Synthesis of Phosphorus(III)-Centered Cations and Their Applications as Ligands

Synthese von Phosphor(III)-Zentrierten Kationen und deren Anwendung als Liganden

DISSERTATION

zur Erlangung des akademischen Grades eines
Doktors der Naturwissenschaften
(Dr. rer. nat.)

dem Fachbereich Chemie
der TU Dortmund vorgelegt von
JEKATERINA PETUŠKOVA

2012

Hiermit versichere ich, dass ich die eingereichte Dissertation selbständig verfasst und keine anderen als die angegebenen Quellen und Hilfsmittel benutzt, sowie Zitate kenntlich gemacht habe.

Datum:_____ _____

(Unterschrift)

1. Berichterstatter: Prof. Dr. Alois Fürstner

2. Berichterstatter: Prof. Dr. Norbert Krause

Die vorliegende Arbeit entstand auf Anregung und unter Anleitung von Herrn Dr. Manuel Alcarazo am Max-Planck-Institut für Kohlenforschung in Mülheim an der Ruhr in der Zeit vom April 2009 bis März 2012. Teile dieser Arbeit wurden in den folgenden Artikeln veröffentlicht: J. Petuškova, H. Bruns, M. Alcarazo, *Angew. Chem. Int. Ed.* **2011**, *50*, 3799 – 3802; J. Petuškova, M. Patil, S. Holle, C. W. Lehmann, W. Thiel, M. Alcarazo, *J. Am. Chem. Soc.* **2011**, *133*, 20758 – 20760.

to my husband Andrejs Petuškovs

Danksagung

Mein herzlichster Dank gilt Herrn Dr. Manuel Alcarazo für die Aufnahme in seinen Arbeitskreis und die Vergabe des interessanten Promotionsthemas.

Herrn Prof. Dr. Alois Fürstner, MPI für Kohlenforschung, und Herrn Prof. Dr. Norbert Krause, TU Dortmund, danke ich für die freundliche Übernahme des Koreferats.

Weiterhin möchte ich der Max-Planck-Gesellschaft und im besonderen dem Max-Planck-Institut für Kohlenforschung für die Bereitstellung meines Arbeitsplatzes und die finanzielle Unterstützung danken.

Mein herzlichster Dank gilt Dr. Manuel Alcarazo für seine große Hilfe, die mich sowohl auf fachlicher und persönlicher Ebene stark zu entwickeln erlaubte. Ich bin ihm zutiefst dankbar für all die Motivation und kompetente Beratung, die er mir zur Verfügung gestellt hat.

Allen Mitgliedern der Arbeitsgruppen Fürstner und Alcarazo danke ich für die gute Zusammenarbeit, das angenehme Arbeitsklima und die schönen Stunden innerhalb und außerhalb des Laboralltags. Ich danke herzlich Helga Krause, Günter Seidel, Daniel Laurich, Karin Radkowski, Roswitha Leichtweiß, Saskia Schulthoff, Gerlinde Mehler und Sigrid Holle für die ständige Hilfsbereitschaft im Labor. Für die große Hilfe bei organisatorischen Angelegenheiten danke ich recht herzlich Frau Lickfeld.

Mein Dank geht an die Mitarbeiter aller analytischen Abteilungen für die zuverlässige und schnelle Durchführung und Auswertung zahlreicher Analysen. Besonders bedanke ich mich bei Frau Phillips, Herrn Dr. Farès und Frau Wirtz aus der NMR-Abteilung, bei Herrn Joppek, Frau Blumenthal und Herrn Klein aus der MS-Abteilung, bei Herrn Deege, Frau Hinrichs und Herrn Breitenbruch aus der HPLC-Abteilung und Herrn Dr. Goddard, Herrn Dr. Lehmann, Frau Dreier und Frau Dreher aus der Kristallographie-Abteilung.

Ich möchte Dr. Georgy Varseev besonders danken für die gemeinsam verbrachte Zeit in Mülheim.
Für das gründliche Korrekturlesen danke ich Dr. Manuel Alcarazo und Dr. Glenn Archibald recht herzlich.

Mein ganz besonderer Dank gilt meinen Ehemann Andrejs für seine Unterstützung! Ich möchte ihm diese Arbeit widmen!

Table of contents

Abbreviations

Å	Angstrom
Ac	Acetyl
Ad	Adamantyl
Aq	Aqueous
atm	Pressure in atmospheres
BAC	Bis(amino)cyclopropenylidene
BIAN	1,2-Bis(imino)acenaphthene
[BMIM][BF_4]	1-Butyl-3-methylimidazolium tetrafluoroborate
Bu	Butyl
Ch	Chalcogene
cod	1,5-Cyclooctadiene
Cy	Cyclohexyl
DAB	1,4-Diazabutadiene
dba	Dibenzylideneacetone
DBN	1,5-Diazabicyclo(4.3.0)non-5-ene
DBU	1,8-Diazabicycloundec-7-ene
DCC	*N*,*N*'-dicyclohexylcarbodiimide
DCE	1,2-Dichloroethane
DCM	Dichloromethane
DHP	3,4-Dihydropyran
DIBAL	Diisobutylaluminium hydride
dipp	2,6-Diisopropylphenyl
DMAP	4-Dimethylaminopyridine
DMF	Dimethylformamide
dmp	2,6-Dimesitylphenyl
DTF	Density functional theory
Δ	Refluxing
δ	Chemical shift (NMR)
E	Ester function
Et	Ethyl
eq	Equivalent
EtOAc	Ethyl acetate

eV	Electronvolt
GC-MS	Gas chromatography – mass spectrometry
h	Hour
Hal	Halogen
Hex	Hexyl
HMPA	Hexamethylphosphoramide
HOMO	Highest occupied molecular orbital
HPLC	High-performance liquid chromatography
HRMS	High-resolution mass spectrometry
Hz	Hertz
IR	Infrared
J	Coupling constant
KHMDS	Potassium hexamethyldisilazane
L	Generalized ligand
L_nM	Generalized metal fragment with *n* ligands
LDA	Lithium diisopropylamide
LUMO	Lowest unoccupied molecular orbital
m	Meta
M	Generalized metal
Me	Methyl
MeO	Methoxy
Mes	Mesityl
min	Minutes
MS	Mass spectrometry
Ms	Methanesulfonate
MTBE	Methyl *tert*-butyl ether
n	Normal
NHC	*N*-Heterocyclic carbenes
NHP	*N*-Heterocyclic phosphines
NMM	*N*-Methylmorpholine
NMR	Nuclear magnetic resonance
$\tilde{\nu}$	Frequency
o	Ortho
p	Para

Ph	Phenyl
PPTS	Pyridinium *p*-toluenesulfonate
Pr	Propyl
PTA	7-Phospha-1,3,5-triazaadamantane
Py	Pyridine
r.t.	Room temperature
t	Tertiary
Tf	Triflate
THF	Tetrahydrofurane
TLC	Thin layer chromatography
TMEDA	*N*,*N*,*N'*,*N'*-Tetramethylethylenediamine
TMS	Trimethylsilyl
Ts	Tosyl
vs	Versus
X	Generalized 1e anionic ligand

1 Subject Overview

The *Lewis*-acid/base reaction between a ligand and a metal fragment to form a complex is one of the fundamental chemical processes. In accordance with their role as *Lewis*-bases, most ligands are neutral species or anions. However, cations may also be employed as ligands. The use of these species, due to their charged nature, may introduce in the resulting metal complexes some interesting properties such as insolubility in organic solvents. That might help to solve one of the problems intrinsically associated with catalytic processes – the separation and recovery of the catalyst. Therefore, the development of stable and recyclable catalysts based on cationic ligands seems to be a promising area of research.

1.1 Cationic Ligands

By definition, all cationic ligands contain moieties in their structure with at least one positive charge. Classical examples are ammonium (**1**, **2**, **4)** or phosphonium (**3**) substituents (Figure 1).[1] Due to their cationic nature, alkylphosphines with positively charged groups such as ammonium or phosphonium substituents are generally less strongly donating than their neutral alkylphosphine analogues.

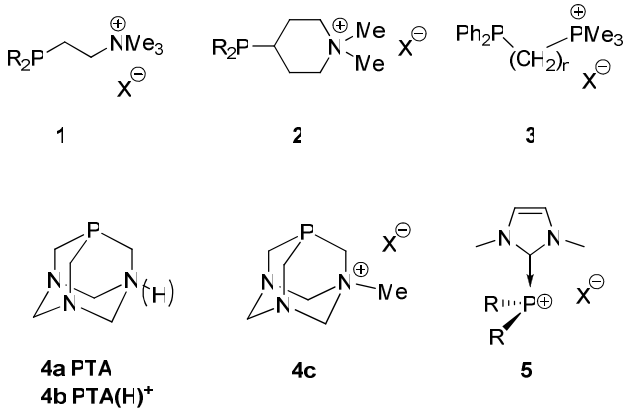

Figure 1. Various phosphine ligands substituted with cationic groups.

It has been reported that the ammonium-functionalized phosphines **1** (R = Cy or *t*Bu) and **2** (R = Cy) are lightly less donating ($\tilde{\nu}$ (CO) of $Ni(CO)_3L$ complexes are 2065, 2064 and 2061 cm^{-1} respectively) than their neutral analogues PCy_3 and $P(tBu)_3$ (2056 cm^{-1} in both

cases).[1] In the same way as alkylammonium groups, alkylphosphonium substituents act as electron-withdrawing moieties in ligands of general structure **3**.[2] An increase in the number of methylene spacers in between the PMe_3^+ moiety and the phosphorus atom reduces this effect.[2] A similar situation takes place by protonation of **4a** to form **4b**.[3]

As an example demonstrating the differences in the behavior of neutral and cationic type ligands in the Pd-catalyzed cross-coupling reaction, the performance of the hexacationic phosphine **7** has been compared with the neutral hexa[(dimethylamino)methyl]-triphenylphosphine **6** as well as the standard triphenyl-phosphine **8** depicted below.[4]

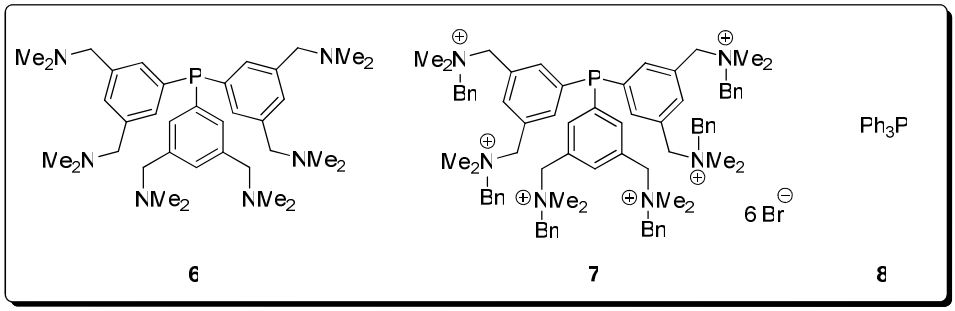

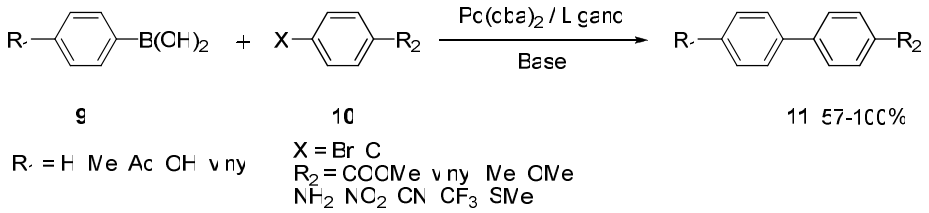

Scheme 1. Pd-catalyzed *Suzuki-Miyaura* cross-coupling reaction.

These experiments showed that **7** exhibited a behavior that is dramatically different from that of PPh_3 (**8**). For example, when four equivalents of **7** were applied at 1 mol% Pd loading in the presence of Na_2CO_3 in aqueous methanol solution, a quantitative yield of the reaction product **11** was reached within ten minutes (R_1 = Me, R_2 = COOMe), whereas in the case of PPh_3 (**8**) the reaction took up to seven hours. The neutral ligand **6** also gave a lower rate (130 min) than the hexaionic species **7**, but still performed better than PPh_3. It has been suggested[4,5] that the phosphine ligand **7** leads to a preferential formation of coordinatively unsaturated and catalytically active Pd(0) species, which may explain the observed high catalytic activity. The presence of six permanent cationic charges in the backbone of this ligand is proposed to result in a significant interligand Coulombic repulsion avoiding the coordination of more than one ligand to the same metal center. This reaction could also be performed in good yields (57-100%) with a significant scope of substrates (R_1 = H, Me, vinyl,

Ac, OH, R_2 = COOMe, vinyl, Me, OMe, NH_2, NO_2, CN, CF_3, SMe, X = Br and Cl) using low catalyst and ligand loadings (0.1 / 0.4 mol%).[4,5] In conclusion, the monodentate, hexacationic triarylphosphine ligand **7** in combination with $Pd(dba)_2$ leads to a very efficient catalytic system for the *Suzuki–Miyaura* cross-coupling reaction that surpasses the results obtained with the nonionic parent compound as well as the benchmark ligand PPh_3.

Finally, *Andrieu et al*. reported the synthesis of cationic imidazolium-2-phosphines **5**. These compounds can be described as a phosphine bearing an imidazolium substituent directly attached to the phosphorus atom, or a phosphenium cation stabilized by a *N*-heterocyclic carbene.[6] In these compounds the lone pair on the phosphorus atom is partially back donated into the imidazolium fragment although it still remains available for coordination to a metal center. This has been demonstrated by measurement of the CO stretching frequency in the corresponding complexes $[RhCl(CO)L_2]$ (L = **5**, ($\tilde{\nu}$ (CO) is 2003 cm^{-1} for R = Ph).[6] These values indicate that these ligands have a behavior similar to phosphites.

1.2 Phosphenium Cations

Phosphenium cations have the general formula $[R_2P:]^+$ and therefore their reactivity is defined by a lone pair that makes them nucleophilic as well as an empty π-orbital that introduces an electrophilic character. Both reactivities have been described. For example, the electrophilic character is observed when they react with *Lewis*-bases[7], when they are involved in C–H bond insertion,[8] or by their reaction with unsaturated organic molecules such as 1,3-dienes[9] or alkynes.[10] Also donative action of the phosphorus lone pair can be shown by their reactivity towards azides[11] and from the fact that phosphenium ions exhibit rich coordination chemistry.

1.2.1 Types of the phosphenium cations

An obvious procedure to stabilize phosphenium cations consists in the donation of electron density to the empty π-orbital at the phosphorus atom. Depending on how this donation takes place, phosphenium cations can be divided into three categories. In type **A** cations, the positive charge is localized exclusively on the substituents (Figure 2). The phosphorus atom is neutral or has even a negative π-charge and is therefore expected to be a mainly nucleophilic centre. In contrast, the phosphorus atom in type **B** cations exhibits a positive charge and may

be classified as an ambiphilic center, which exhibits both electrophilic and nucleophilic (lone pair) character. Finally, in case **C**, an external ligand is used to donate electron density to the phosphorus atom. In this case the electrophilicity of the phosphorus atom is cancelled and its nucleophilic character will strongly depend on the nature of **L**, as will be shown later.

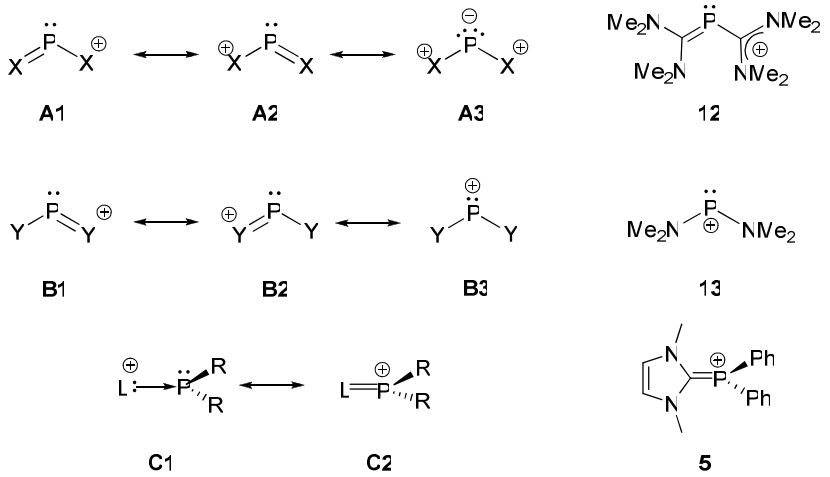

Figure 2. Mesomeric structures of phosphenium cations.

Typical representatives of type **A** cations are 2-phosphaallylic cations **12**,[12] type **B** ions are exemplified by aminophosphenium ions **13**[13] and type **C** cations – by the *Andrieu* system **5** discussed above.

1.2.1.1 Type A phosphenium cations: stabilization by formation of bis(phosphonio)-isophosphindolides

The first bis(phosphonio)isophosphindolide salt was reported by *Schmidtpeter* and *Thiele*.[14] Starting from the *o*-xylylenebis(phosphonium) ion **14**, which is easily prepared from α,α-dibromo-*o*-xylene and the corresponding phosphine (PPh_2R). Subsequent cyclocondensation by reaction with phosphorus trichloride in the presence of triethylamine forms the bis(phosphonio)isophosphindole cations **15** (Scheme 2).[14,15]

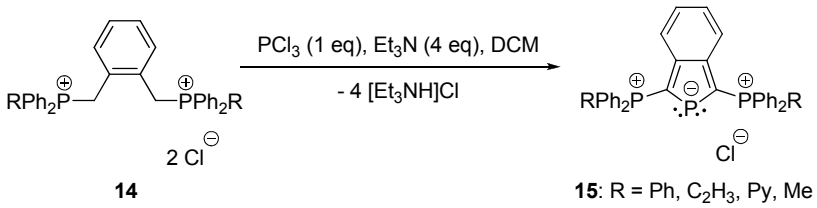

Scheme 2. Synthesis of bis(phosphonio)isophosphindole cations **15**.

Isophosphoindole **15** can be represented by three resonance structures **15a**, **15b**, and **15c** (Figure 3). Mesomer **15a** presents the cation as a phosphenium ion stabilized by two methylenephosphorane groups, **15b** as a phosphonio-substituted phosphaalkene, and **15c** as a phospholide anion modified by two phosphonio substituents.

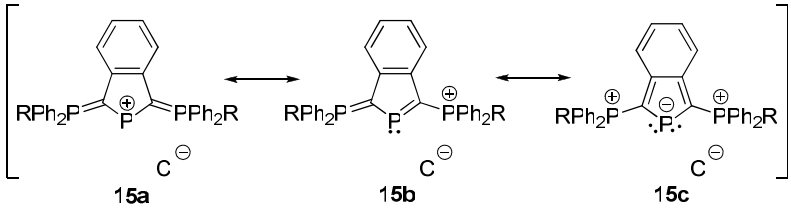

Figure 3. Mesomeric structure of bis(phosphonio)isophosphindole cations **15**.

The known bis(phosphonio)isophosphindolide complexes with group 11 metals can be divided into mono- and dinuclear complexes. In mononuclear complexes, the cation binds to the metal *via* the phosphorus "lone pair" (**D1** and the corresponding example **16**, Figure 4), while in dinuclear complexes a μ^2(P)-bridging coordination of the P-cation to two metals (**D2** and the corresponding example **17**) takes place. In these cases the phosphorus is able to donate up to 4 electrons as depicted in resonance form **15c** (Figure 3).[16]

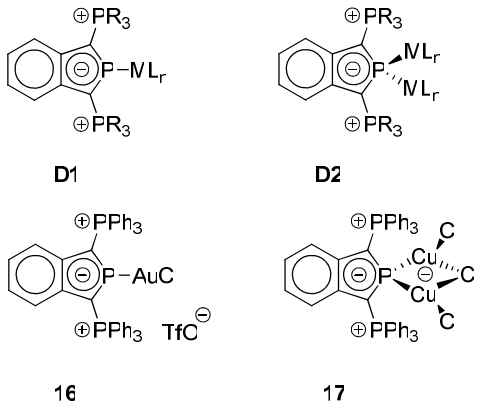

Figure 4. Schematic representation of bis(phosphonio)isophosphindole complexes **D1** and **D2** and their examples **16** and **17**.

1.2.1.2 Type B phosphenium cations: stabilization by introduction in electron rich heterocycles

P-block elements such as P, C and Si can be stabilized in low oxidation states such as +1 or +2 respectively if incorporated in the appropriate organic skeleton. Thus, the first isolated carbenes, silylenes and phosphenium cations shared the general structure **F** (Figure 5). [17] In addition, it has been demonstrated that the saturated counterparts with the general structure **G** can also be isolated despite of the lack of aromatic stabilization.[18]

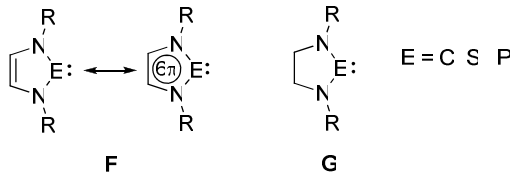

Figure 5. Aromatic 1,3-diazoles (**F**) and non-aromatic 1,3-diazolidines (**G**).

Phosphenium cations of this type (E = P) are usually prepared from chlorophosphines $(R_2N)_2P–Cl$ by two different methods: abstraction of the chloride with *Lewis*-acids such as $GaCl_3$[19] or $AlCl_3$ (Scheme 3, a) or trapping of the chloride anion by silver salts of weakly coordinating anions, especially $AgPF_6$ and $AgBF_4$ (Scheme 3, b).[15]

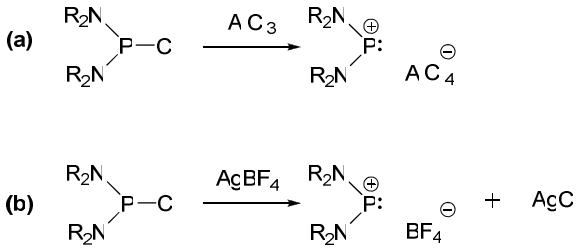

Scheme 3. Formation of phosphenium cations $[(R_2N)_2P]^+$.

As an example, the 1,3-diazolidene derivatives **22a-c** could be prepared starting from glyoxal **18** which is converted to the corresponding diimine derivative **19** by addition of the corresponding amine in ethanol. Subsequent reduction of **19** with $LiAlH_4$ gives the corresponding diamine derivative **20** which, in the reaction with phosphorus trichloride, is transformed to compound **21**. The subsequent anion exchange by the addition of trimethylsilyl trifluoromethanesulfonate or silver tetraflouroborate gives the corresponding products **22a-c** in moderate 43-65% yields (Scheme 4).[20]

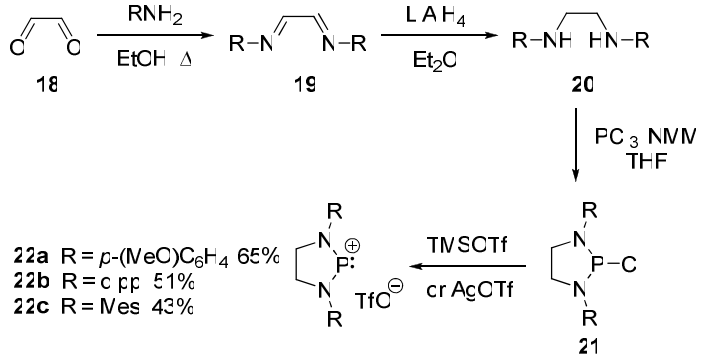

Scheme 4. Synthesis of NHPs derivatives **22a**-**c**.

Additionally, phosphenium cations of this class can be obtained by lithiation of bis-imine **19** followed by reaction with perchlorosilane yielding the dichlorosilane **24** (Scheme 5). The exchange of phosphorus for silicon with PCl_3 in refluxing benzene gives the corresponding chlorophosphine **25**.[18] Simple abstraction of Cl^- from this compound affords the desired phosphenium cation.

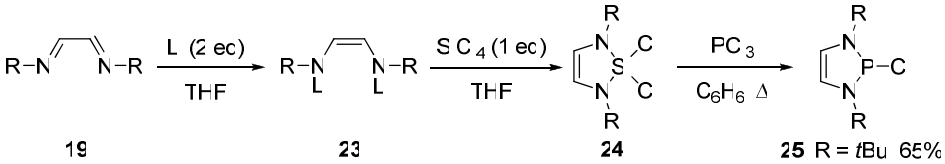

Scheme 5. Synthesis of chlorophosphine derivative **25**.

Interestingly, *N*-heterocyclic carbenes and *N*-heterocyclic phosphenium cations (NHPs) are isovalent and isostructural, but electronically inverse.[21] NHPs are weak σ-donors and good π-acceptors due to the formal positive charge and isotropic s- (as opposed to directional sp^2-) character of the "lone pair" orbital on phosphorus, whereas NHCs are weak π-acceptors and strong σ-donors.[22] Several metal complexes of NHP with late transition metals (groups 9 and 10) have been reported. They are summarized in Figure 6.

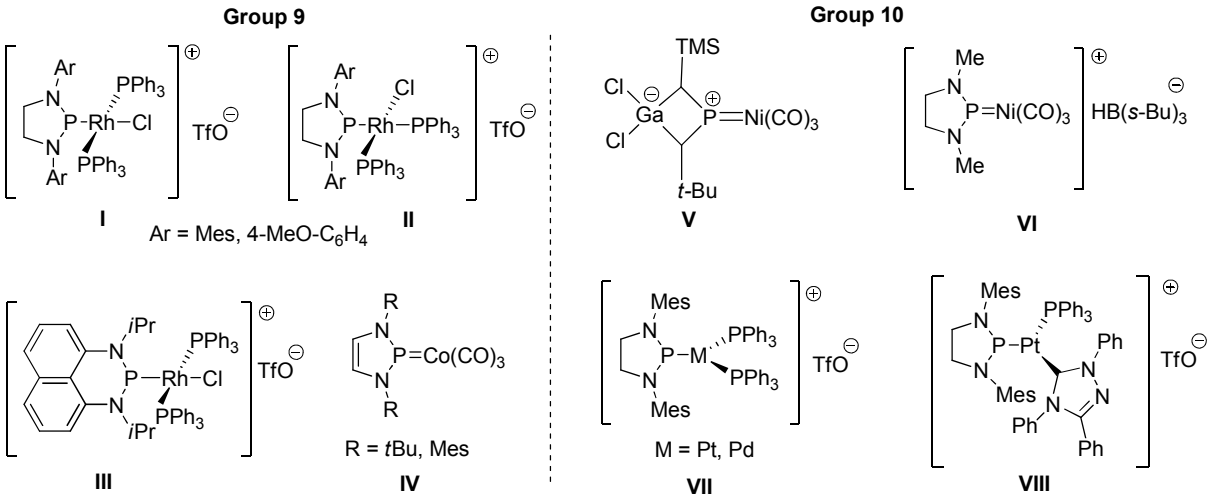

Figure 6. Some reported group 9 and 10 metal–NHP complexes.

The groups of *Baker*[23] and *Richeson*[24] have both prepared NHP-containing analogues of *Wilkinson's* catalyst **I**-**III**, and *Gudat* has described a Co complex (**IV**).[25] NHP complexes of the group 10 metals include the Ni complex with a zwitterionic phosphenium-containing ligand **V** reported by *Niecke*,[26] a Ni complex **VI** made by *Parry*,[27] while *Baker* has shown that [NHP]OTf reacts directly with $Pt(PPh_3)_3$ or $Pd(PPh_3)_3$ affording adducts **VII**.[28] An *Enders*-type NHC can replace one of the PPh_3 ligands in this complex to give complex **VIII**.

1.2.1.3 Type C phosphenium cations: stabilization by formation of complexes with *Lewis*-bases

The bonding interactions in coordination chemistry usually consist in a donation from an electron-rich ligand to an electron-deficient species such as a metal center. With this idea on mind, the phosphinophosphonium cation **26a** can be formally represented as a coordination complex **26b** involving donation of electron density from a chlorophosphine to a phosphenium cation center (Figure 7).[29]

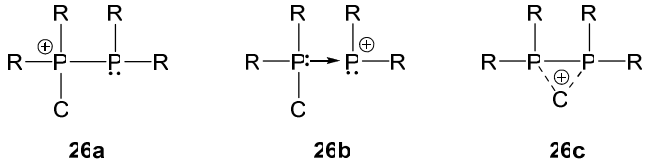

Figure 7. Representative structures of to bonding models for phosphine-stabilized phosphenium cations.

It has been calculated that the transfer of Cl^+ moieties between the phosphorus atoms in compounds with general formula **26** is not kinetically favored.[30] Thus, the R_2ClP fragment of **26b** (R = Ph), that is not a good σ-donor, is available for ligand exchange, which allows the synthesis of some phosphenium cation derivatives, for example – the pentaphenylphosphino-phosphonium salt **27** (Scheme 6).

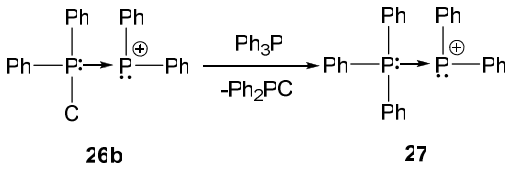

Scheme 6. Synthesis phosphine-stabilized phosphenium cation **27**.

Moreover, the *Lewis*-base in such donor-stabilized phosphenium complexes can be easily substituted by a stronger donor. This approach has been used to synthesize various donor-phosphenium complexes (Do = DMAP, DBN, DBU, NHCs) (Scheme 7).[31]

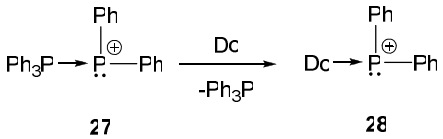

Scheme 7. Ligand exchange for the synthesis of new phosphorus–element bonds; replacement of Ph_3P by a stronger donor (Do).

Another synthetic route able to produce NHC-stabilized phosphenium cations consists in the reaction between 1,3-dialkylimidazolium-2-carboxylates **29** and chlorophosphines R_2PCl (R = phenyl, *iso*-propyl, cyclohexyl). In that manner, adducts **30a-c** were prepared after an anion exchange (Scheme 8).[32] When the reaction was performed with $PhPCl_2$ and 1,3-dimethyl-imidazolium-2-carboxylate **29** in a 1:2 ratio, the phosphine **31**, which contains two imidazolium substituents, was obtained after an anion exchange with KPF_6.[33]

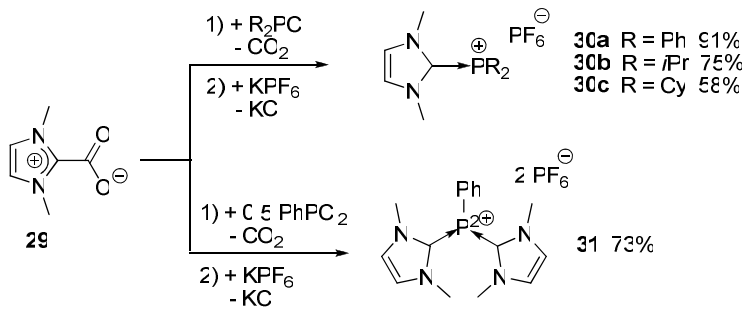

Scheme 8. Synthesis carbene-stabilized phosphenium cations $[LPR_2]^+$ **30a-c** and $[L_2PPh]^{2+}$ **31**.

Imidazolium substituted phosphines have been applied as ligands. For example, reaction of **32** with the benzonitrile complexes $(PhCN)_2MCl_2$ (M = Pd, Pt) gives the electroneutral complexes **33a** (M = Pd) and **33b** (M = Pt) in 90% and 82% yield, respectively (Scheme 9).[34] In **33**, the positive charge of the phosphenium ligand is compensated by the negative charge of the MCl_3^- fragment.

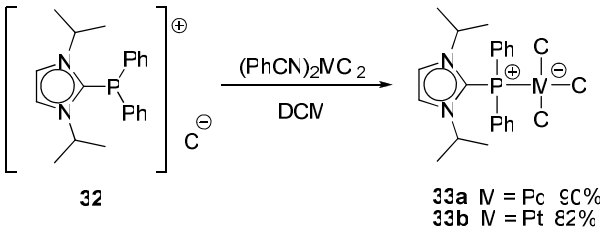

Scheme 9. Synthesis of Pd and Pt complexes **33a** and **33b**.

In addition, these metal complexes have found applications as catalysts. Moreover, these types of complexes are interesting because they strongly decrease the metal leaching in homogeneous polyphasic catalysis, especially when an ionic liquid phase is used.[35] As example, cations **30a** and **37** were employed as ligands in the palladium-catalyzed *Sonogashira* coupling depicted in Scheme 10.

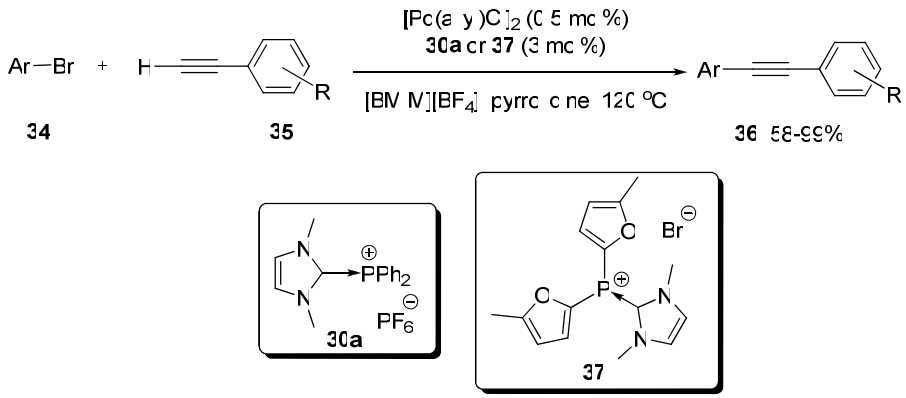

Scheme 10. Palladium-catalyzed aryl alkynylation.

Another example in which these ligands have found application is the platinum-catalyzed hydrogenation of halonitrobenzenes to the corresponding haloanilines,[36] a process that has numerous applications in the manufacture of herbicides, pesticides or chemical fertilizers. The challenge of this transformation consists in minimization of the undesired dehalogenation of the substrates. Thus, complex **30a** was converted to the *trans*-$PtCl_2L_2$ **39**. Using **39** as catalyst, *m*-chloronitrobenzene **38** was converted into *m*-chloroaniline **40** in [BMIM][BF_4] at 20 bars of hydrogen at 110 °C (Scheme 11).

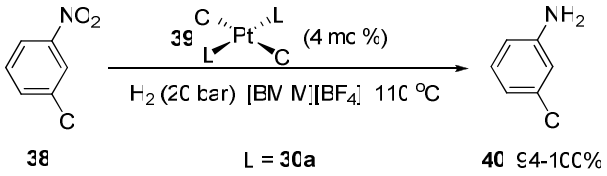

Scheme 11. Platinum-catalyzed hydrogenation of *m*-chloronitrobenzene **38**.

1.3 Summary I

Cationic ligands have recently received considerable attention because of their intrinsic advantages regarding catalyst recycling. In addition, cationic ligands can even increase reaction yields and rates.[4]

2 Carbene-Stabilized Phosphorus(III)-Centered Monocations

2.1 General Introduction

As already mentioned, phosphenium cations of the general formula $[R_2P:]^+$ are isolobal with singlet carbenes and can be stabilized by donation of electron density into their empty orbital.[37] This goal is often reached either by embedding the phosphorous atom into a heterocyclic scaffold[38] as in **B**-type structures, or by reaction with bases of different nature to form the corresponding *Lewis*-adducts **C** (Scheme 12).[39]

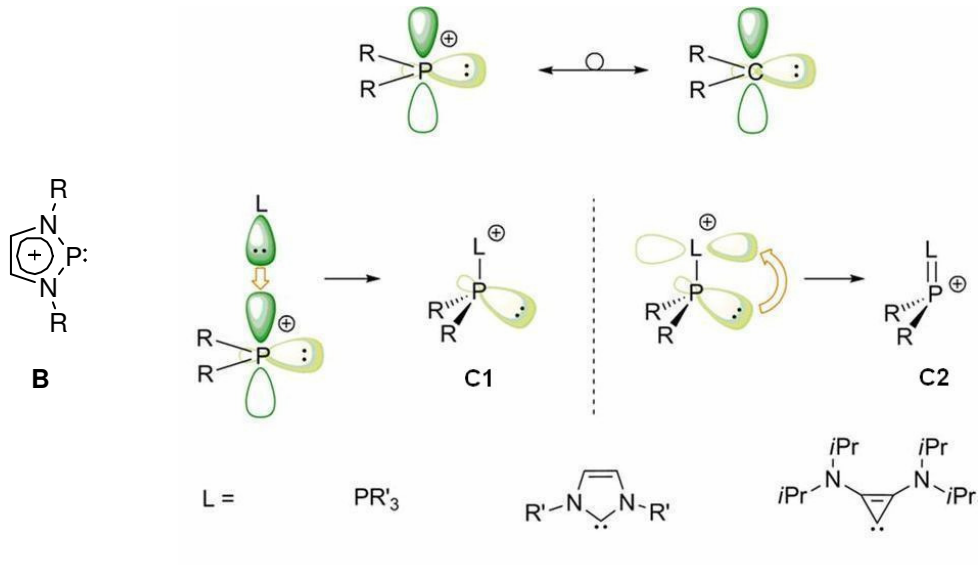

Scheme 12. Representative structures of *N*-heterocyclic phosphenium cations **B** and the conceivable resonance extremes of the phosphenium-base adducts **C1** and **C2**.

In both cases, the presence of an unshared pair of electrons at the phosphorous atom makes the use of these compounds as ligands plausible; however, their intrinsic positive charge renders them poor σ-donors and strong π-acceptors.[40] Specifically, in **C**-type adducts the ground-state structure is dominated by resonance extreme **C2** when L is a phosphine, and therefore, transition-metal coordination complexes derived from these compounds are scarce.[41] Even in the cases in which L is an *N*-heterocyclic carbene (NHC), the coordination properties of the resulting adducts are only comparable to those exhibited by the strongly π-accepting phosphites.[42] However, we imagined that we could generate phosphenium

adducts in which resonance form **C1** might have a decisive contribution to the ground state by selecting an internal ligand L that is a stronger σ-donor and an even poorer π-acceptor than NHCs. This approach should provide systems with phosphine-like coordination behavior while keeping a positive charge that confers them the physicochemical properties of salts. Phosphines containing charged functionalities have already been used in several chemical processes; the hydroformylation of olefins is one remarkable example.[43] Note, however, that in such phosphines, the charged groups are invariably appended to the periphery of the compound and are not directly attached to the phosphorous atom as in the present case.[44]

To put our design concept into practice, we considered 1,2-bis(diisopropylamino)-cyclopropenyl-3-ylidene as the internal ligand that fulfils the necessary electronic requirements.[45] Their HOMO is higher than that of NHC's and therefore they are stronger σ-donors. Similarly, their LUMO has a slightly higher energetic level, making them even less of a π-accetor than NHC's (Figure 8).[46]

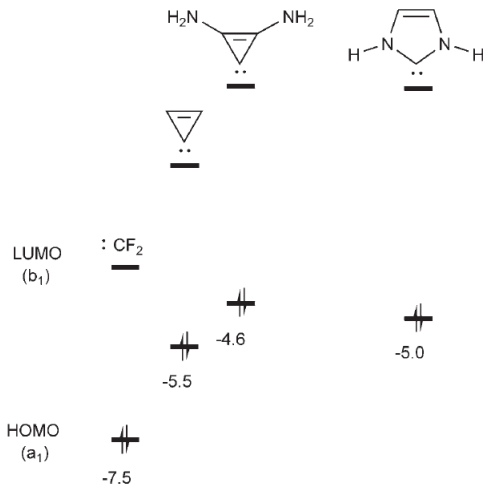

Figure 8. Frontier orbitals of various singlet carbenes obtained at the RI-BP86/TZVP level of theory. HOMO (a_1) energies are given in eV and LUMO refers to the lowest-energy b_1 orbital.

2.2 *Results and Discussion*

2.2.1 Synthesis

Our starting material, the chlorocyclopropenium salt **42** was prepared from tetrachlorocyclopropene **41** and excess of diisopropylamine.[47] Condensation of the salt **42** with a range of secondary aromatic (R = Ph, *p*-(Me)C_6H_4, *p*-(OMe)C_6H_4, *p*-(F)C_6H_4) and aliphatic (R = Cy, Ad) phosphines and subsequent anion exchange gave the desired phosphanylidenes **43a-f** as white, air-stable solids in good to excellent yields (76-96%, Scheme 13).

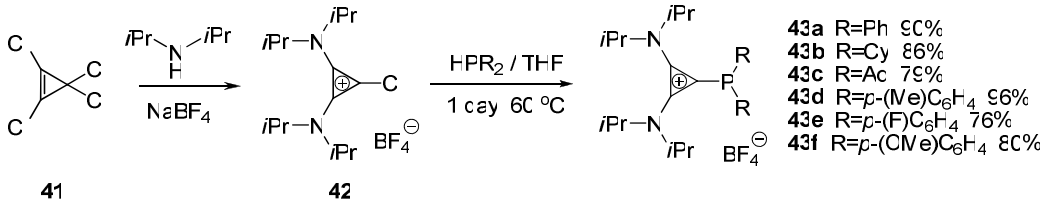

41 42

Scheme 13. Synthesis of diisopropylaminocyclopropenylidene derivatives **43a-f**.

The comparison of the C–P bond lengths in the X-ray structure of **43a** (Figure 9) is especially informative. The C1–P1 bond (1.814 Å) is only slightly shorter than the two other C–P single bonds (1.834 Å and 1.831 Å) connecting the phosphorous atom with the phenyl rings, but is significantly longer than typical C–P double bonds. For comparison, the carbon–phosphorous distance in an unstabilized ylide such as methylenetriphenylphosphorane ($Ph_3P{=}CH_2$) is 1.662(8) Å.[48]

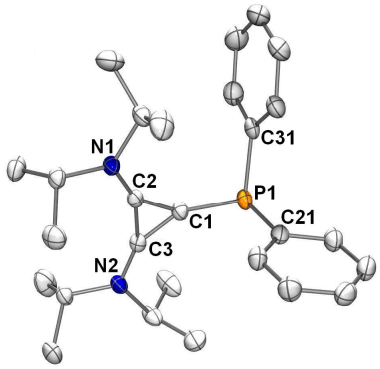

Figure 9. Crystal structure of **43a**. Hydrogen atoms, solvent molecules and the BF_4 anion are omitted for clarity; ellipsoids are set at 50% probability.[49]

This data reveals that, in line with our expectations, back donation from the phosphorous atom to the cyclopropenyl ring must be marginal.

2.2.2 Electronic properties

Evaluation of the CO stretching frequencies in metal carbonyl complexes provides a useful tool to study the electronic properties of the ligands coordinated to a particular metal center. The increase of electron density at a metal generated by the coordination of a new ligand is compensated by the metallic center by increasing its back-donation to the other surrounding ligands. If one of those is CO, the extra back-donation into the π*-orbital will decrease the CO bond order. As a consequence, the CO stretching frequency will be shifted to lower ṽ, thus providing a qualitative measure of the donor ability of the new ligand.

To evaluate the donor ability of the new phosphenium adducts by analysis of the CO stretching frequencies, some rhodium complexes **44a-e** have been prepared in very good yields from phosphanylidenes **43a-e** (Scheme 14).

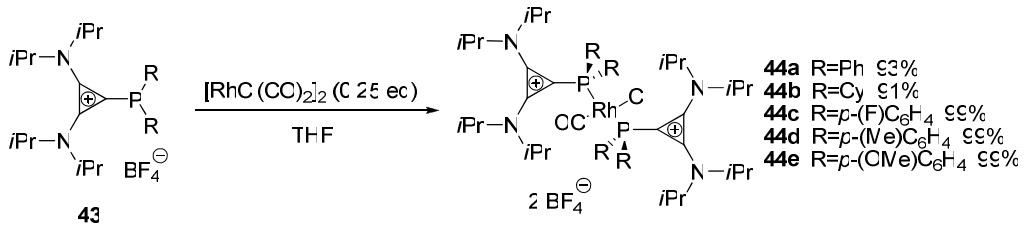

43

Scheme 14. Synthesis of $[RhCl(CO)L_2](BF_4)_2$ type complexes.

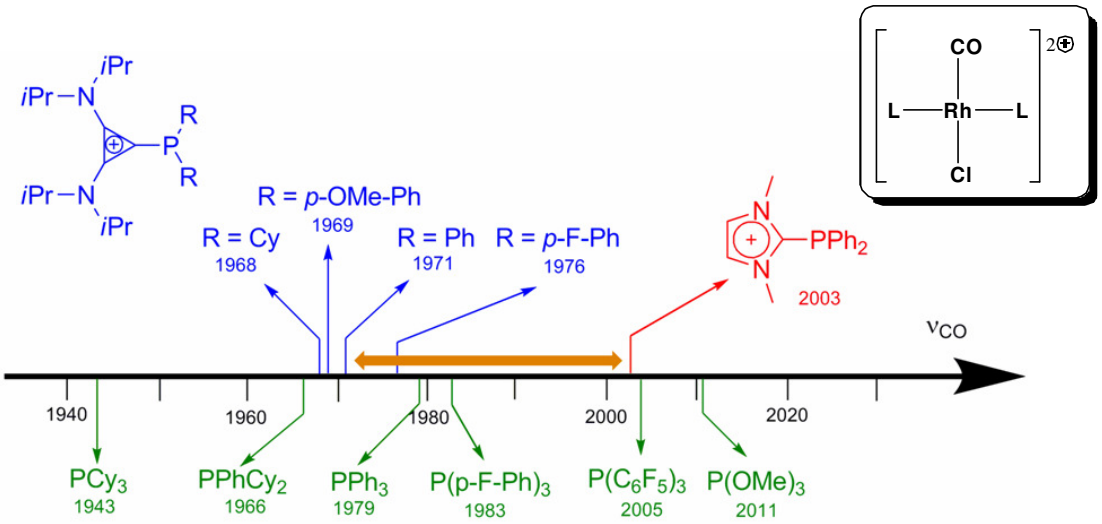

Figure 10. Carbonyl stretching frequences in complexes $[RhCl(CO)L_2](BF_4)_2$

As shown in Figure 10, ligands **43a,b,e,f** have a behavior similar to typical phosphines, even though they are cationic species. They clearly surpass those complexes containing NHCs as internal ligands.[50]

The same conclusion can be extracted from cyclic voltammetry. Rhodium complexes **45a-d** were prepared to measure their electrochemical redox potential (Scheme 15). Table 1 shows the oxidation potentials from Rh(I) to Rh(II) in [RhCl(cod)L] complexes. As it can be seen, the oxidation potential of the complexes containing ligands **43a** and **43b** are nearly identical to those of [RhCl(cod)Ph_3P] and [RhCl(cod)Cy_3P] respectively. As oxidation potentials are directly related to the global electron density of a metal center, it can be concluded that the ligand **43a** and **43b** donate the same amount of electron density as Ph_3P and Cy_3P, respectively.[51]

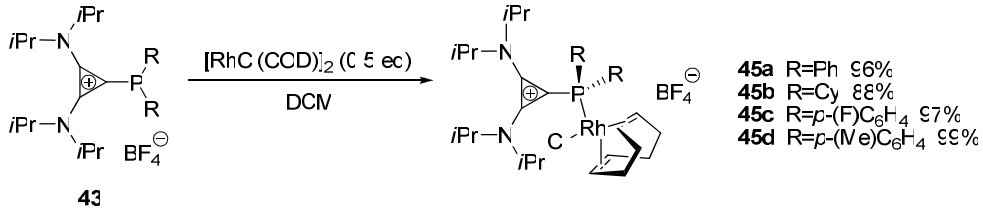

Scheme 15. Synthesis [RhCl(cod)L](BF_4) type complexes.

Table 1: Electrochemical redox potential of complexes [RhCl(cod)L](BF_4) (**45a-d**). The values for commonly used phosphines are also included for comparison.

Entry	Ligand	R	$E_{1/2}$[a] [RhCl(cod)L]BF_4
1	**43a**	Ph	0.955
2	**43b**	Cy	0.911
3	**43e**	*p*-(F)C_6H_4	0.964
4	**43d**	*p*-(Me)C_6H_4	0.915
5		Ph_3P	0.955
6		Cy_3P	0.917

[a] Calibrated versus ferrocene/ferrocenium ($E_{1/2}$ = 0.46 V), Bu_4NPF_6 (0.1M) in CH_2Cl_2.

2.2.3 Coordination properties

Encouraged by the analysis of the electronic properties, we decided to test the potential of these compounds in catalysis and prepared a set of gold complexes in which salts **43a-f** were used as ligands (Scheme 16).

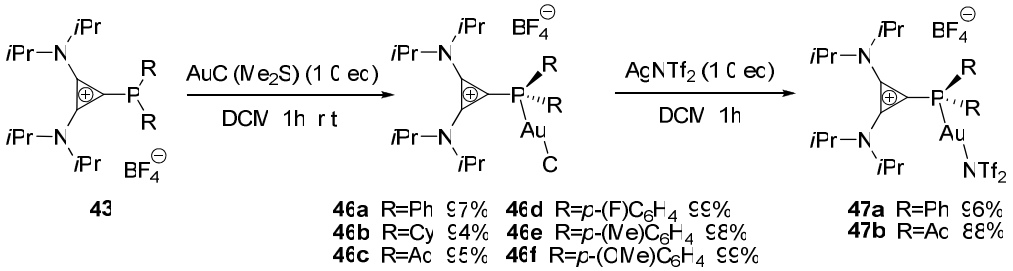

Scheme 16. Preparation of different gold(I) complexes **46a-f** and **47a,b**.

Compounds **46a-f** were obtained as air-stable white solids in excellent yields by addition of [(Me_2S)AuCl] to solutions of **43a-f** in dichloromethane. Subsequent exchange of the chloride anion for the less coordinating bis(trifluoromethanesulfonyl)imidate anion was performed, thus allowing for a convenient way to obtain isolable yet active catalysts **47a,b** without the necessity of using highly hygroscopic silver salts as cocatalysts.[52] Moreover, crystals of **46a** were obtained, and the structure of the complex was determined, thus confirming the expected connectivity (Figure 11).

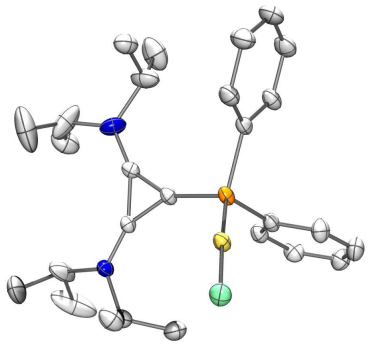

Figure 11. Crystal structure of **46a**. Hydrogen atoms, solvent molecules and the BF_4 anion are omitted for clarity; ellipsoids are set at 50% probability.[49]

In addition, the reactions of phosphanylidene **43a** (R = Ph) or **43e** (R = *p*-(F)C_6H_4) with copper(I) chloride or allylpalladium(II) chloride dimer afforded the corresponding metal complexes **48a-c** in excellent yields (Scheme 17).

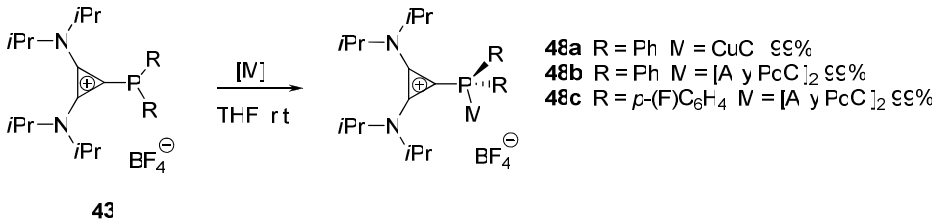

Scheme 17. Preparation of some metal complexes **48a-c**.

The similar reaction between salt **43a** and borane-tetrahydrofuran complex gave the corresponding adduct **49** in 85% yield (Scheme 18).

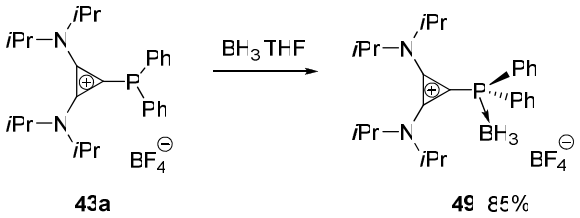

Scheme 18. Preparation of borane complex **49**.

The stability of complex **49** is lower than that of the corresponding metal complexes **48a-d**. This fact could be explained by the lack of back-donation from boron to phosphorus, an energetic contribution that may stabilize complexes **48a-d**. Compound **49** slowly decomposes in solution, but nevertheless its characterization was possible.

The rhodium(III) complex **50** could also be synthesized by refluxing a solution of salt **43a** in ethanol with hydrated rhodium trichloride in the presence of tetraethylammonium chloride to obtain the desired compound in 96% yield (Scheme 19).

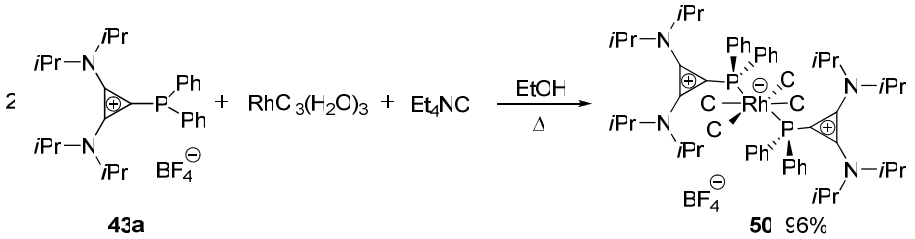

Scheme 19. Preparation of rhodium(III) complex **50**.

Summarizing, we noted that cyclopropenylidene-stabilized phosphenium cations could be successfully used as ligands, producing the corresponding adducts in excellent yields. In order to compare the catalytic performance of the newly synthesized gold(I) compounds with standard gold(I) phosphine complexes, the new catalysts were tested in a range of already reported transformations.[53]

2.2.4 Application in catalysis

2.2.4.1 [2+2] *vs* [2+3] Cycloaddition of ene-allenes

Gold-based catalysts have appeared in the last years as one of the most powerful methods for the electrophilic activation of alkynes toward a variety of nucleophiles under homogeneous conditions. These reactions go through three main stages: (1) activation of the alkyne by coordination of the gold atom, (2) nucleophilic attack and (3) proto-deauration. Therefore, the nature of the ancillary ligand has a tremendous influence on the reaction course and product. The gold(I)-catalyzed [2+2]-cycloaddition of ene-allenes first reported by *Toste et al.*[54] is an interesting transformation and was chosen to evaluate the behavior of our catalysts. The synthesis of the suitable substrate **55** was realized from commercially available starting materials as depicted in Scheme 20.

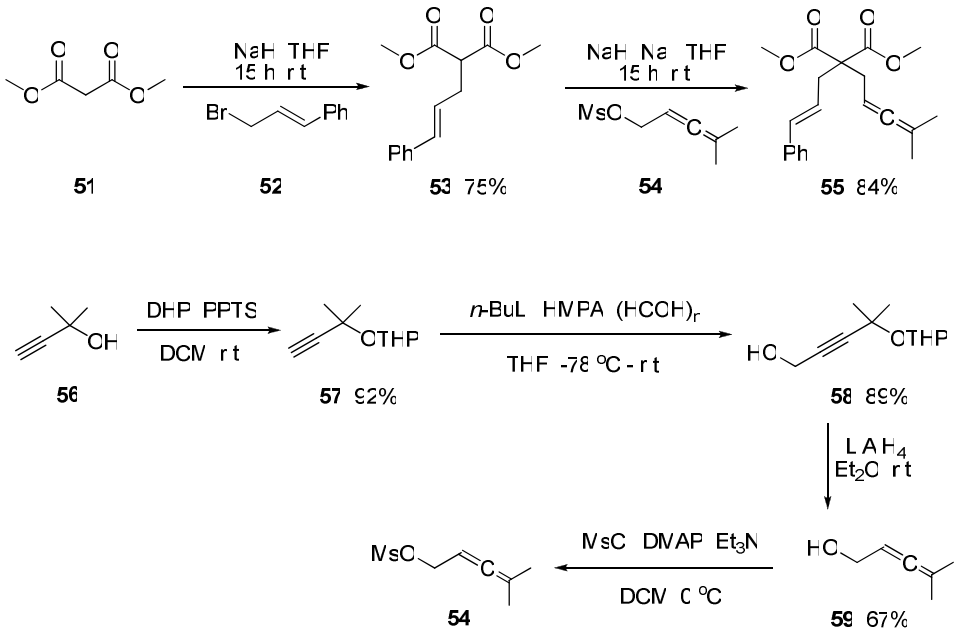

Scheme 20. Synthesis of ene-allene **55**.

After deprotonation of dimethyl malonate **51** with sodium hydride and reaction with cinnamyl bromide **52** in dry THF, the corresponding monoalkylated product **53** was obtained in 75% yield.[54] The mesylate **54** was obtained in a three-step synthesis starting from the reaction of 2-methylbut-3-yne-2-ol **56** with 3,4-dihydropyran in presence of pyridinium *p*-toluenesulfonate.[55] To this end, the THP-protected compound **57** was obtained in 92% yield. Reaction of **57** with *n*-butyllithium and subsequent addition of paraformaldehyde afforded **58** in 89% yield.[56] Treatment of **58** with lithium aluminium hydride gave the desired

allenol **59** in 67% yield,[57] which was later converted into the corresponding mesylate **54** by reaction with methanesulfonyl chloride in the presence of triethylamine and catalytic amount of 4-dimethyl-aminopyridine (DMAP).[58] Deprotonation of cinnamyl malonate **53** with sodium hydride and addition of freshly prepared mesylate **54** in the presence of sodium iodide afforded the desired ene-allene **55** in 84% yield.[54]

Scheme 21 shows the proposed mechanism governing the cycloisomerization of **55**. Once gold coordinates to the substrate, the primarily formed intermediate **60** may evolve following two different reaction pathways.[59]

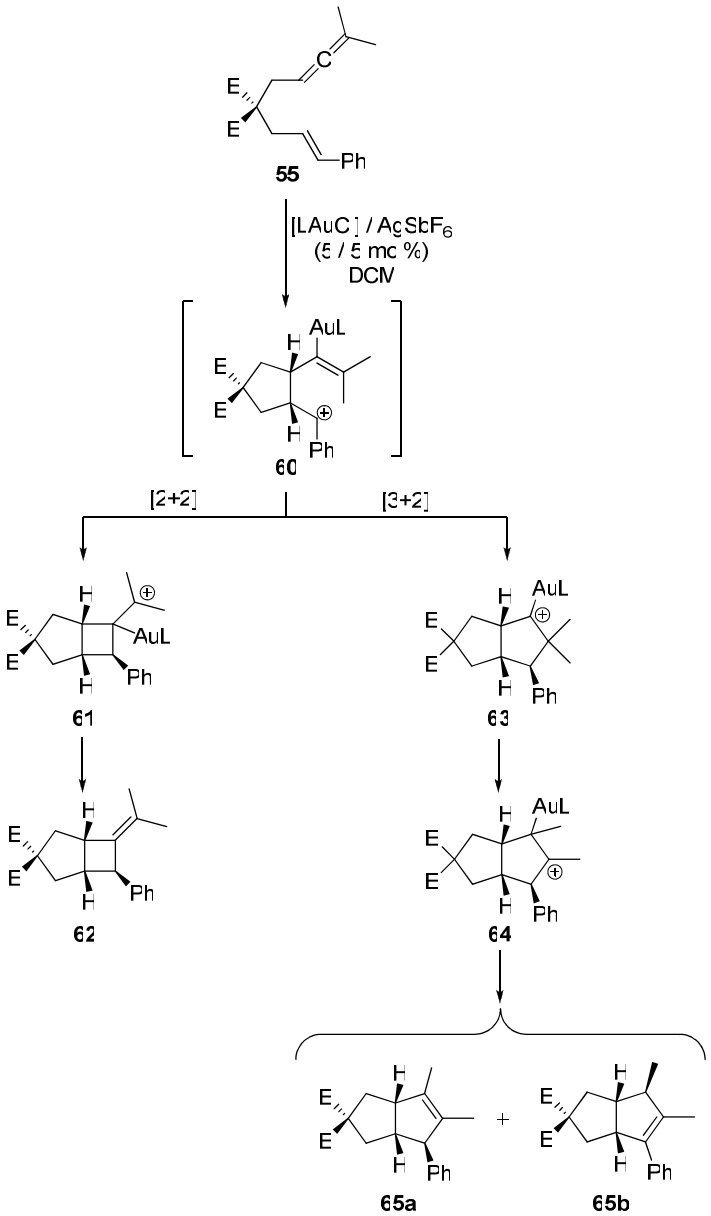

Scheme 21. Control over the cycloaddition of ene-allene **55** by adjusting the π-acceptor properties of the ligand L bound to Au^{+}.

Gold(I) catalysts bearing electron rich ligands may stabilize better an adjacent cation, therefore, they favor the formal [3+2] cycloaddition pathway *via* intermediate **63**. Conversely, electron deficient ligands coordinated to the gold center should promote more effieciently the [2+2] cycloaddition pathway to produce intermediate **61**, in which a carbenium cation is not directly bounded to gold. This route ultimately delivers the known alkylidenecyclobutane **62**.

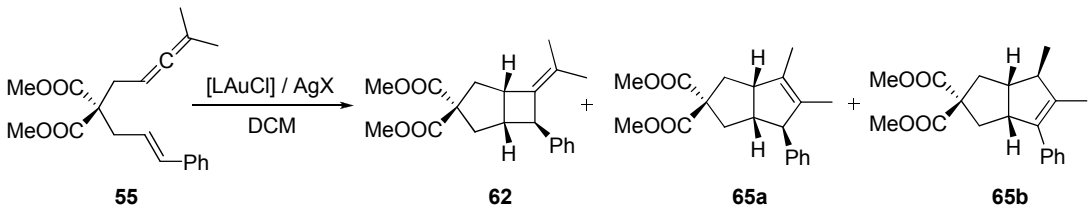

Scheme 22. Gold(I)-catalyzed cycloisomerization of ene-allene **55**.

Table 2 summarizes the behavior of our catalysts in comparison with Ph_3PAuCl and $(PhO)_3PAuCl$.

Table 2: Cycloisomerization of ene-allene **55** catalyzed by different gold complexes.

Entry	Pre-Catalyst	R	Additive	62:65a:65b ratio	Yield (%)
1	**46a** 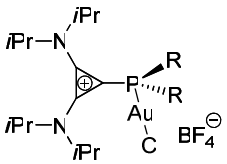	Ph	$AgBF_4$	97:3:0	78
2	**46d**	*p*-FC_6H_4	$AgBF_4$	97:3:0	76
3	**66** Ph_3PAuCl		$AgSbF_6$	50:32:18	83
4	**67** $(PhO)_3PAuCl$		$AgSbF_6$	100:0:0	71

Reaction conditions: 5 mol% of the corresponding gold complex and 5 mol% of appropriate silver salt AgX (X = SbF_6 or BF_4)

The ligand of catalyst **46a** behaves as a good π-acceptor ligand as it gave the [2+2] adduct **62** as the major product. Introduction of a fluoro-substituent into the aromatic rings of the ligand in catalyst **46d** did not show any significant influence on the reaction course, as the yields and regioisomer ratios were comparable. To put these results into perspective, two control experiments with Ph_3PAuCl (**66**) and $(PhO)_3PAuCl$ (**67**) were performed. While **66** delivered the mixture of all possible products **62** and **65a,b** under the chosen conditions, the triphenylphosphite gold(I) complex **67** produced **62** as the only regioisomer due to the excellent π-accepting properties of the ligand. Thus, it can be concluded that our catalyst perfectly compares with phosphite-based catalysts.

2.2.4.2 [2+4] *vs* [3+4] Cycloaddition of allene-dienes

As a second model reaction, the cycloisomerization of allene diene **68** was chosen to generalize our previous conclusions (Scheme 23). This transformation is also known to be dependent on the global electron density at the gold atom, thus providing an additional measure for the donor properties of our ligands, based on reactivity parameters.[60]

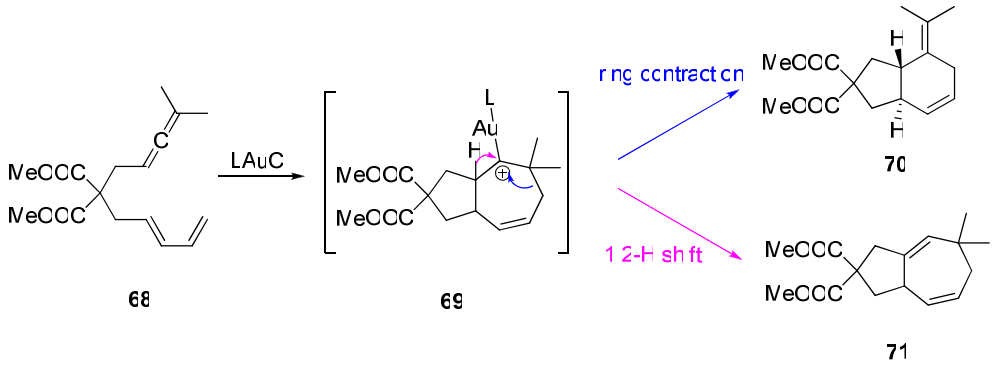

Scheme 23. Effect of the ligands with different π-acceptor properties on the gold-catalyzed cyclization of allene-diene **68**.

When π-acceptor ligands L are used, the carbocationic nature of intermediate **69** is enhanced, thus promoting ring contraction by a 1,2-alkyl shift. In contrast, strongly σ-donating ligands at the gold center increase the carbene character of **69**, thus favoring the 1,2-hydride shift.

The synthesis of allene-diene **68** began with the reaction between dimethyl malonate **51** and (*E*)-5-bromopenta-1,3-diene **72** to give the corresponding monoalkylated dimethyl malonate derivative **73** (Scheme 24). The necessary bromide **72** was prepared by the reduction of the (*E*)-1,4-pentadienoic acid **74** using lithium aluminium hydride[61] and subsequent reaction of the formed alcohol **75** with phosphorus tribromide.[62] Further reaction between mesylate **54** and the dimethyl malonate derivative **73** in the presence of sodium hydride and sodium iodide gave the desired allene-diene **68** in 75% yield.

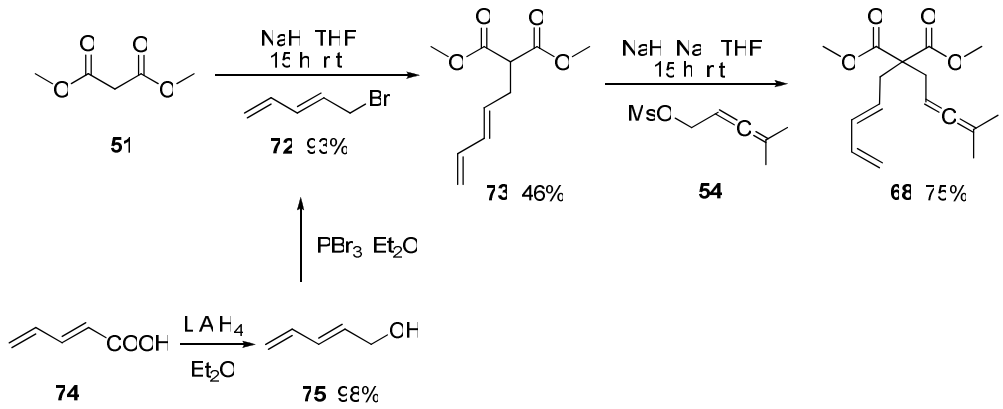

Scheme 24. Synthesis of allene-diene **68**.

Table 3: Cyclization of ene-allene **68** catalyzed by different gold complexes.

Entry	Catalyst	R	Reaction time	70:71 ratio	Yield (%)
1	**47a** 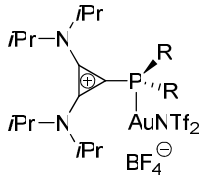	Ph	3 h	87 13	92
2	**47b**	Ac	9 h	61 39	64
3	**76** $MesAuNTf_2$		3 h	1 99	95
4	**77** Me_3PAuCl		9 h	55 45	84
5	**66** Ph_3PAuCl		3 h	75 25	75
6	**67** $(PhO)_3PAuCl$		3 h	97 3	98

Reaction conditions: 2 mol% of [$LAuNTf_2$] (entries 1-3) or 2 mol% of [LAuCl] and 2 mol% of $AgBF_4$ (entries 4–6) stirring at room temperature in DCM solution.

The published results concerning this transformation show that complexes of classical phosphines such as **77** and **66** give a mixture of products, with **70** predominating.[60] The phosphite-based catalyst **67** is, as expected, even more selective for the formation of this product. In contrast, the very electron rich carbene-based catalyst **76** promotes the selective formation of the [3+4] cycloaddion product **71**.

In our case, using catalysts **47a** and **47b**, we obtained again intermediate results, between phosphines and phosphites. Interestingly, alkyl groups in **47b** increase the electron richness at the gold atom giving result similar to phosphines, whereas the phenyl groups in **47a** favor the back-donation from gold, producing reactivity similar to the one observed in phosphites.

2.2.4.3 Other catalytic application examples

In order to validate the applicability of our ligands, two other gold(I)-catalyzed reactions were tried. The first one was the cycloisomerization of the *ortho*-alkynylated phenyl-1*H*-pyrrole derivatives (Scheme 25).[63] Addition of an electrophilic metal salt or metal complex to a phenylpyrrole which contains an alkyne unit at one of its *ortho*-positions should result in an equilibrium between the substrate **76**[64] and the intermediate **77**. If the latter is trapped by the adjacent aromatic ring, a C–C-bond formation with concomitant release of the catalyst will result. This reaction offers a flexible entry into pyrrolo[1,2-*a*]quinolines **78**.

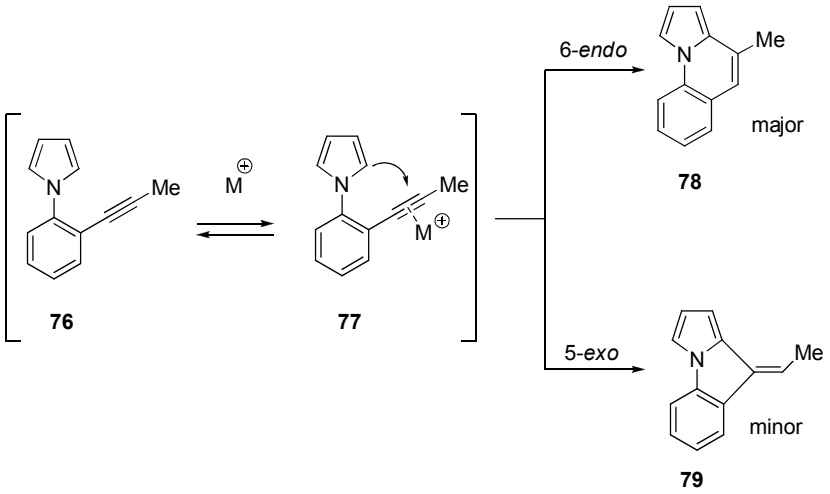

Scheme 25. Mechanistic studies on the cycloisomerization of *ortho*-alkynylated phenylpyrrole **76** catalyzed by transition metal complexes.

4-Methylpyrrolo[1,2-*a*]quinoline **78** was obtained exclusively in excellent yields of 98% and 97% employing only 2 mol% of gold(I) catalyst **47a** or **47b** respectively (Scheme 26).

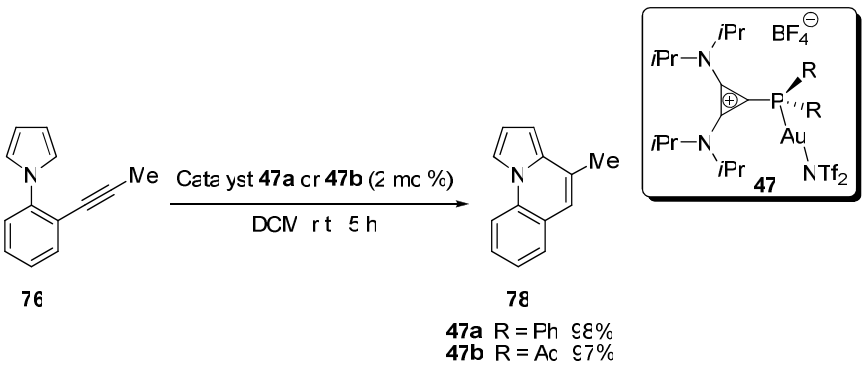

Scheme 26. Cycloisomerization of *ortho*-alkynylated phenylpyrrole **76** catalyzed by gold(I) complexes **47a,b**.

Next, the unprecedented reaction of alcohol **80** in the presence of **46a** was studied (Scheme 27).[65]

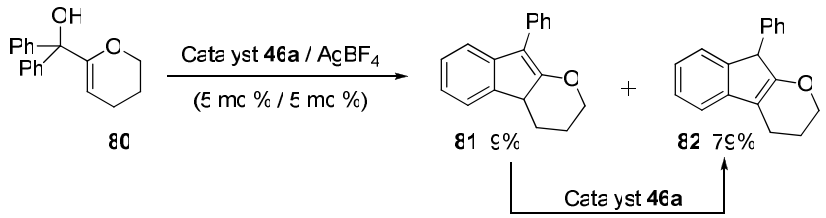

Scheme 27. Transformation of alcohol **80** catalyzed by gold(I) complex **46a**.

Two regioisomeric tetrahydroindeno[2,1-*b*]pyranes **81** and **82** were obtained in 9% and 79% yield respectively. Subsequently, it was found that compound **81** isomerizes in the presence of catalyst to **82**. The mechanism proposed for this conversion includes initial coordination of the gold catalyst to the hydroxyl group (**83**) followed by an elimination that affords carbocation **84** that is stabilized by the conjugation with the aromatic systems (Scheme 28). This carbocation **84** undergoes a *Nazarov*-type cyclization followed by proton elimination to form product **81**.

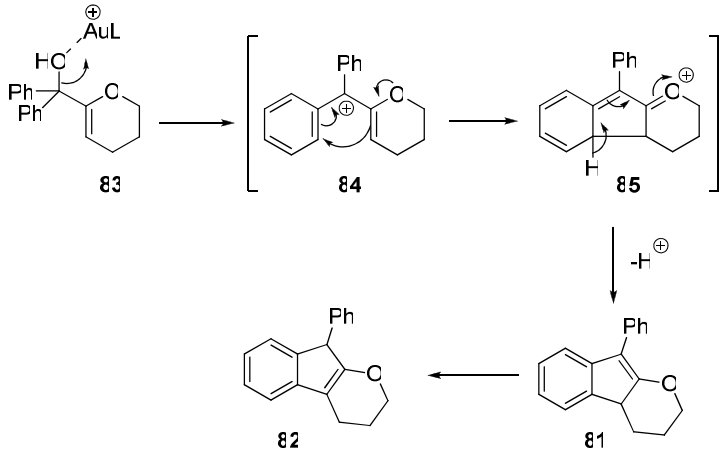

Scheme 28. Proposed mechanism of the formation of tetrahydroindeno[2,1-*b*]pyranes **81** and **82**.

The mechanism of the double bond isomerization in compound **81** forming compound **82** in the presence of gold(I) catalyst has not been studied. We can assume that the isomerization could take place through coordination of the catalyst to the double bond of **81** (Scheme 29) that results in the formation of the carbocation **86**. Protodemetalation from resonance form **86b** produces the final regioisomer **82** and regenerates the gold catalyst.

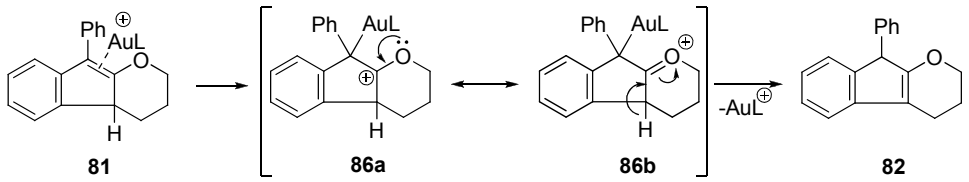

Scheme 29. Feasible mechanism of the compound **81** double bond isomerization forming compound **82**.

The introduction of an extra substituent at the double bond of the pyran ring should lead to the formation of only one reaction product because the isomerization described is no longer possible. In order to prove this hypothesis, we introduced methyl and phenyl substituents in that position.

The corresponding methyl substituted dihydropyran **90a** was prepared from δ-valerolactone **87** (Scheme 30). Alkylation with methyl iodide in the presence of LDA and HMPA in THF solution gave the α-methylated derivative **88** in 81%.[66] Next, reduction with DIBAL in dichloromethane solution gave the corresponding alcohol **89**[66] in excellent yield, which, after dehydratation in the presence of phosphorous pentoxide, gave the expected product **90a** in moderate 52% yield.[67]

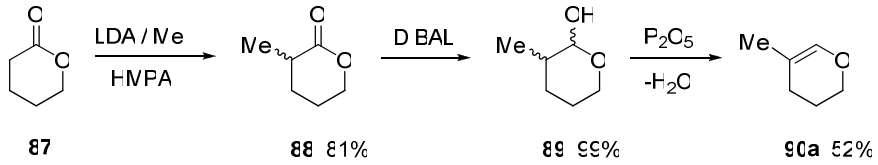

Scheme 30. Synthesis fo 5-methyl-3,4-dihydro-2*H*-pyran **90a**.

The phenyl substituted dihydropyran **90b** was prepared in a different way (Sheme 31) starting by the alkylation of phenylacetic acid **91** with bromochloropropane **92**. After the cyclization of **93** in the presence of DBU,[68] reduction with DIBAL and dehydration afforded the corresponding product **90b** in 72% yield.

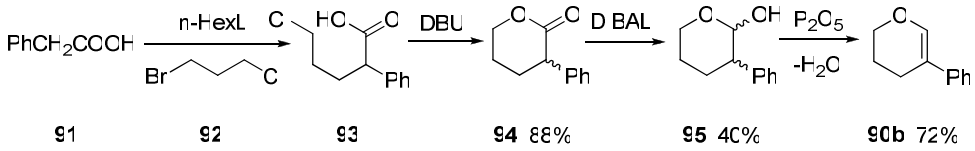

Scheme 31. Synthesis of 5-phenyl-3,4-dihydro-2*H*-pyran **90b**.

The deprotonation of dihydropyrans **90a,b** with *t*-BuLi and addition of benzophenone gave the desired substrates **96a** and **96b** in low but reproducible yields (26% and 24% respectively, Scheme 32).

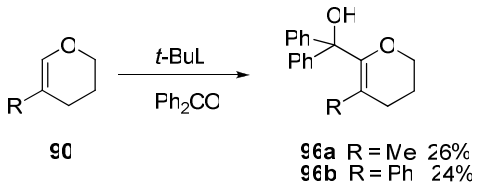

Scheme 32. Synthesis of alcohols **96a,b**.

When substrate **96a** was treated with catalyst **47a,b**, only product **97** was obtained (Scheme 33). Its structure was confirmed by X-ray (Figure 12).

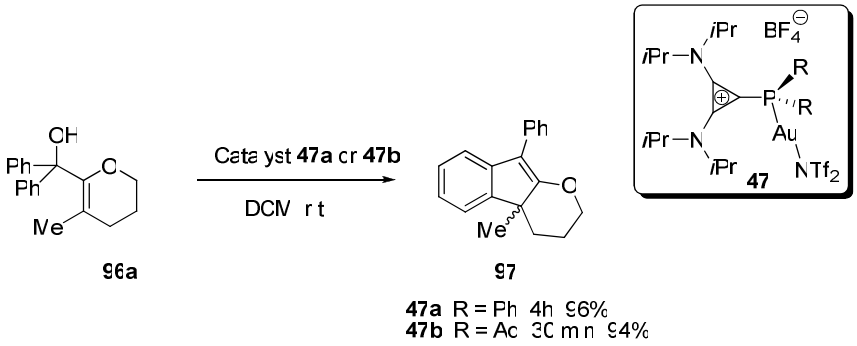

Scheme 33. Transformation of alcohol **96a** catalyzed by gold(I) complex **47a,b**.

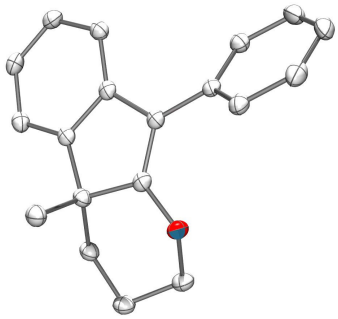

Figure 12. Crystal structure of **97**. Thermal ellipsoids at 50% probability; hydrogen atoms and solvent molecules have been omitted for clarity.

Surprisingly, when alcohol **96b**, which contained a phenyl substituent, was submitted to the same reaction conditions, a mixture of two regioisomeric products **98** and **99** in 1:2 ratio was observed in 82% overall yield (Scheme 34).

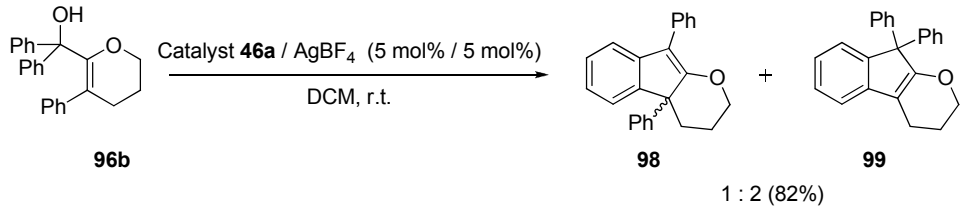

Scheme 34. Transformation of alcohol **96b** catalyzed by gold(I) complex **46a**.

The formation of the two compounds could be explained by the mechanism proposed in Scheme 35. After abstraction of the OH^- moiety by the gold catalyst, the attack of the generated carbocation **100** to the extra phenyl ring takes place *via* intermediate **102** forming the compound **99** after the release of a proton. The cyclization, which occurs through the earlier described mechanism (page 26, Scheme 28) *via* intermediate **101**, leads to the formation of compound **98**.

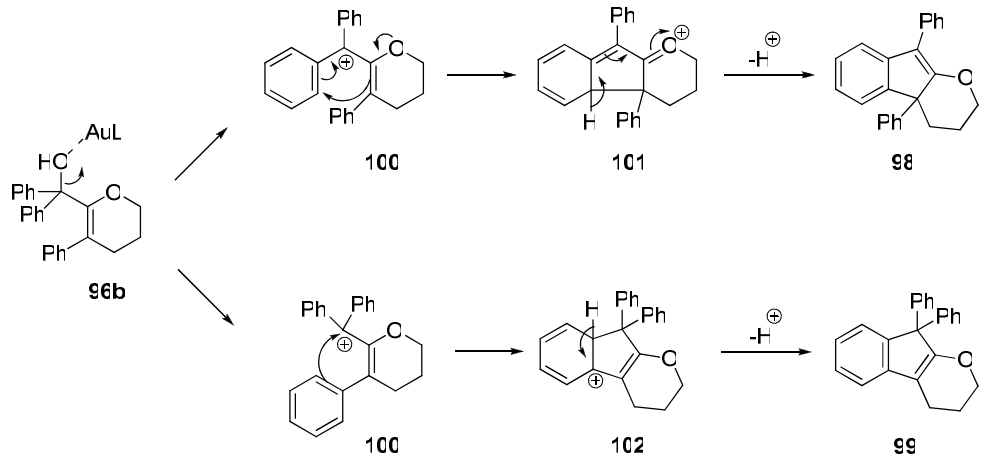

Scheme 35. Proposed mechanism of the formation of tetrahydroindeno[2,1-*b*]pyranes **98** and **99**.

2.2.5. Gold recycling

Once it has been proved that complexes **47a,b** are good catalysts for gold promoted transformations, we decided to make use of the extra positive charge that our ligands bear. Thus, the cycloisomerization of **103**[69] to **104** (Scheme 36) was chosen as a model reaction due to the high solubility of **104** in apolar solvents such as diethyl ether. In contrast, **47a,b** are practically insoluble in this solvent due to the fact that they are salts. Therefore, after full conversion, the DCM used as solvent was removed *in vacuo*, and diethyl ether was added. The catalyst precipitated and could be separated from the product by simple filtration and reused for the next cycle (Figure 13).

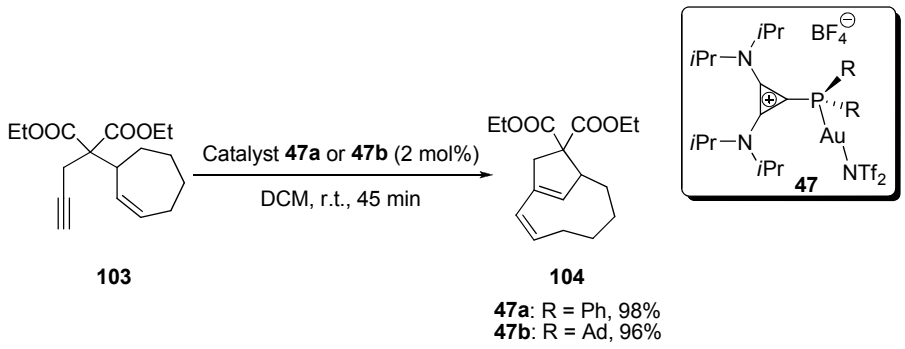

Scheme 36. Cycloisomerization of enyne **103** catalyzed by gold(I) complexes **47a,b**.

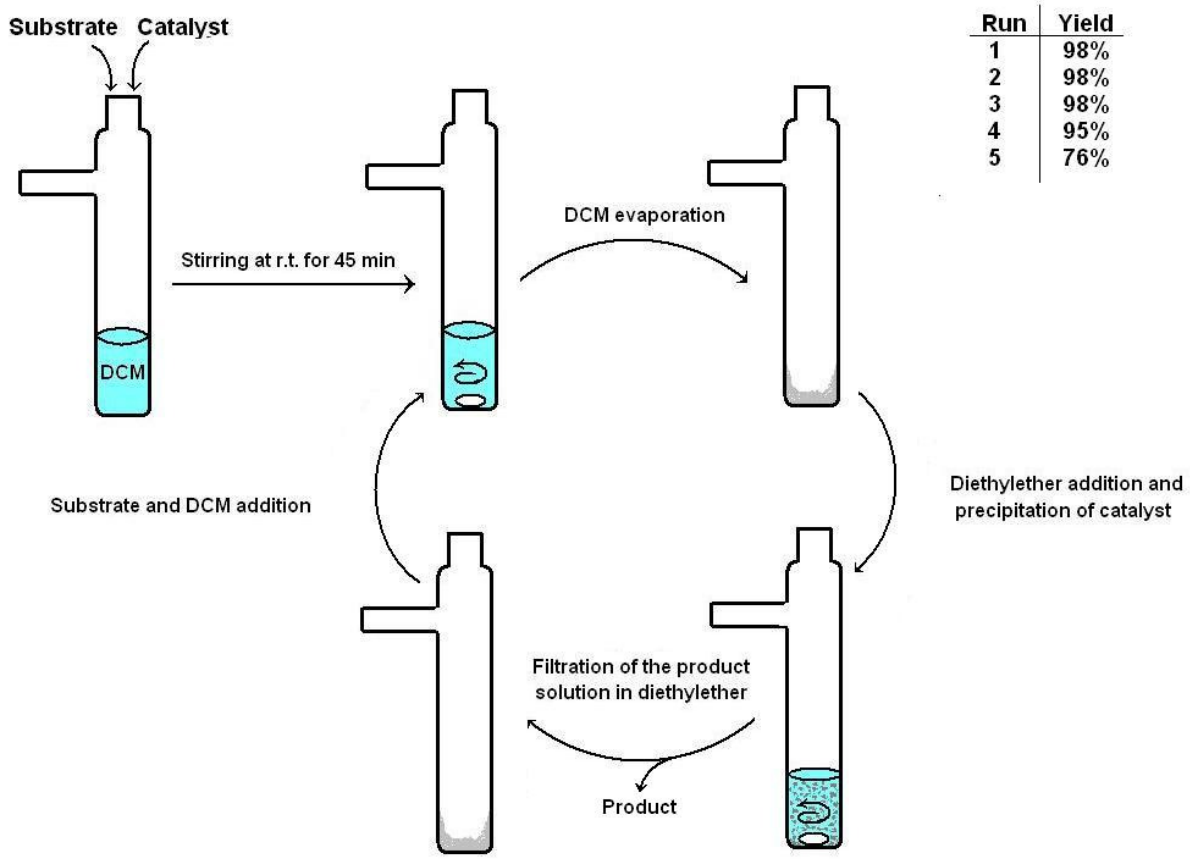

Figure 13. Schematic representation of the recycling process of gold catalyst **47a**.

As shown in Figure 13, the test reaction could be performed up to four times with consistently excellent yields (runs 1–3 yield of isolated product, runs 4, 5 yield determined by gas chromatography).

2.3 Summary II

In conclusion, the synthesis of cyclopropenylidene-stabilized phosphenium adducts has been achieved and their coordination behavior studied. In contrast to other phosphenium-carbene adducts, these compounds exhibit electronic properties that can be ranked in between classical triaryl and trialkyl phosphines and phosphites, even though they carry a global positive charge. Moreover, gold complexes containing these ligands have been synthesized and their practical utility in catalysis was demonstrated in several mechanistically different transformations. Finally, taking advantage of the saline nature of our ligands, the recycling possibilities of the catalysts derived thereof were also explored.

3 Carbene-Stabilized Phosphorus(III)-Centered Dications

3.1 General Introduction

Highly charged cations centered at main group elements are promising reagents for the activation of small molecules.[70] Moreover, their geometries and unusual electronic environments make them interesting targets for theoretical studies as they often have intricate bonding situations not always free of controversy.[71] Therefore, the next challenge of our research after the preparation of monocationic phosphorus(III)-centered compounds was the desing of their dicationic analogues.

The synthesis of few NHC-stabilized dicationic phosphorus(III) species has been achieved by *Andrieu*.[72] Thus, compound **106** could be obtained from the reaction between imidazolium-2-carboxylate **105** and dichlorophenylphosphine (Scheme 37).

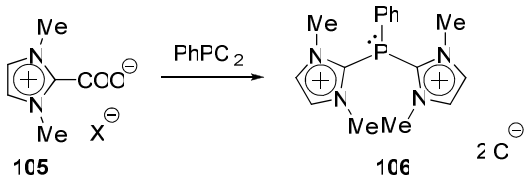

Scheme 37. Preparation of dicationic P(III) species **106**.

It was also found that dicationic adducts of type **112** were not formed in the reaction of free *N*-heterocyclic carbenes **108** (R = Mes, *i*Pr, Et, dipp) with electrophilic phosphorus sources such as PCl_3. Instead, bulky carbenes afford hypervalent (NHC→PCl_3) complexes **107** that do not react further,[73] while less sterically demanding NHCs promote a reductive process which is probably initiated by preferential nucleophilic attack of the carbene at the highly activated Cl-atom, instead of the central P-atom, in intermediates of the general formula $[(NHC)_2PCl]^{2+}$ **112**.[74] Thus, $[(NHC)_2P]^+$ derivatives **109** and **110** are the ultimate result of this transformation (Scheme 38a).

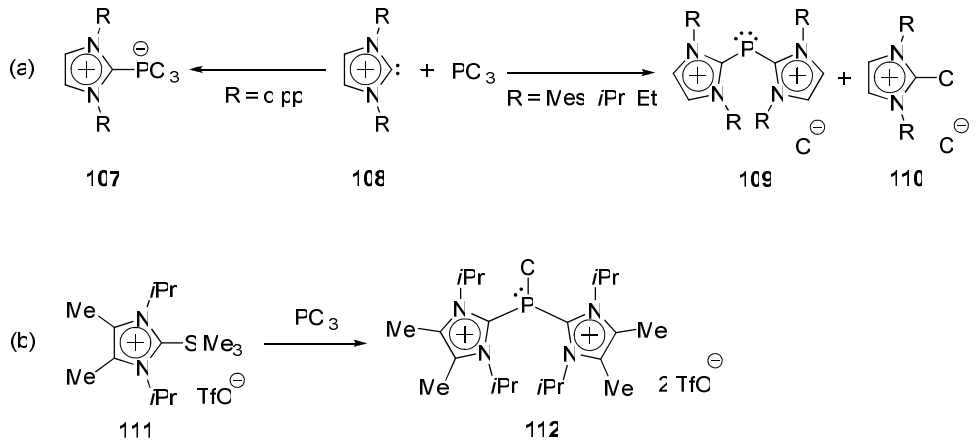

Scheme 38. (a) Reaction of PCl_3 with free carbenes; (b) preparation of dicationic P(III) species *via* "onio-substituent transfer" methodology.

Compound **112** has been synthesized by *Weigand* employing masked carbene **111**.[75] This strategy avoids the undesired reductive pathway (Scheme 38b).

3.2 Results and Discussion

3.2.1 Synthesis

With this idea in mind, we envisaged that the mono-alkyl or aryl substituted phosphanylidenes **113a,b**, prepared by the reaction between chlorocyclopropenium salt **42** and the corresponding monoalkyl- or monoarylphosphine, could serve as convenient starting materials for the preparation of the $[L_2P]^{2+}$ type cations (Scheme 39).

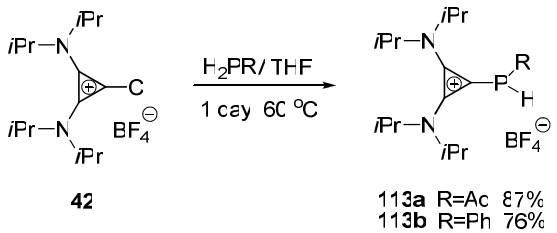

Scheme 39. Synthesis of diisopropylaminocyclopropenylylidene derivatives **113a,b**.

Deprotonation of **113a** and **113b** with KHMDS afforded the very electron rich phosphaalkenes **114a** and **114b**, that were only stable at low temperature (Scheme 40). The most significant changes after this deprotonation were observed in the ^{31}P NMR. While the

resonances of the starting materials **113a** or **113b** appear at -44.8 and -70.9 ppm respectively, they were shifted in the case of **114a** and **114b** to +5.3 and -36.9 ppm respectively.

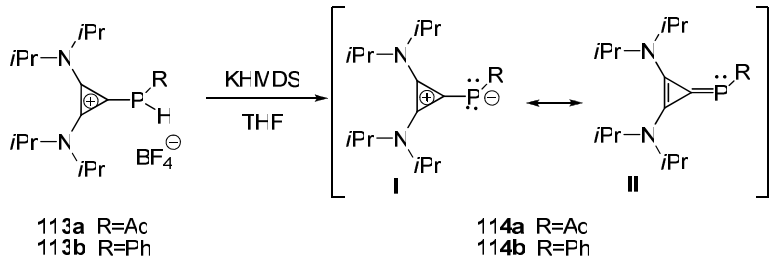

Scheme 40. Deprotonation of **113a,b** with KHMDS.

Further treatment of **114b** with chlorocyclopropenium salt **42** afforded the desired dicationic compound **115** in 69% yield (Scheme 41).

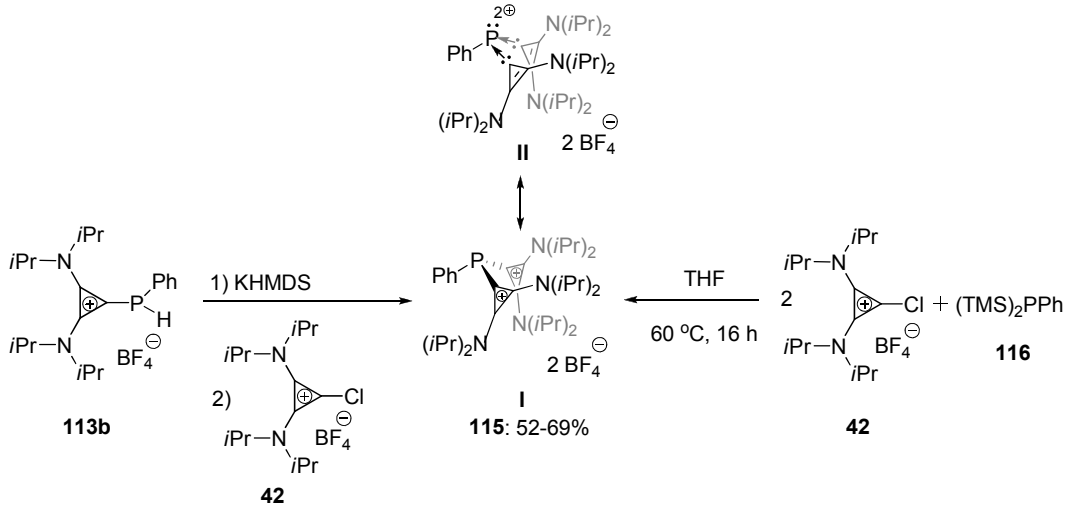

Scheme 41. Synthesis of $[L_2PPh]^{2+}$ type compound **115**.

The same compound **115** could be obtained by the reaction of bis(trimethylsilyl)-phenylphosphine **116** and chlorocyclopropenium salt **42** although in only 52 % yield.[76]

3.2.2 Electronic properties

The formation of dicationic species **115** was indicated by the ^{31}P NMR resonance (δ = -47.9 ppm). This value is comparable to the reported data for imidazolylylidene substituted sister compounds **106** (δ = −50.8 ppm).[77] Moreover, the proposed structure, $[L_2PPh]^{2+}$, has also been confirmed by single X-ray diffraction analysis of **115** (Figure 14).

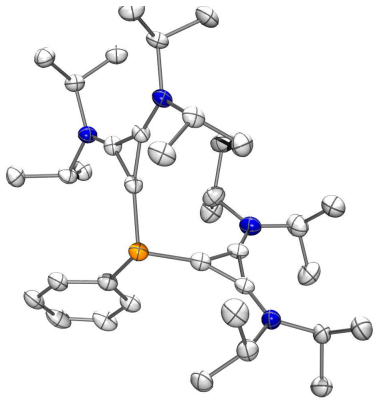

Figure 14. Molecular structure of compound **115** in the solid state. Thermal ellipsoids at 50% probability; tetrafluoroborate counter anions, solvent molecules, and hydrogen atoms have been omitted for clarity.

Two structural parameters are crucial for understanding the electron environment around the phosphorus atom in **115**. The P–C(carbene) bond lengths (both 1.805 Å) are only slightly shorter than those observed in neutral aromatic phosphines but significantly longer than typical P–C double bonds.[78] In addition, the degree of pyramidalization at phosphorus (67.5%) is even higher than that observed for neutral aromatic phosphines (56.7% for PPh_3).[79] Both parameters reveal that back-donation from the phosphorus to the cyclopropenyl rings must be marginal, if any, and suggest retention of a nonbonding electron pair on this atom.

In an attempt to gain insight into the electronic structure of these compounds, density functional calculations at the B3LYP/6-31G* level were performed in cooperation with the theoretical department of the Max Planck Institute for Coal Research under the leadership of Prof. *Thiel*. The optimized structures closely match the experimental crystallographic data (Table 4). In addition, the comparison with classical π-acceptor ligand such as $P(OMe)_3$ and $P(C_6F_5)_3$ is shown.

Table 4: B3LYP/6-31G* results for representative bond lengths (Å) and natural bond orders.

Compounds	Bond length		Bond order	
	P-C(cyclopropyl)	P-C(phenyl)	P-C(cyclopropyl)	P-C(phenyl)
$P(OMe)_3$	1.63[a]	-	0.78[a]	-
$P(C_6F_5)_3$	-	1.86	-	0.890
115 $[L_2PPh]^{2+}$	1.83	1.84	0.909	0.911

[a]P–O(OMe) distance and bond order.

According to natural population analysis, the phosphorus atom in **115** bears a positive charge of +0.88e. This indicates that the real nature of **115** is intermediate between *Lewis*-structures **I** and **II**, (page 35, Scheme 40).

Table 5: Natural population analysis (B3LYP/6-311+G**//6-31G*).

Compounds	Natura charges (e)		Occupancy
	Q(P)	q(substituent)	LP (P)
$P(OMe)_3$	1.53	-0.49[a]	1.96
$P(C_6F_5)_3$	0.93	-0.31[b]	1.90
115 $[L_2PPh]^{2+}$	0.88	0.66	1.87

[a]Sum of natural charges of –OMe group; [b]Sum of natural charges of $–C_6F_5$ group.

Moreover, in line with our analysis of the crystal structure, the *Wiberg* bond index values (0.909 for each C–P bond) support the absence of back-donation from phosphorus to the carbene moieties.

Analysis of the frontier orbitals shows that the HOMO has considerable electron density on the phosphorus and an orbital occupancy of 1.87e (Figure 15). This should provide some *Lewis*-base reactivity to this cation despite the global +2 positive charge that it bears.

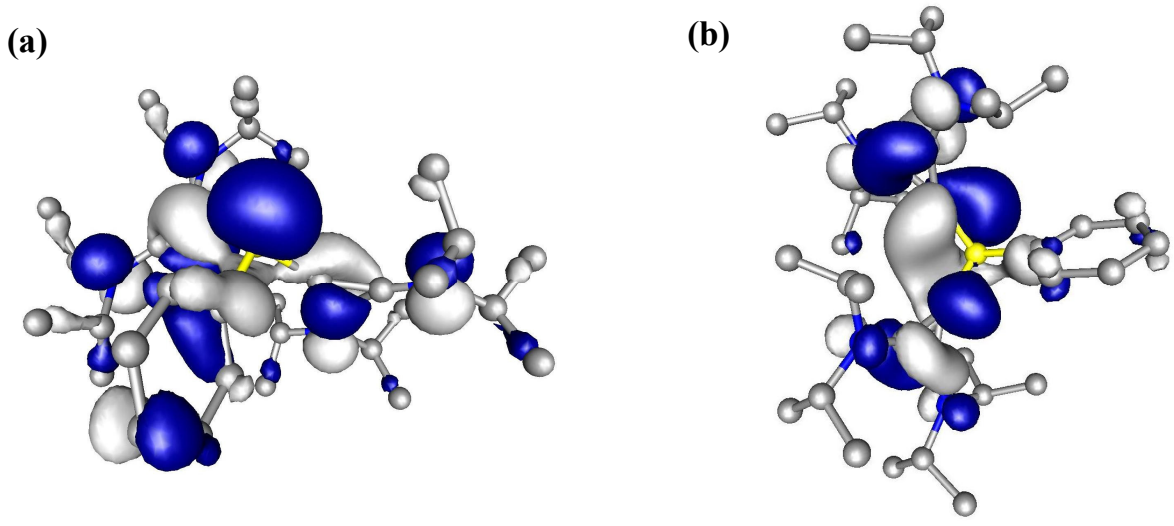

Figure 15. Representation of the calculated HOMO (left) and LUMO (right) for **115**.

In addition, very strong π-acceptor properties must be conferred by the low-lying LUMO if we compare with $P(OMe)_3$ and $P(C_6F_5)_3$ (Table 6).

Table 6: Molecular orbital energies (B3LYP/6-311+G**//6-31G*).

Compounds	Orbital energies (eV)	
	HOMO	LUMO
$P(OMe)_3$	-6.97	-0.03
$P(C_6F_5)_3$	-7.56	-2.44
115 $[L_2PPh]^{2+}$	-11.50	-6.79

3.2.3 Coordination properties

Based on the conclusions from the theoretical analysis of **115** we were expecting that the dication could successfully serve as a strong π-acceptor ligand. Thus, **115** was submitted to reaction with chloro(dimethylsulfide)gold(I), potassium tetrachloroplatinate(II) or tetrachloropalladate(II) (Scheme 42).

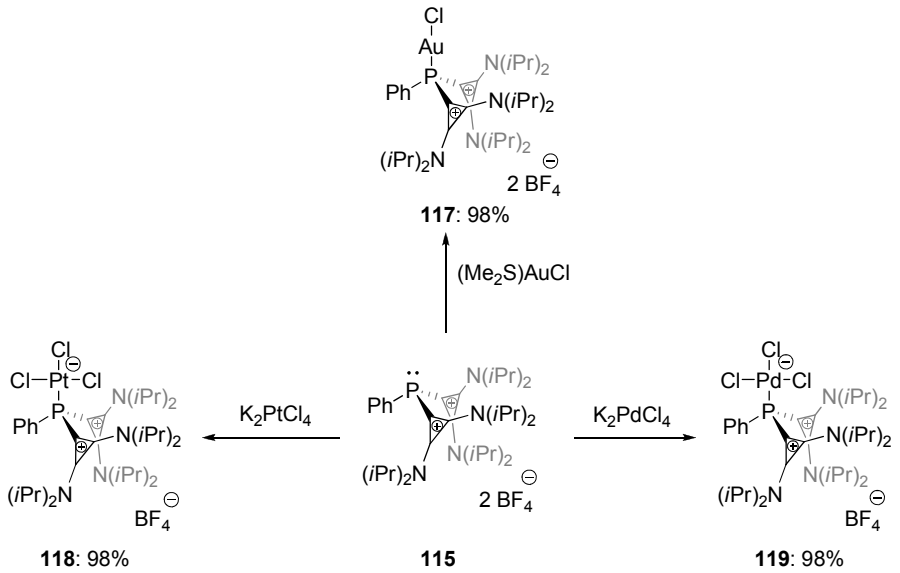

Scheme 42. Synthesis of gold, platinum and palladium complexes **117-119**.

Compound **115** reacted with all three metallic salts affording complexes **117**, **118** and **119** as white or slightly orange solids in excellent yield (98%) in each case. Importantly, the coordination of phosphorus to the platinum centre in complex **118** was confirmed by a new resonance in the ^{31}P NMR (δ = -21.2 ppm, $^{1}J_{P\text{-}Pt}$ = 1994.8 Hz) and ultimately by X-ray diffraction (Figure 16).

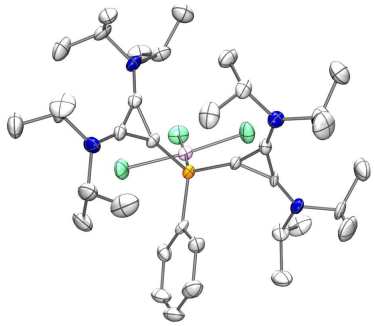

Figure 16. Molecular structure of compound **118** in the solid state. Thermal ellipsoids at 50% probability; hydrogen atoms, tetrafluoroborate counter anion and solvent molecules have been omitted for clarity.

In order to generate the required vacant coordination site on Au for the application of complex **117** in catalysis, it is necessary the abstraction the chloride and replacement by a non-coordinating anion. The use of the bis(trifluoromethanesulfonyl)imidate moiety has been suggested as a convenient way to get active and at the same time stable catalysts.

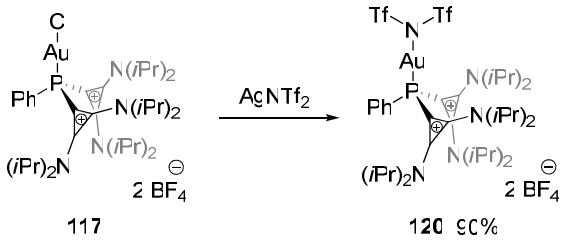

117 120 90%

Scheme 43. Synthesis of the compex **120**.

Making the same manipulation with **117**, the corresponding complex **120** was obtained in 90% yield (Scheme 43). Unfortunately, the stability of the **120** was low and it underwent slow decomposition in DCM solution at room temperature.

Despite the reactivity of **115** towards gold, platinum and palladium, the rhodium complexes (using $[Rh(cod)Cl]_2$ and $[Rh(CO)_2Cl]_2$) were never obtained. This created some difficulties in the evaluation of the donor ability of $[L_2PPh]^{2+}$ type ligands by measuring IR-stretching frequencies of the carbonyl group. However, a qualitative idea of their donor properties can be obtained by screening reactions that dramatically depend on the ligand electronic properties.

3.2.4 Application in catalysis

3.2.4.1 [2+4] *vs* [3+4] Cycloaddition of allene-dienes

The gold(I)-catalyzed cyclization of allene-diene **68** discussed in the second chapter (see page 23 and Scheme 44) was used again as a practical tool to estimate the donor ability of **115**, because the evolution of intermediate **69** depends on the global electron density at the gold atom.

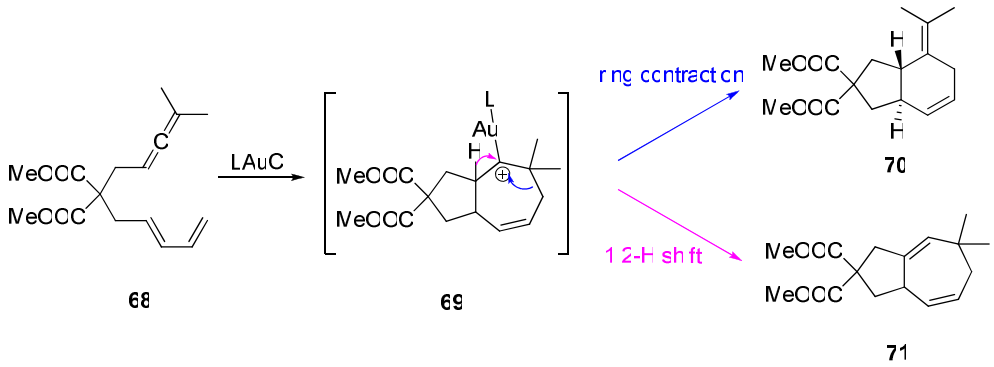

Scheme 44. Effect of the ligands with different π acceptor properties on the gold-catalyzed cyclization of allene-diene **68**.

The cyclization of **68** catalyzed by 2 mol% of catalyst **117** and 2 mol% of $AgBF_4$ gave a mixture of **70** and **71** in 86% overall yield with a **70:71** ratio of 97:3 (determined by ^1H NMR). This result confirms our predictions about the strong π-acceptor behavior of this ligand. By comparison, the **70:71** ratio in the case of phosphites (L = $(PhO)_3P$, see page 24) was also 97:3. Moreover, this reaction is a successful example for the catalytic application of the double charged compounds as ligands. The stronger π-acidity of $[L_2PPh]^{2+}$ compared to $[LPR_2]^+$ is now clear and might allow to find new specific applications for this ligand in catalysis.[53]

3.2.4.2 Cycloisomerization of 1,6-enynes

Enynes are the most-widely studied substrate class in the field of Au- and Pt-catalyzed cycloisomerization. Especially in the cycloisomerization of 1,6-enynes platinum catalysts

have been successfully employed. The mechanistic considerations of the possible pathways of that transformation are shown in Scheme 45.[80] Specifically, when arylated enynes (R = Ph) are used as substrates, the cycloizomerization leads to the formation of cyclobutenes because of the extra stabilization of carbocation **B** due to the aromatic group. Interestingly, this reaction allows the formation of highly strained cyclobutene derivatives in a single operation that are difficult to prepare otherwise. Conversely, in the case of non-substituted alkynes, evolution through intermediate **A** predominates and the formation of 1,3-diene products is observed.

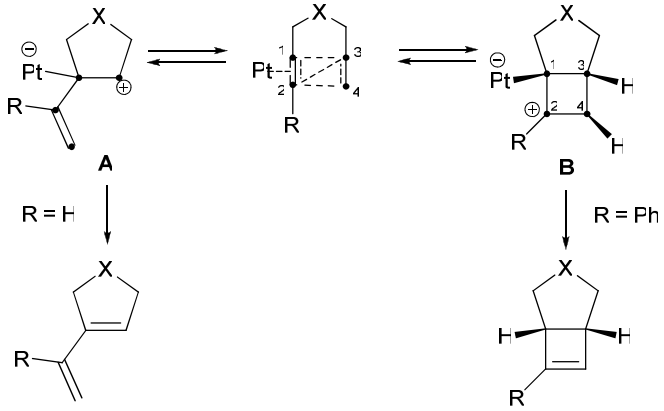

Scheme 45. Mechanistic considerations of the platinum-catalyzed cycloisomerization of 1,6-enynes.

It is known that this and many other Pt(II)-catalyzed reactions are accelerated in presence of CO.[81] Thus, enhancing *Lewis*-acidity of the platinum catalyst by coordination of π-acceptor ligands provides a good strategy to facilitate this reaction. Therefore, this transformation seems appropriate to test our π-acceptor $[L_2PPh]^{2+}$ ligand.

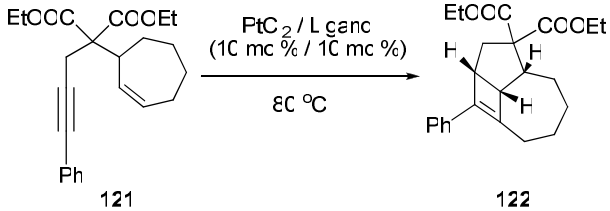

Scheme 46. Platinum-catalyzed cycloisomerization of enyne **121**.

The necessary substrate **121** was prepared by palladium-catalyzed *Sonogashira* coupling from the enyne **103**[82] and iodobenzene in presence of $PdCl_2(Ph_3P)_2$, CuI and Et_3N in 70% yield (Scheme 47).[81]

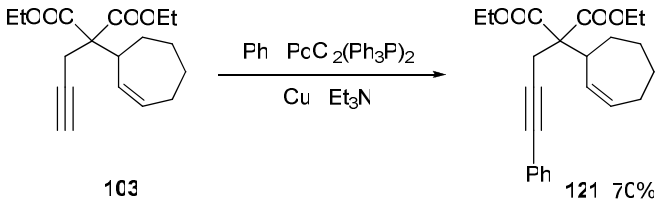

Scheme 47. *Sonogashira* reaction of enyne **103**.

As depicted in Scheme 46 we have pursued this cycloisomerization reaction using 10 mol% of $PtCl_2$ and 10 mol% of ligand **115** in DCE at 80 °C. Although this reaction was described in toluene, we have replaced toluene by dichloroethane in order to improve the solubility of our cationic ligands while still being able to heat to the same temperature. Under the indicated conditions, we obtained complete conversion after 3 hours and an excellent isolated yield of 95%.

The conversion of **121** in **122** was screened by GC-MS, and the results are summarized in Figure 17. In the absence of any ligand a slow reaction was observed that did not reach full conversion even after 24 h. The use of the carbon monoxide (1 atm), clearly improved the reaction rate. The same behavior was observed for Ph_3P and $(C_6F_5)_3P$. Triphenylphosphite, another typical π-acceptor ligand, performed even better reaching a conversion of 97% after 6 h. Interestingly, our cationic ligands **43a** and **115** showed excellent behavior due to their π-acceptor properties, giving 88% and 95% yield, respectively, in only 3 hours (Figure 17).

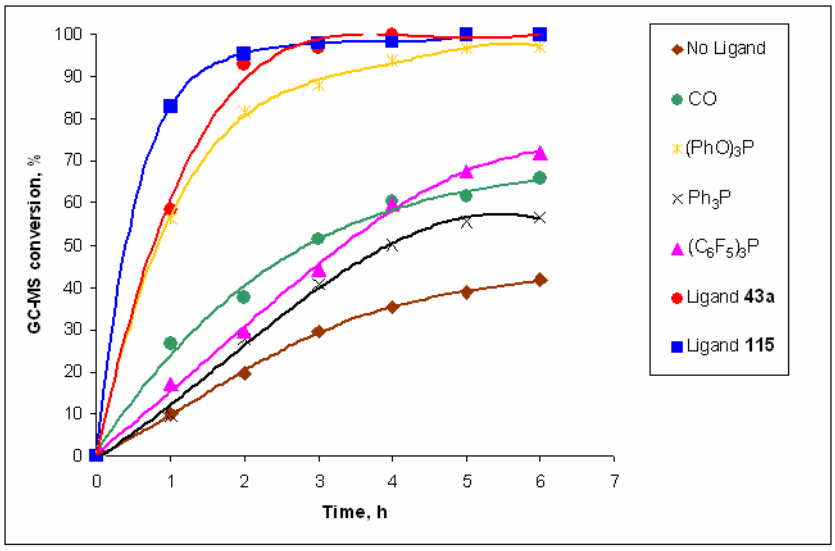

Ligand	Yield
CO	76%
$(PhO)_3P$	97%
Ph_3P	76%
$(C_6F_5)_3P$	95%
43a	88%
115	95%
-	- %

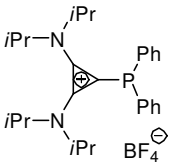

43a

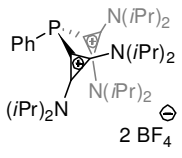

115

Figure 17. Comparison of $[LPPh_2]^+$ and $[L_2PPh]^{2+}$ type ligands properties with a commonly used classical ligands.

Under the previously described conditions, the related substrate **123**[83] containing a cyclohexenyl instead of the cycloheptenyl of **121**, also showed good reactivity, affording **124** in excellent yield (Scheme 48).

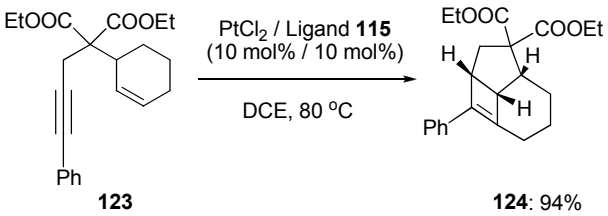

Scheme 48. Platinum-catalyzed cycloisomerization of enyne **123**.

3.3 Trapping Intermediate 114a

During the synthesis of compound **115**, the formation of phosphaalkenes **114a** and **114b** was proposed. Unfortunately, we were not able to isolate them; therefore we tried to trap them by reaction with different electrophiles. The presence of two non-shared electron pairs on the phosphorus atom of **114** can be postulated and therefore it might react with up to two *Lewis*-acids. To check this hypothesis, adamantyl phosphanylidene **113a** was deprotonated with potassium hexamethyldisilazane and treated with two equivalents of chloro(dimethylsulfide)-gold(I) or borane-tetrahydrofuran complex. Thus, we were able to obtain the corresponding adducts **125** and **126** in 99% and 39% yields respectively (Scheme 49). These results support our assumption about the existence of two lone electron pairs on phosphorus.

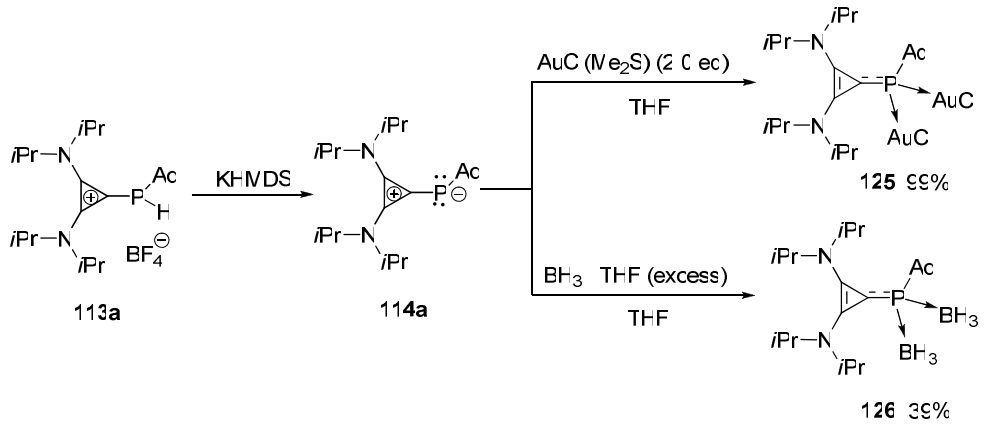

Scheme 49. Synthesis of gold and boron adducts **125** and **126**.

Additionally, the structure of the compound **126** was confirmed by X-ray diffraction analysis (see page 189, Appendix 7.2.16).

3.4 Summary III

In summary, an efficient synthesis of the carbene stabilized $[L_2PPh]^{2+}$ cations has been introduced by the deprotonation of monophenyl-substituted phosphanylidene **113b** and further reaction with the corresponding chlorocyclopropenium salt **42**. Despite the presence of two positive charges, the coordination ability of **115** to gold, platinum and palladium has been demonstrated. In these complexes $[L_2PPh]^{2+}$ ligands showed strong π-acceptor character that we used in Pt(II) and Au(I)-catalyzed reactions, improving the already reported catalytic systems in terms of reactivity.

4 Carbene-Stabilized Phosphorus(III)-Centered Trications

4.1 General Introduction

The synthesis of carbene-stabilized phosphorus(III)-centered trications was defined as our next task. As previously discussed, many compounds based on p-block elements can promote transformations that traditionally were reserved to transition metals (see page 33). In addition, their sometimes unusual electronic properties and geometry make them interesting targets for investigation. Herein we present our results associated with the synthesis and applications of $[L_3P]^{3+}$ trications.

There are only three reported examples of $[L_3P]^{3+}$ trications stabilized by *N*-based ligands. For example, 4-dimethyl-aminopyridine is able to form the tris-pyridino-substituted phosphorus(III) compounds of type **129** containing three positive charges.[84] Scheme 50 resumes it synthesis and the quinuclidine analogue.[85]

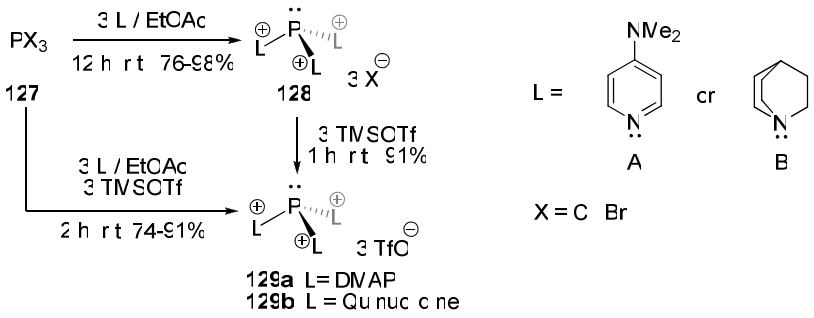

Scheme 50. Synthesis of *N*-based $[L_3P]^{3+}$ cations **129a,b**.

Attempts to carry out the same reaction with a stronger neutral base such as 1,5-diaza-bicyclo[4.3.0]non-5-ene (DBN) **130** surprisingly led to a complicated mixture.[86] In order to overcome this problem, compound **130** was converted into the cationic silyl protected salt **131** by treatment with trimethylsilyl triflate (Scheme 51). It was proposed that the intrinsic reactivity of trimethylsilyl groups towards halogens should improve the reaction rate and purity of the products. This methodology to obtain highly charged base-stabilized cations has been named the "onio-substituent transfer" reaction. Thus, trionio-substituted phosphine **132** was obtained in 40 % yield by treating PCl_3 with three equivalents of the silyl derivative **131**.

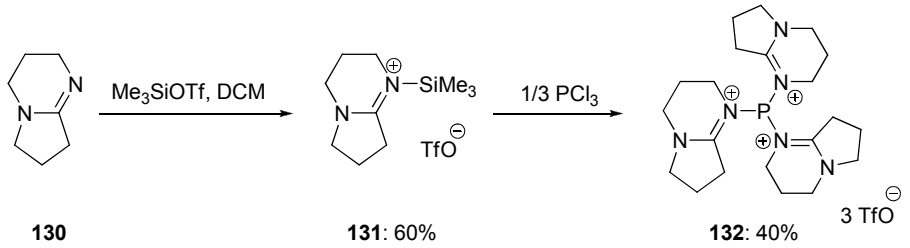

130 **131**: 60% **132**: 40%

Scheme 51. Synthesis of *N*-based $[L_3P]^{3+}$ cation **132**.

It is worth noting that, up to now, no solid-state structural analysis of such a species has been reported. Their connectivities were thus determined only on the basis of spectroscopic and chemical data. In addition, all obtained compounds were stabilized by *N*-based ligands.

The outstanding donor properties exhibited by *N*-heterocyclic carbenes (NHCs) have rendered them privileged ligands for the stabilization of metal complexes and highly electrophilic species.[87] The synthesis of mono- and dicationic P(III) species has been accomplished already using these ligands. However, in the case of P^{3+} centers no success has been achieved.

It is our objective in this section to find a synthesis for these elusive $[L_3P]^{3+}$ type cations. Our strategy consists in the use of an alternative synthetic approach, based on the use of an unprecedented "reverse electron demand" onio-substituent transfer strategy where an umpolung of reagents has been achieved by introduction of trimethylsilyl groups as substituents on the phosphorus atom and a chloride as the substituent on the carbene precursor.

4.2 Results and Discussion

4.2.1 Synthesis

To put this concept into practice, 1-chlorocyclopropenium cations were deliberately chosen as carbene precursors instead of the more common chloroimidazolium salts due to the simultaneous convergence of three beneficial factors: (a) an enhanced tendency to undergo nucleophilic attack at the chlorinated carbon;[88] (b) the smaller steric demand derived from a carbene embedded in a three membered ring that facilitates the coordination of several of these ligands to the same central atom,[89] and (c) the stronger σ-donor and weaker π-acceptor

properties of cyclopropenylidenes as compared with NHCs. Note that the net donation from the carbene ligand must compensate for the continuous increase of formal positive charge on the phosphorus atom in order to allow the consecutive nucleophilic substitution process to take place.[90]

Thus, by gentle heating of a mixture of the 1-chloro-2,3-bis(diisopropylamino)cyclopropenium salt **42** or **133** with $P(SiMe_3)_3$ in THF, the desired P(III)-centered trications **134a** and **134b** were isolated for the first time as white solids in moderate yields (Scheme 52).[91]

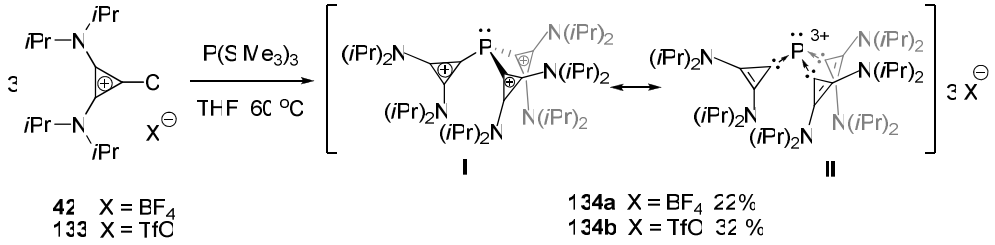

Scheme 52. Synthesis of $[L_3P]^{+3}$ cations **134a,b**.

Surprisingly, the use of "umpoled" reaction partners, the corresponding TMS-substituted compound **136**[92] and PCl_3, gave no reaction under the same conditions (Scheme 53).

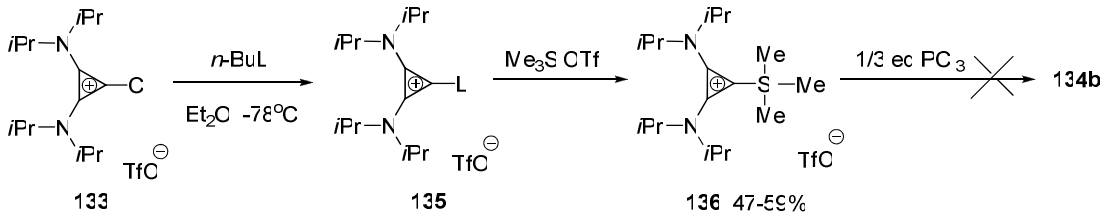

Scheme 53. Synthesis of $[L_3P]^{+3}$ cation **134b**.

An alternative method to synthesize $[L_3P]^{3+}$ type compounds was also attempted. After Li/Cl exchange with BuLi in **133**, the lithiated species was reacted with phosphorus trichloride to afford the corresponding compound **134b** (Scheme 54).[93] This strategy allowed us to increase the yield of this reaction from 32% to 45%.

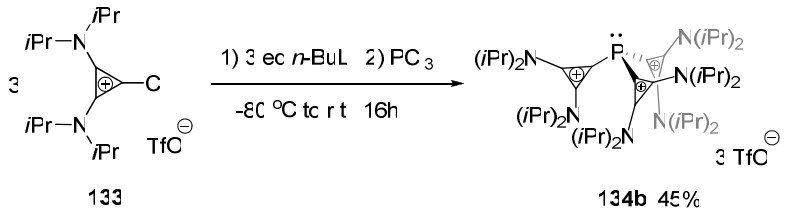

Scheme 54. Alternative synthesis of the compound **134b**.

One explanation for the low yields in the preparation of $[L_3P]^{3+}$ type cations could be steric hindrance. Therefore, the reduction of steric demand of the carbenes moieties was carried out by exchanging the *iso*-propyl groups for methyl groups on the nitrogen atoms. Thus, the chlorocyclopropenium cation **140** was prepared following reported procedures (Scheme 55).[94]

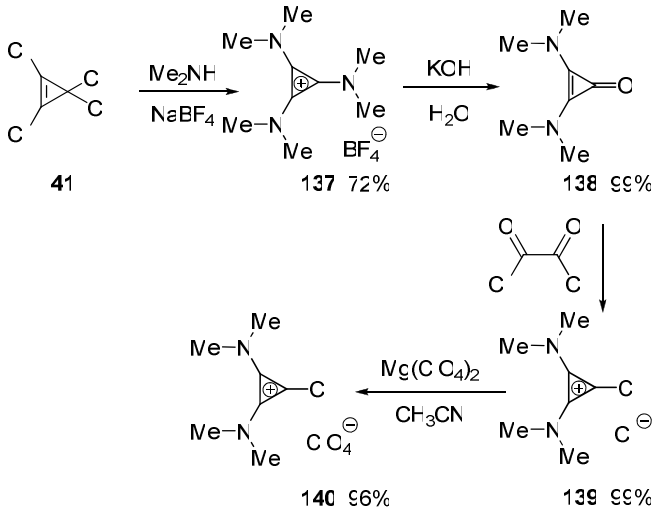

Scheme 55. Synthesis of the chlorocyclopropenium salt **140**.

Reaction of this salt with tris(trimethylsilyl)phosphine afforded the desired product **141** in 68% yield. This improved yield confirms our hypothesis about the influence of the steric factors on this reaction (Scheme 56).

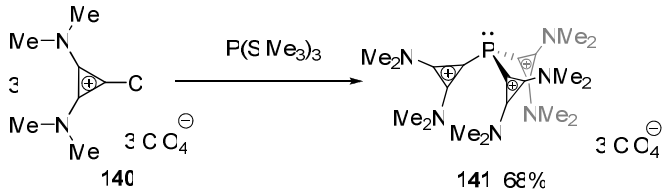

Scheme 56. Synthesis of the compound **141**.

The tricationic character of **134a**, **134b** and **141** was suggested by the increased shielding of the P center (^{31}P NMR resonances at δ = −76.5, −76.4, and −93.5 ppm, respectively) when compared with the data reported for dicationic bis-imidazolylidene substituted sister compounds **106** (δ = −50.8 ppm).[95] Subsequently, single crystal X-ray diffraction analysis unambiguously confirmed the proposed connectivity for the cationic part of **134a** (Figure 18).

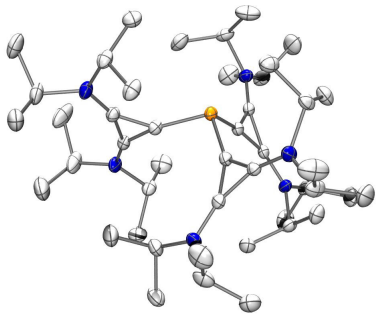

Figure 18. Molecular structure of compound **134a** in the solid state. Thermal ellipsoids at 50% probability; tetrafluoroborate counterions, solvent molecules, and hydrogen atoms have been omitted for clarity.

As in the case of $[L_2PPh]^{2+}$ **115**, the P–C(carbene) bond distances in **134a** are only slightly shorter (1.787, 1.790 and 1.796 Å) than those observed in neutral aromatic phosphines but significantly longer than typical P–C double bonds.[78] The pyramidalization degree at phosphorus (55.4%) is perfectly comparable to those observed for neutral aromatic phosphines (56.7% for PPh_3).[79]

Some interesting conclusions could also be made by exploring the NMR spectra of **115** and **134a**. In the ^{1}H NMR spectrum of **115** the methyl groups signals appear as four doublets (1.21, 1.25, 1.38 and 1.44 ppm, J = 6.9 Hz for each case, 4 × 12H), indicating their nonequivalence (Figure 19). In the ^{13}C NMR spectrum we observed six signals corresponding to the methyl groups (21.2, 21.5, 21.5, 21.6, 21.6 and 21.7 ppm) (Figure 20).

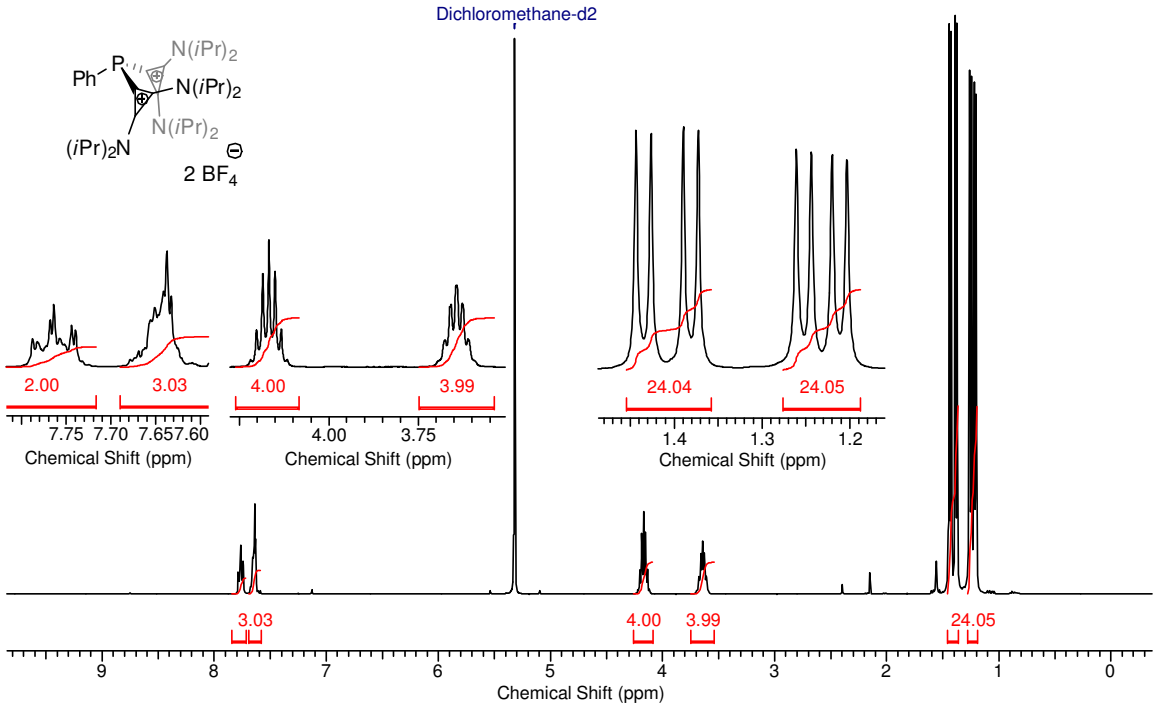

Figure 19. ^{1}H NMR of **115** in CD_2Cl_2.

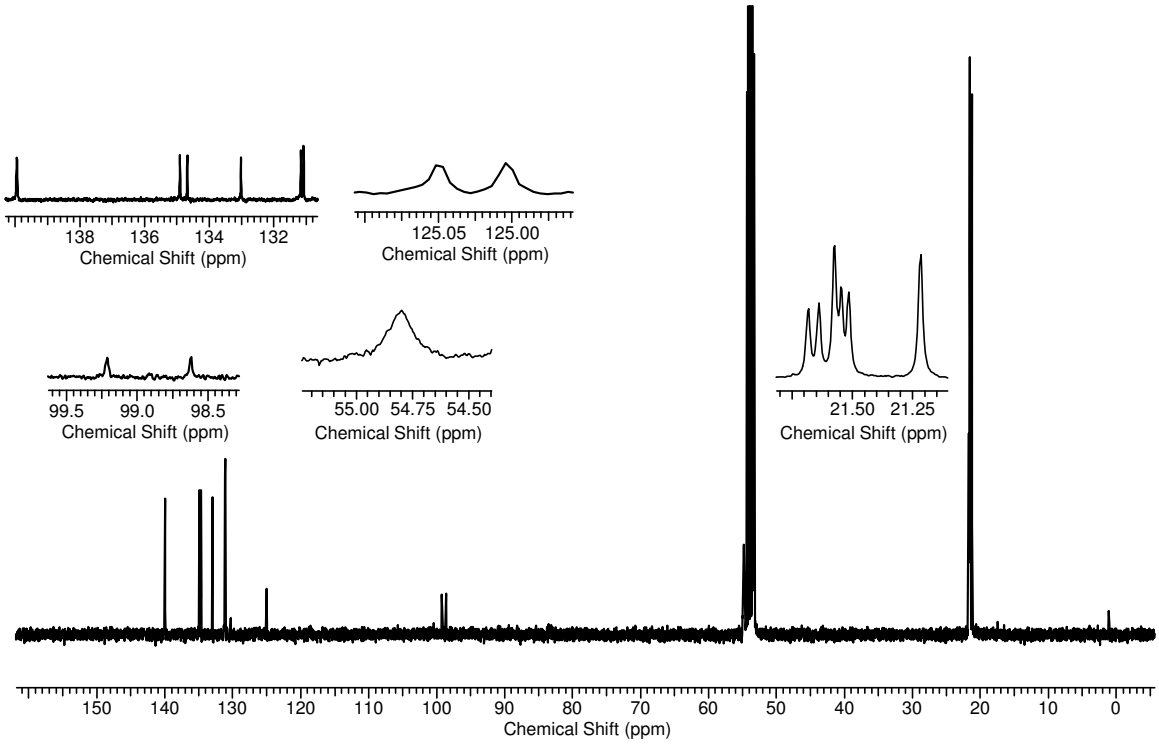

Figure 20. ^{13}C NMR of **115** in CD_2Cl_2.

However, in the ^{1}H NMR spectrum of **134a** (Figure 21) the methyl groups signals appear only as two doublets (1.40 and 1.46 ppm, J = 6.9 Hz in both cases, 2 × 36H). The total number of methyl group signals was also reduced by half in the ^{13}C NMR spectrum (21.4, 21.9 and

22.0 ppm, Figure 22). An increase of the number of nonequivalent methyl groups in **115** may be indicative of a higher phosphorus inversion barrier than in the triple charged salt **134a**.

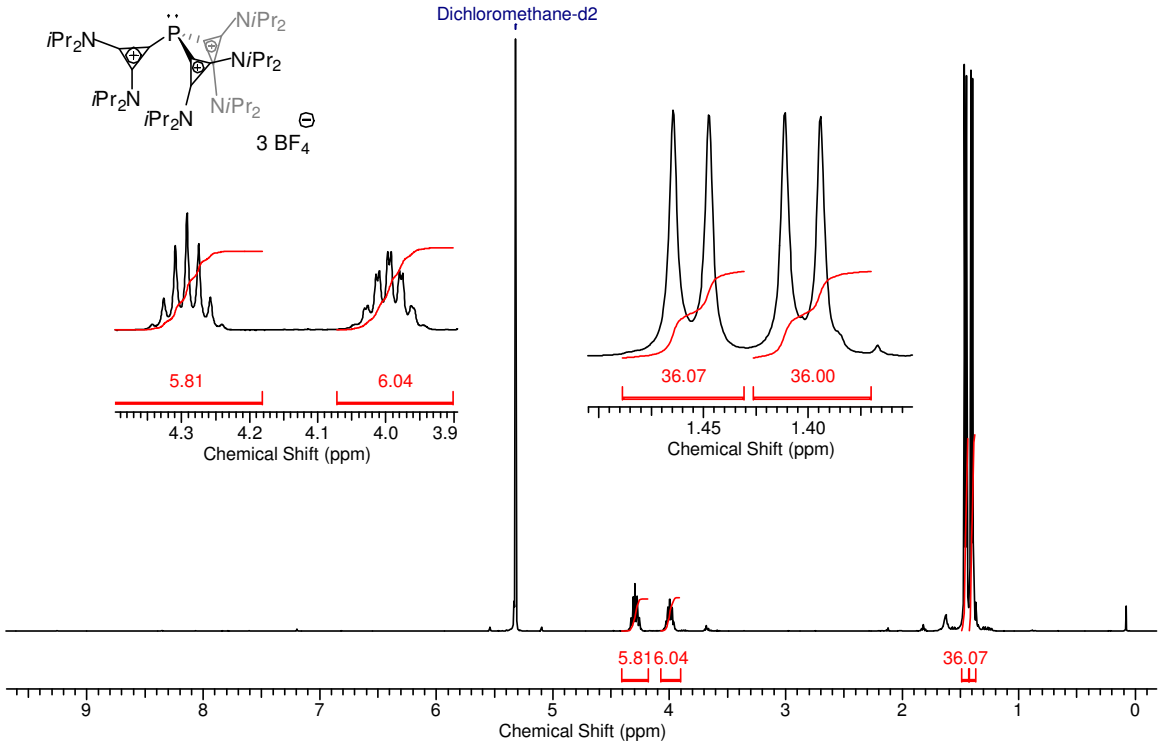

Figure 21. ^{1}H NMR of **134a** in CD_2Cl_2.

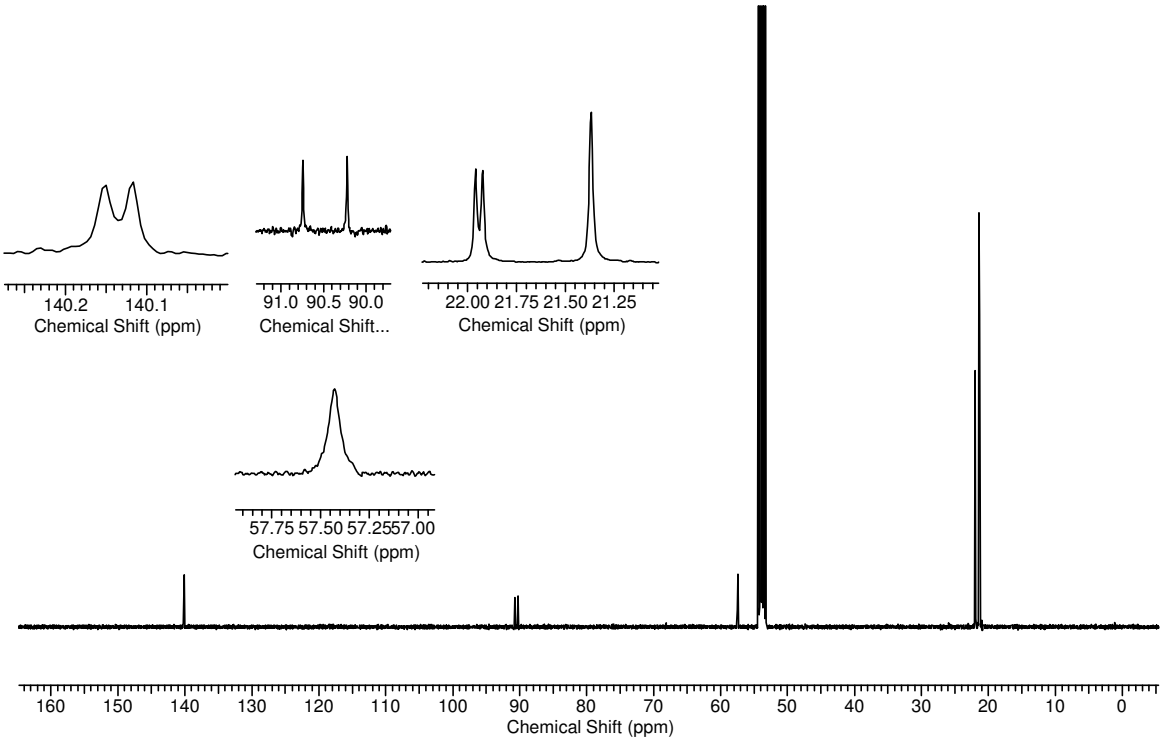

Figure 22: ^{13}C NMR of **134a** in CD_2Cl_2.

4.2.2 Electronic properties

The calculated bond order between phosphorus and carbon in these structures is 0.919. According to natural population analysis, the phosphorus atom in **134a** bears a positive charge of (+0.88e). The optimized DTF structures closely match the experimental ones: the calculated bond length between phosphorus atom and carbon atom of cyclopropenyl moiety in the compound **134a** (1.82 Å) are in agreement with the results obtained from X-ray diffraction analysis (1.787, 1.7901 and 1.7964 Å for each C-P bond respectively).

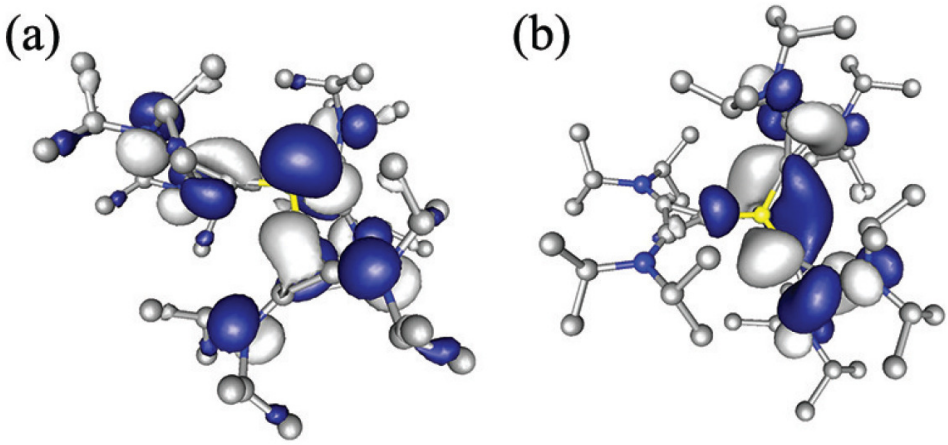

Figure 23. Representation of the calculated HOMO (left) and LUMO (right) for **134a**.

Inspection of the frontier orbitals shows that the HOMO has substantial lone pair character at phosphorus, with a natural orbital occupancy of 1.84e (Figure 23). This might provide some *Lewis*-base reactivity to this cation in spite of the global +3 charge that it formally bears. More importantly, the very low-lying LUMO is expected to confer remarkably strong π-acceptor properties (Figure 24).

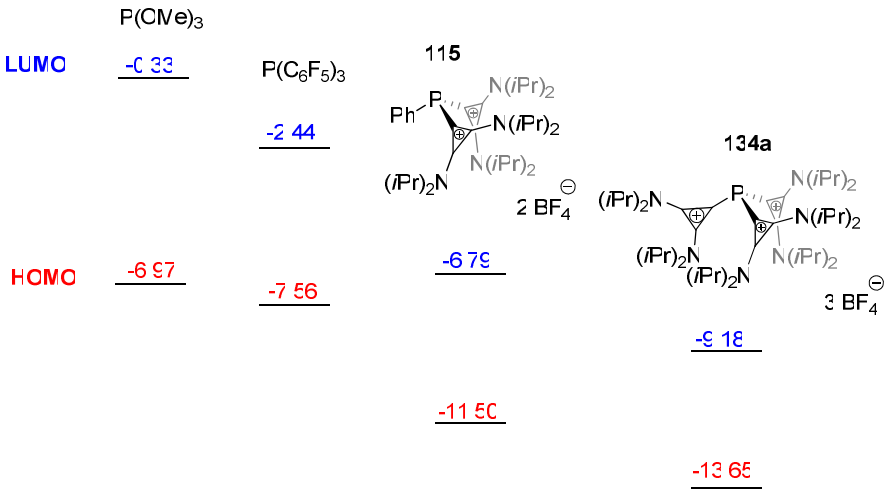

Figure 24. Molecular orbital energies (B3LYP/6-311+G**//6-31G*).

4.2.3 Coordination properties

Encouraged by the distinctive electronic properties, electron-rich metal-containing moieties able to engage in gentle back-donation were chosen in an attempt to ascertain whether these trications could actually be employed as ligands. Thus, when **141** was reacted with K_2PdCl_4 and K_2PtCl_4 in acetonitrile, complexes **142** and **143** were efficiently obtained in 92% and 87% yields respectively (Scheme 57). The triple charged compound **134a** reacted neither with the Pd nor Pt metallic sources. This lack of reactivity might be attributable to steric factors, because the smaller compound **141**, also with three positive charges, reacted efficiently under the same conditions.

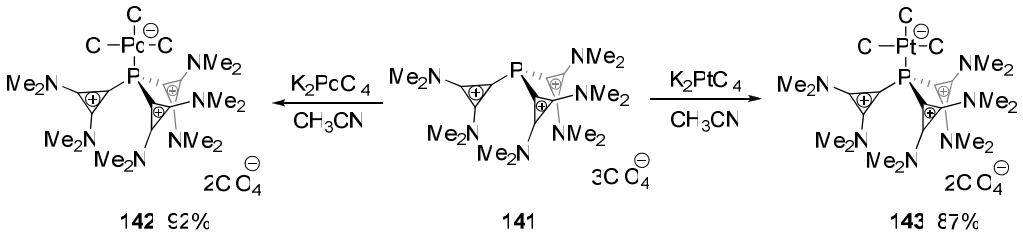

Scheme 57. Formation of Pd and Pt complexes **142** and **143**.

The coordination of phosphorus to Pd and Pt in **142** and **143** was primarily suggested by the appearance of new resonances in the ^{31}P NMR spectra (δ = −46.1 and −62.4 ppm, respectively). Especially informative are the satellite signals in **143** ($^1J_{P-Pt}$= 2033 Hz) that are indicative of Pt–P bond formation. Ultimately, the structure of **143** was confirmed by X-ray diffraction analysis (Figure 25).

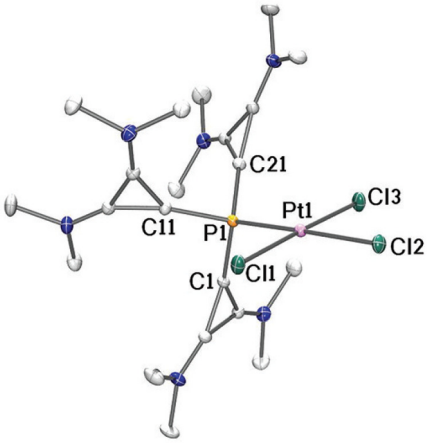

Figure 25. Molecular structure of compound **143** in the solid state. Thermal ellipsoids at 50% probability; perchlorate counterions, solvent molecules, and hydrogen atoms have been omitted for clarity.

The nature of this metal–ligand bond has been further examined by quantum chemical calculations. Charge decomposition analysis reveals that the total L→M σ-donation (0.31e) is lower than the M→L π-back-donation (0.43e) which should hence be regarded as the main interaction in **143** and thus as the principal source of its stability. Generally, ligands are anionic or neutral species and monocationic ligands are rare.[96] Compounds of this type, formally constituted by a tricationic ligand with no spacer between the donor atom and the positive charged groups, seem to be unknown.[1]

It was found that the coordination of **141** to the gold(I) moiety was also possible (Scheme 58). The adduct **144** was isolated in 94% yield, but the stability of this complex is lower than the corresponding Pd and Pt complexes. Although it could be stored at -40 °C, it decomposes at room temperature. The low stability of **144** may be due to the weakening of metal back-donation to the phosphorus atom.

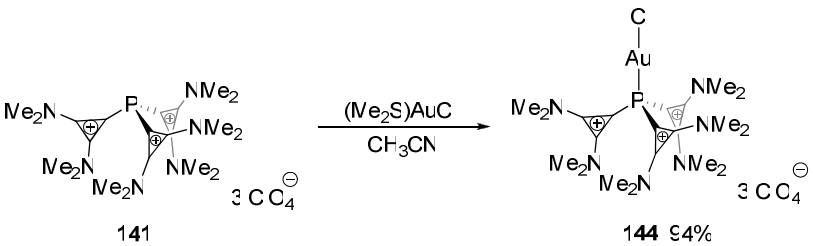

Scheme 58. Formation of Au(I) complexe **144**.

Next, we assumed that if an electron pair remains on the phosphorus, compound **141** might be able to be protonated with the concomitant formation of an adduct which is able to carry four positive charges (Scheme 59).

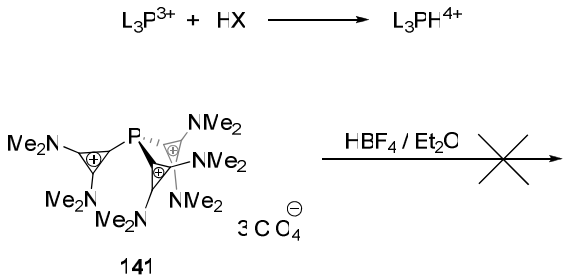

Scheme 59. Protonation of the compound **141**.

However, compound **141** gave no reaction with an excess of tetrafluoroboric acid. This failure can be considered as an evidence of the electron poorness of the phosphorus atom in this compound.

4.3 Summary IV

In summary, we have synthesized for the first time a tricationic P(III)-carbene stabilized center. Unexpectedly, despite the presence of three positive charges, coordination of **134a** to electron-rich transition metals such as Pt and Pd has been possible and their stability demonstrated in both the solid state and in solution. The coordination to less electron-rich metals such gold, was also possible. Additionally, the nature of the metal–ligand interaction has been analyzed by DFT calculations. Whether this and related compounds could have applications in catalysis is under investigation.

5 Carbene-Stabilized Chalcogenoid Dications

5.1 General Introduction

Due to the recent development of p-block-centered polycation chemistry, an interesting addition to this work could be the synthesis of cyclopropenylidene-stabilized chalcogenium polycations.

It is known that cationic chalcogenium-centered compounds are usually very reactive species if they are not stabilized by donating heteroatoms.[97] For example, sulfenium cations can be generated by electrochemical oxidation of various disulfides and are applied for some reactions such as the α-thiolation of alkyl ketones or the preparation of electron rich methylsulfanyl aromatic compounds (Scheme 60).

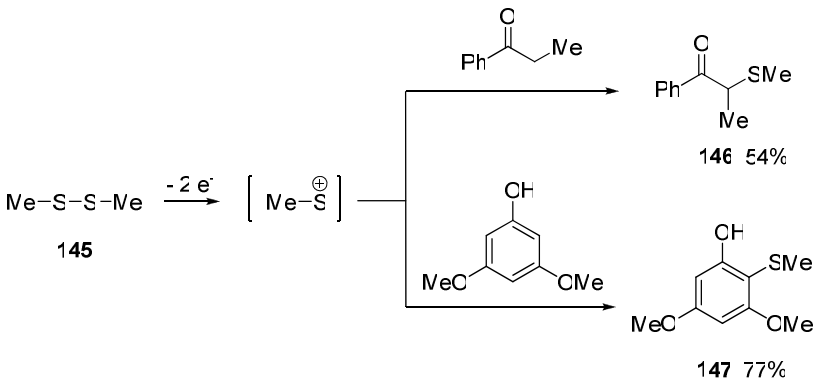

Scheme 60. Reaction of MeS^+ cation with ketone and phenol derivatives.

Similar to the already described phosphenium cations, the stabilization of chalcogenium cationic species can be achieved by incorporation of the chalcogen into electron rich heterocycles (structure **148**, Scheme 61) or by formation of complexes with *Lewis*-bases (structures **149** and **150**).

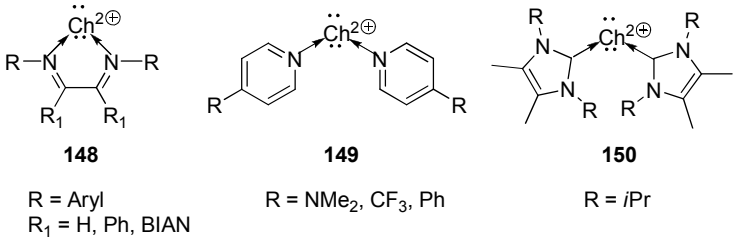

Scheme 61. Examples of Ch^{2+} dications, stabilized by imines, amines and carbenes.

5.1.1. Stabilization by incorporation in electron rich heterocycles

Bidentate ligands such 1,2-diimines can stabilize chalcogenium dications. For example, 1,2,5-chalcogenadiazolium compounds **148** were synthesized by the reaction of chalcogen dichloride (Ch = S, Se) with the 1,2-diimine **151** (R = Cy, dipp, dmp, *p*MeOPh, R_1 = H, Me, Ph, BIAN) followed by treatment with TMSOTf (Scheme 62).[98]

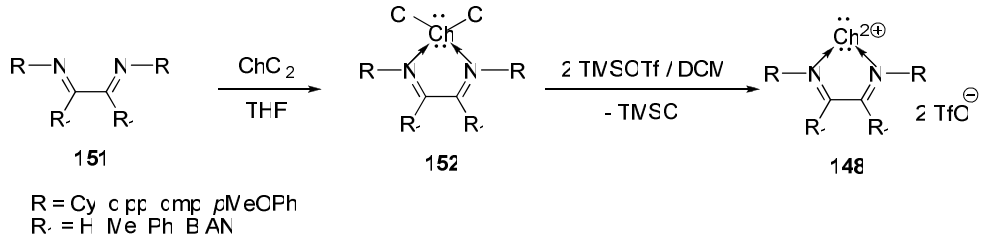

Scheme 62. Synthesis of 1,2,5-chalcogenadazolium compounds **148**.

Tellurium dichloride has a "transient nature", therefore, tellurium containing analogues of type **148** (Ch = Te) could not be obtained using the methodology just described. Thus, the tellurenium dication **156** was prepared by the alternative way using ligand exchange from **153** to **155** and halide abstraction with an excess of AgOTf (Scheme 63).[99]

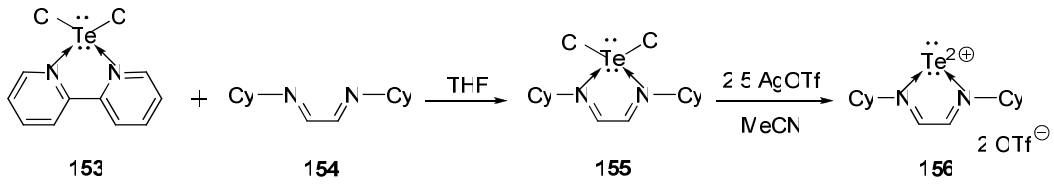

Scheme 63. Synthesis of the dicationic tellurium compound **156**.

5.1.2 Stabilization by formation of complexes with *Lewis*-bases

The most common way for the preparation of stabilized chalcogenium monocations is the abstraction of a Cl^- group of the corresponding sulfenyl, selenyl or telluryl chlorides with non-coordinating anions.[100] For example, selenyl chloride, formed by the oxidation of methyl selenide **157** with *t*-BuOCl, is dechlorinated by treatment with KPF_6 to give compound **158** (Scheme 64).

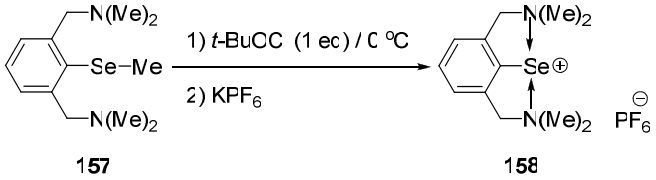

Scheme 64. Synthesis of N-stabilized selenenium monocation **158**.

Similar methods were used for the generation of chalcogen-centered dications. For example, pyridine-stabilized sulfenium(II) dications **162** were prepared by treatment of sulfur dichloride with TMSOTf and subsequent treatment with pyridines (Scheme 65).[70]

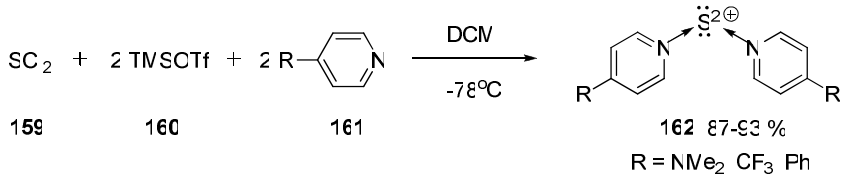

Scheme 65. Synthesis of pyridine-stabilized S^{2+} dications **162**.

Recently, bis-imines were identified as appropriate ligands for the transfer of Ch^{2+} to other neutral two-electron donor ligands. For example, the addition of two equivalents of 1,3-diisopropylimidazol-2-ylidene **164** to **163** gives the dication **150** (Scheme 66).[101]

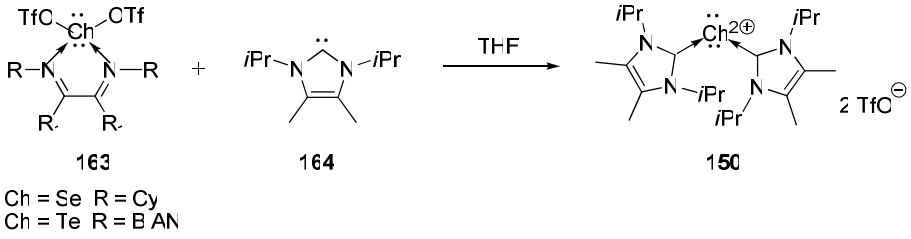

Scheme 66. Synthesis of NHC-stabilized dications **150**.

Cyclopropenylidenes, that have already been successfully used for the stabilization of polycharged phosphorus-centered cations, might also be used for the synthesis of other p-block element analogues applying the same "reverse electron demand" onio-substituent transfer methodology. Therefore, we decided to investigate its scope by reaction with bis(trimethylsilyl)-chalcogenides.

5.2 Results and Discussion

5.2.1 Synthesis of carbene-stabilized sulfenium, selenenium and tellurenium cations

The reaction of silylated chalcogenides **165** (Y = S, Se and Te) and chlorocyclopropenium salts **42** or **133** afforded the desired carbene-stabilized sulfenium and selenenium dications **166a,b** and **167a,b** in moderate to good yields (66-85%), proving the generality of our strategy (Scheme 67 and 68).

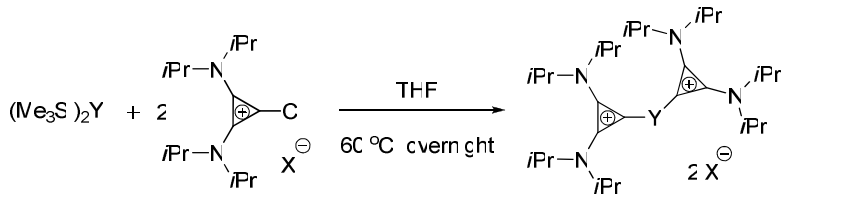

Scheme 67. Synthesis of the sulfenium and selenenium cations **166a,b** and **167a,b**.

The synthesis of the corresponding tellurium compound **169** using this methodology was not as efficient as in the sulfur and selenium case, probably because bis(trimethyl-silyl)telluride **168** partially decomposes in the reaction conditions releasing metallic tellurium. The use of chlorocyclopropenium salt **42** with a tetrafluoroborate counteranion led to the formation of considerable amounts of byproduct **170** (Scheme 68). Compound **170** was isolated in 55-83% yields and its structure has been confirmed by X-ray diffraction analysis (see page 199, Appendix 7.2.21).

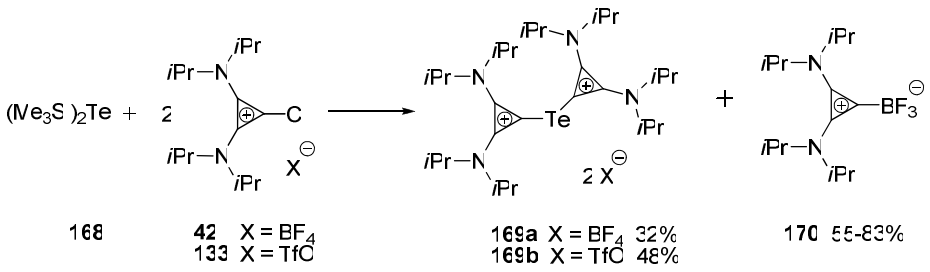

Scheme 68. Synthesis of the tellurenium cations **169a,b**.

The formation of byproduct **170** could be explained by the reaction of the already formed product **169a** with BF_3 that may be present in the reaction medium due to the following equilibrium (Scheme 69).

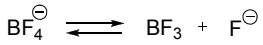

Scheme 69. An equilibrium between tetrafluoroborate anion, boron trifluoride and fluoride anion.

This side reaction could be explained by the weaker tellurium-carbon bond in comparison with the sulfur-carbon and selenium-carbon bonds, which is probably due to an inefficient (C)sp^2-(Te)5p orbital overlap. This also explains the absence of the side reaction in the case of sulfur and selenium where (C)sp^2-(S)3p and (C)sp^2-(Se)4p overlaps are more efficient. The increase in the yield of the reaction in the sequence S>Se>Te (85%, 66% and 32%, Schemes 67 and 68) speaks in favor of this explanation.

Due to the bad results obtained with $(TMS)_2Te$ **168**, we investigated an alternative approach to synthesis of tellurenium compounds **169a,b**. An alternative could be the use a different source of tellurium such as sodium telluride **172**.[102] Thus, treatment of tellurium powder with sodium naphthalide yielded $TeNa_2$ **172** (Scheme 70), which was reacted with chlorocyclopropenium triflate **133** to yield the desired product **169b** in 53% yield. However, the reaction of sodium telluride **172** with chlorocyclopropenium tetrafluoroborate **42** did not afford any identicable product, probably because of the instability of BF_4^- under these highly reducing conditions.

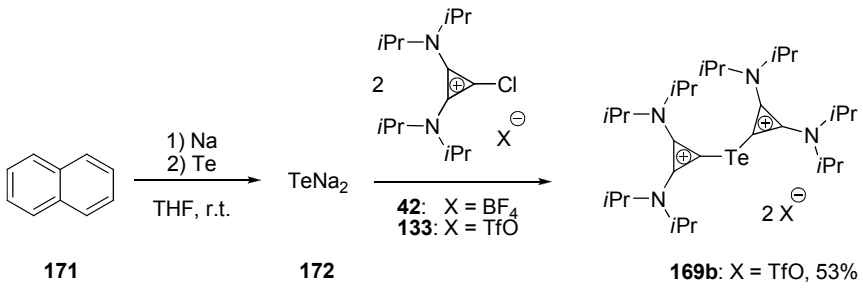

Scheme 70. Alternative synthesis of the tellurenium compound **169b**.

The structures of all produced chalcogenenium cations **166a**, **167a** and **169b** have been confirmed by X-ray diffraction (Figure 26, 27 and 28).

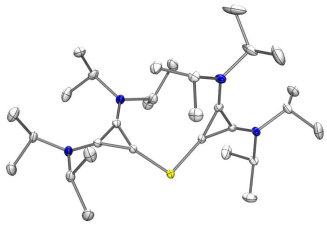

Figure 26. Molecular structure of compound **166a** in the solid state. Hydrogen atoms, tetraflouroborate counter anions and solvent molecules have been omitted for clarity. Thermal ellipsoids at 50% probability.

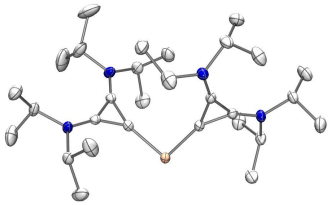

Figure 27. Molecular structure of compound **167a** in the solid state. Hydrogen atoms, tetraflouroborate counter anions and solvent molecules have been omitted for clarity. Thermal ellipsoids at 50% probability.

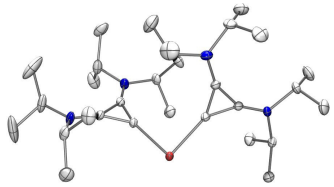

Figure 28. Molecular structure of compound **169b** in the solid state. Hydrogen atoms, triflate counter anions and solvent molecules have been omitted for clarity. Thermal ellipsoids at 50% probability.

The bond lengths between the chalcogen atom and the adjacent carbon atoms as well as bond angles (C-Ch-C) in compounds **166a**, **167a** and **169b** were compared. Compounds **166a** and **167a** have the same counter anion (BF_4^-); in the case of **169b** the counter anion is different (TfO^-) and in the X-ray structure we can see the Te-OTf interaction. The observed bond lengths (C–Ch) for **166a** are 1.7297(13) Å and 1.7394(13) Å, for **167a** are 1.8847(16) Å and 1.8773(16) Å, for **169b** are 2.085(3) Å and 2.087(3) Å. The bond angles are 100.14(6)°, 97.30(7)° and 95.44(10)° for **166a**, **167a** and **169b** respectively. This comparison clearly shows that the increasing of the sizes S<Se<Te correlates with an increase in the carbon–chalcogen bond length and a decreased angle between these two bonds. This might be explained by less efficient hybridization between the s- and p-orbitals. Therefore, the bond angle changes from 120°, which is characteristic for the sp^2 hybridization, to close to 90° which is typical for the orthogonal p-orbitals.

5.3 Summary V

In summary, a new synthetic approach for preparation of cyclopropenylidene-stabilized chalcogenoid-centered dications have been developed. The compounds were isolated in moderate to good yields and their molecular structures were confirmed by X-ray diffraction.

6 Experimental Part

6.1 General Experimental Conditions

6.1.1 Working techniques

All moisture- and oxidation-sensitive reactions were performed in carefully dried glassware under an argon atmosphere. The saturated aqueous solutions of sodium chloride, sodium bicarbonate, sodium carbonate and ammonium chloride, were saturated over sediment, unless indicated otherwise.

Solvents and reagents

All solvents were purified by distillation before use following standard procedures. Dry solvents were obtained by distillation over the appropriate drying agent (*vide infra*) and then kept under an atmosphere of argon: diethyl ether, tetrahydrofuran, toluene, benzene, pentane and *n*-hexane (sodium, benzophenone as indicator); *N*,*N*′-dimethylformamide (Desmodur®, dibutyltin dilaurate); dichloromethane, acetone, acetonitrile, triethylamine (calcium hydride); fluorobenzene (phosphorus pentoxide), methanol and ethanol (magnesium). 1,2-Dichloroethane was purchased from Sigma-Aldrich and used as received. Other commercial reagents were obtained from various sources and used without further purification.

Inert gas atmosphere

Air and moisture-sensitive reactions were conducted under an argon atmosphere. Argon was obtained from *Air Liquide* with higher than 99.5% purity.

Chromatographic methods

Reactions were mostly monitored by **thin layer chromatography** (**TLC**) using silica gel pre-coated polyester sheets (40 × 80 mm, Polygram® SIL G/UV254 from Macherey-Nagel). The spots were visualized with UV-light (λ = 254 nm) and/or by staining with phosphomolybdic acid or potassium permanganate stains.

Flash column chromatography was performed using silica gel 60 (Merck, 60 Å, 230-400 mesh 0.040-0.063 mm) and separations were conducted at slightly elevated pressure in a glass column.

6.1.2 Analytical methods

Nuclear magnetic resonance spectroscopy (NMR)

Spectra were recorded on Bruker DPX 300 (^{1}H: 300 MHz, ^{13}C: 75 MHz, ^{31}P: 121 MHz), Bruker AV 400 (^{1}H : 400 MHz, ^{13}C: 100 MHz, ^{31}P: 161 MHz), and Bruker AV 500 (^{1}H: 500 MHz, ^{13}C: 125 MHz, ^{31}P: 202 MHz) spectrometers at room temperature (298 K). Chemical shifts (δ) are given in parts per million (ppm) relative to tetramethylsilane (^{1}H and ^{13}C, internal standard) and H_3PO_4 (^{31}P, external standard) and coupling constants (*J*) in Hertz (Hz). The corresponding solvent signals were used as a references: $CDCl_3$: δC 77.0 ppm, δH 7.26 ppm; CD_2Cl_2: δC 54.0 ppm, δH 5.32 ppm; CD_3CN: δC 1.32 ppm, δC 118.26 ppm δH 1.94 ppm; [D8]-toluene δC 20.4 ppm, δC 125.5 ppm, δC 128.3 ppm, δC 129.2 ppm, δC 137.9 ppm, δH 2.08 ppm, δH 6.97 ppm, δH 7.01 ppm and δH 7.09 ppm. The ^{1}H NMR multiplicities are assigned as follows: singlet (s), doublet (d), triplet (t), quartet (q), quintet (quin), sextet (sext), septet (sept), multiplet (m), broad (br.). The signals have been assigned using 1D and 2D experiments.

Infrared spectroscopy

IR spectra were recorded using ATR (attenuated total reflection) on a Spectrum One (Perkin-Elmer) spectrometer at room temperature. The characteristic absorption bands are given in wavenumbers [cm^{-1}].

Analytical gas chromatography

GC-MS couplings were performed on an *Agilent Technology* GC 6890 Series and MSD 5973 (carrier gas: helium) with HP6890 Series Injector, employing an MN Optima®5 column (30 m × 0.25 mm × 0.25 mm). The mass spectra were recorded with an *Agilent Technology* 5973 Network MSD spectrometer. Quantitative evaluation of the integration was based on the substance peaks without considering response factors, unless stated otherwise.

Mass spectrometry (MS)

Mass spectra were measured on a Finnigan MAT 8200 (70 eV) or MAT 8400 (70 eV) spectrometer by electron ionization, chemical ionization, or fast atom/ion bombardment techniques. High resolution masses were determined on a Bruker APEX III FT-MS spectrometer (7 T magnet). All masses are given in atomic units per elementary charge (*m/z*) and reported in percentage relative to the basic peak. The mechanistic studies (cf. Chapter 4.5.2) were performed by ESI-MS with a Finnigan Ultra Mass TSQ 7000.

X-ray crystal structure analysis

The crystal structures were measured in the X-ray department of the Max Planck Institute for Coal Research in Mülheim an der Ruhr, led by Dr. C. W. Lehmann. The measurements were made using a Bruker-AXS Kappa CCD diffractometer.

6.1.3 Starting materials as well as in working group-made chemicals

Commercially available chemicals were used without further purification unless otherwise stated. Working group's internal chemicals: diethyl 2-(cyclohept-2-enyl)-2-(prop-2-ynyl)malonate **103** and diethyl 2-(cyclohex-2-enyl)-2-(3-phenylprop-2-ynyl)malonate **123**,[69] 1-(2-(prop-1-ynyl)phenyl)-1*H*-pyrrole **76**.[64]

6.2 Synthesis

Compound 43a

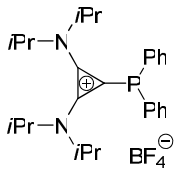

Diphenylphosphine (2.9 mL, 16.7 mmol) was added to a mixture of chlorocyclopropenium salt **42** (2.0 g, 5.58 mmol) in THF (20 mL) and the resulting mixture was heated at 60 °C for 24 hours. After cooling to room temperature, the solvent was removed *in vacuo*, the residue dissolved in DCM (30 mL) and washed with a saturated solution of $NaBF_4$ (3 × 25 mL). Once dried over Na_2SO_4, the organic phase was concentrated and the residue washed with Et_2O (3 × 10 mL) affording the desired compound as a white solid (2.55 g, 90%). ^{1}H NMR (300 MHz, CD_2Cl_2) δ = 0.98 (d, *J* = 6.8 Hz, 12H), 1.29 (d, *J* = 6.8 Hz, 12H), 3.34 (sept, *J* = 6.8 Hz, 2H), 3.99 (sept, *J* = 6.8 Hz, 2H), 7.32-7.47 ppm (m, 10H). ^{31}P NMR (121 MHz, CD_2Cl_2) δ = -23.61 ppm. ^{13}C NMR (75 MHz, CD_2Cl_2) δ = 21.6, 22.0, 53.6, 107.1 (d, *J* = 66.8 Hz), 130.5 (d, *J* = 8.1 Hz), 131.4 (d, *J* = 8.1 Hz), 131.7, 134.7 (d, *J* = 21.2 Hz), 139.7 ppm. IR (neat) $\tilde{\nu}$ = 695, 752, 1047, 1547, 1867, 2974 cm^{-1}. HRMS *calcd*. for $C_{27}H_{38}N_2P^+$: 421.276711; *found* 421.276467.

Compound 43b

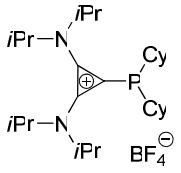

Dicyclohexylphosphine (0.84 mL, 4.17 mmol) was added to a mixture of chlorocyclopropenium salt **42** (500 mg, 1.39 mmol) in THF (5 mL) and the resulting mixture was heated at 60 °C for 24 hours. After cooling to room temperature, the solvent was removed *in vacuo*, the residue dissolved in DCM (20 mL) and washed with a saturated solution of $NaBF_4$ (3 × 15 mL). Once dried over Na_2SO_4, the organic phase was concentrated and the residue washed with Et_2O (3 × 5 mL) affording the desired compound as a white solid

(620 mg, 86%). ^{1}H NMR (300 MHz, CD_2Cl_2) δ = 0.96-1.24 (m, 8H), 1.31 (d, *J* = 6.6 Hz, 12H), 1.33 (d, *J* = 6.8 Hz, 12H), 1.35-1.51 (m, 6H), 1.55-1.95 (m, 8H), 3.94 (sept, *J* = 7.2 Hz, 2H), 4.08 (sept, *J* = 7.2 Hz, 2H). ^{31}P NMR (121 MHz, CD_2Cl_2) δ = -16.77 ppm. ^{13}C NMR (100 MHz, CD_2Cl_2) δ = 21.1, 21.2, 22.0 (br.s), 26.5, 27.3, 27.4, 27.6, 27.7, 31.5, 31.6, 31.9, 32.1, 36.2 (d, *J* = 13.7 Hz), 53.2 (br.s), 107.1 (d, *J* = 78.8 Hz), 142.2 ppm. IR (neat) ν̃ = 680, 1035, 1050, 1548, 1862, 2847, 2919 cm^{-1}. (ESI) MS *calcd*. for $C_{27}H_{50}N_2P^+$: 433.4; *found* 433.5.

Compound 43c

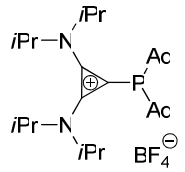

Diadamantylphosphine (1.26 g, 4.17 mmol) was added to a mixture of chlorocyclopropenium salt **42** (500 mg, 1.39 mmol) in THF (5 mL) and the resulting mixture was heated at 60 °C for 72 hours. After cooling to room temperature, the solvent was removed *in vacuo*, the residue dissolved in DCM (20 mL) and washed with a saturated solution of $NaBF_4$ (3 × 15 mL). Once dried over Na_2SO_4, the organic phase was concentrated and the residue washed with Et_2O (3 × 10 mL) affording the desired compound as a white solid (680 mg, 79%). ^{1}H NMR (300 MHz, CD_2Cl_2) δ = 1.30 (d, *J* = 6.9 Hz, 6H), 1.38 (d, *J* = 6.9 Hz, 12H), 1.45 (d, *J* = 6.9 Hz, 6H), 1.56-1.77 (m, 12H), 1.84 (br.s, 12H), 2.04 (br.s, 6H), 3.76-3.83 (m, 1H), 3.92 (sept, *J* = 7.2 Hz, 1H), 4.36 (sept, *J* = 6.9 Hz, 1H), 4.57 (sept, *J* = 6.9 Hz, 1H); ^{31}P NMR (121 MHz, CD_2Cl_2) δ = 15.63 ppm. ^{13}C NMR (75 MHz, CD_2Cl_2) δ = 20.9, 21.4, 21.5, 21.6, 23.3, 29.5 (d, *J* = 8.5 Hz), 37.0, 39.5 (d, *J* = 25.2 Hz), 42.9 (d, *J* = 11.5 Hz), 49.9, 57.5, 57.6, 105.0 (d, *J* = 90.5 Hz), 145.2 ppm (d, *J* = 22.4 Hz). IR (neat) ν̃ = 1033, 1048, 1089, 1375, 1452, 1539, 1851, 2848, 2901 cm^{-1}. HRMS *calcd*. for $C_{35}H_{58}N_2P^+$: 537.433212; *found* 537.433029.

Compound 43d

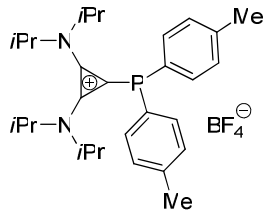

Di(*p*-tolyl)phosphine (1.80 g, 8.40 mmol) was added to a mixture of chlorocyclopropenium salt **42** (1.00 g, 2.80 mmol) in THF (20 mL) and the resulting mixture was heated at 60 °C for 24 hours. After cooling to room temperature, the solvent was removed *in vacuo*, the residue dissolved in DCM (20 mL) and washed with a saturated solution of $NaBF_4$ (3 × 15 mL). Once dried over Na_2SO_4, the organic phase was concentrated and the residue washed with Et_2O (3 × 20 mL) affording the desired compound as a white solid (1.44 g, 96%). ^{1}H NMR (400 MHz, CD_2Cl_2) δ = 0.97 (d, *J* = 6.6 Hz, 12H), 1.27 (d, *J* = 6.8 Hz, 12H), 2.31 (s, 6H), 3.32 (sept, *J* = 6.6 Hz, 2H), 3.98 (sept, *J* = 6.8 Hz, 2H), 7.20-7.21 ppm (m, 8H). ^{31}P NMR (161 MHz, CD_2Cl_2) δ = -24.12 ppm. ^{13}C NMR (100 MHz, CD_2Cl_2) δ = 21.5, 21.6, 21.9, 22.0 (br.s), 53.4 (br.s), 108.1 (d, *J* = 67,8 Hz), 127.9 (d, *J* = 6.1 Hz), 131.2 (d, *J* = 8.1 Hz), 134.6 (d, *J* = 22.3 Hz), 139.4, 142.4 ppm. IR (neat) ν̃ = 686, 811, 1048, 1547, 1863, 2976 cm^{-1}. HRMS *calcd*. for $C_{29}H_{42}N_2P^+$: 449.308012; *found* 449.308455.

Compound 43e

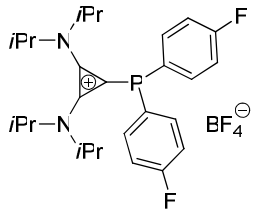

Di(*p*-fluorophenyl)phosphine (2.67 g, 12.0 mmol) was added to a mixture of chlorocyclopropenium salt **42** (1.44 g, 4.00 mmol) in THF (20 mL) and the resulting mixture was heated at 60 °C for 24 hours. After cooling to room temperature, the solvent was removed *in vacuo*, the residue dissolved in DCM (20 mL) and washed with a saturated solution of $NaBF_4$ (3 × 15 mL). Once dried over Na_2SO_4, the organic phase was concentrated and the residue washed with Et_2O (3 × 20 mL) affording the desired compound as a white solid (1.65 g, 76%). ^{1}H NMR (400 MHz, CD_2Cl_2) δ = 0.99 (d, *J* = 6.8 Hz, 12H), 1.29 (d,

J = 6.9 Hz, 12H), 3.35 (sept, *J* = 6.8 Hz, 2H), 4.00 (sept, *J* = 6.9 Hz, 2H), 7.15 (m, 4H), 7.41 ppm (m, 4H). ^{31}P NMR (161 MHz, CD_2Cl_2) δ = -24.57 ppm. ^{13}C NMR (100 MHz, CD_2Cl_2) δ = 21.5, 21.6, 21.9, 54.0 (br.s), 108.8 (d, *J* = 58.5 Hz), 117.8 (dd, *J* = 21.2 Hz, *J* = 9.2 Hz), 127.0 (dd, *J* = 7.1 Hz, *J* = 4.0 Hz), 137.1 (dd, *J* = 23.2 Hz, *J* = 9.1 Hz), 139.6, 165.4 ppm (d, *J* = 252.6 Hz). IR (neat) ṽ = 691, 836, 1049, 1552, 1869, 2987 cm^{-1}. (ESI) MS calcd. for $C_{27}H_{36}F_2N_2P^+$ 457.26, found 457.29. HRMS *calcd*. for $C_{27}H_{36}N_2F_2P^+$: 457.257868; *found* 457.257700.

Compound 43f

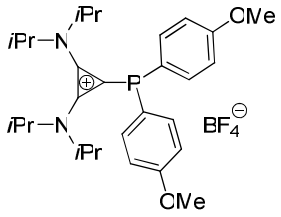

Di(*p*-methoxyphenyl)phosphine (0.875 g, 3.6 mmol) was added to a mixture of chlorocyclopropenium salt **42** (430 mg, 1.2 mmol) in THF (5 mL) and the resulting mixture was heated at 60 °C for 12 hours. After cooling to room temperature, the solvent was removed *in vacuo*, the residue dissolved in DCM (20 mL) and washed with a saturated solution of $NaBF_4$ (3 × 15 mL). Once dried over Na_2SO_4, the organic phase was concentrated and the residue purified by silica gel flash chromatography (9:1 DCM : Acetone) affording the desired compound as a white solid (0.55 g, 80%).^{1}H NMR (300 MHz, CD_2Cl_2) δ = 0.97 (d, *J* = 6.8 Hz, 12H), 1.27 (d, *J* = 6.9 Hz, 12H), 3.34 (sept, *J* = 6.8 Hz, 2H), 3.76 (s, 6H), 3.97 (sept, *J* = 6.9 Hz, 2H), 6.94 (m, 4H), 7.31 ppm (m, 4H). ^{31}P NMR (121 MHz, CD_2Cl_2) δ = -23.83 ppm. ^{13}C NMR (75 MHz, CD_2Cl_2) δ = 21.6, 21.7, 22.0, 56.3, 108.1 (d, *J* = 67.4 Hz), 116.0 (d, *J* = 9.1 Hz), 122.0 (d, *J* = 3.3 Hz), 136.6 (d, *J* = 23.4 Hz), 139.2 (d, *J* = 1.3 Hz), 162.8 ppm. IR (neat) ṽ = 684, 834, 1024, 1247, 1553, 1866, 2982 cm^{-1}; (ESI) MS calcd. for $C_{29}H_{42}N_2O_2P^+$: 481.30 found 481.37. HRMS *calcd*. for $C_{29}H_{42}N_2O_2P^+$: 481.297843; *found* 481.297370.

Compound 44a

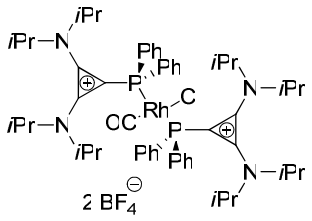

Dry THF (2 mL) was added to a cooled (- 20 °C) solid mixture of $[RhCl(CO)_2]_2$ (10 mg, 0.025 mmol) and chlorophosphenium salt **43a** (50 mg, 0.1 mmol). The reaction mixture was allowed to warm to room temperature and then stirred additionally for 30 min. After removal of the solvents *in vacuo*, the solid residue was washed with pentane (3 × 1 mL) and dried, affording the desired product as a yellow solid (56 mg, 93%).^{1}H NMR (400 MHz, CD_2Cl_2) δ = 0.89 (d, *J* = 6.9 Hz, 24H), 1.27 (d, *J* = 6.9 Hz, 24H), 3.39 (m, 4H), 4.04 (m, 4H), 7.52-7.62 (m, 12H), 8.08-8.16 ppm (m, 8H). ^{31}P NMR (161 MHz, CD_2Cl_2) δ = 30.15 ppm (d, *J* = 133.1 Hz). ^{13}C NMR (100 MHz, CD_2Cl_2) δ = 21.2, 21.6, 55.0 (br.s), 101.4 (t, *J* = 13.4 Hz), 128.5 (t, *J* = 25.8 Hz), 130.1 (t, *J* = 5.8 Hz), 133.5, 134,3 (d, *J* = 21.6 Hz), 136.1 (t, *J* = 7.8 Hz),139.2 ppm (t, *J* = 4.3 Hz). IR (neat) ṽ = 700, 800, 1036, 1053, 1552, 1865, 1970, 2975 cm^{-1}. HRMS *calcd*. for $C_{53}H_{76}BClF_4N_4OP_2Rh^+$: 1095.427971; *found* 1095.427645.

Compound 44c

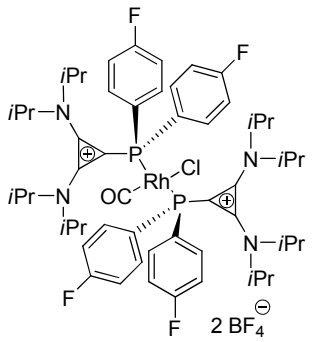

Dry THF (2 mL) was added to a cooled (-20 °C) solid mixture of $[RhCl(CO)_2]_2$ (12 mg, 0.030 mmol) and phosphenium salt **43e** (65 mg, 0.12 mmol). The reaction mixture was allowed to warm to room temperature and then stirred additionally for 30 min. After removal of the solvents *in vacuo*, the solid residue was washed with pentane (3 × 1 mL) and dried, affording the desired product as a yellow solid (74 mg, 99%).^{1}H NMR (300 MHz, CD_2Cl_2)

δ = 1.02 (d, *J* = 7.0 Hz, 24H), 1.36 (d, *J* = 7.0 Hz, 24H), 3.45 (sept, *J* = 7.0 Hz, 4H), 4.13 (sept, *J* = 7.0 Hz, 4H), 7.34 (m, 8H), 8.28 ppm (m, 8H). ^{31}P NMR (121 MHz, CD_2Cl_2) δ = 26.12 ppm (d, *J* = 131.3 Hz). ^{13}C NMR (75 MHz, CD_2Cl_2) δ = 21.3, 21.6, 54.0, 100.6 (t, *J* = 15.1 Hz), 117.5 (dd, *J* = 21.5, 6.3 Hz), 124.4 (t, *J* = 4.7 Hz), 138.8 (dt, *J* = 9.7 Hz, *J* = 8.5 Hz), 139.3 (dd, *J* = 7.0 Hz, *J* = 3.7 Hz), 166.0 ppm (d, *J* = 256.0 Hz). IR (neat) ṽ = 687, 814, 1035, 1239, 1556, 1865, 1976, 2972 cm^{-1}. HRMS *calcd*. for $C_{55}H_{72}B_3ClF_{16}N_4OP_2Rh^-$: 1341.399085; *found* 1341.398831.

Compound 44d

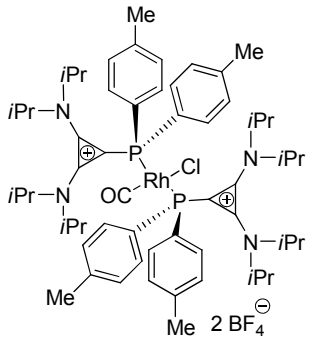

Dry THF (2 mL) was added to a cooled (-20 °C) solid mixture of $[RhCl(CO)_2]_2$ (13 mg, 0.031 mmol) and phosphenium salt **43d** (67 mg, 0.12 mmol). The reaction mixture was allowed to warm to room temperature and then stirred additionally for 30 min. After removal of the solvents *in vacuo*, the solid residue was washed with pentane (1 × 15 mL) and dried, affording the desired product as a yellow solid (76 mg, 99%).^{1}H NMR (300 MHz, CD_2Cl_2) δ = 0.89 (d, *J* = 6.8 Hz, 24H), 1.26 (d, *J* = 6.8 Hz, 24H), 2.37 (s, 12H), 3.39 (sept, *J* = 7.0 Hz, 4H), 4.03 (sept, *J* = 7.0 Hz, 4H), 7.35 (d, *J* = 7.9 Hz, 8H), 7.93-8.00 ppm (m, 8H). ^{31}P NMR (121 MHz, CD_2Cl_2) δ = 28.82 ppm (d, *J* = 131.2 Hz). ^{13}C NMR (75 MHz, CD_2Cl_2) δ = 21.5, 21.9, 22.0, 53.4 (br.s) 55.1 (br.s), 100.2 (d, *J* = 12.6 Hz), 125.5 (dd, *J* = 27.8 Hz, *J* = 26.5 Hz), 131.1 (t, *J* = 6.4 Hz), 136.4 (t, *J* = 7.9 Hz), 139.3 (d, *J* = 3.3 Hz), 145.0 (t, *J* = 1.3 Hz), 163.4 ppm. IR (neat) ṽ = 664, 807, 1031, 1357, 1554, 1866, 1969, 2969 cm^{-1}. HRMS *calcd*. for $C_{59}H_{84}BClF_4N_4OP_2Rh^+$: 1151.488064; *found* 1151.491726.

Compound 44e

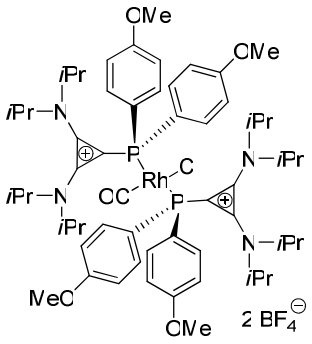

Dry THF (2 mL) was added to a cooled (-20 °C) solid mixture of $[RhCl(CO)_2]_2$ (9.0 mg, 0.023 mmol) and phosphenium salt **43f** (52 mg, 0.091 mmol). The reaction mixture was allowed to warm to room temperature and then stirred additionally for 30 min. After removal of the solvents *in vacuo*, the solid residue was washed with pentane (3 × 1 mL) and dried, affording the desired product as a yellow solid (61 mg, 99%). ^{1}H-NMR (300 MHz, CD_2Cl_2) δ = 0.91 (d, *J* = 6.9 Hz, 24H), 1.25 (d, *J* = 6.9 Hz, 24H), 3.42 (sept, *J* = 6.9 Hz, 4H), 3.81 (s, 12H), 4.02 (sept, *J* = 6.9 Hz, 4H), 7.04 (m, 8H), 8.02 ppm (m, 8H). ^{31}P NMR (121 MHz, CD_2Cl_2) δ = 27.12 ppm (d, *J* = 130.3 Hz). ^{13}C NMR (100 MHz, CD_2Cl_2) δ = 21.5, 21.9, 24.0, 56.6, 103.2 (t, *J* = 13.0 Hz), 115.8 (t, *J* = 6.7 Hz), 119.8 (t, *J* = 29.0 Hz), 138.3 (t, *J* = 8.5 Hz), 139.3, (t, *J* = 4.5 Hz), 164.2 ppm. IR (neat) $\tilde{\nu}$ = 685, 800, 1053, 1257, 1551, 1864, 1977, 2979 cm^{-1}. HRMS *calcd*. for $C_{59}H_{84}B_3ClF_{12}N_4O_5P_2Rh^-$: 1389.479175; *found*: 1389.478116.

Compound 45a

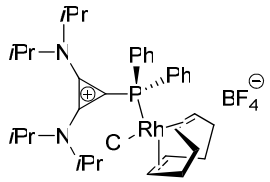

$[RhCl(cod)]_2$ (24.6 mg, 0.05 mmol) was added to a solution of **43a** (50.9 mg, 0.10 mmol) in DCM (2 mL) and the resulting mixture stirred for 1 h at room temperature. Then the solvent was evaporated and the resulting yellow residue washed with pentane (2 mL) and dried to afford **45a** as a yellow solid (72.4 mg, 96%). ^{1}H NMR (400 MHz, CD_2Cl_2) δ = 1.09 (d, *J* = 6.4 Hz, 12H), 1.33 (d, *J* = 6.8 Hz, 12H), 1.98 (m, 2H), 2.08 (m, 2H), 2.29 (m, 4H), 3.54 (br.s, 2H), 3.94 (br.m, 2H), 4.10 (br.m, 2H), 5.58 (br.s, 2H), 7.39-7.70 ppm (m, 10H).

^{31}P NMR (161 MHz, CD_2Cl_2) δ = 25.30 ppm (d, *J* = 150.6 Hz). ^{13}C NMR (100 MHz, CD_2Cl_2) δ = 21.9, 22.4, 29.5 (bs), 33.7 (d, *J* = 2.0 Hz), 53.3(br.s), 59.1(br.s), 72.9 (d, *J* = 12.9 Hz), 102.9 (d, *J* = 12.9 Hz), 108.6 (dd, *J* = 7.0, 12.6 Hz), 128.0 (d, *J* = 43.9 Hz), 130.3 (d, *J* = 10.7 Hz), 133.3 (d, *J* = 1.9 Hz), 135.1 (d, *J* = 12.0 Hz), 139.2 ppm (d, *J* = 7.9 Hz). IR (neat) ṽ = 696, 752, 996, 1032, 1049, 1091, 1376, 1552, 1868, 2938, 2975 cm^{-1}; HRMS *calcd.* for $C_{35}H_{50}ClN_2PRh^+$: 667.244969; *found*: 667.245253.

Compound 45b

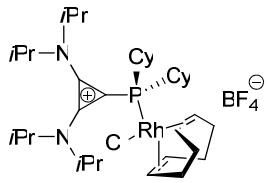

$[RhCl(cod)]_2$ (24.6 mg, 0.05 mmol) was added to a solution of **43b** (52.0 mg, 0.10 mmol) in DCM (2 mL) and the resulting mixture stirred for 1 h at room temperature. Then the solvent was evaporated and the resulting yellow residue washed with pentane (2 mL) and dried to afford **45b** as a yellow solid (67.4 mg, 88%). ^{1}H NMR (400 MHz, CD_2Cl_2) δ = 1.23-1.45 (m, 8H), 1.50 (br.s, 12H), 1.57 br.s, 12H), 1.84 (br.s, 4H), 1.96 (br.s, 8H), 2.11-2.27 (m, 4H), 2.31-2.42 (m, 2H), 2.42-2.57 (m, 2H), 3.78 (br.s, 2H), 4.22 (br.s, 2H), 4.83 (br.s, 2H) 5.51 ppm (br.s, 2H). ^{31}P NMR (161 MHz, CD_2Cl_2) δ = 28.3 ppm (d, *J* = 150.5 Hz). ^{13}C NMR (100 MHz, CD_2Cl_2) δ = 22.2 (br.s), 23.0 (br.s), 26.2 (d, *J* = 1.3 Hz), 27.2, 27.3, 27.4, 27.5, 28.8 (d, *J* = 1.2 Hz), 30.5 (br.s), 31.3, 31.6 (d, *J* = 2.6 Hz), 33.6 (d, *J* = 2.5 Hz), 34.6 (br.s). 34.9 (br.s), 58.8 (br.s), 71.4 (d, *J* = 13.0 Hz), 102.2, 107.8 (dd, *J* = 12.0 Hz, *J* = 6.9 Hz), 141.4 ppm (br.s). IR (neat) ṽ = 727, 1004, 1050, 1093, 1535, 1860, 2852, 2933 cm^{-1}. HRMS *calcd.* for $C_{35}H_{62}ClN_2PRh^+$: 679.338870; *found*: 679.338987.

Compound 45c

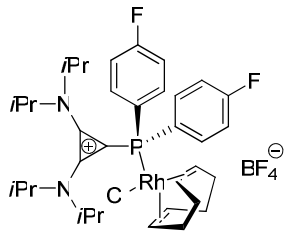

$[RhCl(cod)]_2$ (25.0 mg, 0.05 mmol) was added to a solution of **43e** (54.0 mg, 0.10 mmol) in DCM (2 mL) and the resulting mixture stirred for 1 h at room temperature. Then the solvent was evaporated and the resulting yellow residue washed with pentane (2 mL) and dried to afford **45c** as a yellow solid (77.0 mg, 97%). ^{1}H NMR (300 MHz, CD_2Cl_2) δ = 1.22 (d, *J* = 6.7 Hz, 12H), 1.45 (d, *J* = 6.5 Hz, 12H), 2.05-2.28 (m, 4H), 2.30-2.56 (m, 4H), 3.65 (m, 2H), 4.03 (m, 2H), 4.21 (m, 2H), 5.70 (m, 2H), 7.26-7.37 (m, 4H), 7.73-7.86 ppm (m, 4H). ^{31}P NMR (121 MHz, CD_2Cl_2) δ = 22.65 ppm (d, *J* = 153.0 Hz). ^{13}C NMR (100 MHz, CD_2Cl_2) δ = 21.6, 21.9, 29.1 (br.s), 33.3 (d, *J* = 2.4 Hz), 55.5 (br.s), 57.6, 72.4 (d, *J* = 13.0 Hz), 101.6 (d, *J* = 19.3 Hz), 108.5 (dd, *J* = 12.4 Hz, *J* = 7.2 Hz), 117.3 (dd, *J* = 21.5 Hz, *J* = 11.5 Hz), 123.5 (dd, *J* = 45.9 Hz, *J* = 2.5 Hz), 137.4 (dd, *J* = 14.4 Hz, *J* = 8.9 Hz), 138.9 (dd, *J* = 7.2 Hz, *J* = 1.4 Hz), 165.6 ppm (dd, *J* = 256.0 Hz, *J* = 2.4 Hz). IR (neat) $\tilde{\nu}$ = 681, 815, 1053, 1548, 1865, 2976 cm^{-1}. HRMS *calcd*. for $C_{35}H_{48}ClF_2N_2PRh^+$: 703.226126; *found* 703.225916.

Compound 45d

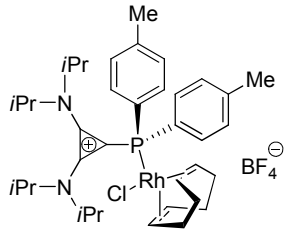

$[RhCl(cod)]_2$ (25.0 mg, 0.05 mmol) was added to a solution of **43d** (54.0 mg, 0.10 mmol) in DCM (2 mL) and the resulting mixture stirred for 1 h at room temperature. Then the solvent was evaporated and the resulting yellow residue washed with pentane (2 mL) and dried to afford **45d** as a yellow solid (77.0 mg, 99%). ^{1}H NMR (400 MHz, CD_2Cl_2) δ = 1.08 (d, *J* = 6.5 Hz, 12H), 1.32 (d, *J* = 6.7 Hz, 12H), 1.92-2.11 (m, 4H), 2.18-2.33 (m, 4H), 2.35 (s, 6H), 3.51 (m, 2H), 3.95 (m, 2H), 4.08 (m, 2H), 5.54 (m, 2H), 7.23-7.29 (m, 4H), 7.43-7.50

ppm (m, 4H). ^{31}P NMR (161 MHz, CD_2Cl_2) δ = 24.66 ppm (d, *J* = 151.0 Hz). ^{13}C NMR (100 MHz, CD_2Cl_2) δ = 21.9, 22.0, 22.4, 29.5, 33.7 (d, *J* = 2.9 Hz), 53.2 (br.s), 56.0 (br.s), 72.7 (d, *J* = 12.9 Hz), 103.5 (d, *J* = 15.7 Hz), 108.3 (dd, *J* = 12.7 Hz, *J* = 6.9 Hz), 124.5 (d, *J* = 46.0 Hz), 130.9 (d, *J* = 10.1 Hz), 135.0 (d, *J* = 12.2 Hz), 139.1 (d, *J* = 8.4 Hz), 142.2 ppm (d, *J* = 2.0 Hz). IR (neat) ṽ = 677, 808, 1053, 1552, 1863, 2969 cm^{-1}. HRMS *calcd*. for $C_{37}H_{54}ClN_2PRh^+$: 695.276269; *found* 695.276236.

Compound 46a

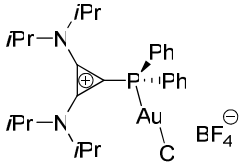

[AuCl(Me_2S)] (63.0 mg, 0.20 mmol) was added to a cooled (-20 °C) suspension of salt **43a** (109.0 mg, 0.20 mmol) in dry THF (3 mL) and the solution stirred at this temperature for 1 h. The solvent was then removed *in vacuo* at 0 °C, affording the desired product as an off white solid (154 mg, 97%).^{1}H NMR (400 MHz, CD_2Cl_2) δ = 0.96 (d, *J* = 6.9 Hz, 12H), 1.33 (d, *J* = 6.9 Hz, 12H), 3.35 (sept, *J* = 6.9 Hz, 2H), 4.07 (sept, *J* = 6.9 Hz, 2H), 7.54-7.64 (m, 6H), 7.86-7.93 ppm (m, 4H). ^{31}P NMR (161 MHz, CD_2Cl_2) δ = 17.86 ppm. ^{13}C NMR (75 MHz, CD_2Cl_2) δ = 21.9, 22.0, 68.5, 96.8 (d, *J* = 45.3 Hz), 125.5 (d, *J* = 67.5 Hz), 131.1 (d, *J* = 13.6 Hz), 134.7 (d, *J* = 2.6 Hz), 135.9 (d, *J* = 16.2 Hz), 138.7 ppm. IR (neat) ṽ = 692, 751, 1057, 1568, 1866, 2979 cm^{-1}. HRMS *calcd*. For $C_{27}H_{38}AuClN_2P^+$: 653.212121; *found* 653.213006.

Compound 46b

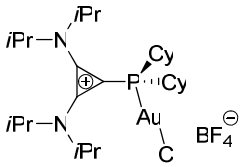

[AuCl(Me_2S)] (29.5 mg, 0.10 mmol) was added to a cooled (-20 °C) suspension of salt **43b** (52.0 mg, 0.10 mmol) in dry DCM (3 mL) and the solution stirred at this temperature for 1 h. The solvent was then removed *in vacuo* at 0 °C, affording the desired product as an off white solid (70.8 mg, 94%).^{1}H NMR (300 MHz, CD_2Cl_2) δ = 1.23-1.45 (m, 10H), 1.51 (d, *J* =

5.7 Hz, 12H), 1.63 (d, *J* = 6.9 Hz, 12H), 1.65-1.82 (m, 4H), 1.94 (br.s, 4H), 2.10-2.16 (m, 2H), 2.36-2.50 (m, 2H), 4.16 (sept, *J* = 6.9 Hz, 2H), 4.27 ppm (sept, *J* = 6.9 Hz, 2H). ^{31}P NMR (121 MHz, CD_2Cl_2) δ = 33.31 ppm. ^{13}C NMR (75 MHz, CD_2Cl_2) δ = 22.0, 22.1, 25.8 (br.s), 26.8 (d, *J* = 15.5 Hz), 27.1 (d, *J* = 13.4 Hz), 30.8, 30.9, 32.1, 32.2, 38.0 (d, *J* = 32.1 Hz), 54.5 (br.s), 68.5, 95.1 (br.s), 141.1 ppm. IR (neat) ṽ = 682, 1029, 1051, 1558, 1863, 2851, 2928 cm^{-1}. HRMS *calcd*. for $C_{27}H_{50}AuClN_2P^+$: 665.306018; *found* 665.306796.

Compound 46c

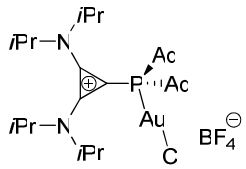

[AuCl(Me$_2$S)] (29.5 mg, 0.10 mmol) was added to a cooled (-20 °C) suspension of salt **43c** (62.5 mg, 0.10 mmol) in dry DCM (3 mL) and the solution stirred at this temperature for 1 h. The solvent was then removed *in vacuo* at 0 °C, affording the desired product as an off white solid (81.4 mg, 95%).^{1}H NMR (400 MHz, CD_2Cl_2) δ = 1.28 (d, *J* = 6.4 Hz, 8H), 1.39 (d, *J* = 6.8 Hz, 12H), 1.62 (br.s, 6H), 1.71 (s, 10H), 2.00-2.14 (m, 18H), 4.12 (br.s, 1H), 4.36 (br.s, 1H), 4.43 ppm (sept, *J* = 6.8 Hz, 2H). ^{31}P NMR (161 MHz, CD_2Cl_2) δ = 33.31 ppm (br.s). ^{13}C NMR (100 MHz, CD_2Cl_2) δ = 21.7 (br.s), 22.7 (br.s), 23.0, 28.9, 29.1, 36.0, 36.1, 42.3, 42.4, 44.7 (br.s), 54.0, 54.2, 54.3, 58.2, 93.7 (br.s), the two C-N from the cyclopropenium cations were not detected after prolonged measurement. IR (neat) ṽ = 672, 734, 1055, 1551, 1842, 2899 cm^{-1}. HRMS *calcd*. for $C_{35}H_{58}AuClN_2P^+$: 769.368616; *found* 769.368204.

Compound 46d

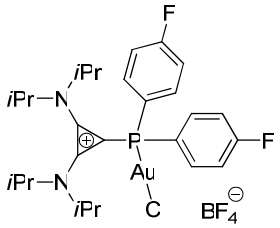

[AuCl(Me$_2$S)] (29.0 mg, 0.098 mmol) was added to a cooled (-20 °C) suspension of salt **43e** (54.0 mg, 0.098 mmol) in dry THF (2 mL) and the solution stirred at this temperature for 1 h.

The solvent was then removed *in vacuo* at 0 °C, affording the desired product as an off white solid (75 mg, 99%). ^{1}H NMR (300 MHz, CD_2Cl_2) δ = 1.00 (d, *J* = 6.8 Hz, 12H), 1.33 (d, *J* = 6.8 Hz, 12H), 3.38 (sept, *J* = 6.8 Hz, 2H), 4.08 (sept, *J* = 6.8 Hz, 2H), 7.29 (dt, *J* = 8.6 Hz, *J* = 2.0 Hz, 4H), 7.89-8.02 ppm (m, 4H). ^{31}P NMR (121 MHz, CD_2Cl_2) δ = 15.73 ppm. ^{13}C NMR (75 MHz, CD_2Cl_2) δ = 21.9, 22.0, 50.0, 58.1, 96.0 (d, *J* = 47.9 Hz), 118.5 (dd, *J* = 22.1 Hz, *J* = 14.9 Hz), 121.6 (dd, *J* = 70.5 Hz, *J* = 3.5 Hz), 138.6 (dd, *J* = 9.7 Hz, *J* = 2.0 Hz), 138.8 (dd, *J* = 7.7 Hz, *J* = 2.6 Hz), 167.0 ppm (dd, *J* = 257.6 Hz, *J* = 2.6 Hz). IR (neat) ṽ = 829, 1052, 1236, 1496, 1566, 1864, 2978 cm^{-1}. HRMS *calcd*. for $C_{27}H_{36}AuClF_2N_2P^+$: 689.193278; *found* 689.192744.

Compound 46e

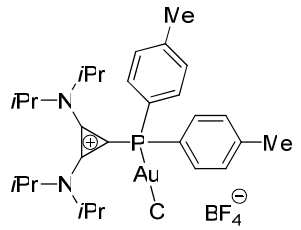

[AuCl(Me_2S)] (25.0 mg, 0.085 mmol) was added to a cooled (-20 °C) suspension of salt **43d** (46.0 mg, 0.085 mmol) in dry THF (2 mL) and the solution stirred at this temperature for 1 h. The solvent was then removed *in vacuo* at 0 °C, affording the desired product as an off white solid (64 mg, 98%). ^{1}H NMR (300 MHz, CD_2Cl_2) δ = 0.97 (d, *J* = 7.0 Hz, 12H), 1.32 (d, *J* = 7.0 Hz, 12H), 2.36 (s, 6H), 3.36 (sept, *J* = 7.0 Hz, 2H), 4.06 (sept, *J* = 7.0 Hz, 2H), 7.36 (dd, *J* = 7.8 Hz, *J* = 2.6 Hz, 4H), 7.73 ppm (dd, *J* = 14.5 Hz, *J* = 7.8 Hz, 4H). ^{31}P NMR (121 MHz, CD_2Cl_2) δ = 16.13 ppm. ^{13}C NMR (75 MHz, CD_2Cl_2) δ = 21.9, 22.0, 22.1, 22.2, 87.5 (d, *J* = 13.6 Hz), 122.2 (d, *J* = 69.2 Hz), 131.7 (d, *J* = 13.6 Hz), 135.8 (d, *J* = 16.2 Hz), 138.6 (d, *J* = 7.6 Hz), 146.0 ppm (d, *J* = 2.6 Hz). IR (neat) ṽ = 658, 814, 1051, 1375, 1567, 1866, 2972 cm^{-1}. HRMS *calcd*. for $C_{29}H_{42}AuClN_2P^+$: 681.243414; *found* 681.243078.

Compound 46f

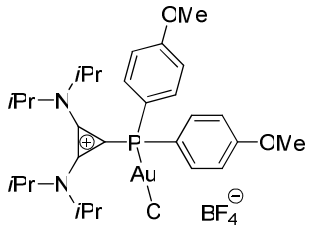

[AuCl(Me$_2$S)] (30.0 mg, 0.10 mmol) was added to a cooled (-20 ^{o}C) suspension of salt **43f** (57.0 mg, 0.10 mmol) in dry THF (4 mL) and the solution stirred at this temperature for 1 h. The solvent was then removed *in vacuo* at 0 ^{o}C, affording the desired product as an off white solid (79 mg, 99%). ^{1}H NMR (300 MHz, CD_2Cl_2) δ = 0.98 (d, *J* = 6.7 Hz, 12H), 1.32 (d, *J* = 6.7 Hz, 12H), 3.39 (sept, *J* = 6.7 Hz, 2H), 3.79 (s, 6H), 4.05 (sept, *J* = 6.7 Hz, 2H), 7.05 (dd, *J* = 13.9 Hz, *J* = 8.8 Hz, 4H), 7.80 ppm (dd, *J* = 8.8 Hz, *J* = 2.2 Hz, 4H). ^{31}P NMR (121 MHz, CD_2Cl_2) δ = 14.37 ppm. ^{13}C NMR (75 MHz, CD_2Cl_2) δ = 20.4, 20.5, 55.0, 97.2 (d, *J* = 42.0 Hz), 114.8 (d, *J* = 73.3 Hz), 115.0 (d, *J* = 14.8 Hz), 136.2 (d, *J* = 18.1 Hz), 136.9 (d, *J* = 7.1 Hz), 163.3 ppm (d, *J* = 2.6 Hz). IR (neat) $\tilde{\nu}$ = 688, 800, 1052, 1260, 1567, 1867, 2973 cm^{-1}. HRMS *calcd*. for $C_{29}H_{42}AuClO_2N_2P^+$: 713.233248; *found* 713.233797.

Compound 47a

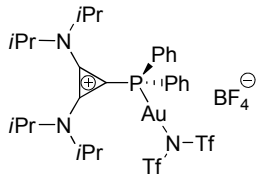

$AgNTf_2$ (77.6 mg, 0.20 mmol) was added to a cooled (0 ^{o}C) suspension of complex **46a** (148.2 mg, 0.20 mmol) in dry DCM (3 mL) and the solution stirred at this temperature for 1 h. The reaction mixture was then filtered through a Celite plug. After evaporation of the filtrate *in vacuo* the desired product was obtained as an off white solid (196 mg, 96%). ^{1}H NMR (400 MHz, CD_2Cl_2) δ = 0.95 (d, *J* = 7.2 Hz, 12H), 1.32 (d, *J* = 7.2 Hz, 12H), 3.27 (sept, *J* = 6.8 Hz, 2H), 4.08 (sept, *J* = 6.8 Hz, 2H), 7.52-7.66 (m, 6H), 7.81-7.95 ppm (m, 4H). ^{31}P NMR (161 MHz, CD_2Cl_2) δ = 14.47 ppm. ^{13}C NMR (100 MHz, CD_2Cl_2) δ = 21.9, 22.0, 55.4 (br.s), 94.6 (d, *J* = 54.8 Hz), 120.2 (q, *J* = 320.2 Hz), 124.3 (d, *J* = 71.6 Hz), 131.4 (d, *J* = 13.5 Hz), 135.2 (d, *J* = 2.5 Hz), 135.9 (d, *J* = 16.8 Hz), 139.0 ppm (d, *J* = 7.6 Hz).

IR (neat) $\tilde{\nu}$ = 691, 956, 1052, 1130, 1182, 1351, 1401, 1439, 1567, 1866, 2986 cm^{-1}. HRMS *calcd*. for $C_{29}H_{38}AuClN_3O_4F_6PS_2^{+}$: 898.160568; *found* 898.160583.

Compound 48a

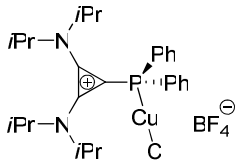

To a cooled (-20 °C) solid mixture of CuCl (26 mg, 0.26 mmol) and compound **43a** (67 mg, 0.13 mmol) a dry THF (2 mL) was added and the solution stirred at this temperature for 5 h. The solvent was removed *in vacuo*, the precipitate was dissolved in DCM (2 mL) and the resulting solution was filtered under argon and the filtrate concentrated *in vacuo* to give the desired product as a white solid (79 mg, 99%). ^{1}H NMR (300 MHz, CD_2Cl_2) δ = 0.93 (d, *J* = 6.9 Hz, 12H), 1.29 (d, *J* = 6.9 Hz, 12H), 3.31 (sept, *J* = 6.9 Hz, 2H), 4.02 (sept, *J* = 6.9 Hz, 2H), 7.41-7.56 (m, 6H), 7.67-7.77 ppm (m, 4H). ^{31}P NMR (121 MHz, CD_2Cl_2) δ = -15.24 ppm. ^{13}C NMR (75 MHz, CD_2Cl_2) δ = 23.4, 23.5, 55.5, 103.0 (d, *J* = 53.0 Hz), 129.3 (d, *J* = 38.2 Hz), 132.2 (d, *J* = 11.0 Hz), 134.8 (d, *J* = 1.9 Hz), 136.7 (d, *J* = 17.4 Hz), 140.1 ppm (d, *J* = 5.5 Hz). IR. (neat) $\tilde{\nu}$ = 694, 750, 1032, 1547, 1864, 2979 cm^{-1}. (ESI) MS *calcd*. for $C_{27}H_{38}ClCuN_2P^{+}$: 519.2; *found* 519.0.

Compound 48b

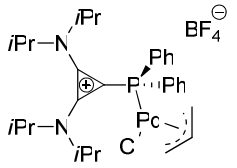

To a cooled (-20 °C) solid mixture of allyl palladium chloride dimer (24 mg, 0.06 mmol) and compound **43a** (66 mg, 0.13 mmol) a dry THF (6 mL) was added and the solution stirred at this temperature for 30 min. The solvent was removed *in vacuo*, affording the desired product as a white solid (89 mg, 99%). ^{1}H NMR (300 MHz, $CDCl_3$) δ = 0.94-1.00 (m, 12H), 1.42 (d, *J* = 7.0 Hz, 12H), 3.07 (d, *J* = 12.3 Hz, 1H), 3.38 (sept, *J* = 7.0 Hz, 2H), 3.82-3.93 (m, 1H), 4.07-4.22 (m, 3H), 4.97-5.06 (m, 1H), 5.64-5.80 (m, 1H), 7.52-7.68 (m, 6H), 7.85-7.99 (m, 2H), 7.99-8.12 ppm (m, 2H). ^{31}P NMR (121 MHz, $CDCl_3$) δ = 26.94 ppm. ^{13}C NMR

(100 MHz, $CDCl_3$) δ = 21.1, 21.2, 21.4, 53.6 (d, *J* = 122.0 Hz), 58.9, 77.2, 81.2 (d, *J* = 31.6 Hz), 100.3 (d, *J* = 23.1 Hz), 118.0 (d, *J* = 5.4 Hz), 127.9 (dd, *J* = 45.9 Hz, *J* = 24.6 Hz), 129.8 (t, *J* = 11.3 Hz), 132.5 (dd, *J* = 6.2 Hz, *J* = 2.2 Hz), 135.2 (d, *J* = 15.9 Hz), 138.9 ppm (d, *J* = 8.0 Hz). IR. (neat) ṽ = 699, 756, 1036, 1372, 1435, 1552, 1864, 2977 cm^{-1}. HRMS *calcd*. for $C_{30}H_{43}N_2ClPPd^+$: 603.189045; *found* 603.189620.

Compound 48c

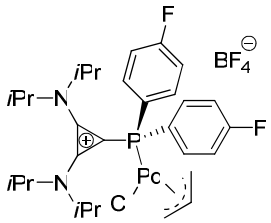

To a cooled (-20 °C) solid mixture of allyl palladium chloride dimer (17.6 mg, 0.05 mmol) and compound **43e** (52.0 mg, 0.10 mmol) a dry THF (4 mL) was added and the solution stirred at this temperature for 30 min. The solvent was removed *in vacuo*, affording the desired product as a pale yellow solid (69 mg, 99%). ^1H NMR (400 MHz, CD_2Cl_2) δ = 0.85-0.93 (m, 12H), 1.30 (d, *J* = 7.0 Hz, 12H), 3.00 (d, *J* = 12.0 Hz, 1H), 3.34 (sept, *J* = 7.0 Hz, 2H), 3.72-3.81 (m, 1H), 3.98-4.10 (m, 3H), 4.84-4.92 (m, 1H), 5.60-5.73 (m, 1H), 7.17-7.28 (m, 4H), 7.73-7.82 (m, 2H), 7.86-7.95 ppm (m, 2H). ^{31}P NMR (161 MHz, CD_2Cl_2) δ = 25.49 ppm. ^{13}C NMR (100 MHz, CD_2Cl_2) δ = 21.6, 21.6, 22.0, 55.1 (br.s), 60.6, 81.9 (d, *J* = 32.3 Hz), 101.1 (d, *J* = 21.3 Hz), 118.0 (ddd, *J* = 21.3 Hz, *J* = 13.1 Hz, *J* = 7.5 Hz), 119.4 (d, *J* = 5.2 Hz), 124.5 (dd, *J* = 48.7 Hz, *J* = 22.8 Hz), 138.4 (m), 139.3 (d, *J* = 7.7 Hz), 166.2 ppm (dd, *J* = 255.6 Hz, *J* = 5.3 Hz). IR. (neat) ṽ = 674, 844, 1031, 1230, 1359, 1548, 1854, 2987 cm^{-1}. HRMS *calcd*. for $C_{30}H_{41}N_2ClF_2PPd^+$: 639.170431; *found* 639.170937.

Compound 49

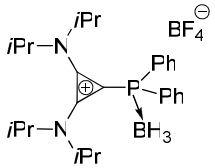

To a suspension of phosphenium salt **43a** (51 mg, 0.1 mmol) in dry THF a BH_3·THF solution (1M, 0.2 mL, 0.2 mmol) was added and the reaction mixture was stirred at room temperature

for 3h. The solvent was removed *in vacuo*, the residue washed with Et_2O (3 × 8 mL) and dried *in vacuo*. The product was obtained as a white solid (45 mg, 85%). ^{1}H NMR (400 MHz, CD_2Cl_2) δ = 0.88 (d, *J* = 6.9 Hz, 12H), 1.29-1.45(m, 15H), 3.42 (sept, *J* = 6.9 Hz, 2H), 4.04 (sept, *J* = 6.9 Hz, 2H), 7.49-7.61 (m, 6H), 7.82-7.90 ppm (m, 4H). ^{31}P NMR (161 MHz, CD_2Cl_2) δ = 14.97 ppm. ^{11}B (128 MHz, CD_2Cl_2) δ = -1.16, -37.80 (br.s). ^{13}C NMR (75 MHz, CD_2Cl_2) δ = 20.9, 22.1, 53.3 (br.s), 99.3 (d, *J* = 38.3 Hz), 125.6 (d, *J* = 60.7 Hz), 130.6 (d, *J* = 11.0 Hz), 134.2 (d, *J* = 2.5 Hz), 134.5 (d, *J* = 11.0 Hz), 138.8 ppm (d, *J* = 8.1 Hz). IR (neat) $\tilde{\nu}$ = 701, 741, 1048, 1558, 1866, 2378, 2973 cm^{-1}.

Compound 50

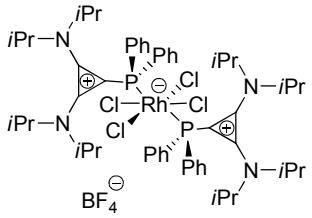

The mixture of phosphenium salt **43a** (60 mg, 0.118 mmol), $RhCl_3(H_2O)_3$ (12.3 mg, 0.059 mmol) and Et_4NCl (10.0 mg, 0.059 mmol) in ethanol (2.5 mL) was refluxed for 3 h. The solvent was removed *in vacuo* and the residue was purified by column chromatography (4:1 DCM : Acetone). The product was isolated from the first fraction as a dark-yellow solid (66.0 mg, 96%). ^{1}H NMR (300 MHz, CD_2Cl_2) δ = 1.03 (d, *J* = 6.6 Hz, 24H), 1.37 (d, *J* = 6.6 Hz, 24H), 3.83 (sept, *J* = 6.6 Hz, 4H), 4.00-4.18 (m, 4H), 7.26-7.39 (m, 12H), 8.27-8.37 ppm (m, 8H). ^{31}P NMR (121 MHz, CD_2Cl_2) δ = 16.67 ppm (d, *J* = 94.7 Hz). ^{13}C NMR (100 MHz, CD_2Cl_2) δ = 21.2, 21.6, 58.1, 100.5 (t, *J* = 13.4 Hz), 127.4 (t, *J* = 5.4 Hz), 129.0 (t, *J* = 26.3 Hz), 130.2, 134,2 (t, *J* = 5.5 Hz), 140.1 ppm (t, *J* = 3.5 Hz). IR (neat) $\tilde{\nu}$ = 697, 1055, 1435, 1538, 1873, 2980 cm^{-1}. HRMS *calcd*. for $C_{54}H_{76}Cl_4N_4P_2Rh^+$: 1085.334184; *found* 1085.334199.

Compound 53

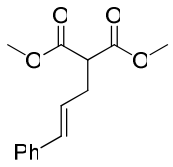

To a cooled (0 ºC) suspension of NaH (260 mg, 10.8 mmol) in dry THF (75 mL) dimethyl malonate **51** (1.4 mL, 11.9 mmol) was added dropwise and the mixture stirred for 30 min. Cinnamyl bromide **52** (1.6 mL, 10.8 mmol) was added dropwise and the solution was stirred overnight at room temperature. The reaction was quenched with sat. aq. NH_4Cl (75 mL). The aqueous layer was extracted with MTBE (3 × 75 mL) and the combined organic layers were washed with brine (2 × 25 mL) and dried over Na_2SO_4, filtered and concentrated *in vacuo*. The crude oil was purified by flash column chromatography (1:9 MTBE : hexane) to give the monoallylmalonate as transparent oil from the second fraction (2.02 g, 75%). ^{1}H NMR (400 MHz, $CDCl_3$) δ = 2.81 (dt, *J* = 7.4 Hz, *J* = 1.2 Hz, 2H), 3.54 (t, *J* = 7.6 Hz, 1H), 3.74 (s, 6H), 6.14 (dt, *J* = 15.7 Hz, *J* = 7.2 Hz, 1H), 6.48 (d, *J* = 15.7 Hz, 1H), 7.19-7.35 ppm (m, 5H). ^{13}C NMR (100 MHz, $CDCl_3$) δ = 32.2, 51.7, 52.5, 125.3, 126.2, 127.4, 128.4, 132.9, 136.9, 169.2 ppm; The spectroscopic data were consistent with the previously published values.[54]

Compound 54

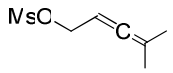

Methanesulfonyl chloride (0.95 mL, 12.1 mmol) was added dropwise *via* syringe to a cooled (0 °C) solution of 4-methyl-2,3-pentadien-1-ol **59** (0.99 g, 10.1 mmol), 4-(dimethylamino)-pyridine (124 mg, 1.01 mmol) and triethylamine (2.1 mL, 15.1 mmol) in dry DCM (50 mL), and the resulting mixture was stirred for 1 h at 0 °C. After that water (20 mL) was added to the reaction mixture and the aqueous layer was extracted with DCM (3 × 25 mL). The combined organic layers with ca. 10g crushed ice were washed with aq. HCl (1M, 1 × 50 mL), sat. aq. $NaHCO_3$ (2 × 50) mL and brine (2 × 50 mL), dried over anhydrous Na_2SO_4 and filtered. Removal of the volatile material *in vacuo* gave 4-methyl-2,3-pentadienyl methanesulfonate **54** as orange oil (1.58 g, 89%). The crude mesylate was used in the next step without further purification. ^{1}H NMR (400 MHz, $CDCl_3$) δ = 1.72 (d, *J* = 2.8 Hz, 6H), 3.02 (s, 3H), 4.68 (d, *J* = 7.3 Hz, 2H), 5.13-5.21 ppm (m, 1H). ^{13}C NMR (100 MHz, $CDCl_3$)

δ = 20.0, 31.5, 38.3, 69.5, 83.7, 98.2, 204.6 ppm; The spectroscopic data were consistent with the previously published values.[58]

Compound 55

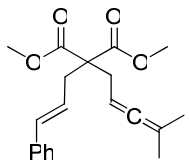

Dimethyl-2-cinnamylmalonate **53** (900 mg, 3.6 mmol) was added dropwise to a cooled (0 ºC) suspension of NaH (96 mg, 4.0 mmol) in dry THF (50 mL). After 30 min, a solution of allenyl mesylate **54** (828 mg, 4.7 mmol) in dry THF (15 mL) was added dropwise, followed by the addition of NaI (706 mg, 4.7 mmol) in one portion. The formed yellow suspension was stirred overnight at room temperature. The reaction mixture was quenched with sat. aq. NH_4Cl (50 mL). The aqueous layer was extracted with Et_2O (3 × 25 mL) and the combined organic layers were washed with brine (3 × 50 mL), dried over Na_2SO_4, filtered and evaporated. The crude oil was purified by column chromatography (1:9 MTBE : hexane) to give the desired product (1.0 g, 84%). ^{1}H NMR (400 MHz, $CDCl_3$) δ = 1.67 (s, 3H), 1.68 (s, 3H), 2.60 (d, *J* = 7.6 Hz, 2H), 2.85 (dd, *J* = 7.6 Hz, *J* = 1.3 Hz, 2H), 3.73 (s, 6H), 4.78-4.85 (m, 1H), 6.03 (dt, *J* = 15.5 Hz, *J* = 7.7 Hz, 1H), 6.44 (d, *J* = 15.5 Hz, 1H), 7.18-7.33 ppm (m, 5H). ^{13}C NMR (100 MHz, $CDCl_3$) δ = 20.5, 32.9, 36.0, 52.4, 58.2, 82.7, 95.2, 124.0, 126.2, 127.4, 128.5, 133.9, 137.1, 171.2, 203.8 ppm. The spectroscopic data were consistent with the previously published values.[54]

Compound 57

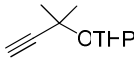

2-Methylbut-3-yne-2-ol (6.0 mL, 60 mmol) and 3,4-dihydro-2*H*-pyran (22.6 mL, 240 mmol) were added to a stirred solution of PPTS (0.77 g, 3.0 mmol) in DCM (30 mL). The reaction mixture was stirred at room temperature for 16 h and then concentrated under reduced pressure. The residue was dissolved in Et_2O (50 mL) and washed with water (25 mL). The organic phase was dried over Na_2SO_4, filtered and concentrated *in vacu*o. After vacuum distillation (85 °C, 13.4 mbar) the desired product was obtained as transparent liquid (9.31 g,

92%). ^{1}H NMR (400 MHz, $CDCl_3$) δ = 1.44-1.60 (m, 10H), 1.66-1.76 (m, 1H), 2.43 (s, 1H), 1.78-1.89 (m, 1H), 3.54-3.47 (m, 1H), 3.95 (ddd, *J* = 10.3 Hz, *J* = 5.9 Hz, *J* = 4.3 Hz, 1H), 5.06 ppm (dd, *J* = 5.4, 3.2 Hz, 1H). ^{13}C NMR (100 MHz, $CDCl_3$) δ = 20.4, 25.3, 29.8, 30.6, 31.9, 63.3, 70.8, 71.8, 86.4, 96.1 ppm. The spectroscopic data were consistent with the previously published values.[55]

Compound 58

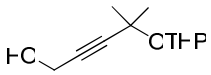

n-BuLi (1.6 M in hexane, 45.0 mL, 71.9 mmol) was added dropwise over 30 min to a cooled (-78 °C) solution of 2-(2-methylbut-3-yne-2-yloxy)tetrahydro-2*H*-pyran **57** (9.31 g, 55.3 mmol) in dry THF (150 mL). The mixture was allowed to warm to 0 °C and HMPA (12.0 mL, 65.6 mmol) and paraformaldehyde (3.32 g, 110.6 mmol) were added. The reaction mixture was stirred at room temperature for 2 h, and then quenched by a phosphate buffer solution (pH 6.9, 25 mL). The mixture was extracted with Et_2O (3 × 70 mL). The combined organic layer was washed with water (1M, 2 × 60 mL), dried over anhydrous Na_2SO_4 and filtered. After concentration and vacuum distillation (100 °C, 2.4 mbar) the desired product was obtained as transparent liquid (9.76 g, 89%). ^{1}H NMR (400 MHz, $CDCl_3$) δ = 1.47-1.54 (m, 9H), 1.64-1.95 (m, 4H), 3.45-3.56 (m, 1H), 3.90-3.98 (m, 1H), 4.26-4.31 (m, 2H), 5.02-5.08 ppm (m, 1H). ^{13}C NMR (100 MHz, $CDCl_3$) δ = 20.2, 25.4, 29.9, 30.5, 31.9, 51.1, 63.1, 70.9, 82.2, 88.1, 95.8 ppm. The spectroscopic data were consistent with the previously published values.[56]

Compound 59

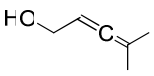

A solution of 4-methyl-4-(tetrahydropyran-2-yloxy)pent-2-yn-1-ol (9.76 g, 49.2 mmol) in dry Et_2O (30 mL) was added dropwise over 30 min to a cooled (0 °C) suspension of $LiAlH_4$ (4.67 g, 123 mmol) in dry Et_2O (120 mL). After being stirred at room temperature for 3 h, the reaction was quenched by addition of a mixture of Celite and sodium sulfate decahydrate (v/v = 1/1), and the mixture was filtered. The solvent was removed and the residue was

distilled under reduced pressure (35 °C, 2.4 mbar) to give pure methylpenta-2,3-dien-1-ol **59** as transparent oil (3.27 g, 67%). ^{1}H NMR (400 MHz, $CDCl_3$) δ = 1.65-1.75 (br.s, 1H), 1.70 (d, *J* = 3.2 Hz, 6H), 4.07 (d, *J* = 5.6 Hz, 2H), 5.16-5.22 ppm (m, 1H). ^{13}C NMR (100 MHz, $CDCl_3$) δ = 15.2, 20.6, 60.9, 65.8, 89.9, 200.5 ppm. The spectroscopic data were consistent with the previously published values.[57]

Compounds 62 and 65a

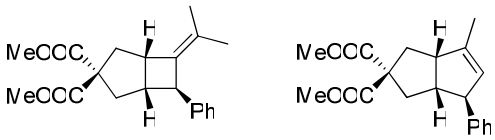

A mixture of gold catalyst **46a** (4.3 mg, 5.8 µmol) and $AgBF_4$ (1.1 mg, 5.8 µmol) in dry DCM (0.5 mL) was stirred at room temperature for 10 min. Then a solution of ene-allene **55** (38 mg, 116 µmol) in dry DCM (1.0 mL) was added to the reaction mixture. The reaction was stirred at room temperature and monitored by TLC analysis and GC-MS. Upon completion (2 h), the mixture was filtered through a short silica plug and eluted with DCM. Evaporation of the filtrate afforded the mixture of isomeric cycloadducts **62** and **65a** as transparent oil (30 mg, 78%). The ratio of the isomers was determined by ^{1}H NMR spectroscopy as **62**:**65a** = 97:3. The isomers were separated by flash column chromatography (2:1 DCM : Hexane). Compound **62** was isolated as major product. ^{1}H NMR (400 MHz, $CDCl_3$) δ = 1.29 (s, 3H), 1.60 (s, 3H), 2.22 (dd, *J* = 13.7 Hz, *J* = 8.8 Hz, 1H), 2.34 (dd, *J* = 13.3 Hz, *J* = 7.7 Hz, 1H), 2.57-2.63 (m, 1H), 2.71 (d, *J* = 13.4 Hz, 1H), 2.77 (dd, *J* = 13.8 Hz, *J* = 1.6 Hz, 1H), 3.71 (s, 3H), 3.55-3.62 (m, 1H), 3.67-3.70 (m, 1H), 3.72 (s, 3H), 7.14-7.20 (m, 3H), 7.25-7.32 ppm (m, 2H). ^{13}C NMR (100 MHz, $CDCl_3$) δ = 18.8, 18.8, 39.0, 40.1, 44.4, 44.6, 51.8, 52.4, 52.8, 62.6, 125.7, 127.0, 128.4, 129.2, 134.0, 144.9, 172.0, 172.8 ppm.

Compound **65a** was isolated as minor product. ^{1}H NMR (400 MHz, $CDCl_3$) δ = 1.37 (s, 3H), 1.64 (s, 3H), 2.11 (dd, *J* = 13.2 Hz, *J* = 4.8 Hz, 1H), 2.19 (dd, *J* = 12.8 Hz, *J* = 6.3 Hz, 1H), 2.49 (ddd, *J* = 12.5 Hz, *J* = 8.8 Hz, *J* = 1.0 Hz, 1H), 2.46 (ddd, *J* = 12.8, *J* = 8.4 Hz, *J* = 1.0 Hz, 1H), 2.54 (tdd, *J* = 8.3 Hz, *J* = 7.2 Hz, 2.0 Hz, 1H), 3.29-3.37 (m, 2H), 3.69 (s, 3H), 3.69 (s, 3H), 7.05 (d, *J* = 7.0 Hz, 2H), 7.17 (tt, *J* = 7.8 Hz, *J* = 1.4 Hz, 1H), 7.26 ppm (t, *J* = 7.0 Hz, 2H). ^{13}C NMR (100 MHz, $CDCl_3$) δ = 12.3, 12.6, 38.7, 41.8, 49.0, 52.4, 52.7, 53.7, 61.2, 63.5, 126.0, 127.3, 128.4, 133.6, 134.0, 146.1, 171.9, 172.6 ppm. The spectroscopic data were consistent with the previously published values.[54]

Compound 68

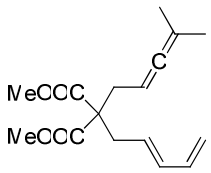

(*E*)-dimethyl-2-(penta-2,4-dienyl)malonate **73** (308 mg, 1.6 mmol) solution in dry THF (5 mL) was added dropwise to a cooled (0 ºC) suspension of NaH (41 mg, 1.7 mmol) in dry THF (10 mL). After 30 min, a solution of allenyl mesylate **54** (336 mg, 2.0 mmol) in dry THF (5 mL) was added dropwise, followed by the addition of NaI (303 mg, 2.0 mmol) in one portion. The formed suspension was stirred overnight at room temperature. The reaction mixture was quenched with sat. aq. $NaHCO_3$ (30 mL). The aqueous layer was extracted with EtOAc (3 × 20 mL), the organic phases dried over Na_2SO_4, filtered and evaporated. The crude oil was purified by column chromatography (1:15 EtOAc : hexane) to give the desired product (324 mg, 75%). ^{1}H NMR (400 MHz, $CDCl_3$) δ = 1.65 (s, 3H), 1.66 (s, 3H), 2.54 (d, *J* = 7.6 Hz, 2H), 2.72 (d, *J* = 7.6 Hz, 2H), 3.71 (s, 6H), 4.72-4.80 (m, 1H), 5.00 (d, *J* = 10.0 Hz, 1H), 5.51 (dt, *J* = 15.2 Hz, *J* = 7.6 Hz, 1H), 5.11 (d, *J* = 16.8 Hz, 1H), 6.09 (dd, *J* = 15.0 Hz, *J* = 10.4 Hz, 1H), 6.27 ppm (dt, *J* = 16.9 Hz, *J* = 10.3 Hz, 1H). ^{13}C NMR (100 MHz, $CDCl_3$) δ = 20.5, 32.8, 35.5, 52.4, 58.1, 82.6, 95.2, 116.4, 128.0, 135.0, 136.7, 171.2, 203.8 ppm. The spectroscopic data were consistent with the previously published values.[103]

Compounds 70 and 71

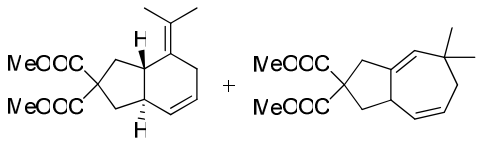

A mixture of gold catalyst **133** (2.1 mg, 2 µmol) and $AgBF_4$ (0.4 mg, 2 µmol) in dry DCM (0.5 mL) was stirred at room temperature for 10 min. Then, the solution was filtered and added to a stirred solution of (*E*)-dimethyl 2-(4-methylpenta-2,3-dienyl)-2-(penta-2,4-dienyl)malonate **68** (29 mg, 104 µmol) in dry DCM (1.0 mL). The reaction was stirred at room temperature and monitored by GC-MS analysis. Upon completion (after 1.5 h), the mixture was filtered through a short silica plug and eluted with DCM (2 × 2 mL). The filtrate

was evaporated and the obtained residue was subjected to column chromatography (1:10 EtOAc:hexane) to afford the mixture of desired isomers **70** and **71** as transparent oils (25 mg, 86%). The ratio of the isomers was determined by ^{1}H NMR spectroscopy as **70**:**71** = 97:3. Compound **70**:^{1}H NMR (400 MHz, $CDCl_3$) δ = 1.64 (s, 3H), 1.78 (s, 3H), 2.13-2.26 (m, 3H), 2.65 (dd, *J* = 12.8 Hz, *J* = 6.4 Hz, 1H), 2.74 (d, *J* = 20.1 Hz, 1H), 2.85 (d, *J* = 19.7 Hz, 1H), 2.99 (d, *J* = 7.6 Hz, 1H), 3.69-3.72 (m, 1H), 3.72 (s, 3H), 3.73 (s, 3H), 5.69-5.76 (m, 1H), 5.83 ppm (d, *J* = 9.2 Hz, 1H).^{13}C NMR (100 MHz, $CDCl_3$) δ = 21.8, 21.9, 31.4, 37.4, 39.8, 44.2, 48.2, 52.7, 52.7, 58.4, 123.9, 127.9, 127.9, 129.1, 173.2, 173.3 ppm.

Compound **71**: ^{1}H NMR (400 MHz, $CDCl_3$) δ = 0.95 (s, 3H), 1.00 (s, 3H), 1.83-1.89 (m, 1H), 2.07 (dd, *J* = 12.6 Hz, *J* = 11.1 Hz, 1H), 2.48 (dd, *J* = 14.9 Hz, *J* = 4.0 Hz, 1H), 2.60 (dddd, *J* = 12.6 Hz, *J* = 8.3 Hz, *J* = 1.3 Hz, *J* = 0.3 Hz, 1H), 2.88 (dt, *J* = 16.5 Hz, *J* = 2.3 Hz, 1H), 2.99 (dq, *J* = 16.4 Hz, *J* = 1.6 Hz, 1H), 3.49-3.57 (m, 1H), 3.71 (s, 3H), 3.74 (s, 3H), 5.15-5.19 (m, 1H), 5.67-5.76 (m, 2H). ^{13}C NMR (100 MHz, $CDCl_3$) δ = 28.6, 31.5, 34.3, 39.0, 39.1, 41.0, 41.9, 52.7, 52.8, 58.2, 129.1, 132.5, 135.0, 136.5, 172.0, 172.2. The spectroscopic data were consistent with the previously published values.[104]

Compound 72

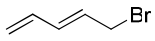

Phosphorus tribromide (1.03 mL, 10.9 mmol) was added to a cooled (0 °C) solution of (*E*)-penta-2,4-dien-1-ol (0.91 g, 10.9 mmol) in dry Et_2O (20 mL). After stirring at 0 °C for 1 h, water (10 mL) was carefully added. The layers were separated, the aqueous layer extracted with Et_2O (3 × 20 mL). The combined organic layers were washed with water (1 × 20 mL), $NaHCO_3$ (1 × 20 mL) and brine (1 × 20 mL), dried over Na_2SO_4, filtered and carefully concentrated under reduced pressure, using an ice bath, to afford bromide **72** as a pale yellow liquid (1.48 g, 93%). ^{1}H NMR (300 MHz, $CDCl_3$) δ = 4.04 (d, *J* = 7.9 Hz, 2H), 5.15 (d, *J* = 10.2 Hz, 1H), 5.26 (d, *J* = 16.2 Hz, 1H), 5.83 (dt, *J* = 13.9 Hz, *J* = 7.9 Hz, 1H), 6.23-6.39 ppm (m, 2H). ^{13}C NMR (75 MHz, $CDCl_3$) δ = 32.8, 119.4, 129.1, 135.2, 135.5 ppm. The spectroscopic data were consistent with the previously published values.[62]

Compound 73

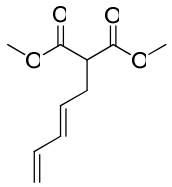

Dimethyl malonate **51** (0.53 mL, 4.5 mmol) was added dropwise to a cooled (0 ºC) suspension of NaH (98 mg, 4.1 mmol) in dry THF (30 mL) and the mixture stirred for 30 min. The solution of dienyl bromide **72** (60 mg, 4.1 mmol) was added dropwise. The obtained mixture was stirred overnight at room temperature and then quenched with sat. aq. NH_4Cl (30 mL). Aqueous layer was extracted with MTBE (3 × 30 mL) and combined organic layers were washed with brine (2 × 20 mL) and dried over Na_2SO_4, filtered and concentrated *in vacuo*. The crude oil was purified by flash column chromatography (1:9 MTBE : hexane) to give the monoallylmalonate as transparent oil from the second fraction (372 mg, 46%). ^{1}H NMR (400 MHz, $CDCl_3$) δ = 2.68 (t, *J* = 7.3 Hz, 2H), 3.45 (t, *J* = 7.6 Hz, 1H), 3.74 (s, 3H), 3.74 (s, 3H), 5.02 (d, *J* = 10.1 Hz, 1H), 5.14 (d, *J* = 16.9 Hz, 1H), 5.62 (dt, *J* = 15.7 Hz, *J* = 7.4 Hz, 1H), 6.12 (dd, *J* = 14.9 Hz, *J* = 10.6 Hz, 1H), 6.27 ppm (dd, *J* = 17.0 Hz, *J* = 10.2 Hz, 1H). ^{13}C NMR (100 MHz, $CDCl_3$) δ = 31.8, 51.6, 52.6, 116.6, 129.3, 133.8, 136.5, 169.2 ppm. The spectroscopic data were consistent with the previously published values.[61]

Compound 75

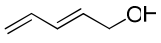

(*E*)-1,4-pentadienoic acid **74** (2.94 g, 30 mmol) was added to a cooled (-78 °C) suspension of $LiAlH_4$ (2.28 g, 60 mmol) in dry Et_2O (200 mL). The reaction mixture was stirred at -78 °C for 30 min, then allowed to warm to 0 °C and stirred for 2 h at that temperature, then allowed to warm to room temperature and stirred overnight. The reaction was quenched with water (10 mL), the precipitate was filtered, the filtrate was dried over Na_2SO_4 and concentrated under reduced pressure obtaining the product as transparent liquid (2.48 g, 98%). ^{1}H NMR (400 MHz, $CDCl_3$) δ = 4.16 (d, *J* = 5.7 Hz, 2H), 5.07 (dd, *J* = 10.1 Hz, *J* = 1.7 Hz, 1H), 5.19 (dd, *J* = 17.0 Hz, *J* = 1.7 Hz, 1H), 5.88 (dt, *J* = 15.2 Hz, *J* = 5.7 Hz, 1H), 6.22-6.38 ppm (m,

2H). ^{13}C NMR (100 MHz, $CDCl_3$) δ = 62.9, 117.3, 131.6, 132.7, 136.3 ppm. The spectroscopic data were consistent with the previously published values.[61]

Compound 78

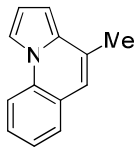

Catalyst **47a** (6.3 mg, 0.006 mmol) was added to a stirred solution of alkynylated phenylpyrrole **76** (58 mg, 0.32 mmol) in dry DCM (2.0 mL). The reaction mixture was stirred at room temperature for 5 h. Solvent was removed *in vacuo* and after column chromatography (1:20 EtOAc : hexane) the desired pyrrolo[1,2-*a*]quinoline **78** was isolated (57 mg, 98%). ^{1}H NMR (400 MHz, $CDCl_3$) δ = 2.47 (s, 3H), 6.57 (dd, *J* = 3.8 Hz, *J* = 1.4 Hz, 1H), 6.82 (dd, *J* = 3.7 Hz, *J* = 3 Hz, 1H), 6.87 (s, 1H), 7.35 (dt, *J* = 7.9 Hz, *J* = 1 Hz, 1H), 7.50 (dt, *J* = 7.3 Hz, *J* = 1.4 Hz, 1H), 7.65 (dd, *J* = 7.8 Hz, *J* = 1.3 Hz, 1H), 7.91 ppm (m, 2H). ^{13}CNMR (100 MHz, $CDCl_3$) δ = 18.7, 101.9, 113.0, 113.1, 114.7, 118.0, 124.2, 125.1, 127.5, 128.5, 132.7 ppm. The spectroscopic data were consistent with the previously published values.[63]

Compound 80

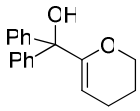

tert-Butyllithium (1.7 M in pentane, 8.4 mL, 14.2 mmol) was added dropwise to a cooled (-78 ºC) solution of 3,4-dihydro-2*H*-pyran (1.84 g, 21.6 mmol) in Et_2O (15 mL) and the mixture was stirred for 1 h, then was allowed to warm to 0 ºC and stirred for 3 h. The mixture was cooled to -78 ºC and benzophenone (2.59 g, 14.2 mmol) was added. The reaction mixture was allowed to warm to room temperature and stirred overnight. Saturated aqueous NH_4Cl (20 mL) was added to the reaction mixture followed by extraction with Et_2O (4 × 30 mL). The combined organic extracts were washed with brine (4 × 30 mL) and dried over Na_2SO_4 and concentrated *in vacuo*. The product was isolated after column chromatography (1:9 MTBE : hexane) as white solid (2.88 g, 76%). ^{1}H NMR (CD_2Cl_2,

300 MHz) δ = 1.71-1.81 (m, 2H), 1.93-2.01 (m, 2H), 3.34 (s, 1H), 3.94-4.00 (m, 2H), 4.29 (t, *J* = 3.8 Hz, 1H), 7.12-7.26 (m, 6H), 7.27-7.33 ppm (m, 4H). ^{13}C NMR (CD_2Cl_2, 75 MHz) δ = 21.0, 22.9, 67.5, 81.3, 102.2, 127.9, 128.4, 128.5, 145.4, 156.4 ppm. IR (neat) ṽ = 746, 890, 1019, 1061, 1153, 1446, 1665, 3446 cm^{-1}. HRMS *calcd*. for $C_{18}H_{18}O_2Na^+$: 289.119897; *found*: 289.119790.

Compounds 81 and 82

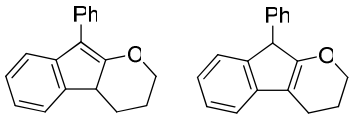

A mixture of the gold compound **46a** (5.0 mg, 0.007 mmol) and $AgBF_4$ (1.3 mg, 0.007 mmol) in dry DCM (1.0 mL) was stirred at room temperature for 10 min and then the precipitate was filtered off. The filtrate was added to a stirred solution of alcohol **80** (36.0 mg, 0.140 mmol) in dry DCM (1 mL) and stirred at room temperature overnight. After evaporation of the solvent the two isomeric products were separated by column chromatography (9:1 Hex : MTBE). The isomer **82** was isolated from the first fraction (27 mg, 79% yield). ^{1}H NMR (400 MHz, $CDCl_3$) δ = 1.98-2.07 (m, 2H), 2.41-2.55 (m, 2H), 4.12-4.24 (m, 2H), 4.41-4.45 (m, 1H), 6.95-7.00 (m, 1H), 7.04-7.09 (m, 2H), 7.11-7.15 (m, 2H), 7.18-7.25 (m, 2H), 7.26-7.31 ppm (m, 2H). ^{13}C NMR (100 MHz, $CDCl_3$) δ = 18.4, 22.2, 53.4, 68.2, 111.2, 116.4, 123.0, 123.4, 126.9, 127.0, 128.1, 128.7, 138.7, 141.4, 144.4, 161.8 ppm. IR (neat) ṽ = 697, 947, 1050, 1281, 1454, 1639, 2925 cm^{-1}. HRMS *calcd*. for $C_{18}H_{16}O$: 248.120116; *found*: 248.120154.

The minor isomer **81** was isolated from the second fraction (3.0 mg, 9%) ^{1}H NMR (400 MHz, CD_2Cl_2) δ = 1.32-1.43 (m, 1H), 1.74-1.83 (m, 1H), 1.98-2.11 (m, 1H), 2.49-2.59 (m, 1H), 3.25 (dd, *J* = 12.4 Hz, *J* = 6.6 Hz, 1H), 3.81 (dt, *J* = 10.7 Hz, *J* = 3.4 Hz, 1H), 4.23-4.31 (m, 1H), 7.03 (dt, *J* = 7.3 Hz, *J* = 1.0 Hz, 1H), 7.13-7.18 (m, 1H), 7.19-7.24 (m, 1H), 7.25-7.28 (m, 1H), 7.32-7.38 (m, 3H), 7.51-7.54 ppm (m, 2H). ^{13}C NMR (100 MHz, CD_2Cl_2) δ = 25.2, 26.7, 44.1, 71.3, 94.7, 119.5, 123.0, 123.9, 127.3, 127.5, 129.0, 129.3, 134.2, 141.9, 144.3, 162.3 ppm.

Compound 88

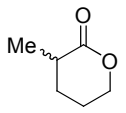

A solution of *n*-BuLi in hexane (1.6 M, 82.2 mL, 131.5 mmol) was added dropwise over 10 min to a cooled (0 ºC) solution of diisopropylamine (18.6 mL, 131.5 mmol) in dry THF (200 mL). The resulting solution was cooled to -78 ºC and stirred for 30 min. Then a solution of δ-valerolactone (10.0 mL, 107.8 mmol) and HMPA (23.1 mL, 131.5 mmol) in dry THF (100 mL) was added dropwise over 10 min and the reaction mixture was stirred at this temperature for 1 h. Methyl iodide (7.1 mL, 113.2 mmol) was added dropwise over 5 min and the resulting mixture was stirred for 2 h at -78 ºC. The reaction was quenched with sat. aq. NH_4Cl solution (200 mL) and heated to room temperature. The organic layer was separated; the water layer was extracted with Et_2O (3 × 200 mL) and the combined organic layers were dried over Na_2SO_4. After evaporation of the solvent, the residue was purified by column chromatography (1:1 Et_2O : pentane) to give the desired product (9.96 g, 81%). ^1H NMR (300 MHz, $CDCl_3$) δ = 1.28 (d, *J* = 6.9 Hz, 3H), 1.49-1.64 (m, 1H), 1.85-1.98 (m, 2H), 2.04-2.19 (m, 1H), 2.52-2.68 (m, 1H), 4.30-4.37 ppm (m, 2H). The spectroscopic data were consistent with the previously published values.[66]

Compound 89

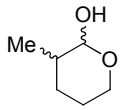

A solution of diisobutylaluminium hydride in hexane (1.0 M, 7.7 mL, 7.7 mmol) was added dropwise over 7 min to a cooled (-78 ºC) stirred solution of α-methyl-δ-valerolactone **88** (0.80 g, 7.0 mmol) in dry DCM (20 mL). The mixture was stirred for 30 min and then quenched with EtOAc (3 mL). The mixture was warmed to room temperature and then poured into a solution of sat. aq. Na-K tartrate (250 mL). The resulting mixture was vigorously stirred until both (aqueous and organic) layers were clear (2 h). The layers were separated, and the aqueous layer was extracted with DCM (4 × 100 mL). The combined organic layers were dried over Na_2SO_4, filtered, concentrated and purified by flash column chromatography (1:1 Et_2O : pentane) affording the desired product as mixture of diastereomers in ratio 0.3:0.7

(0.80 g, 99%). ^{1}H NMR (300 MHz, $CDCl_3$) δ = 0.95 (d, *J* = 6.9 Hz, 0.9H), 1.00 (d, *J* = 6.7 Hz, 2.1H), 1.19-1.28 (m, 2H), 1.42-1.66 (m, 2H), 1.79-1.90 (m, 1H), 2.39-2.62 (m, 0.3H), 2.76-2.99 (m, 0.7H), 3.45-3.57 (m, 1H), 3.89-4.06 (m, 1H), 4.35 (d, *J* = 7.7 Hz, 0.7H) 5.00 ppm (d, *J* = 3.0 Hz, 0.3H). The spectroscopic data were consistent with the previously published values.[66]

Compound 90a

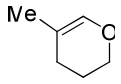

Heating a mixture of δ-lactol **89** (2.06 g, 17.8 mmol) and phosphorus pentoxide (0.02 g) in a short-path distillation apparatus afforded a distillate that was dried (K_2CO_3) and redistilled (100 °C, 200 mbar), yielding 2-methyl-3,4-dihydro-2*H*-pyran **90a** (0.91 g, 52%). ^{1}H NMR (300 MHz, $CDCl_3$) δ = 1.55-1.57 (m, 3H), 1.82-1.98 (m, 4H), 3.86-3.92 (m, 2H), 6.21-6.24 ppm (m, 1H). ^{13}C NMR (75 MHz, $CDCl_3$) δ = 19.1, 23.0, 25.5, 65.4, 109.1, 138.9 ppm. The spectroscopic data were consistent with the previously published values.[67]

Compound 90b

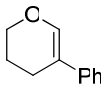

The mixture of δ-lactol **95** (0.68 g, 3.8 mmol) and phosphorus pentoxide (7.0 mg) in toluene (30 mL) was heated at 105 °C for 30 min. The sat. aq. $NaHCO_3$ (30 mL) was added, the organic layer was separated, the water layer was extracted with EtOAc (3 × 30 mL), the combined organic layers were dried over Na_2SO_4 and evaporated. The product was purified by column chromatography (5:1 hexane : EtOAc), yielding 2-phenyl-3,4-dihydro-2*H*-pyran **90b** (0.44 g, 72%). ^{1}H NMR (300 MHz, $CDCl_3$) δ = 1.98-2.08 (m, 2H), 2.41-2.48 (m, 2H), 4.05 (t, *J* = 5.2 Hz, 2H), 6.96 (s, 1H), 7.15-7.40 ppm (m, 5H). ^{13}C NMR (100 MHz, $CDCl_3$) δ = 23.1, 23.2, 66.4, 113.7, 124.7, 126.5, 129.1, 140.5, 142.8 ppm. IR (neat) $\tilde{\nu}$ = 698, 755, 1067, 1448, 1722, 2930 cm^{-1}.

Compound 94

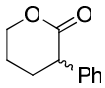

A solution of n-HexLi in hexane (2.47 M, 20.8 mL, 51.4 mmol) was added dropwise over 15 min to a cooled (-60 ºC) solution of phenylacetic acid (3.5 g, 25.7 mmol) in dry THF (100 mL). The reaction mixture was warmed to 0 ºC and stirred for 2 h. 1-Bromo-3-chloropropane (2.8 mL, 28.3 mmol) was added to a reaction mixture, the mixture was allowed to warm to room temperature and stirred for 18 h. The reaction was quenched with NaOH (1N, 50 mL). The aqueous layer was separated; the organic layer was extracted with NaOH (1N, 50 mL). The combined aqueous cuts were re-acidified with HCl (1N, 130 mL) and extracted with EtOAc (2 × 60 mL). The organic phase was washed with water (50 mL) and concentrated *in vacuo* to give oil that contains intermediate **93**. The oil was redissolved in THF (50 mL), treated with DBU (3.9 mL, 25.7 mmol) and heated at 60 ^{o}C for 18 h. The resultant slurry was cooled to room temperature, diluted with EtOAc (50 mL), filtered, the residue was washed with EtOAc (2 × 25 mL). The combined filtrates were concentrated *in vacuo* (at or below 25 ^{o}C). The product was purified by flash column chromatography (1:3 hexane : EtOAc) yielding the desired lactone **94** (4.00 g, 88%). ^{1}H NMR (300 MHz, $CDCl_3$) δ = 1.95-2.19 (m, 3H), 2.26-2.39 (m, 1H), 3.76-3.85 (m, 1H), 4.41-4.55 (m, 2H), 7.23-7.42 ppm (m, 5H). ^{13}C NMR (75 MHz, $CDCl_3$) δ = 22.4, 28.6, 47.5, 69.6, 127.7, 128.6, 129.1, 139.3, 172.8 ppm. The spectroscopic data were consistent with the previously published values.[68]

Compound 95

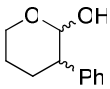

A solution of diisobutylaluminium hydride in hexane (1.0 M, 25.0 mL, 25.0 mmol) was added dropwise over 10 min to a cooled (-78 ºC) stirred solution of α-phenyl-δ-valerolactone **94** (4.0 g, 22.7 mmol) in dry DCM (50 mL). The mixture was stirred for 30 min and then quenched with EtOAc (6 mL). The mixture was warmed to room temperature and then poured into a solution of sat. aq. Na-K tartrate (1000 mL). The resulting mixture was vigorously stirred until both the aqueous and organic layers were clear (2 h). The layers were separated,

and the aqueous layer was extracted with DCM (4 × 300 mL). The combined organic layers were dried over Na_2SO_4, filtered, concentrated and purified by flash column chromatography (1:1 Et_2O : pentane), affording the desired product as mixture of diastereomers in ratio 0.4:0.6 (1.62 g, 40%). ^{1}H NMR for the diastereomer mixture (300 MHz, $CDCl_3$) δ = 1.43-1.98 (m, 4H), 1.99-2.40 (m, 1H), 2.56-3.10 (m, 1H), 3.44-3.81 (m, 1H), 3.99-4.19 (m, 1H), 4.81-4.88 (m, 0.6H), 5.25-5.35 (m, 0.4H), 7.19-7.44 ppm (m, 5H). ^{13}C NMR for the major diastereomer (300 MHz, $CDCl_3$) δ = 25.6, 30.7, 49.9, 66.7, 99.5, 127.2, 128.3, 128.6, 128.9 ppm. ^{13}C NMR for the minor diastereomer (300 MHz, $CDCl_3$) δ = 23.3, 26.1, 47.1, 60.0, 94.8, 127.1, 127.8, 128.3, 128.7 ppm.

Compound 96a

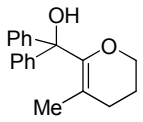

tert-Butyllithium (1.7 M in pentane, 1.2 mL, 2.1 mmol) was added dropwise to a cooled (-78 ºC) stirred solution of 5-methyl-3,4-dihydro-2*H*-pyran **90a** (0.30 g, 3.1 mmol) in dry Et_2O (3 mL) and the mixture was stirred for 1 h. The mixture was allowed to warm to 0 ºC and stirred for 3 h. After cooling down to -78 ºC a benzophenone (0.37 g, 2.1 mmol) was added. The reaction mixture was allowed to warm to room temperature and stirred overnight. Saturated aqueous NH_4Cl (20 mL) was added to the reaction mixture, and the mixture was extracted with Et_2O (4 × 15 mL). The combined organic extracts were washed with brine (2 × 15 mL) and dried over Na_2SO_4 and concentrated *in vacuo*. The residue was isolated after column chromatography (1:9 MTBE : hexane) as white solid (0.15 g, 26%). ^{1}H NMR (CD_2Cl_2, 300 MHz) δ = 0.93-0.95 (m, 3H), 1.74-1.84 (m, 2H), 1.96 (t, *J* = 6.6 Hz, 2H), 3.83 (t, *J* = 5.1 Hz, 2H), 3.88 (s, 1H), 7.14-7.29 ppm (m, 10H). ^{13}C NMR (CD_2Cl_2, 75 MHz) δ = 19.1, 24.0, 29.4, 66.9, 81.6, 108.1, 128.0, 128.5, 128.8, 146.5, 149.6 ppm. IR (neat) $\tilde{\nu}$ = 695, 761, 891, 1010, 1126, 1236, 1445, 1666, 3527 cm^{-1}. HRMS *calcd*. for $C_{19}H_{20}O_2Na^+$: 303.135551; *found*: 303.135833.

Compound 96b

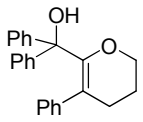

tert-Butyllithium (1.7 M in pentane, 0.7 mL, 1.2 mmol) was added dropwise to a cooled (-78 ºC) stirred solution of 5-phenyl-3,4-dihydro-2*H*-pyran **90b** (0.28 g, 1.8 mmol) in dry Et_2O (3 mL) and the mixture was stirred for 1 h. The mixture was allowed to warm to 0 ºC and stirred for 3 h. After cooling down to -78 ºC a benzophenone (0.21 g, 1.2 mmol) was added. The reaction mixture was allowed to warm to room temperature and stirred overnight. Saturated aqueous NH_4Cl (15 mL) was added to the reaction mixture, and the mixture was extracted with Et_2O (4 × 15 mL). The combined organic extracts were washed with brine (2 × 15 mL) and dried over Na_2SO_4 and concentrated *in vacuo*. The residue was isolated after column chromatography (1:9 MTBE : hexane) as white solid (0.10 g, 24%). ^{1}H NMR ($CDCl_3$, 400 MHz) δ = 1.83-1.91 (m, 2H), 2.23 (t, *J* = 6.6 Hz, 2H), 2.79 (s, 1H), 3.94 (t, *J* = 5.1 Hz, 2H), 6.80-6.85 (m, 2H), 6.95-7.00 (m, 3H), 7.07-7.17 (m, 6H), 7.18-7.24 ppm (m, 4H). ^{13}C NMR ($CDCl_3$, 100 MHz) δ = 22.7, 30.4, 65.4, 81.4, 112.8, 126.7, 127.1, 127.1, 127.9, 128.8, 141.1, 145.6, 151.2 ppm. IR (neat) $\tilde{\nu}$ = 695, 748, 1052, 1446, 1492, 1718, 2929 cm^{-1}. HRMS *calcd*. for $C_{24}H_{22}O_2Na^+$: 365.151195; *found*: 365.151081.

Compound 97

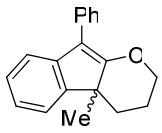

Catalyst **47a** (1.0 mg, 0.001 mmol) was added to a stirred solution of alcohol **96a** (0.1 mmol) in dry DCM (2 mL) and the reaction mixture stirred at room temperature for 30 min. The reaction mixture was then filtered through a silica plug. After evaporation of the filtrate the title compound was obtained (27 mg, 96% yield). ^{1}H NMR (300 MHz, CD_2Cl_2) δ = 1.30 (s, 3H), 1.45-1.61 (m, 2H), 2.13-2.31 (m, 2H), 3.54-3.64 (m, 1H), 4.28-4.36 (m, 1H), 7.06 (dt, *J* = 7.3, 1.3 Hz, 1H), 7.14 (dt, *J* = 7.4, 1.4 Hz, 1H), 7.18-7.26 (m, 2H), 7.31-7.38 (m, 3H), 7.47-7.52 ppm (m, 2H). ^{13}C NMR (75 MHz, CD_2Cl_2) δ = 22.9, 23.0, 33.8, 45.2, 73.3, 118.2, 120.3, 121.8, 124.6, 127.3, 127.5, 129.0, 129.4, 133.9, 142.3, 149.7, 166.2 ppm. IR (neat)

$\tilde{\nu}$ = 757, 1002, 1069, 1140, 1305, 1445, 1619, 2874, 2931 cm^{-1}. HRMS *calcd*. for $C_{19}H_{18}O$: 262.135762; *found*: 262.135495.

Compounds 98 and 99

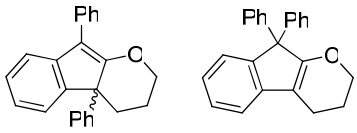

The mixture of the gold compound **46a** (5.1 mg, 0.0067 mmol) and $AgBF_4$ (1.3 mg, 0.0067 mmol) in dry DCM (1.0 mL) was stirred at room temperature for 10 min and then the precipitate was filtered off. The filtrate was added to a stirred solution of alcohol **96b** (47.0 mg, 0.140 mmol) in dry DCM (2 mL) and stirred at room temperature for 30 min. After evaporation of the solvent the two isomeric products were separated by preparative HPLC (150 mm YMC Pack ODS-A, 5 μm, 20 mm, Acetonitrile/Water 80:20). The compound **98** was isolated as a white solid (12 mg, 26% yield). ^{1}H NMR (400 MHz, CD_2Cl_2) δ = 1.55-1.63 (m, 1H), 1.71 (dt, *J* = 12.3 Hz, *J* = 4.0 Hz, 1H), 1.77-1.90 (m, 1H), 3.00-3.08 (m, 1H), 3.74 (dt, *J* = 11.0 Hz, *J* = 3.5 Hz, 1H), 4.13-4.21 (m, 1H), 6.96 (dt, *J* = 7.6 Hz, *J* = 1.3 Hz, 1H), 7.08 (dt, *J* = 7.6 Hz, *J* = 1.2 Hz, 1H), 7.12-7.17 (m, 2H), 7.20-7.35 (m, 4H), 7.37-7.43 (m, 4H), 7.58-7.64 ppm (m, 2H). ^{13}C NMR (100 MHz, CD_2Cl_2) δ = 23.0, 32.6, 72.7, 120.4, 121.0, 121.4, 123.0, 124.9, 127.1, 127.4, 127.5, 127.8, 129.1, 129.5, 129.7, 133.7, 142.2, 142.5, 148.5, 163.8 ppm. IR (neat) $\tilde{\nu}$ = 698, 747, 1051, 1631, 2924, 3356 cm^{-1}. HRMS *calcd*. for $C_{24}H_{20}O$: 324.151418; *found*: 324.151288.

The compound **99** was isolated as a white solid (25 mg, 56% yield). ^{1}H NMR (400 MHz, CD_2Cl_2) δ = 1.91-1.98 (m, 2H), 2.40 (t, *J* = 6.3 Hz, 2H), 4.13 (t, *J* = 5.2 Hz, 2H), 6.93 (dt, *J* = 7.5 Hz, *J* = 1.3 Hz, 1H), 7.00-7.03 (m, 1H), 7.05-7.08 (m, 1H), 7.09-7.19 ppm (m, 11H). ^{13}C NMR (100 MHz, CD_2Cl_2) δ = 19.1, 22.8, 64.5, 69.2, 111.8, 117.9, 123.9, 125.1, 127.5, 127.9, 128.8, 129.0, 143.8, 144.3, 145.6, 163.6 ppm. IR (neat) $\tilde{\nu}$ = 700, 740, 1050, 1645, 2923 cm^{-1}. HRMS *calcd*. for $C_{24}H_{20}O$: 324.151414; *found*: 324.151238.

Compound 113a

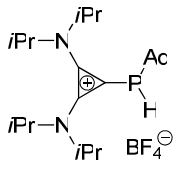

Adamantylphosphine (2.401 g, 14.3 mmol) was added to a mixture of chlorocyclopropenium salt **42** (2.559 g, 7.1 mmol) in THF (15 mL) and the resulting mixture was heated at 60 °C overnight. After cooling to room temperature, the solvent was removed *in vacuo*, the residue dissolved in DCM (40 mL) and the solution was washed with a saturated solution of $NaBF_4$ (6 × 35 mL). Once dried over Na_2SO_4, the organic phase was concentrated and the residue was purified by column chromatography (9:1 DCM : Acetone), getting the product from the first fraction as a white solid (3.030 g, 87%). ^{1}H NMR (400 MHz, $CDCl_3$) δ = 1.35 (d, *J* = 6.8 Hz, 18H), 1.41 (d, *J* = 6.8 Hz, 6H), 1.66-1.70 (m, 6H), 1.80-1.85 (m, 6H), 1.95-2.00 (m, 3H), 3.96 (sept, *J* = 6.8 Hz, 2H), 3.99 (d, *J* = 221.3 Hz, 1H), 4.13 ppm (sept, *J* = 6.8 Hz, 2H). ^{31}P NMR (161 MHz, $CDCl_3$) δ = -44.48 ppm. ^{13}C NMR (100 MHz, $CDCl_3$) δ = 20.6, 20.9, 21.0, 21.4, 28.4 (d, *J* = 8.6 Hz), 35.5, 36.7 (d, *J* = 11.2 Hz), 42.7 (d, *J* = 9.5 Hz), 51.4, 53.6, 101.9 (d, *J* = 67.7 Hz), 140.3 ppm. IR (neat) ν̃ = 607, 1045, 1153, 1376, 1543, 1863, 2903 cm^{-1}. HRMS *calcd*. for $C_{25}H_{44}N_2P^+$: 403.323658; *found* 403.323727.

Compound 113b

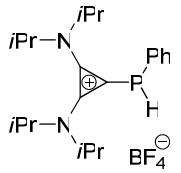

A solution of phenylphosphine in hexane (7.4 mL, 5.3 mmol, 10 %) was added to a mixture of chlorocyclopropenium salt **42** (630.0 mg, 1.8 mmol) in THF (6.0 mL) and the resulting mixture was heated at 60 °C overnight. After cooling to room temperature, the solvent was removed *in vacuo*, the residue dissolved in DCM (15 mL) and the solution was washed with a saturated solution of $NaBF_4$ (3 × 25 mL). Once dried over Na_2SO_4, the organic phase was concentrated and the residue washed with pentane (3 × 10 mL), affording the desired compound as a white solid (575 mg, 76%). ^{1}H NMR (300 MHz, $CDCl_3$) δ = 1.12 (d, *J* = 6.9 Hz, 6H), 1.31-1.46 (m, 18H), 3.64-3.80 (m, 2H), 4.14 (sept, *J* = 6.9 Hz, 2H), 5.63 (d,

J = 233.6 Hz, 1H) 7.44-7.51 (m, 3H), 7.64-7.72 ppm (m, 2H). ^{31}P NMR (161 MHz, $CDCl_3$) δ = -70.88 ppm. ^{13}C NMR (100 MHz, CD_2Cl_2) δ = 21.6, 21.8, 22.9, 50.8, 56.7, 105.5 (d, *J* = 58.7 Hz), 126.0, 130.4 (d, *J* = 8.1 Hz), 132.3, 137.1 (d, *J* = 20.2 Hz), 138.7 ppm (d, *J* = 4.1 Hz). IR (neat) $\tilde{\nu}$ = 729, 1032, 1349, 1558, 1872, 2984 cm^{-1}. HRMS *calcd*. for $C_{21}H_{34}N_2P^+$: 345.245415; *found* 345.245568.

Compound 114a

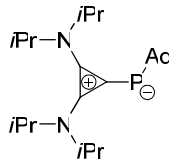

KHMDS (88.0 mg, 0.44 mmol) was added to a cooled (-40 °C) suspension of adamantylphosphanylidene **113a** (216.0 mg, 0.44 mmol) in dry THF (5 mL) and the resulting mixture was stirred for 1.5 h. The solvent was removed *in vacuo*, the yellowish residue was dissolved in dry DCM (3.0 mL) and the mixture was filtered under argon atmosphere. The filtrate was concentrated *in vacuo* and the residue was washed with Et_2O (6 × 5 mL). The corresponding product is stable at -20 °C (176 mg, 99%). ^{1}H NMR (300 MHz, toluene-d_8, -40 °C) δ = 0.95 (d, *J* = 6.7 Hz, 12H), 1.20 (d, *J* = 6.7 Hz, 12H), 1.83-1.89 (m, 6H), 2.10-2.15 (m, 3H), 2.38-2.44 (m, 6H), 3.39-3.56 (m, 2H), 3.99 ppm (sept, *J* = 6.7 Hz, 2H). ^{31}P NMR (121 MHz, toluene-d_8, -40 °C) δ = 2.28 ppm. ^{13}C NMR (75 MHz, toluene-d_8, -40 °C) δ = 21.4, 23.7 (br.s), 29.8, 29.9, 31.9, 32.4, 37.5, 45.4 (d, *J* = 13.2 Hz), 48.6, 49.3 (br.s), 123.3 (d, *J* = 30.3 Hz), 126.5 ppm (d, *J* = 16.1 Hz).

Compound 114b

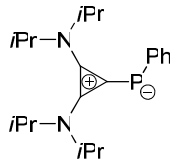

KHMDS (20.0 mg, 0.095 mmol) was added to a cooled (-40 °C) suspension of phenylphosphanylidene **113b** (41.0 mg, 0.095 mmol) in dry toluene-d_8 (1.5 mL) and the resulting mixture was stirred for 30 min. The suspension was filtered under argon atmosphere. After NMR experiments, the solution was concentrated *in vacuo*. The corresponding product

is stable at -20 °C (32 mg, 97%). ^{1}H NMR (300 MHz, toluene-d_8) δ = 0.95 (br.s, 24H), 3.31 (br.s, 4H), 7.12-7.17 (m, 3H), 8.03-8.10 ppm (m, 2H). ^{31}P NMR (121 MHz, toluene-d_8) δ = -36.86 ppm. ^{13}C NMR (75 MHz, toluene-d_8) δ = 22.5 (br.s), 49.3 (br.s), 82.4 (d, *J* = 239.9 Hz), 125.0 (d, *J* = 1.5 Hz), 125.6 (d, *J* = 4.9 Hz), 127.4 (d, *J* = 3.6 Hz), 137.0 ppm (d, *J* = 14.1 Hz).

Compound 115

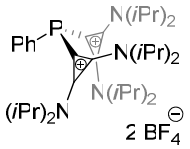

Dry THF (6 mL) was added to a cooled (- 40 °C) solid mixture of KHMDS (215.7 mg, 1.08 mmol) and phosphenium salt **113b** (425.0 mg, 0.98 mmol) and the solution stirred at this temperature for 2 h. Then chlorocyclopropenium salt **42** (353.0 mg, 0.98 mmol) was added, the reaction mixture was allowed to warm to room temperature and stirred overnight. The solvent was removed *in vacuo*, the residue was dissolved in DCM (15 mL) and the solution washed with a saturated solution of $NaBF_4$ (3 × 15 mL). Once dried over Na_2SO_4, the organic phase was concentrated and the residue washed with THF (3 × 10 mL) affording the desired compound as a white solid (516 mg, 69%). ^{1}H NMR (400 MHz, CD_2Cl_2) δ = 1.21 (d, *J* = 6.9 Hz, 12H), 1.25 (d, *J* = 6.9 Hz, 12H), 1.38 (d, *J* = 6.9 Hz, 12H), 1.44 (d, *J* = 6.9 Hz, 12H), 3.64 (sept, *J* = 6.9 Hz, 4H), 4.17 (sept, *J* = 6.9 Hz, 4H), 7.62-7.68 (m, 3H), 7.73-7.80 ppm (m, 2H). ^{31}P NMR (161 MHz, CD_2Cl_2) δ = -48.31 ppm. ^{13}C NMR (100 MHz, CD_2Cl_2) δ = 21.2, 21.5, 21.5, 21.6, 21.6, 21.7, 53.4, 54.8, 98.2 (d, *J* = 59.5 Hz), 125.0 (d, *J* = 4.6 Hz), 131.1 (d, *J* = 8.9 Hz), 133.0, 134.8 (d, *J* = 22.9 Hz), 140.0 ppm. IR (neat) ν̃ = 694, 1029, 1151, 1357, 1555, 1858, 2974 cm^{-1}. HRMS *calcd*. for $C_{36}H_{61}BF_4N_4P^+$: 667.467509; *found* 667.467401.

Compound 117

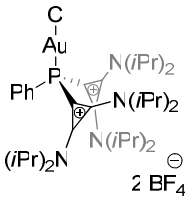

[AuCl(Me_2S)] (39.0 mg, 0.13 mmol) was added to a cooled (-20 °C) suspension of salt **115** (100.0 mg, 0.13 mmol) in dry THF (4 mL). The reaction mixture was allowed to warm to room temperature and stirred at this temperature for 2 h. The solvent was then removed *in vacuo* affording the desired product as a white solid (129 mg, 98%). ^{1}H NMR (400 MHz, CD_2Cl_2) δ = 1.25 (d, *J* = 7.0 Hz, 12H), 1.34 (d, *J* = 7.0 Hz, 12H), 1.45 (d, *J* = 7.0 Hz, 24H), 3.86 (sept, *J* = 7.0 Hz, 4H), 4.24 (sept, *J* = 7.0 Hz, 4H), 7.72-7.78 (m, 3H), 8.08-8.17 ppm (m, 2H). ^{31}P NMR (161 MHz, CD_2Cl_2) δ = -9.96 ppm. ^{13}C NMR (100 MHz, CD_2Cl_2) δ = 21.5, 21.7, 21.9, 55.5, 56.0, 90.9 (d, *J* = 53.2 Hz), 121.9 (d, *J* = 69.4 Hz), 131.5 (d, *J* = 14.2 Hz), 135.4, 135.4 (d, *J* =17.9 Hz), 138.9 ppm (d, *J* = 6.3 Hz). IR (neat) $\tilde{\nu}$ = 694, 1030, 1151, 1358, 1556, 1858, 2973 cm^{-1}. HRMS *calcd*. for $C_{36}H_{61}AuBClF_4N_4P^+$: 899.401161; *found* 899.401924.

Compound 118

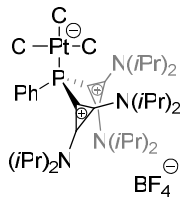

K_2PtCl_4 (48.4 mg, 0.117 mmol) was added to a solution of salt **115** (88.0 mg, 0.117 mmol) in dry DCM (3.0 mL). The reaction mixture was allowed to warm to room temperature and stirred overnight. The solvent was then removed *in vacuo* affording the desired product as a pale yellow solid (111 mg, 98%). ^{1}H NMR (400 MHz, CD_2Cl_2) δ = 1.10 (d, *J* = 6.4 Hz, 12H), 1.14 (d, *J* = 6.4 Hz, 12H), 1.33 (d, *J* = 7.0 Hz, 12H), 1.36 (d, *J* = 7.0 Hz, 12H), 4.05-4.18 (m, 4H), 4.29-4.43 (m, 4H), 7.58-7.67 (m, 3H), 8.37-8.46 ppm (m, 2H). ^{31}P NMR (161 MHz, CD_2Cl_2) δ = -21.24 ppm (*J* = 1994.8 Hz). ^{13}C NMR (100 MHz, CD_2Cl_2) δ = 17.5, 18.1, 18.5, 53.4, 90.6 (d, *J* = 51.5 Hz), 118.9 (d, *J* = 70.8 Hz), 126.8 (d, *J* = 12.9 Hz), 130.9 (d, *J* = 2.3 Hz), 133.5 (d, *J* = 13.5 Hz), 134.7 ppm (d, *J* = 8.6 Hz). IR (neat) $\tilde{\nu}$ = 679, 1050, 1148,

1376, 1557, 1850, 2977 cm^{-1}. HRMS *calcd*. for $C_{36}H_{61}Cl_3N_4PPt^+$: 880.333066; *found* 880.333903.

Compound 119

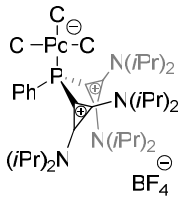

K_2PdCl_4 (18 mg, 0.053 mmol) was added to a solution of salt **115** (40 mg, 0.053 mmol) in dry DCM (2.0 mL). The reaction mixture was stirred overnight, then filtered through the syringe filter and the filtrate was concentrated *in vacuo* affording the desired product as a yelllow solid (46 mg, 98%). ^{1}H NMR (400 MHz, CD_2Cl_2) δ = 1.12 (d, *J* = 6.7 Hz, 12H), 1.16 (d, *J* = 6.7 Hz, 12H), 1.33 (d, *J* = 7.0 Hz, 12H), 1.36 (d, *J* = 7.0 Hz, 12H), 4.05-4.19 (m, 4H), 4.21-4.38 (m, 4H), 7.62-7.69 (m, 3H), 8.43-8.54 ppm (m, 2H). ^{31}P NMR (161 MHz, CD_2Cl_2) δ = -2.62 ppm. ^{13}C NMR (100 MHz, CD_2Cl_2) δ = 20.2, 20.2, 20.7, 21.2, 56.4 (br.s), 95.0 (d, *J* = 39.7 Hz), 121.1 (d, *J* = 59.2 Hz), 129.6 (d, *J* = 12.5 Hz), 134.0 (d, *J* = 2.8 Hz), 137.0 (d, *J* = 13.9 Hz), 137.2 ppm (d, *J* = 8.2 Hz). IR (neat) $\tilde{\nu}$ = 694, 1032, 1376, 1556, 1852, 2978 cm^{-1}. HRMS *calcd*. for $C_{36}H_{61}Cl_3N_4PPd^+$: 791.273514; *found* 791.273504.

Compound 120

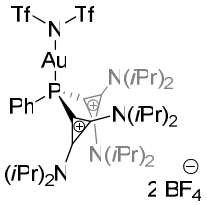

$AgNTf_2$ (9.0 mg, 0.023 mmol) was added to a cooled (0 °C) suspension of complex **117** (23.0 mg, 0.023 mmol) in dry DCM (2 mL) and the solution stirred at this temperature for 1 h. The reaction mixture was then filtered through a Celite plug. After evaporation of the filtrate *in vacuo* the desired product as an off white solid (26 mg, 90%). ^{1}H NMR (400 MHz, CD_2Cl_2) δ = 1.14 (d, *J* = 6.7 Hz, 12H), 1.23 (d, *J* = 6.7 Hz, 12H), 1.38 (d, *J* = 7.0 Hz, 24H), 3.78 (sept, *J* = 7.0 Hz, 4H), 4.15 (sept, *J* = 6.7 Hz, 4H), 7.70-7.79 (m, 3H), 8.15 ppm (dd, *J* = 16.4 Hz,

J = 6.8 Hz, 2H). ^{31}P NMR (161 MHz, CD_2Cl_2) δ = -5.53 ppm. ^{13}C NMR (100 MHz, CD_2Cl_2) δ = 21.6, 23.1, 23.1, 55.9, 89.5 (d, *J* = 56.6 Hz), 120.5 (d, *J* = 67.9 Hz), 120.1 (q, *J* = 321.5 Hz,), 131.7 (d, *J* = 14.2 Hz), 136.1 (d, *J* =2.8 Hz), 136.4 (br.s), 139.0 ppm (br.s). IR (neat) $\tilde{\nu}$ = 693, 1028, 1151, 1360, 1560, 1868, 2966 cm^{-1}. HRMS *calcd*. for $C_{38}H_{61}AuBF_{10}N_5O_4S_2P^+$: 1144.351283; *found* 1144.352705.

Compound 121

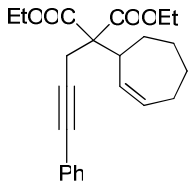

$PdCl_2(PPh_3)_2$ (0.06 g, 0.08 mmol) and CuI (0.02 g, 0.08 mmol) were added to a stirred solution of enyne **103** (1.19 g, 4.1 mmol) and iodobenzene (0.5 mL, 4.5 mmol) in dry Et_3N (40 mL). The reaction mixture was heated at 50 °C overnight. The mixture was cooled to room temperature, then filtered and washed with MTBE (50 mL), and filtrate was concentrated *in vacuo*. The product was purified by bulb-to-bulb distillation followed by column chromatography (1:15 MTBE : hexane), affording the desired product as colorless oil (1.05 g, 70%). ^{1}H NMR (300 MHz, $CDCl_3$) δ = 1.26 (t, *J* = 7.1 Hz, 3H), 1.27 (t, *J* = 7.1 Hz, 3H), 1.30 (m, 2H), 1.71 (m, 2H), 2.01 (m, 2H), 2.24 (m, 2H), 3.07 (s, 2H), 3.29 (m, 1H), 4.23 (m, 4H), 5.83 (m, 2H), 7.27 (m, 3H), 7.36 ppm (m, 2H). ^{13}C NMR (75 MHz, $CDCl_3$): δ = 14.1, 14.2, 24.1, 26.1, 28.0, 29.8, 31.6, 43.0, 60.7, 61.4, 61.5, 83.2, 85.5, 123.6, 127.8, 128.2, 131.5, 131.9, 133.0, 170.0, 170.1 ppm. The spectroscopic data were consistent with the previously published values.[81]

Compound 122

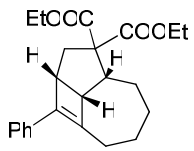

$PtCl_2$ (3.1 mg, 0.012 mmol) and ligand **115** (8.8 mg, 0.012 mmol) were added to a solution of enyne **121** (43 mg, 0.12 mmol) in dry toluene (1.5 mL). The reaction mixture was heated at 80 °C for 3 h. After concentration, the residue was purified by flash column chromatography

(1:10 EtOAc : hexane), affording the product as colorless oil (41 mg, 95%). ^{1}H NMR (400 MHz, $CDCl_3$) δ = 1.19 (t, *J* = 7.1 Hz, 3H), 1.26 (t, *J* = 7.1 Hz, 3H), 1.51 (m, 4H), 1.82 (m, 2H), 2.20 (m, 1H), 2.29 (ddd, *J* = 13.8 Hz, *J* = 8.1 Hz, *J* = 0.9 Hz, 1H), 2.38 (dd, *J* = 13.8 Hz, *J* = 7.3 Hz, 1H), 3.24 (m, 1H), 2.83 (m, 2H), 3.52 (m, 1H), 4.15 (m, 4H), 7.19 (m, 1H), 7.30 ppm (m, 4H). ^{13}C NMR (100 MHz, $CDCl_3$): δ = 14.1, 14.2, 27.5, 27.6, 28.6, 29.6, 32.2, 40.9, 42.5, 49.8, 60.9, 61.3, 71.5, 125.7, 126.7, 128.5, 135.0, 140.3, 145.4, 169.7, 172.4 ppm. The spectroscopic data were consistent with the previously published values.[81]

Compound 124

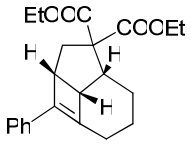

$PtCl_2$ (2.4 mg, 0.009 mmol) and ligand **115** (6.8 mg, 0.009 mmol) were added to a solution of enyne **123** (32 mg, 0.09 mmol) in dry toluene (1.0 mL). The reaction mixture was heated at 80 ^{o}C for 3 h. After concentration, the residue was purified by flash column chromatography (1:10 EtOAc : hexane), affording the product as colorless oil (30 mg, 94%). ^{1}H NMR (400 MHz, $CDCl_3$) δ = 1.14 (t, *J* = 7.1 Hz, 3H), 1.21 (t, *J* = 7.1 Hz, 3H), 1.24-1.30 (m, 1H), 1.48-1.62 (m, 3H), 2.27 (ddd, *J* = 14.1 Hz, *J* = 7.8 Hz, *J* = 0.6 Hz, 1H), 2.47 (dd, *J* = 14.1 Hz, *J* = 5.0 Hz, 2H), 2.52-2.65 (m, 1H), 2.77-2.87 (m, 1H), 3.17-3.24 (m, 1H), 3.31-3.39 (m, 1H), 3.99-4.15 (m, 2H), 4.12-4.29 (m, 2H), 7.16-7.38 ppm (m, 5H). ^{13}C NMR (100 MHz, $CDCl_3$): δ = 12.9, 13.0, 20.5, 22.5, 24.9, 33.0, 39.7, 41.4, 45.4, 59.9, 64.8, 68.0, 124.4, 125.7, 127.4, 133.8, 141.0, 141.8, 169.2, 171.8 ppm. The spectroscopic data were consistent with the previously published values.[81]

Compound 125

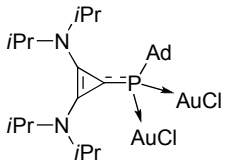

Compound **114a** (0.15 mmol, prepared *in situ* as described above) was dissolved inTHF at -40 °C. Then (Me_2S)AuCl (88.4 mg, 0.30 mmol) was added and the reaction mixture was stirred at room temperature for 30 min. The solvent was removed *in vacuo*, the residue washed with Et_2O (3 × 5 mL) and dried *in vacuo*. The product was obtained as a white solid (129 mg, 99%). ^{1}H NMR (400 MHz, $CDCl_3$) δ = 1.26 (d, *J* = 6.9 Hz, 12H), 1.41 (d, *J* = 6.6 Hz, 12H), 1.48-1.57 (m, 6H), 1.83-1.90 (m, 9H), 3.90-4.05 (m, 2H), 4.72-4.90 ppm (m, 2H). ^{31}P NMR (161 MHz, $CDCl_3$) δ = 10.91 ppm. ^{13}C NMR (100 MHz, $CDCl_3$) δ = 22.2, 28.8 (d, *J* = 11.6 Hz), 30.9, 36.2, 42.2(d, *J* = 26.5 Hz), 43.8 (d, *J* = 3.8 Hz), 55.3, 124.2 (d, *J* = 763.4 Hz), 148.6 ppm (d, *J* = 70.8 Hz). IR (neat) $\tilde{\nu}$ = 677, 840, 1451, 1530, 1853, 2901 cm^{-1}. HRMS *calcd*. for $C_{25}H_{43}N_2Au_2Cl_2PNa^+$: 889.176417; *found* 889.176486.

Compound 126

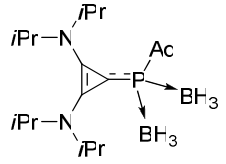

Compound **114a** (0.114 mmol, prepared *in situ* as described above) was dissolved inTHF at -30 °C. Then BH_3·THF solution (1M, 0.34 mL, 0.432 mmol) was added and the reaction mixture was stirred at room temperature for 30 min. The solvent was removed *in vacuo*, the residue washed with Et_2O (3 × 8 mL) and dried *in vacuo*. The product was obtained as a white solid (19 mg, 39%). ^{1}H NMR (400 MHz, CD_2Cl_2) δ = 0.04-0.93 (m, 6H), 1.22-1.41 (m, 24H), 1.55-1.68 (m, 6H), 1.71-1.80 (m, 6H), 1.83-1.93 (m, 3H), 3.90-4.11 (m, 2H), 4.74-4.94 ppm (m, 2H). ^{31}P NMR (161 MHz, CD_2Cl_2) δ = 8.90 ppm. ^{11}B NMR (128 MHz, CD_2Cl_2) δ = -36.0 (d, *J* = 47.6 Hz), δ = -35.6 (d, *J* = 47.6 Hz) ppm. ^{13}C NMR (100 MHz, CD_2Cl_2) δ = 22.0, 23.1, 29.4 (d, *J* = 8.1 Hz), 34.0 (d, *J* = 22.2 Hz), 37.5, 39.1, 57.1, 111.6 (d, *J* = 17.2 Hz), 142.2 (d, *J* = 9.1 Hz) ppm. IR (neat) $\tilde{\nu}$ = 670, 1051, 1359, 1524, 1851, 2356, 2904 cm^{-1}. (ESI) MS *calcd*. for $C_{25}H_{49}B_2N_2P^+$: 430.4; *found* 430.1.

Compound 134a

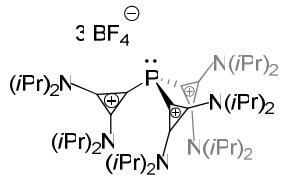

Tris(trimethylsilyl)phosphine (0.1 mL, 0.34 mmol) was added to a stirred suspension of chlorocyclopropenium salt **42** (369.0 mg, 1.03 mmol) in freshly distilled fluorobenzene (5.0 mL) and the solution was heated at 60 °C overnight. After cooling to room temperature, the solvent was removed *in vacuo*, the residue was washed with THF (5 × 8 mL) and dried *in vacuo*, affording the desired product as a white solid (75 mg, 22%). ^{1}H NMR (400 MHz, CD_2Cl_2) δ = 1.40 (d, *J* = 6.9 Hz, 36H), 1.46 (d, *J* = 6.9 Hz, 36H), 3.93-4.04 (m, 6H), 4.29 ppm (sept, *J* = 6.9 Hz, 6H). ^{31}P NMR (161 MHz, CD_2Cl_2) δ = -76.90 ppm. ^{13}C NMR (100 MHz, CD_2Cl_2) δ = 21.4, 21.9, 22.0, 57.4, 90.5 (d, *J* = 52.8 Hz), 140.1 ppm (d, *J* = 3.4 Hz). IR (neat) $\tilde{\nu}$ = 689, 1032, 1146, 1354, 1568, 1852, 2976 cm^{-1}. HRMS *calcd*. for $C_{45}H_{84}B_4F_{16}N_6P^-$: 1087.666055; *found* 1087.665515.

Compound 134b

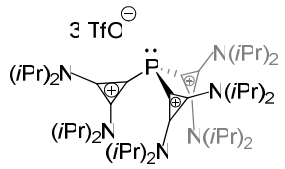

n-BuLi (0.64 mL, 1.6 M, 1.02 mmol) was added dropwise to a cooled (-78 °C) suspension of chlorocyclopropenium salt **133** (430.0 mg, 1.02 mmol) in dry THF (20 mL) and the reaction mixture was stirred for 20 min. Then PCl_3 (30 µL, 0.34 mmol) was added, the reaction mixture slowly allowed to reach room temperature and then stirred overnight. Afterwards, the solvent was removed *in vacuo* and the residue washed with THF (4 × 8 mL) and dried, affording the desired product as a white solid (184 mg, 45%). ^{1}H NMR (400 MHz, CD_2Cl_2) δ = 1.40 (d, *J* = 6.8 Hz, 36H), 1.45 (d, *J* = 6.8 Hz, 36H), 4.03 (dsept, *J* = 1.8 Hz, *J* = 6.8 Hz, 6H), 4.33 ppm (sept, *J* = 6.8 Hz, 6H). ^{31}P NMR (161 MHz, CD_2Cl_2) δ = -76.40 ppm. ^{13}C NMR (100 MHz, CD_2Cl_2) δ = 21.8, 22.4, 22.4, 54.1 (br.s), 57.8 (br.s), 90.8 (d, *J* = 52.5 Hz), 121.6 (q, *J* = 321.6 Hz), 140.4 ppm (d, *J* = 3.1 Hz). IR (neat) $\tilde{\nu}$ = 686, 1029,

1142, 1260, 1378, 1568, 1848, 2984 cm^{-1}. HRMS *calcd*. for $C_{47}H_{84}F_6N_6O_6PS_2^+$: 1037.553010; *found* 1037.553102.

Compound 136

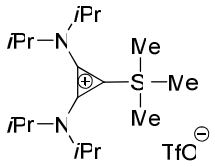

n-BuLi solution in hexane (0.28 mL, 0.45 mmol, 1.6M) was added dropwise to a cooled (-78 ^oC) suspension of chlorocyclopropenium salt **133** (189.0 mg, 0.45 mmol) in dry diethylether (3.0 mL) and the mixture was stirred for 20 min. The mixture was allowed to warm to room temperature and the solvent was removed *in vacuo*. The residue was dissolved with dry fluorobenzene (1.0 mL) and trimethylsilyl trifluoromethanesulfonate (0.17 mL, 0.90 mmol) was added, and then the mixture stirred at room temperature for 1h. The solvent was removed *in vacuo*, the residue was washed with dry DCM (3 × 2 mL), the filtrate was concentrated yielding the corresponding product as pale yellow air sensitive solid (108 mg, 52%). ^1H NMR (400 MHz, CD_2Cl_2) δ = 0.45 (s, 9H), 1.37 (d, *J* = 6.9 Hz, 12H), 1.40 (d, *J* = 6.9 Hz, 12H), 3.99 (sept, *J* = 6.9 Hz, 2H), 4.12 ppm (sept, *J* = 6.9 Hz, 2H). ^{13}C NMR (100 MHz, CD_2Cl_2) δ = -0.1, 20.6, 21.5, 54.4, 111.4, 121.4 (quart, *J* = 321.8 Hz), 141.5 ppm. ^{29}Si NMR (80 MHz, CD_2Cl_2) δ = -7.49 ppm. IR (neat) $\tilde{\nu}$ = 845, 1030, 1138, 1267, 1532, 1864, 2983 cm^{-1}. HRMS *calcd*. for $C_{18}H_{37}N_2Si$: 309.272048; *found*: 309.271979.

Compound 137

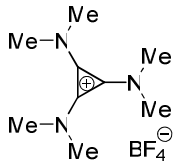

An excess of dimethylamine (~ 15 mL) was condensed in a cooled (-78 ^oC) flask, then dry DCM (40 mL) was slowly added. The solution of 1,1,2,3-tetrachloropropene (7.0 mL, 59.8 mmol) in dry DCM (13 mL) was slowly added to a stirred reaction mixture *via* syringe pump over 1 h. The reaction mixture was stirred at -78 ^oC for 4 h, before it was heated to 0 ^oC and stirred 1 h; then was heated to room temperature and stirred overnight. Then the reaction

mixture was refluxed for 3 h. After cooling to room temperature, HBF_4 (48% solution in water, 15 mL) was added and the reaction mixture stirred for 10 min. The aqueous layer was separated, the organic layer was dried over Na_2SO_4 and concentrated *in vacuo* to give the product as white solid (11.03 g, 72%). ^{1}H NMR (300 MHz, $CDCl_3$) δ = 3.12 ppm (s, 18H). ^{13}C NMR (75 MHz, $CDCl_3$) δ = 42.7, 118.4 ppm. HRMS *calcd*. for $C_9H_{18}N_3BF_4$: 255.152992; *found*: 255.152901. The spectroscopic data were consistent with the previously published values.[105]

Compound 138

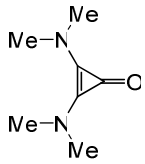

A mixture of cyclopropenium salt **137** (5.50 g, 21.6 mmol) and KOH (12.10 g, 216 mmol) in water (68.5 mL) was heated at 65 °C for 2 h. After cooling to room temperature the mixture was extracted with DCM (4 × 40 mL), the combined extracts were dried over Na_2SO_4 and concentrated *in vacuo* to give the desired product (2.99 g, 99%). ^{1}H NMR (300 MHz, $CDCl_3$) δ = 2.97 ppm (s, 12H). ^{13}C NMR (75 MHz, $CDCl_3$) δ = 41.7, 121.6, 134.4 ppm. IR (neat) $\tilde{\nu}$ = 727, 1181, 1392, 1500, 1594, 1888, 2882 cm^{-1}. HRMS *calcd*. for $C_7H_{12}N_2O$: 140.094960; *found*: 140.094853. The spectroscopic data were consistent with the previously published values.[106]

Compound 139

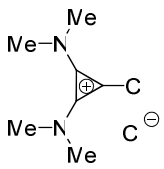

Oxalyl chloride (6.4 mL, 73.5 mmol) was slowly added to cooled (0 °C) ketone **138** (3.22 g, 23.0 mmol). The strong gas evolution was observed. The reaction mixture was stirred at room temperature for 15 min, then excess of oxalyl chloride was removed *in vacuo*, getting the chlorochyclopropenium salt (4.47 g, 99%). ^{1}H NMR (300 MHz, $CDCl_3$) δ = 3.37 ppm (d,

J = 27.9 Hz 12H). ^{13}C NMR (75 MHz, $CDCl_3$) δ = 42.3, 43.3, 92.2, 135.2 ppm. The spectroscopic data were consistent with the previously published values.[107]

Compound 140

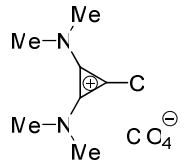

A solution of chlorocyclopropenium salt **139** (5.2 g, 26.6 mmol) in dry acetonitrile (20 mL) was added to a solution of magnesium perchlorate (3.00 g, 13.3 mmol) in dry acetonitrile (25 mL). The formed precipitate was filtered off and washed with acetonitrile (10 mL). After evaporation of the filtrate, the desired salt was obtained (6.62 g, 96%). ^{1}H NMR (300 MHz, CD_2Cl_2) δ = 3.18 ppm (d, *J* = 3.8 Hz, 12H). ^{13}C NMR (100 MHz, CD_2Cl_2) δ = 42.0, 42.7, 92.5, 135.0 ppm. The spectroscopic data were consistent with the previously published values.[108]

Compound 141

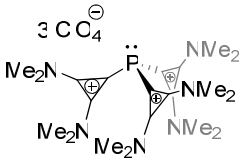

Tris(trimethylsilyl)phosphine (0.1 mL, 0.34 mmol) was added to a stirred suspension of chlorocyclopropenium salt **140** (267.0 mg, 1.03 mmol) in freshly distilled fluorobenzene (6.0 mL) and the solution was heated at 60 °C for 3 days. After cooling to room temperature, the solvent was removed *in vacuo*, the residue was washed with CH_2Cl_2 (3 × 10 mL) and dried *in vacuo*, affording the desired product as a pale orange solid (175 mg, 73%). ^{1}H NMR (500 MHz, CD_3CN) δ = 3.20 (s, 18H), 3.27 ppm (s, 18H). ^{31}P NMR (202 MHz, CD_3CN) δ = -93.48 ppm. ^{13}C NMR (125 MHz, CD_3CN) δ = 43.7, 43.8, 93.2 (d, *J* = 51.8 Hz), 142.4 ppm. IR (neat) $\tilde{\nu}$ = 752, 1073, 1217, 1409, 1620, 1902, 2947, 3597 cm^{-1}. HRMS *calcd*. for $C_{21}H_{36}N_6O_8Cl_2P^+$: 601.170382; *found* 601.171374.

Compound 142

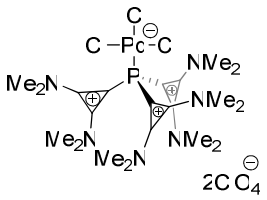

K_2PdCl_4 (10 mg, 0.03 mmol) was added to a cooled (-20 ^oC) solution of **141** (21 mg, 0.03 mmol) in dry acetonitrile (2.5 mL). The reaction mixture was allowed to reach room temperature and stirred overnight. The precipitate was filtered off and the filtrate concentrated *in vacuo* to afford the desired product as an orange solid (22 mg, 92%). ^1H NMR (400 MHz, CD_3CN) δ = 3.30 (s, 18H), 3.36 ppm (s, 18H). ^{31}P NMR (161 MHz, CD_3CN) δ = -46.10 ppm. ^{13}C NMR (100 MHz, CD_3CN) δ = 44.1, 44.6, 86.7 (d, *J* = 60.0 Hz), 140.8 ppm (d, *J* = 7.8 Hz). IR (neat) $\tilde{\nu}$ = 742, 1075, 1221, 1410, 1615, 1902, 3434 cm^{-1}. HRMS *calcd*. for $C_{21}H_{36}Cl_{14}N_6O_4PPd^+$: 713.031965; *found* 713.032286.

Compound 143

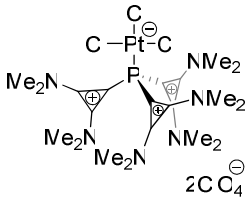

K_2PtCl_4 (39 mg, 0.094 mmol) was added solution of salt **141** (66 mg, 0.094 mmol) in dry acetonitrile (3 mL) and the reaction mixture was stirred overnight. The precipitate was filtered off and the filtrate concentrated *in vacuo* to afford the desired product as an yellow-orange solid (74 mg, 87%). ^1H NMR (400 MHz, CD_3CN) δ = 3.34 (s, 18H), 3.40 ppm (s, 18H). ^{31}P NMR (161 MHz, CD_3CN) δ = -62.43 ppm. ^{13}C NMR (100 MHz, CD_3CN) δ = 42.8, 43.2, 84.4 (d, *J* = 73.2 Hz), 139.5 ppm (d, *J* = 7.6 Hz). IR (neat) $\tilde{\nu}$ = 755, 1077, 1217, 1407, 1633, 1897, 2948 cm^{-1}. HRMS *calcd*. for $C_{21}H_{36}Cl_{14}N_6O_4PPt^+$: 802.091664; *found* 802.092584.

Compound 144

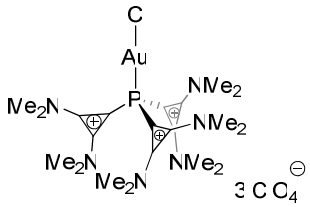

Dry acetonitrile (2.0 mL) was added to a cooled (-20 °C) mixture of salt **141** (24 mg, 0.03 mmol) and (Me_2S)AuCl (10 mg, 0.03 mmol). The mixture was stirred for 1 h and concentrated *in vacuo* at 0 °C to give the product as pale yellow solid (30 mg, 94%). ^{1}H NMR (400 MHz, CD_3CN) δ = 3.27 (s, 18H), 3.28 ppm (s, 18H). ^{31}P NMR (161 MHz, CD_3CN) δ = -49.67 ppm. ^{13}C NMR (100 MHz, CD_3CN) δ = 43.1, 43.7, 102.9 (d, *J* = 68.2 Hz), 140.2 ppm (d, *J* = 5.0 Hz). IR (neat) ṽ = 749, 1075, 1217, 1408, 1622, 1898, 3429 cm^{-1}. HRMS *calcd*. for $C_{21}H_{36}Cl_3N_6O_8PAu^+$: 833.105788; *found* 833.106459.

Compound 166a

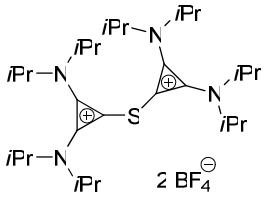

Bis(trimethylsilyl)sulfide (77 µL, 0.41 mmol) was added to a stirred suspension of chlorocyclopropenium salt **42** (294 mg, 0.82 mmol) in dry THF (7.0 mL) and the reaction mixture was heated at 60 °C overnight. Then the mixture was cooled to room temperature, the precipitate was filtered off and washed with THF (3 × 9 mL), affording the desired compound as a white solid (236 mg, 85%). ^{1}H NMR (400 MHz, CD_2Cl_2) δ = 1.31 (d, *J* = 6.9 Hz, 24H), 1.33 (d, *J* = 6.9 Hz, 24H), 3.86 (sept, *J* = 6.9 Hz, 4H), 4.06 ppm (sept, *J* = 6.9 Hz, 4H). ^{13}C NMR (100 MHz, CD_2Cl_2) δ = 21.4, 22.7, 51.7, 57.5, 92.7, 136.9 ppm. IR (neat) ṽ = 893, 1045, 1350, 1562, 1873, 2979 cm^{-1}. HRMS *calcd*. for $C_{30}H_{56}BF_4N_4S^+$: 591.426501; *found* 591.427218.

Compound 166b

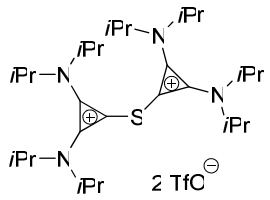

Bis(trimethylsilyl)sulfide (94.8 µL, 0.50 mmol) was added to a stirred suspension of chlorocyclopropenium salt **133** (425 mg, 1.01 mmol) in dry THF (10.0 mL) and the reaction mixture was heated at 60 °C overnight. Then the mixture was cooled to room temperature, the precipitate was filtered off and washed with THF (3 × 12 mL), affording the desired compound as a white solid (713 mg, 88%). ^{1}H NMR (400 MHz, CD_2Cl_2) δ = 1.31 (d, *J* = 7.0 Hz, 24H), 1.33 (d, *J* = 7.0 Hz, 24H), 3.87 (sept, *J* = 7.0 Hz, 4H), 4.06 ppm (sept, *J* = 7.0 Hz, 4H). ^{13}C NMR (100 MHz, CD_2Cl_2) δ = 21.1, 22.4, 51.4, 56.9, 92.9, 121.8 (q, *J* = 321.4 Hz), 136.6 ppm. IR (neat) ṽ = 1029, 1140, 1260, 1558, 1588, 1877, 2975 cm^{-1}. HRMS *calcd*. for $C_{31}H_{56}N_4O_3F_3S_2^+$: 653.374049; *found* 653.374644.

Compound 167a

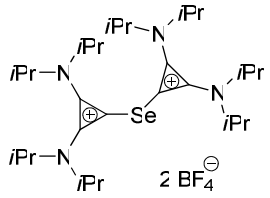

Bis(trimethylsilyl)selenide (50 µL, 0.20 mmol) was added to a stirred suspension of chlorocyclopropenium salt **42** (143 mg, 0.40 mmol) in dry THF (4.0 mL) and the reaction mixture was heated at 60 °C overnight. Then the mixture was cooled to room temperature, the solvent was removed *in vacuo* and the residue was dissolved in DCM (10 mL). The resulting solution was filtered through the syringe filter and the filtrate concentrated *in vacuo*. The residue was washed with THF (2 × 8 mL), affording the desired compound as a white solid (96 mg, 66%). ^{1}H NMR (300 MHz, CD_2Cl_2) δ = 1.31 (d, *J* = 6.9 Hz, 24H), 1.32 (d, *J* = 6.9 Hz, 24H), 3.90 (sept, *J* = 6.9 Hz, 4H), 4.04 ppm (sept, *J* = 6.9 Hz, 4H). ^{13}C NMR (75 MHz, CD_2Cl_2) δ = 21.5, 22.6, 51.6, 57.2, 87.1, 139.9 ppm. IR (neat) ṽ = 680, 890, 1057, 1354, 1549, 1872, 2974 cm^{-1}. HRMS *calcd*. for $C_{30}H_{56}BF_4N_4Se^+$: 639.371658; *found* 639.372040.

Compound 167b

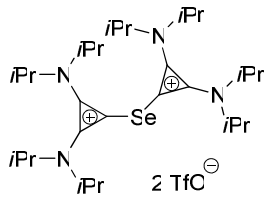

Bis(trimethylsilyl)selenide (0.3 mL, 1.20 mmol) was added to a stirred suspension of chlorocyclopropenium salt **133** (1.00 g, 2.40 mmol) in dry THF (10.0 mL) and the reaction mixture was heated at 60 °C overnight. Then the mixture was cooled to room temperature, the solvent was removed *in vacuo* and the residue was dissolved in DCM (25 mL). The resulting solution was filtered through the syringe filter and the filtrate concentrated *in vacuo*. The residue was washed with THF (2 × 10 mL), affording the desired compound as a white solid (714 mg, 70%). ^{1}H NMR (400 MHz, CD_2Cl_2) δ = 1.32 (d, *J* = 6.8 Hz, 48H), 3.91 (sept, *J* = 6.8 Hz, 4H), 4.05 ppm (sept, *J* = 6.8 Hz, 4H). ^{13}C NMR (100 MHz, CD_2Cl_2) δ = 21.2, 22.3, 51.4, 56.4, 87.9, 121.3 (q, *J* = 320.9 Hz), 139.5 ppm. IR (neat) ṽ = 800, 1028, 1139, 1258, 1558, 1872, 2973 cm^{-1}. HRMS *calcd*. for $C_{31}H_{56}F_3N_4O_3SSe^+$: 701.318486; *found* 701.320843.

Compound 169a

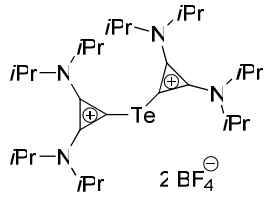

Bis(trimethylsilyl)telluride (50 µL, 0.17 mmol) was added to a stirred suspension of chlorocyclopropenium salt **42** (123 mg, 0.34 mmol) in dry THF (3.0 mL) and the reaction mixture was heated at 60 °C overnight. Then the mixture was cooled to room temperature, the solvent was removed *in vacuo* and the residue was dissolved in DCM (5 mL). The resulting solution was filtered through the syringe filter and the filtrate concentrated *in vacuo*. The residue was washed with THF (2 × 10 mL), affording the desired compound as a white solid (43 mg, 32%). ^{1}H NMR (400 MHz, CD_2Cl_2) δ = 1.30 (d, *J* = 6.9 Hz, 24H), 1.33 (d, *J* = 6.9 Hz, 24H), 4.02 (sept, *J* = 6.9 Hz, 4H), 4.03 ppm (sept, *J* = 6.9 Hz, 4H). ^{13}C NMR (100 MHz, CD_2Cl_2) δ = 21.2, 22.3, 51.3, 56.1, 71.4, 143.6 ppm. IR (neat) ṽ = 669, 889, 1013,

1063, 1141, 1354, 1539, 1575, 1863, 2973 cm^{-1}. HRMS *calcd*. for $C_{30}H_{56}BN_4F_4Te^+$: 689.360549; *found* 689.360863.

Compound 169b

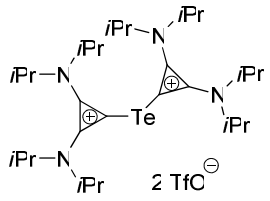

Freshly dried THF (6 mL) was added to a mixture of sodium (28.0 mg, 1.22 mmol) and naphthalene (156 mg, 1.22 mmol). A dark green solution was formed which was stirred at room temperature for 1h. Pulverized tellurium (78 mg, 0.61 mmol) was added to the reaction mixture which was stirred overnight. The chlorocyclopropenium salt **133** (512 mg, 1.22 mmol) was added to a white suspension of sodium telluride and the mixture was stirred overnight. The solvent was removed *in vacuo*, the dark residue was washed with pentane (4 × 5 mL) to remove the naphthalene. The remaining residue was washed with DCM (4 × 2 mL) to dissolve the product. The filtrate was concentrated *in vacuo*, then washed with hot THF (~ 60 °C, 6 × 7 mL) affording the desired compound as a white solid (289 mg, 53%). ^{1}H NMR (400 MHz, CD_2Cl_2) δ = 1.30 (d, *J* = 6.9 Hz, 24H), 1.33 (d, *J* = 6.9 Hz, 24H), 4.03 (sept, *J* = 6.9 Hz, 4H), 4.04 ppm (sept, *J* = 6.9 Hz, 4H). ^{13}C NMR (100 MHz, CD_2Cl_2) δ = 21.4, 22.3, 51.4, 55.4, 74.3, 121.1 (q, *J* = 321.0 Hz), 143.4 ppm. IR (neat) $\tilde{\nu}$ = 1027, 1152, 1263, 1553, 1862, 2984 cm^{-1}. HRMS *calcd*. for $C_{31}H_{56}N_4O_3F_3STe^+$: 751.308665; *found* 751.309581.

Compound 170

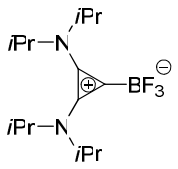

The compound was obtained as a by-product from the reaction between chlorocyclopropenium salt **42** (246 mg, 0.68 mmol) and bis(trimethylsilyl)telluride (0.1 mL 0.34 mmol) upon heating in dry THF (4.0 mL) at 65 °C overnight. The solvent was removed

in vacuo, the residue was dissolved in DCM (5.0 mL) and the mixture was filtered through the syringe filter. After concentration of the filtrate, the residue was recrystallized from DCM/Et_2O, obtaining the title compound (139 mg, 67%) ^{1}H NMR (400 MHz, CD_2Cl_2) δ = 1.21 (d, *J* = 6.7 Hz, 12H), 1.34 (d, *J* = 6.7 Hz, 12H), 3.70-3.89 ppm (m, 4H). ^{11}B NMR (96 MHz, CD_2Cl_2) δ = -0.54 ppm (q, *J* = 35.9 Hz). ^{13}C NMR (100 MHz, CD_2Cl_2) δ = 20.5, 21.3, 49.2, 55.3, 84.3, 139.0 ppm (q, *J* = 2.9 Hz). IR (neat) $\tilde{\nu}$ = 682, 939, 1028, 1345, 1515, 1871, 2981 cm^{-1}. HRMS *calcd*. for $C_{15}H_{28}N_2BF_3Na^+$: 327.218891; *found* 327.219088.

7 Appendix

7.1 NMR Spectra of Representative Compounds

Compound 43a

^{1}H NMR

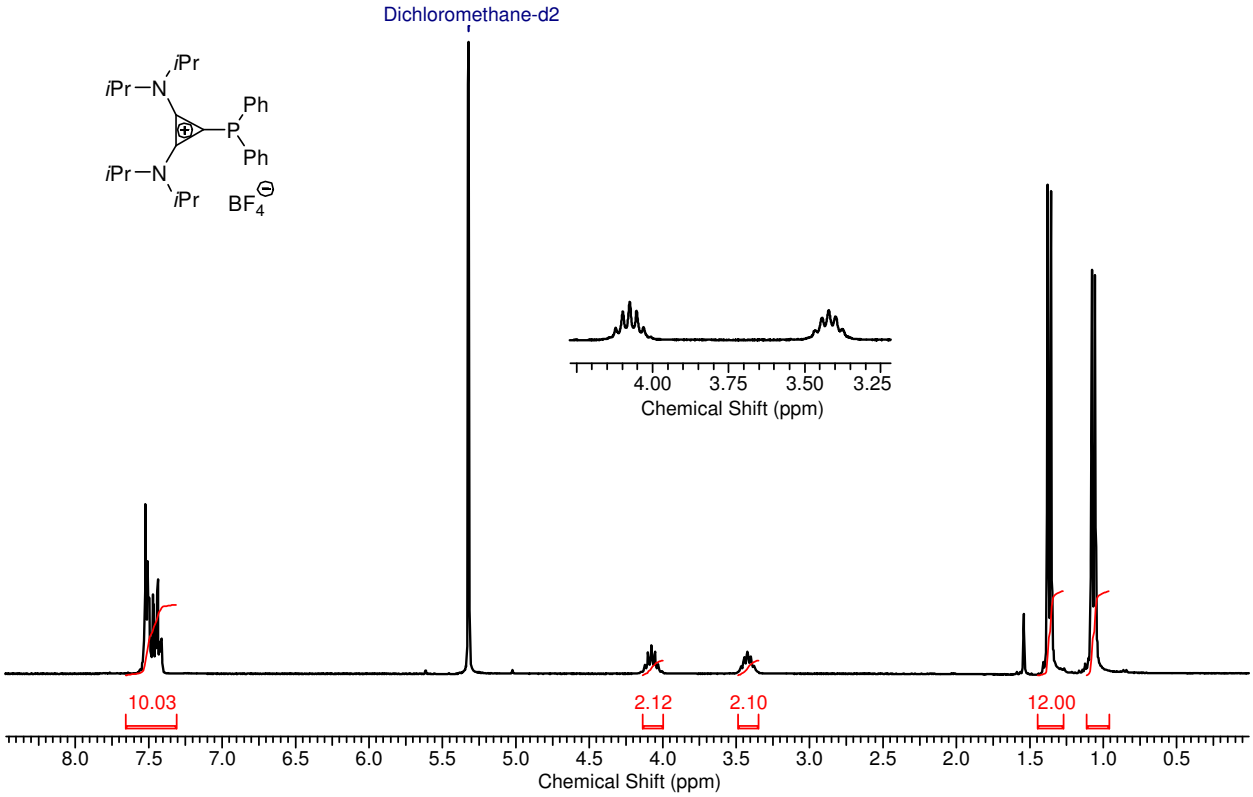

^{31}P NMR

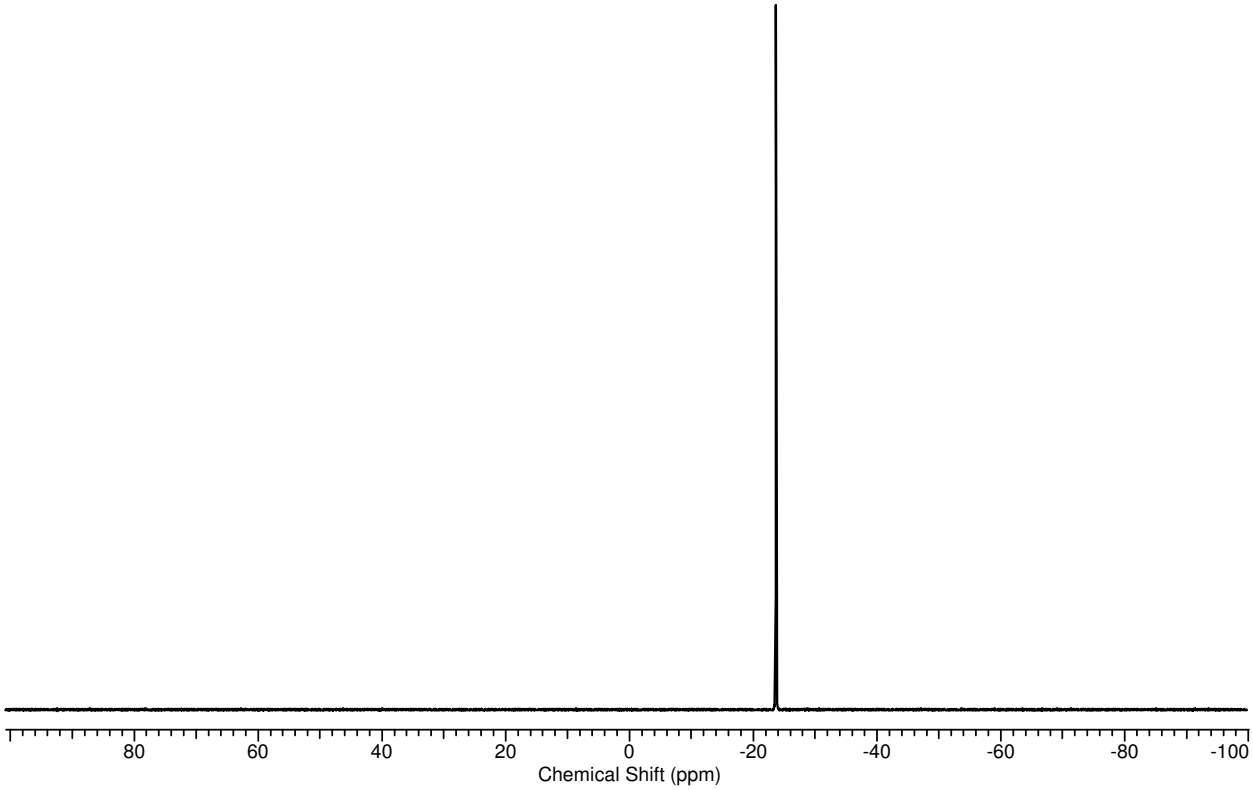

^{13}C NMR

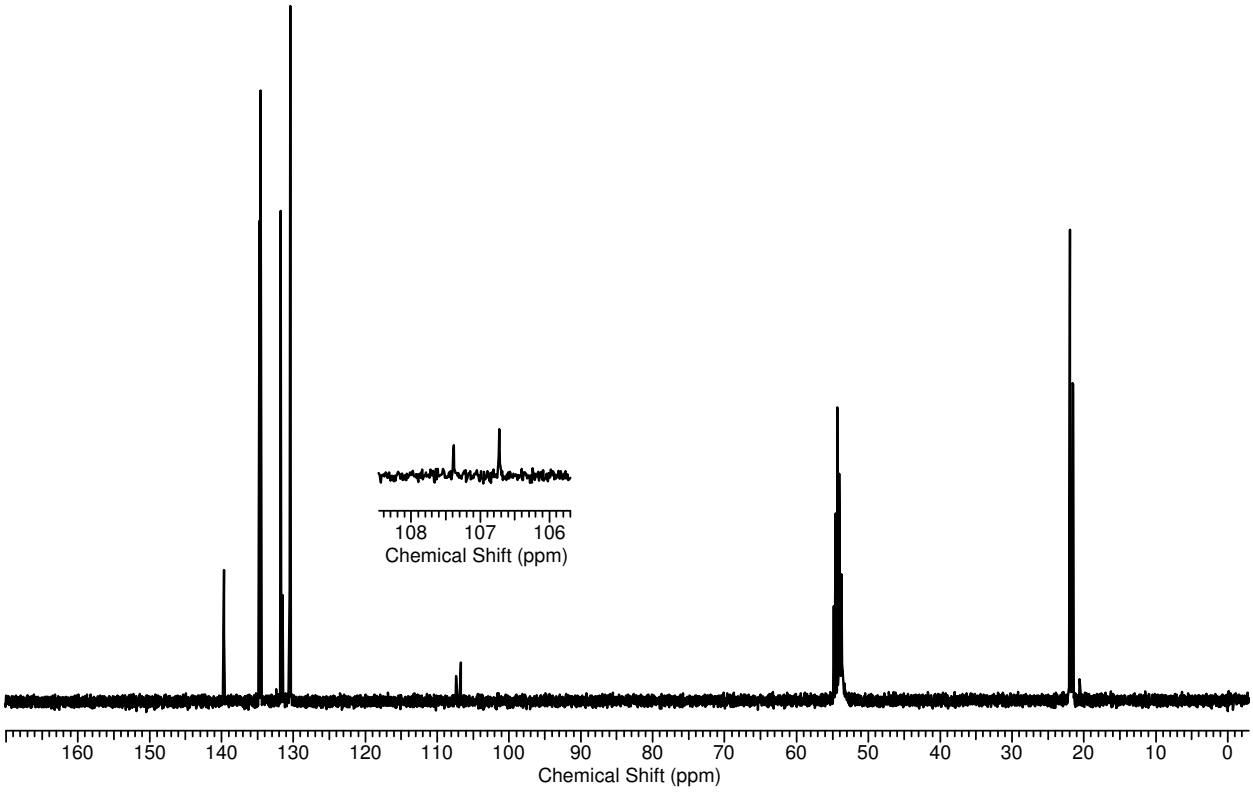

Compound 43c

^{1}H NMR

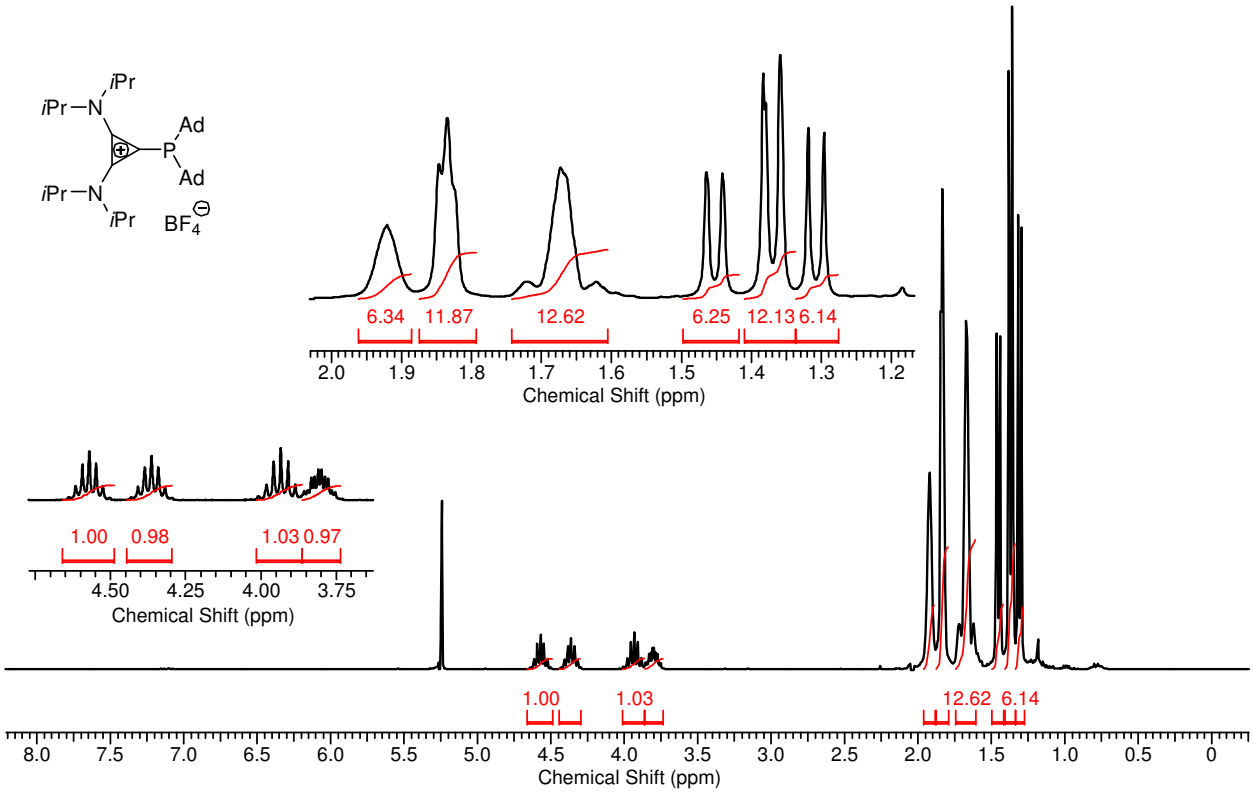

^{31}P NMR

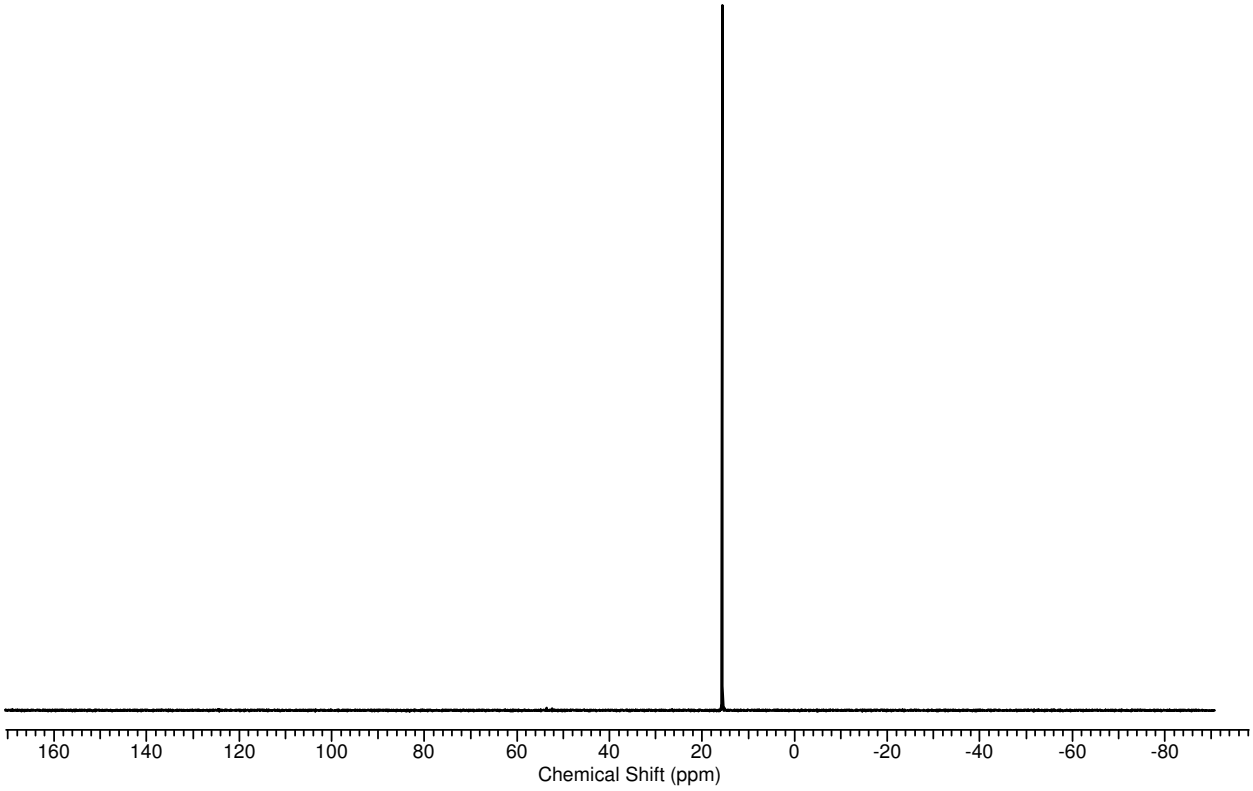

^{13}C NMR

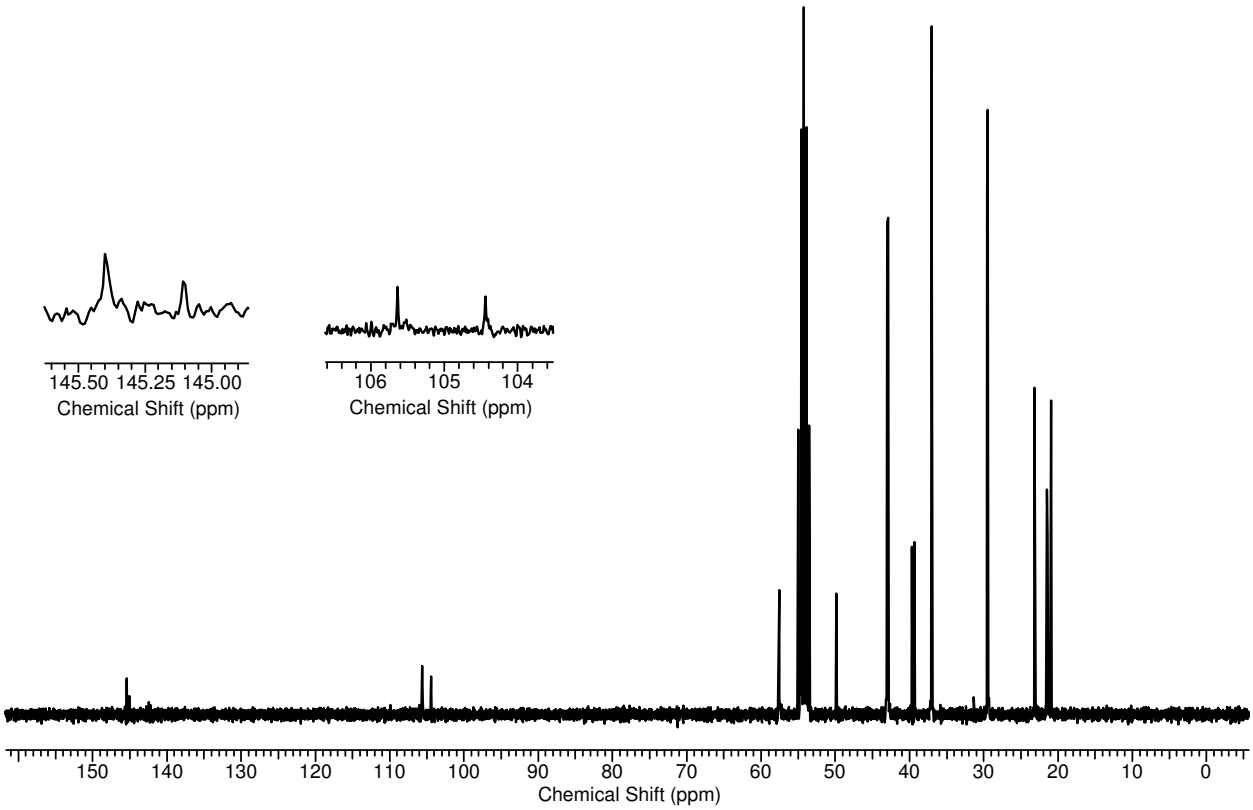

Compound 44d

^{1}H NMR

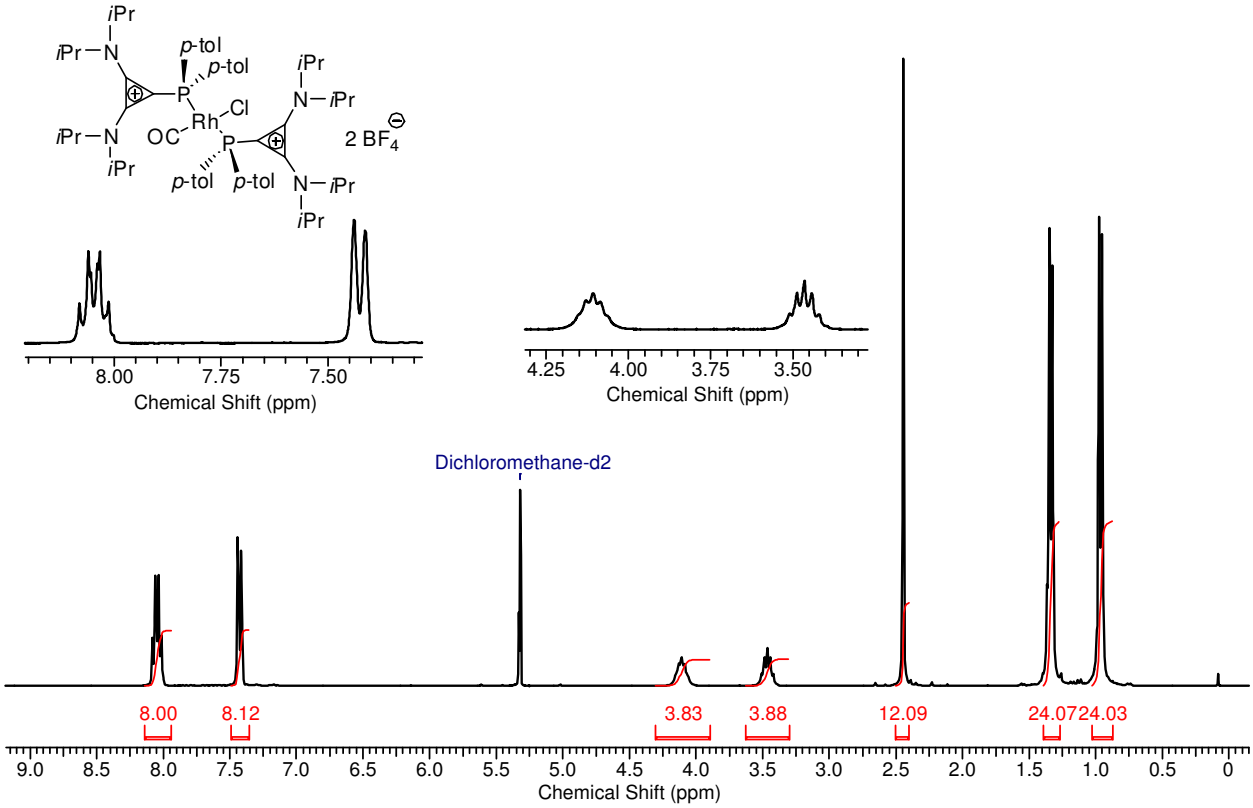

^{31}P NMR

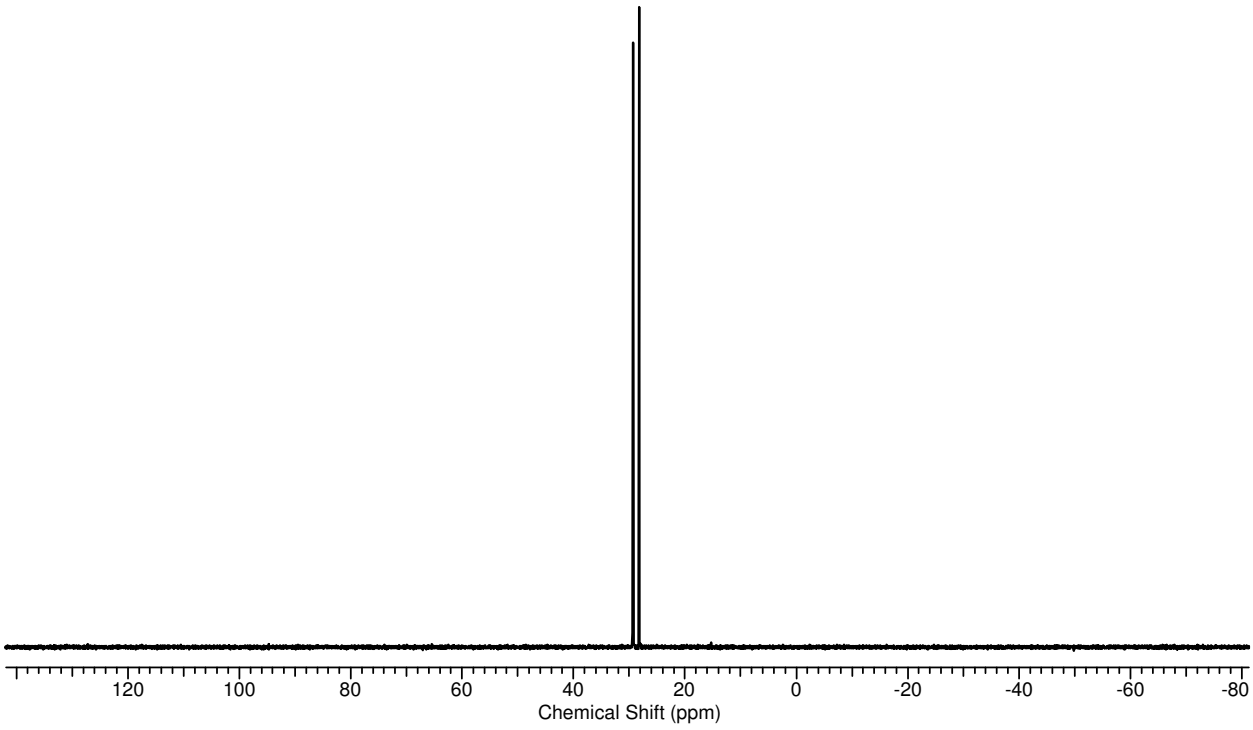

^{13}C NMR

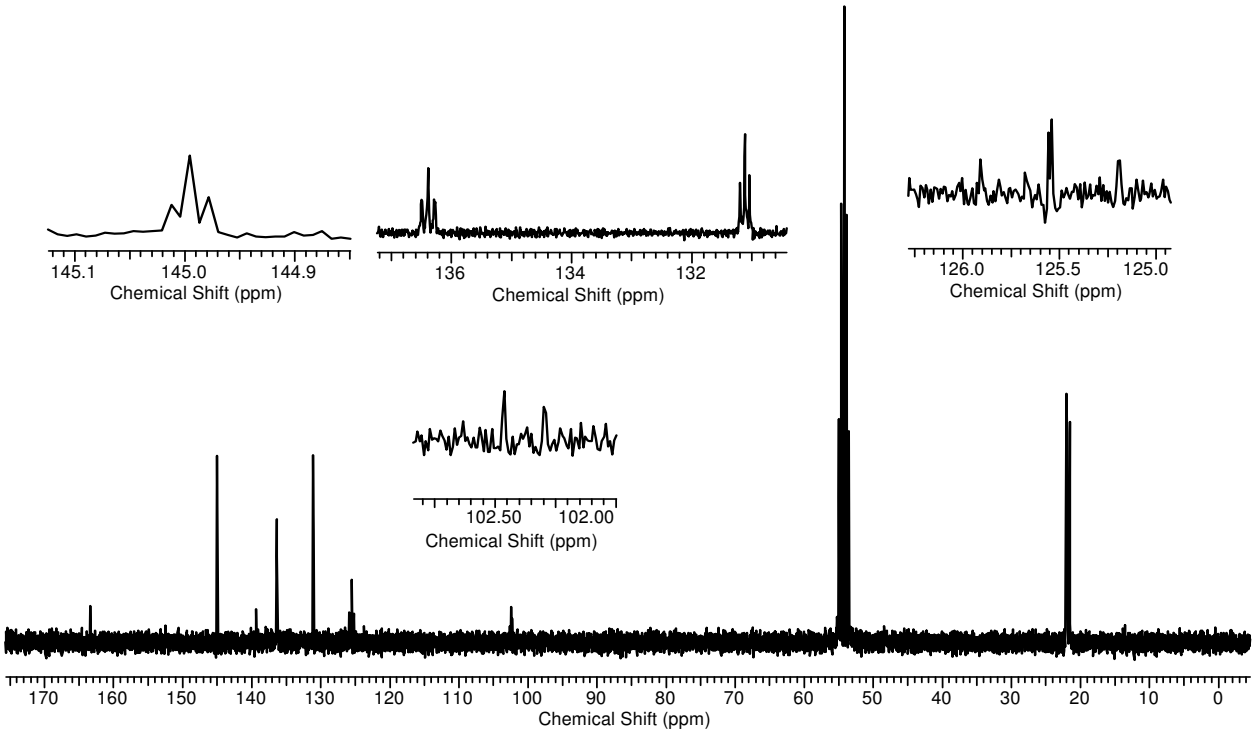

Compound 45d

^{1}H NMR

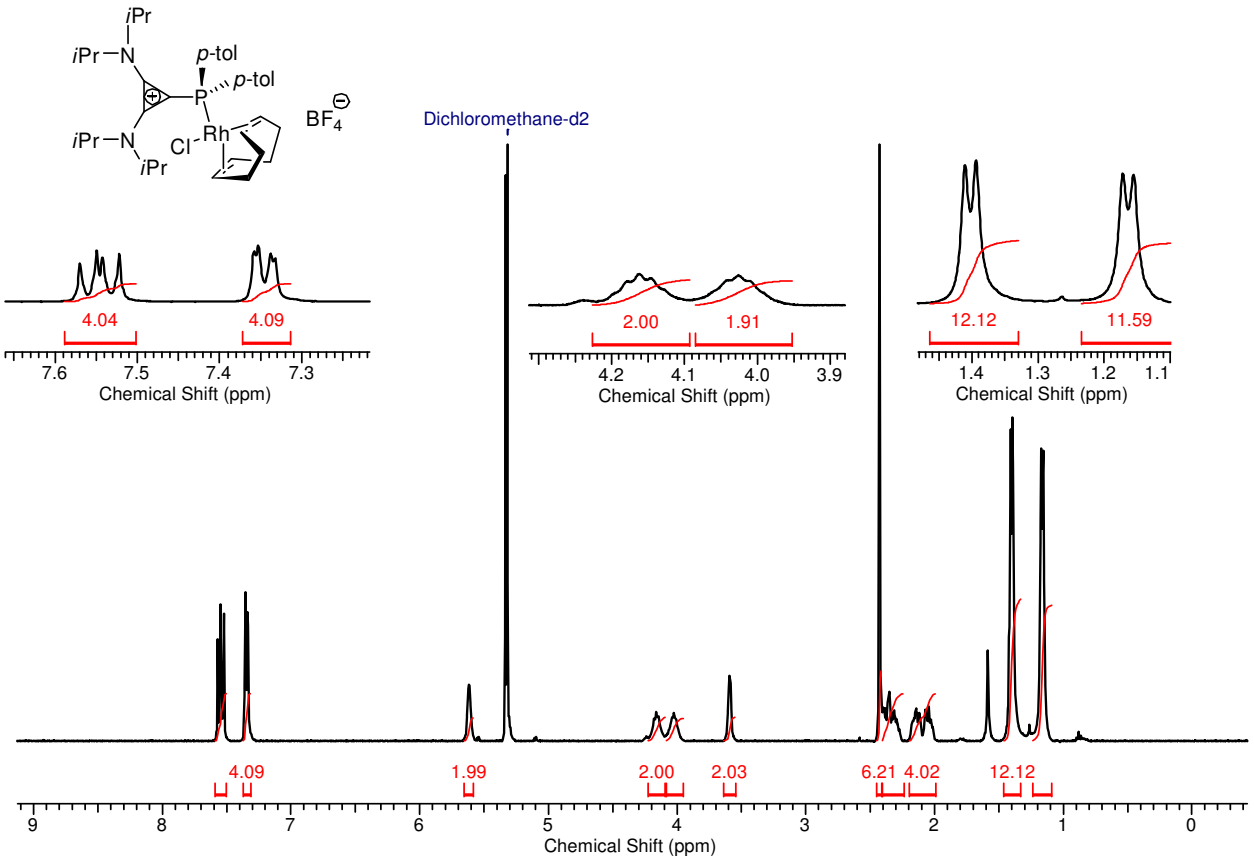

^{31}P NMR

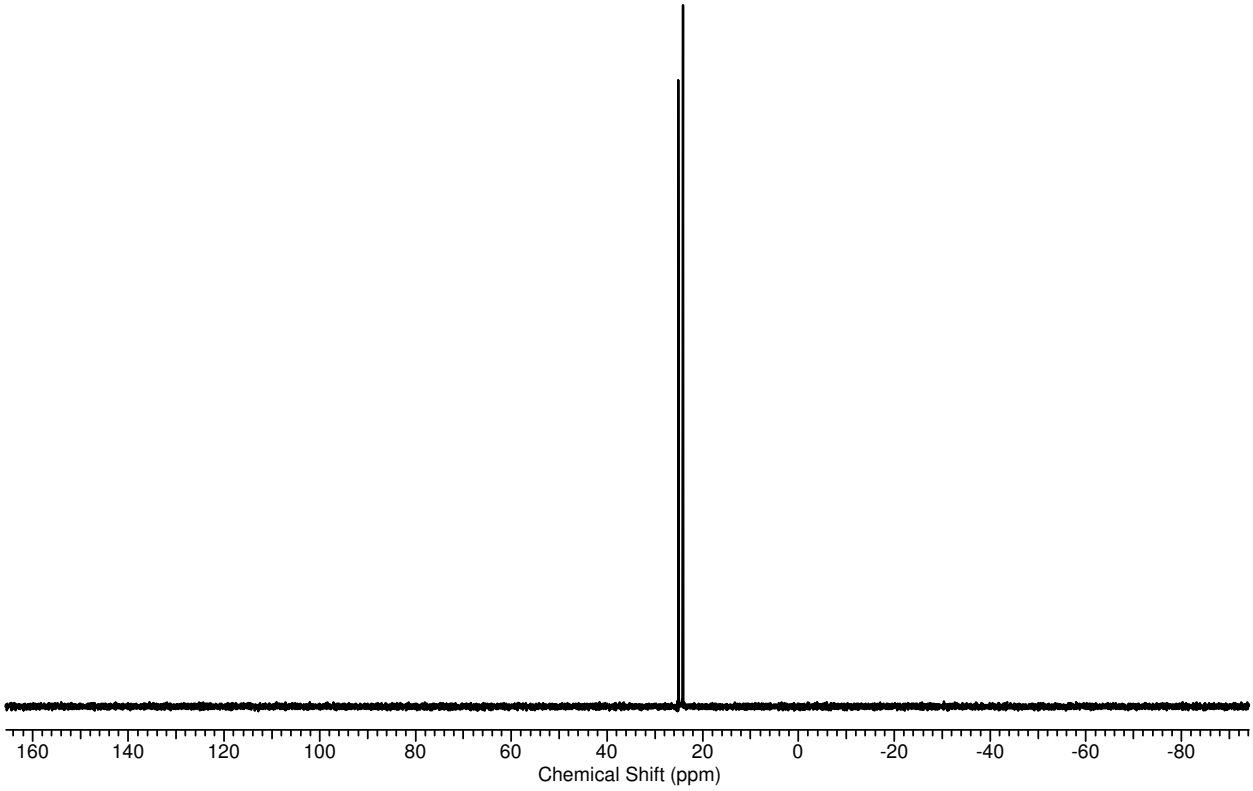

^{13}C NMR

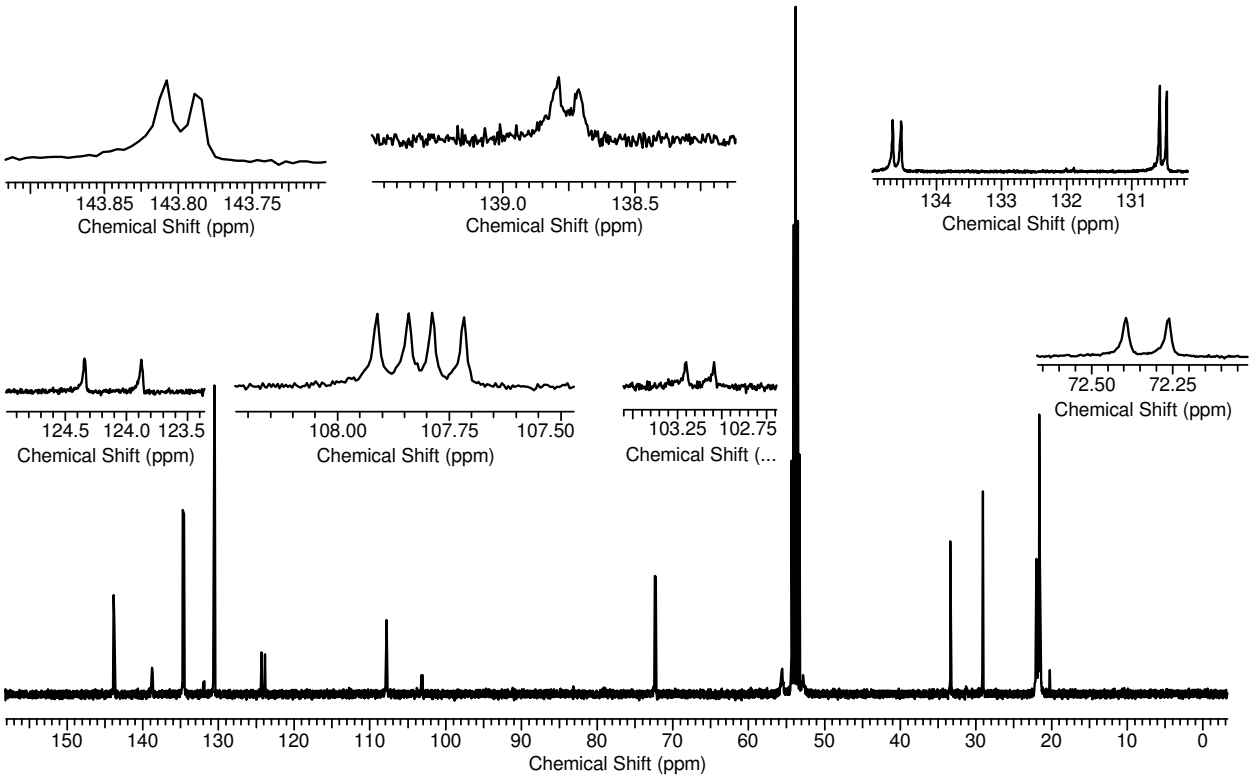

Compound 46a

^{1}H NMR

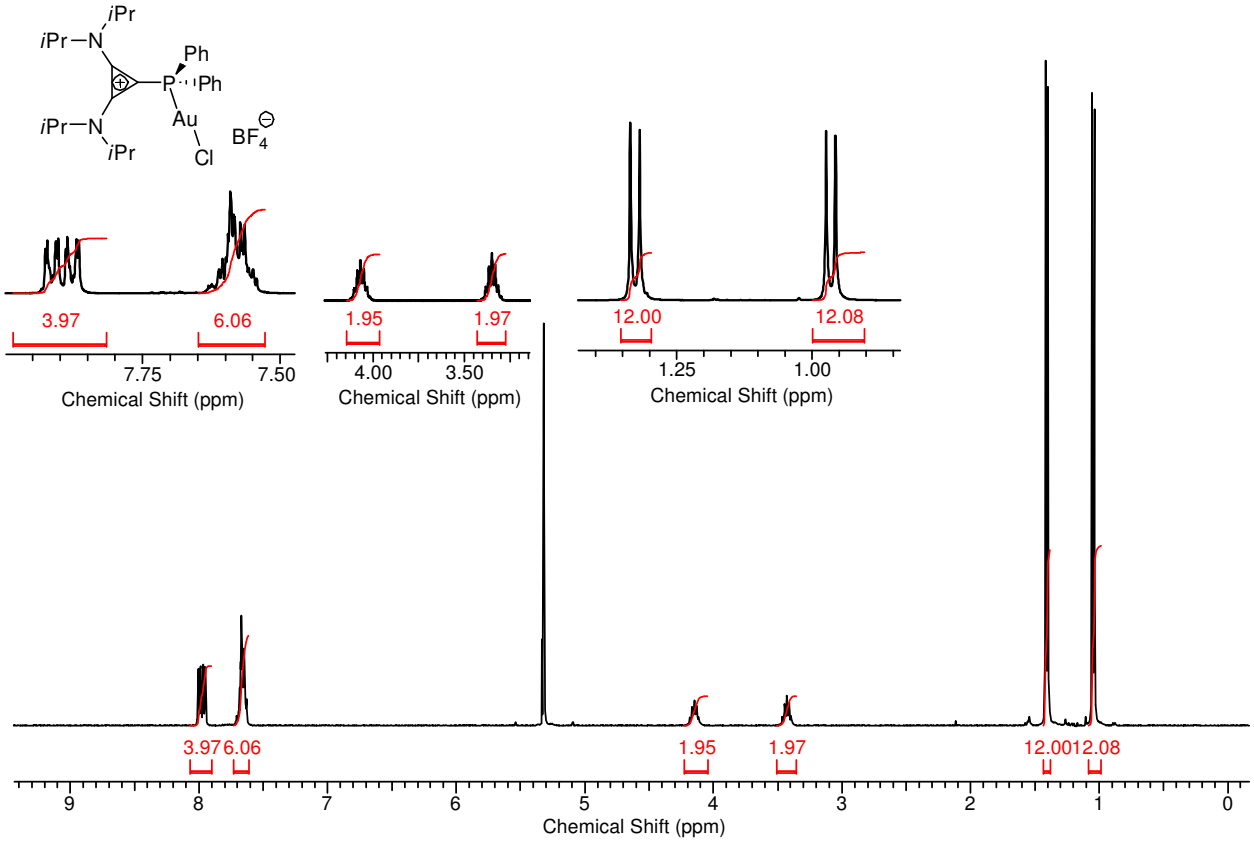

^{31}P NMR

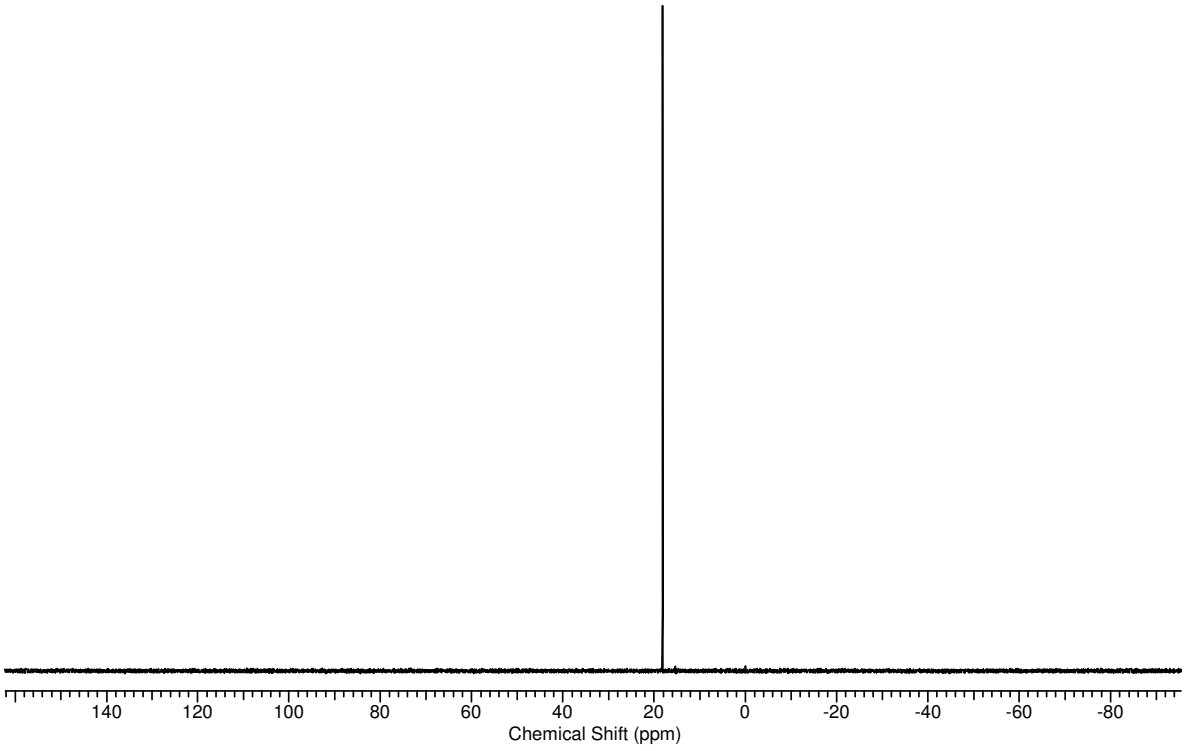

^{13}C NMR

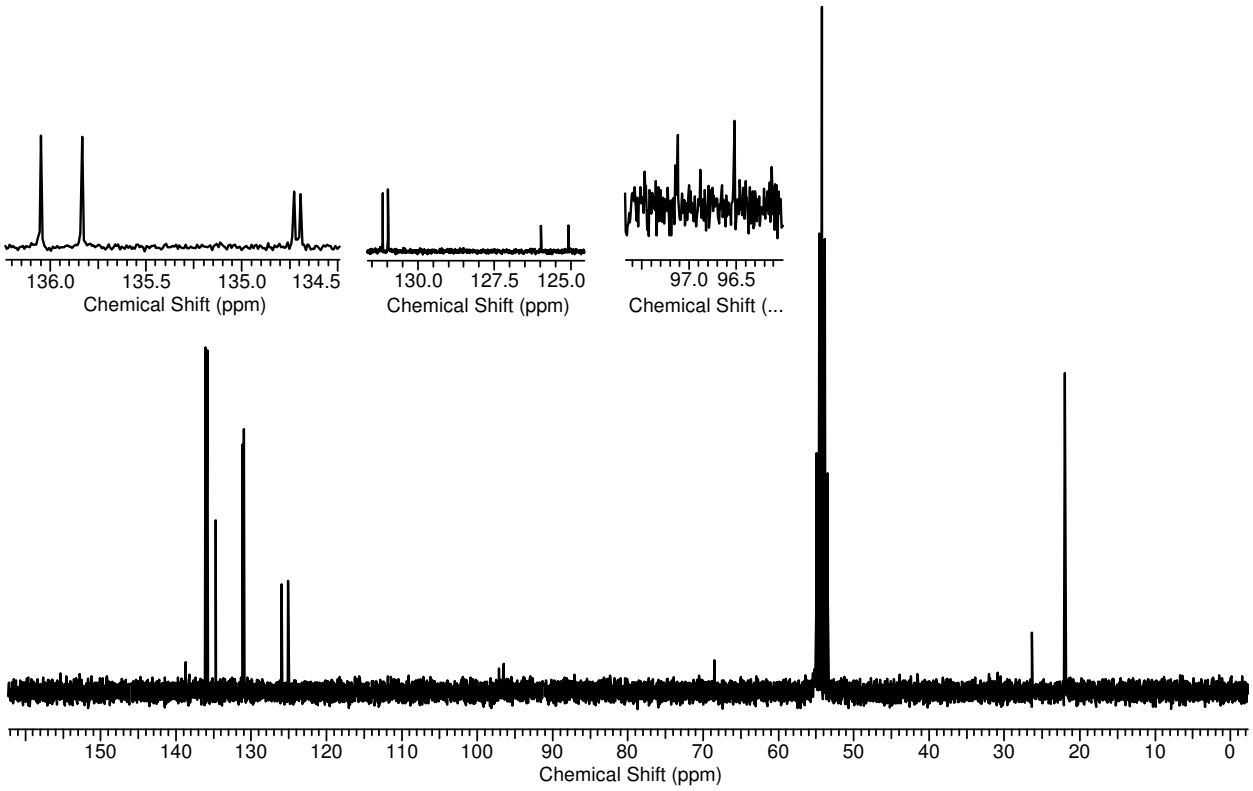

Compound 48a

^{1}H NMR

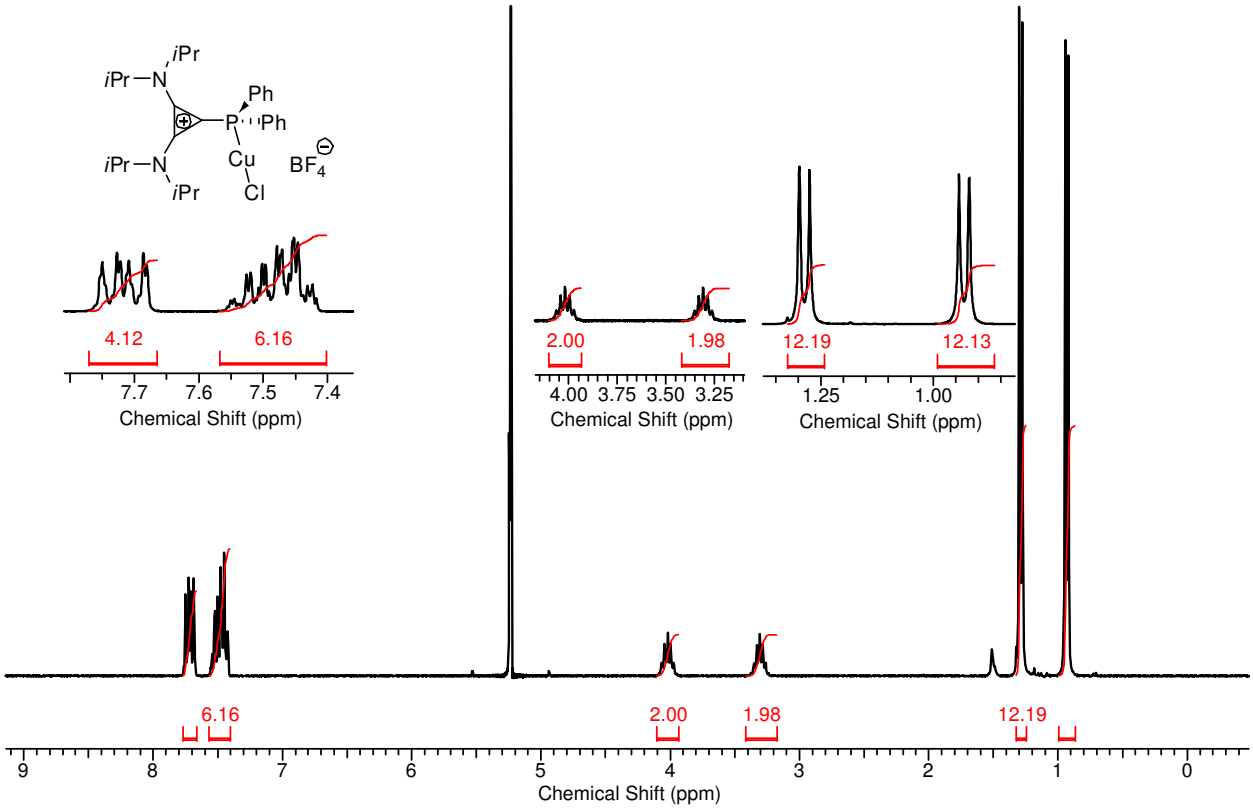

^{31}P NMR

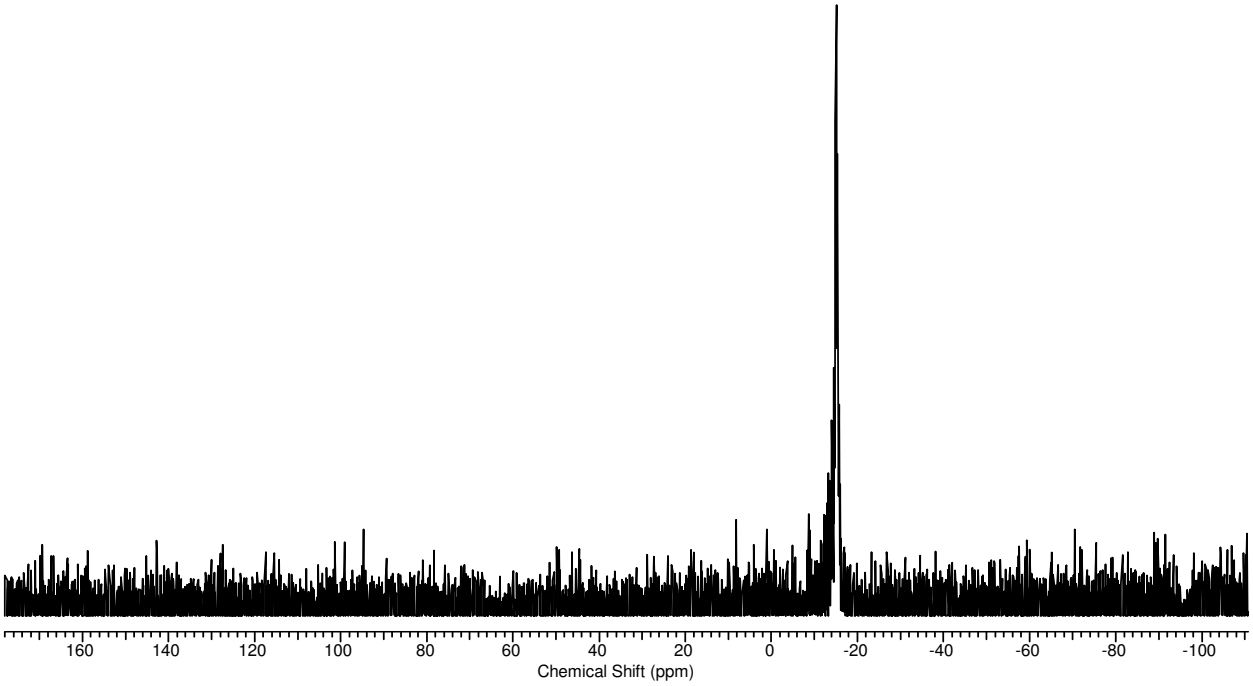

^{13}C NMR

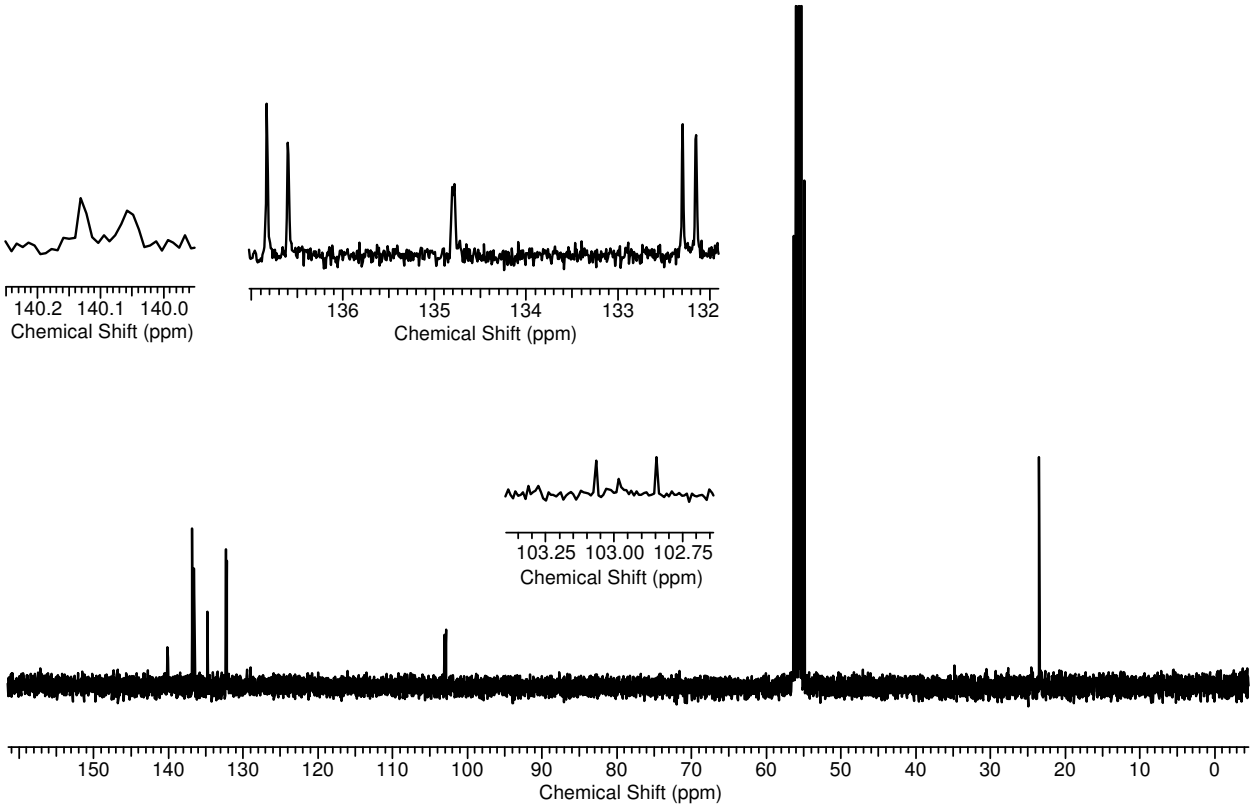

Compound 48b

^{1}H NMR

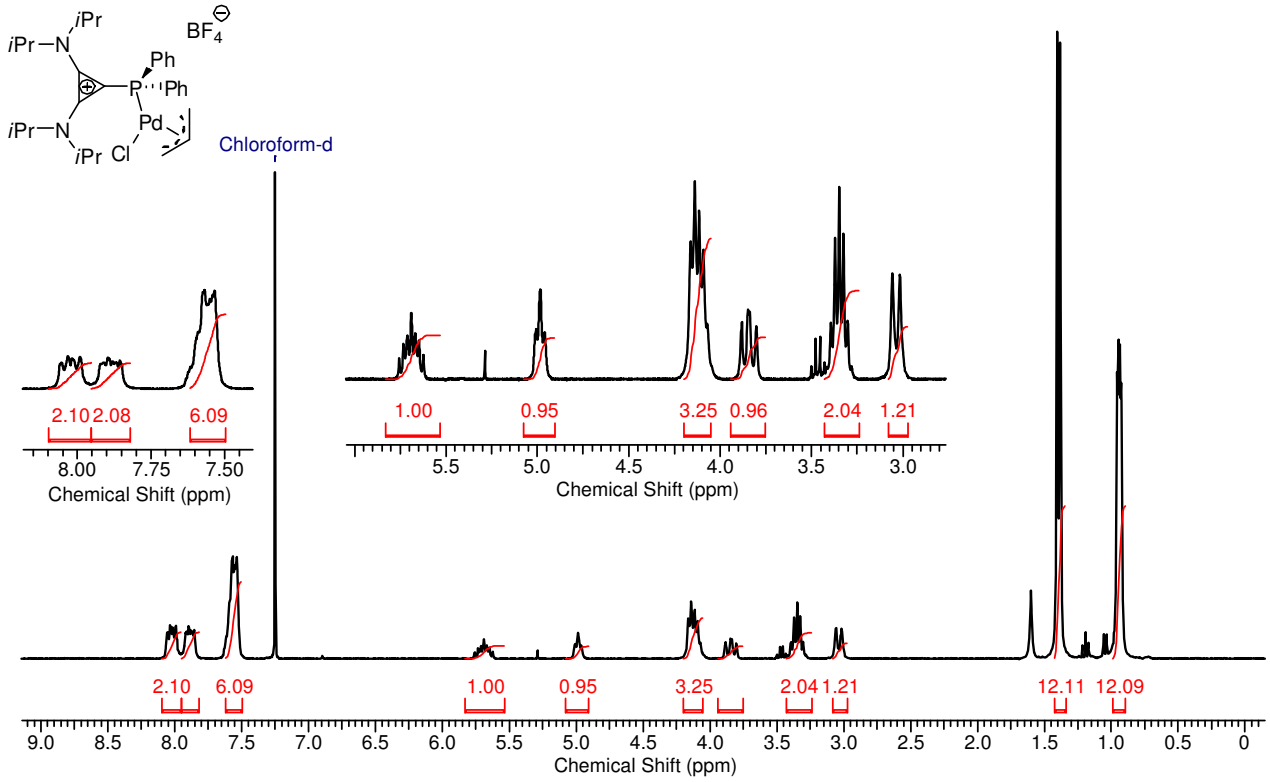

^{31}P NMR

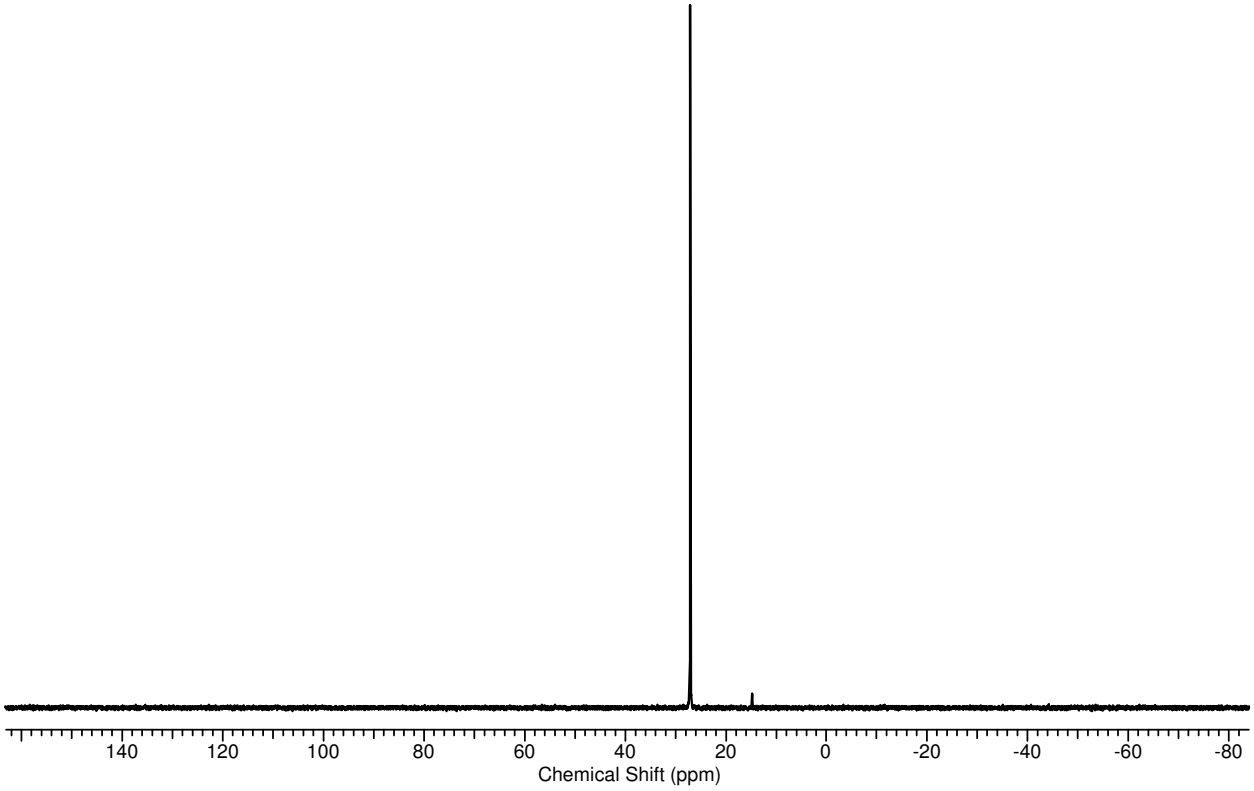

^{13}C NMR

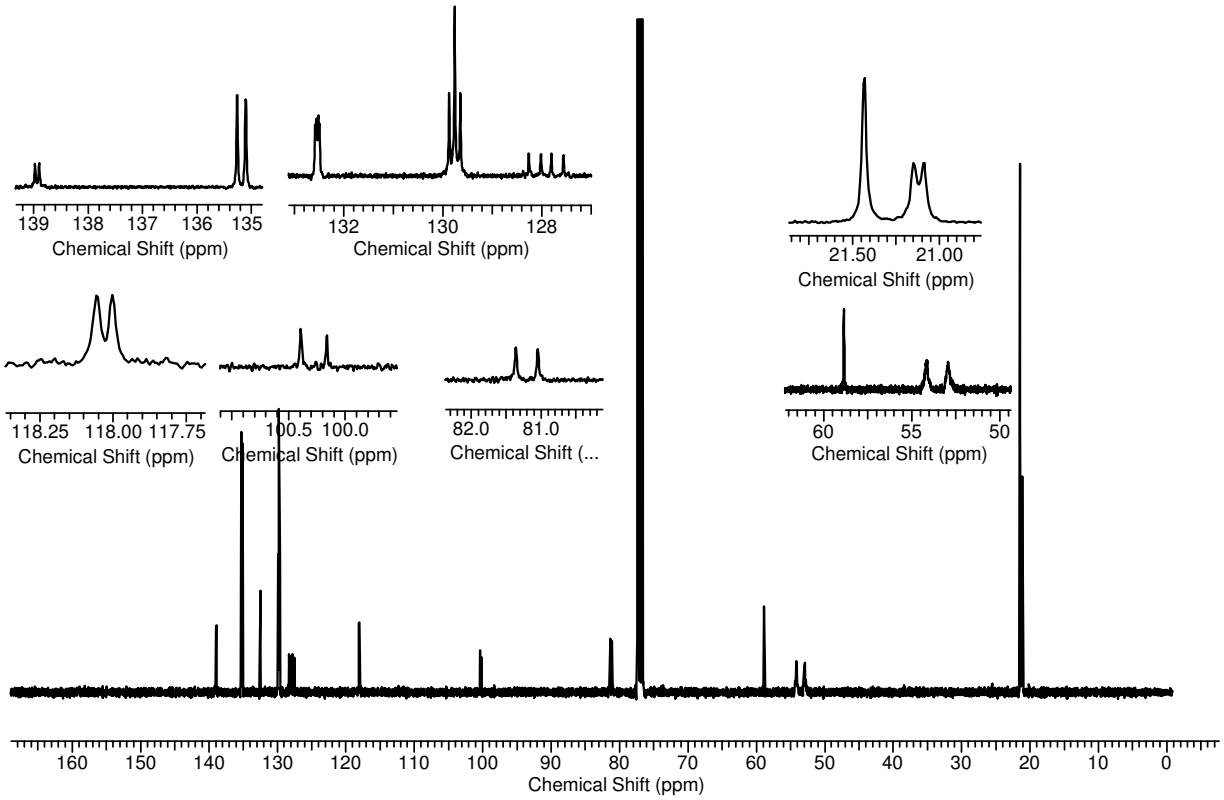

Compound 49

^{1}H NMR

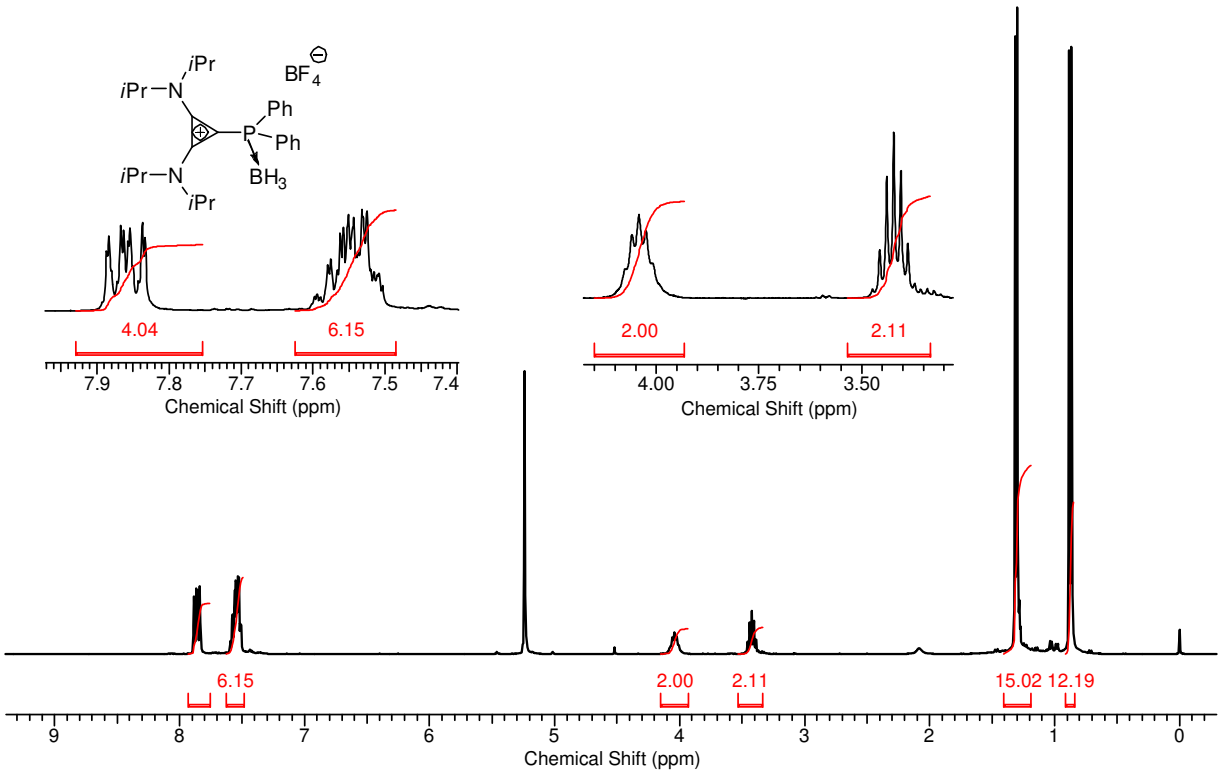

^{31}P NMR

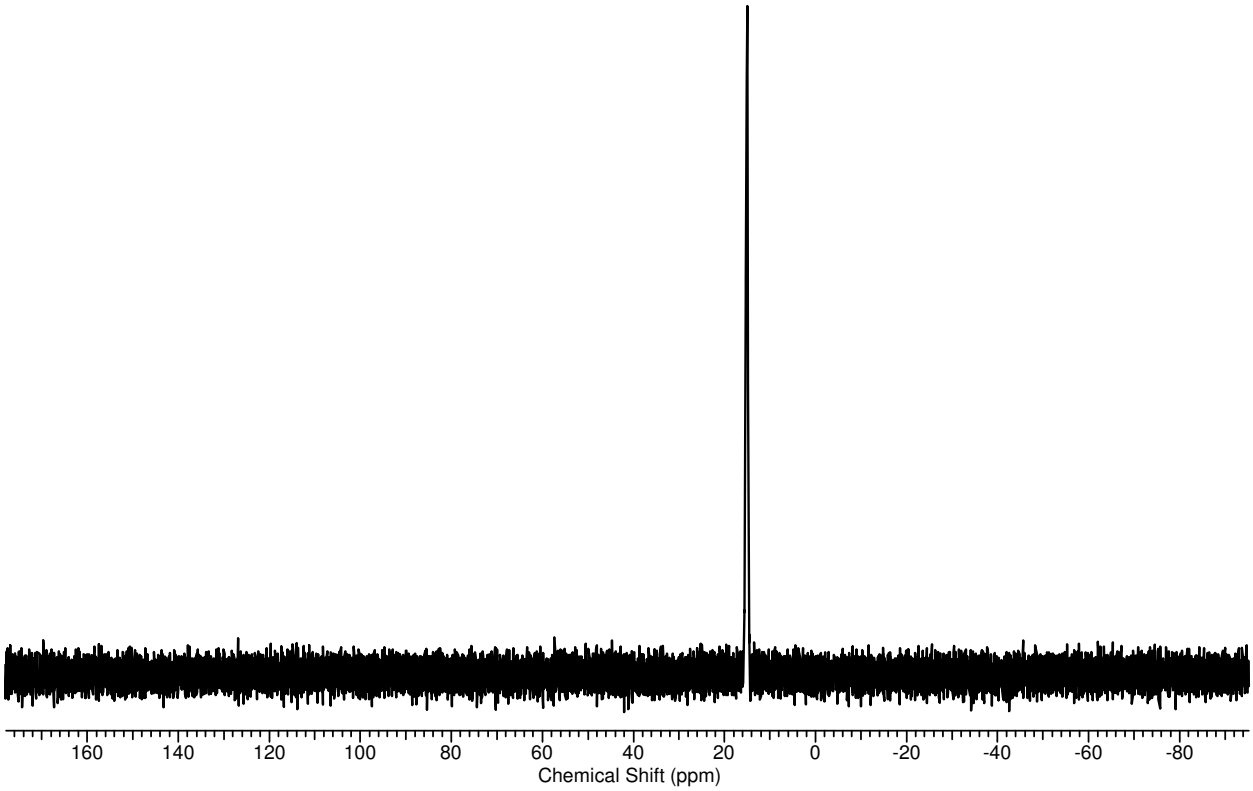

^{11}B NMR

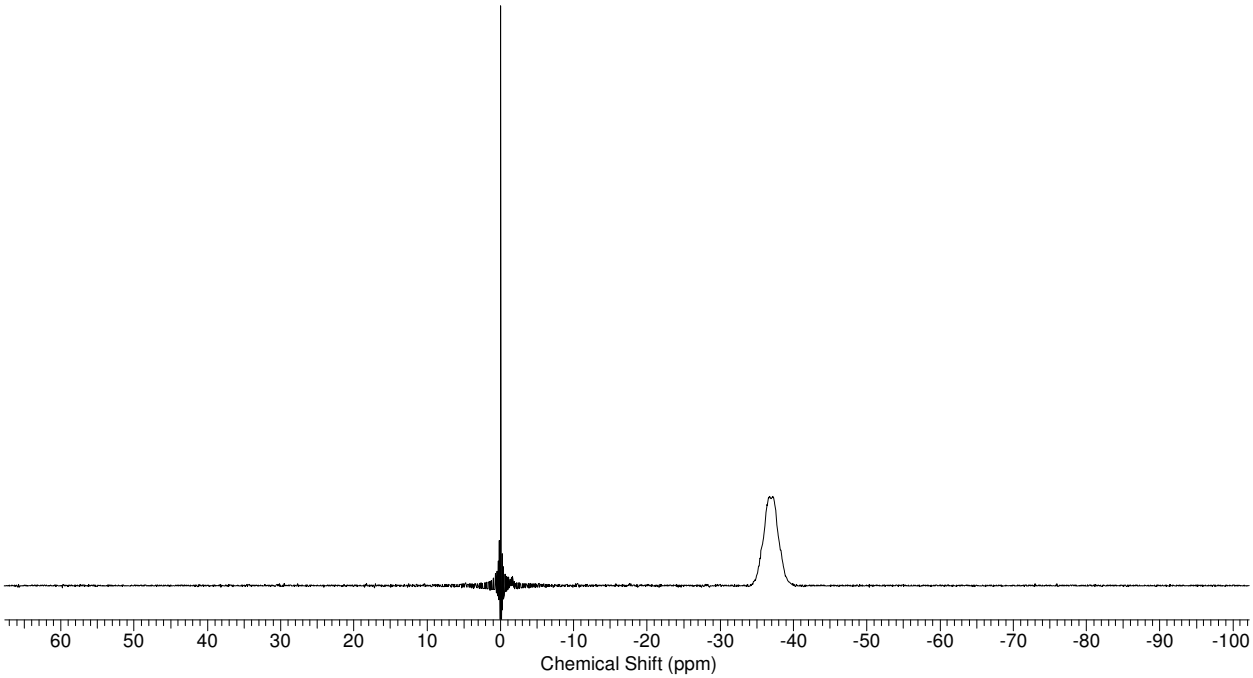

^{13}C NMR

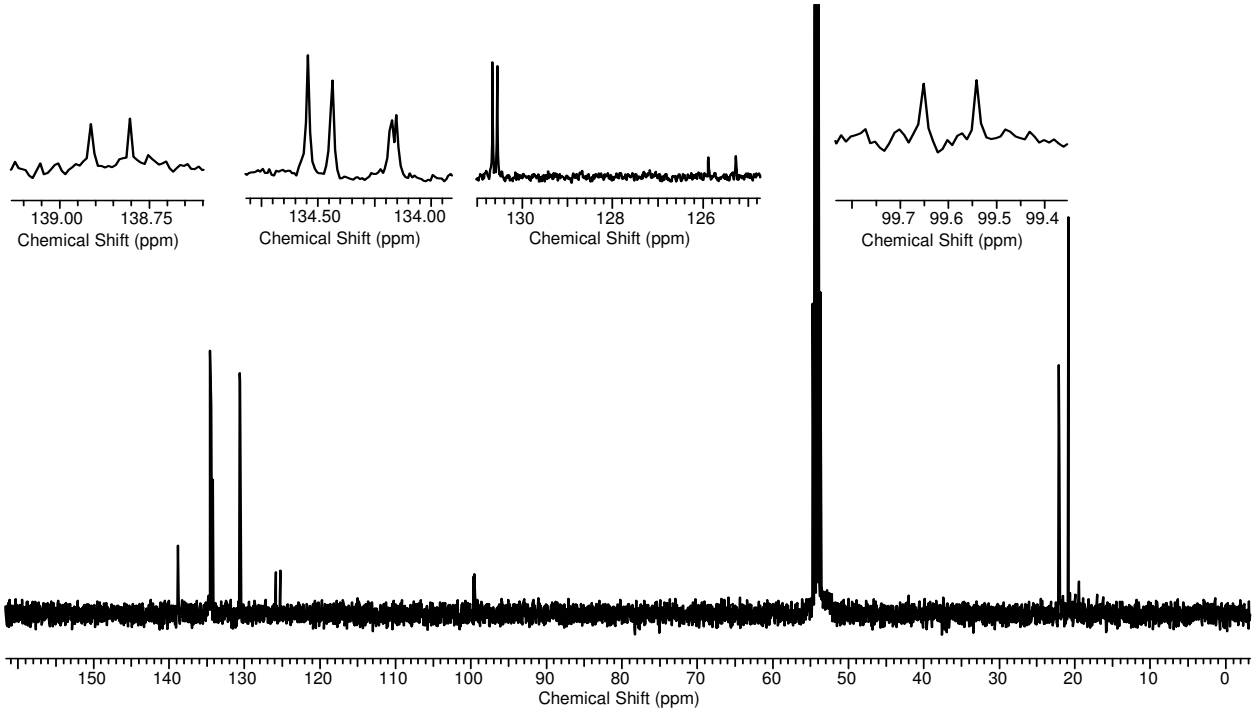

Compound 50

^{1}H NMR

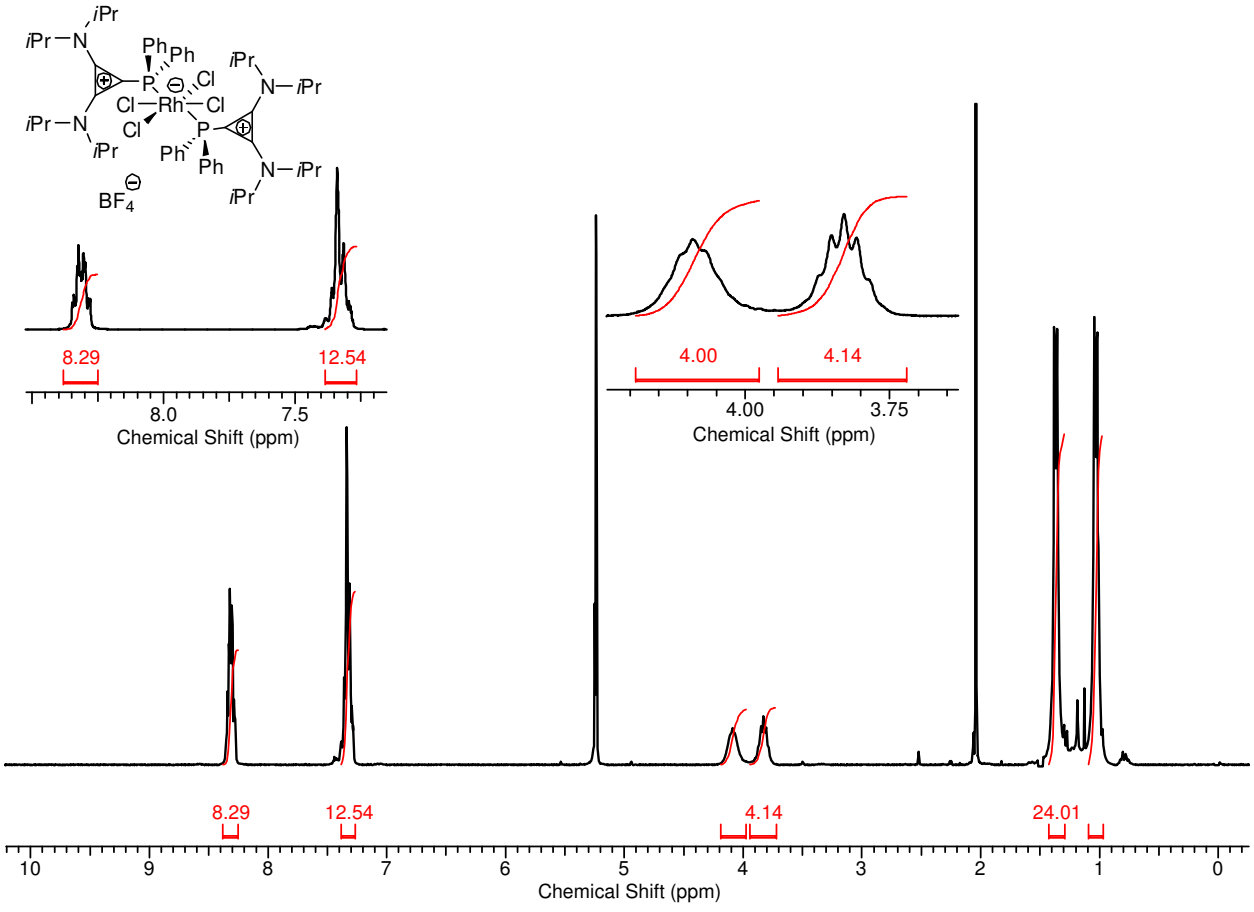

^{31}P NMR

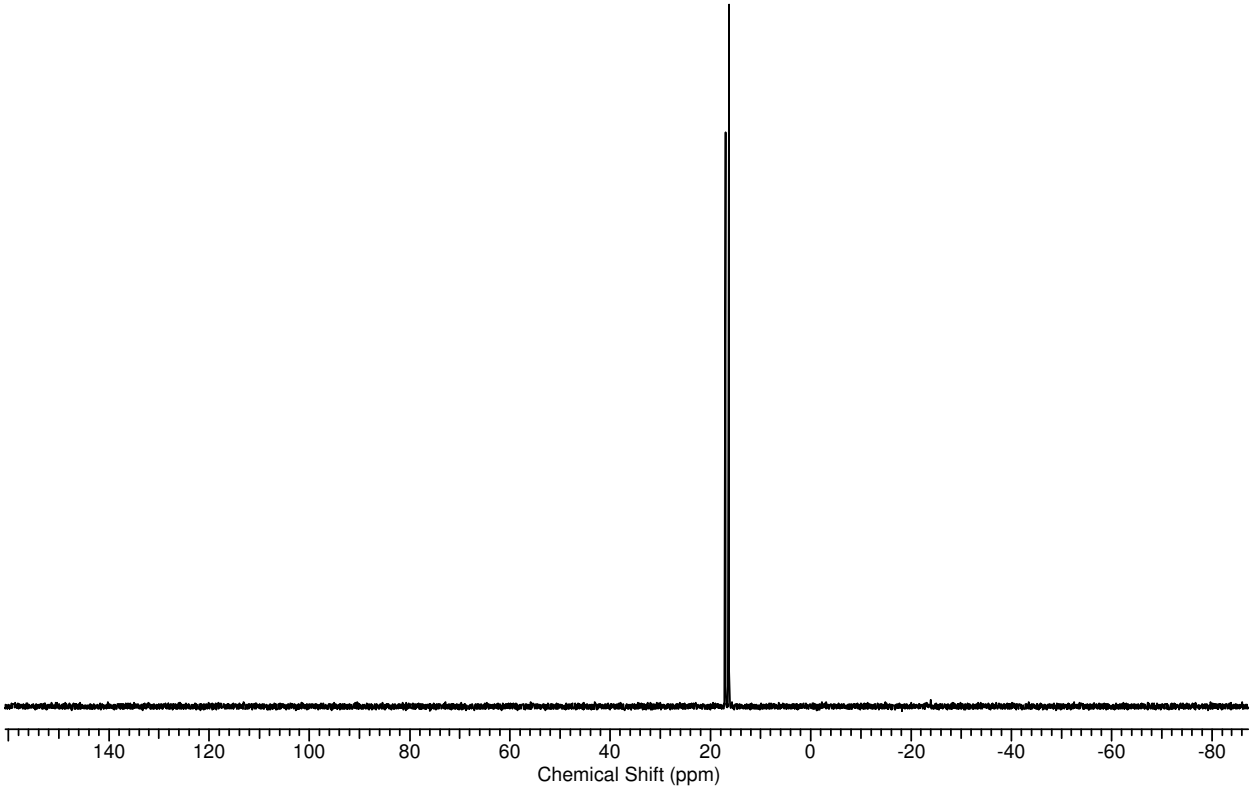

^{13}C NMR

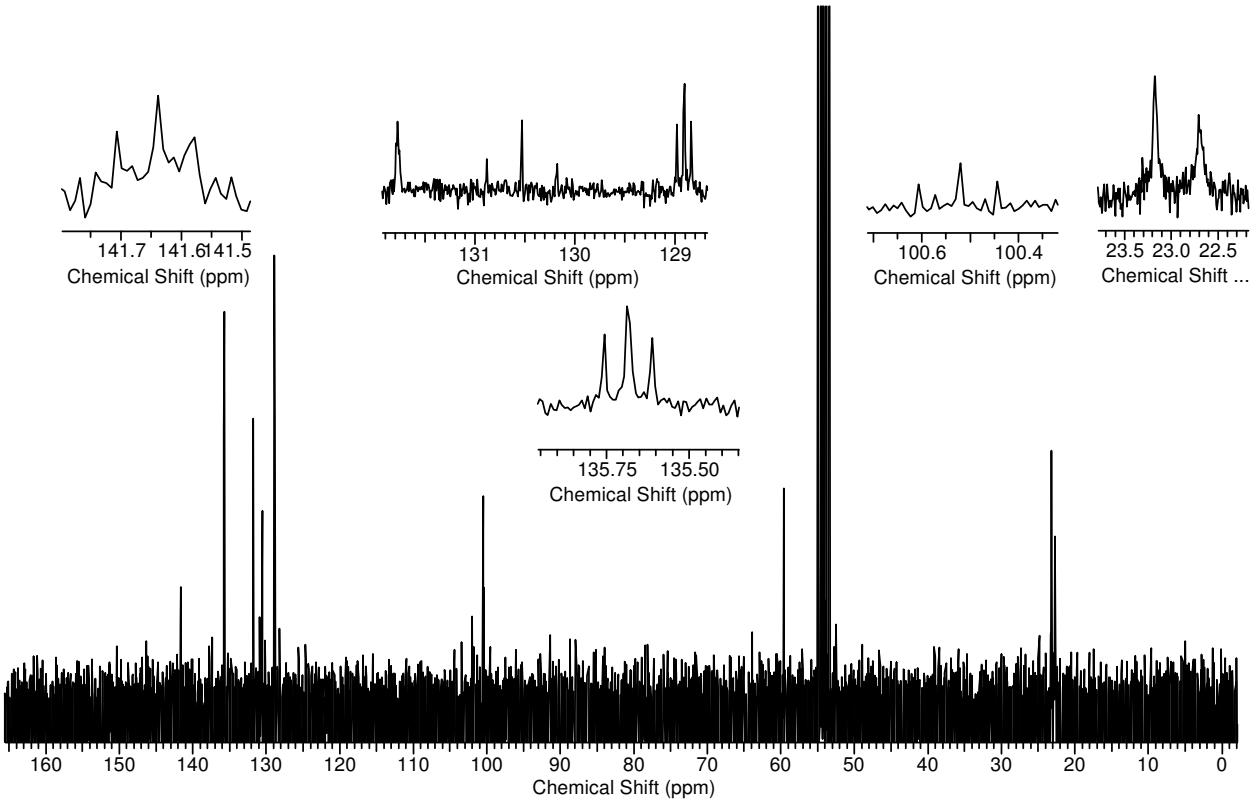

Compound 81

^{1}H NMR

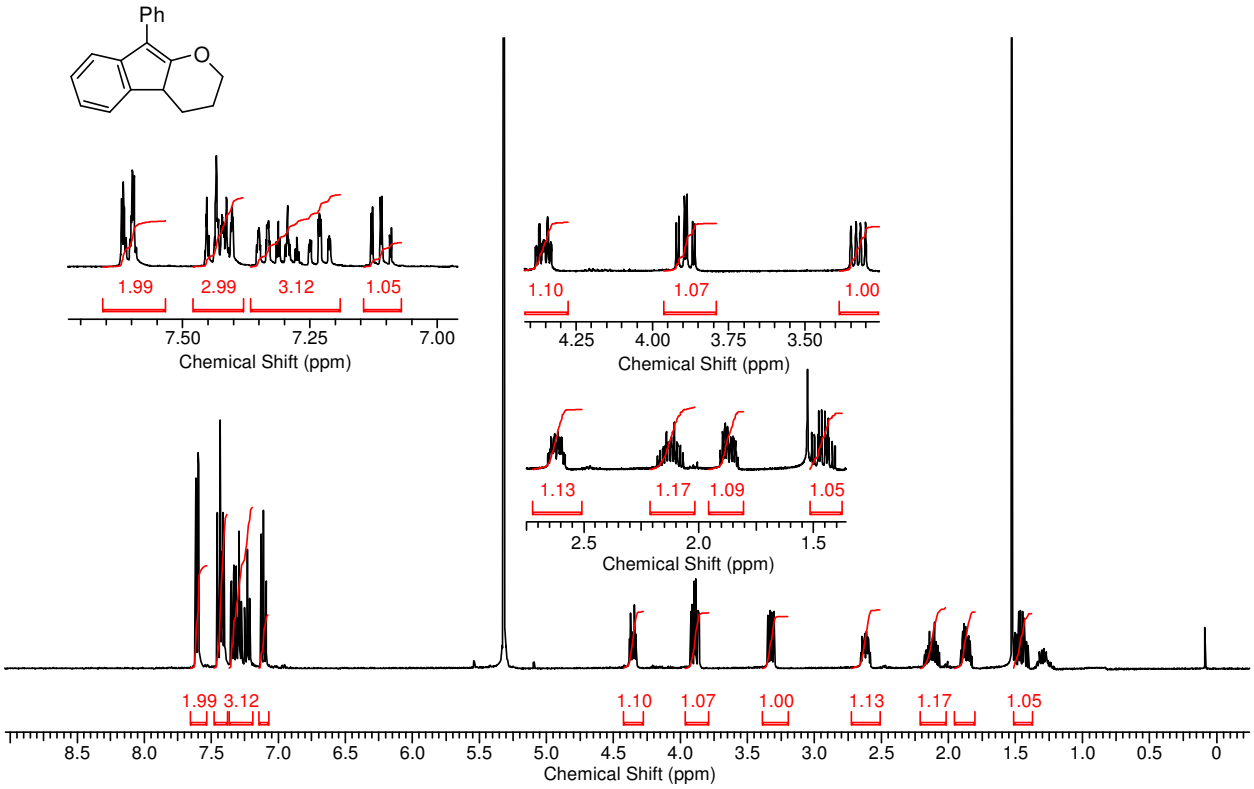

^{13}C NMR

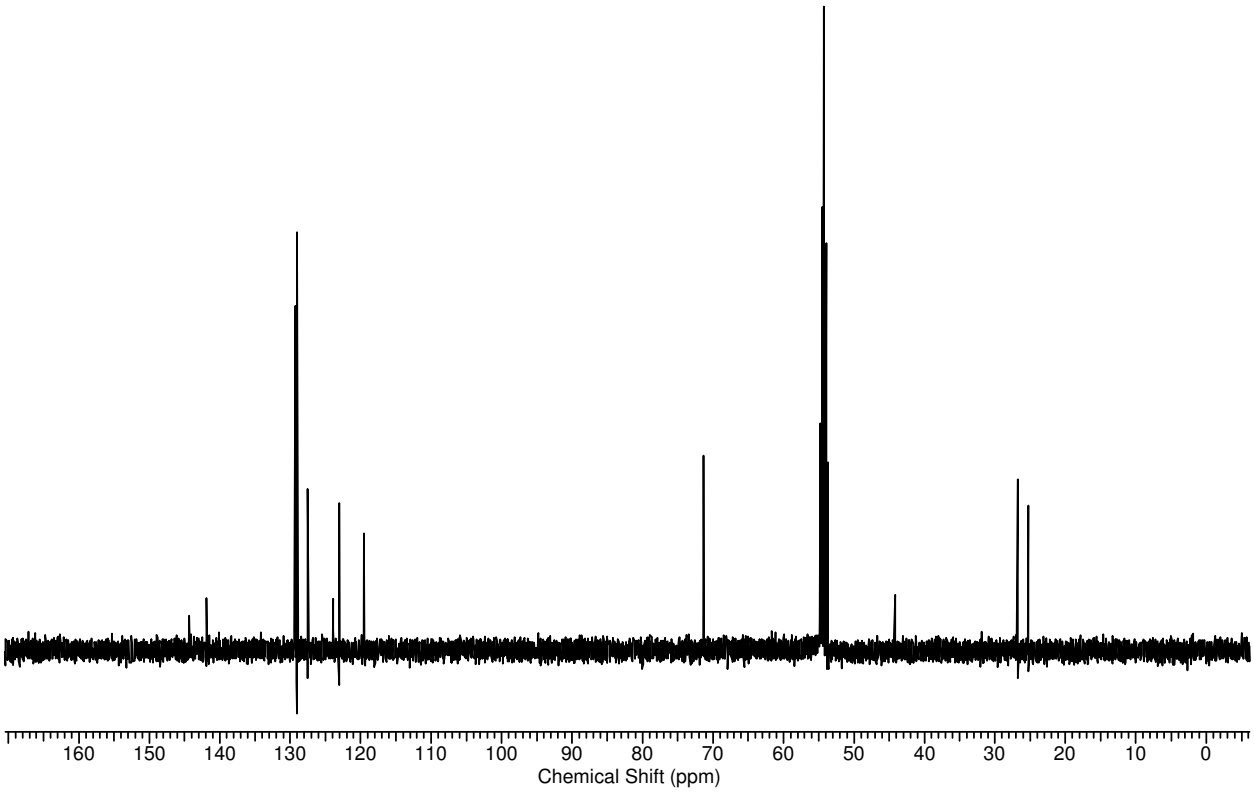

Compound 82

^{1}H NMR

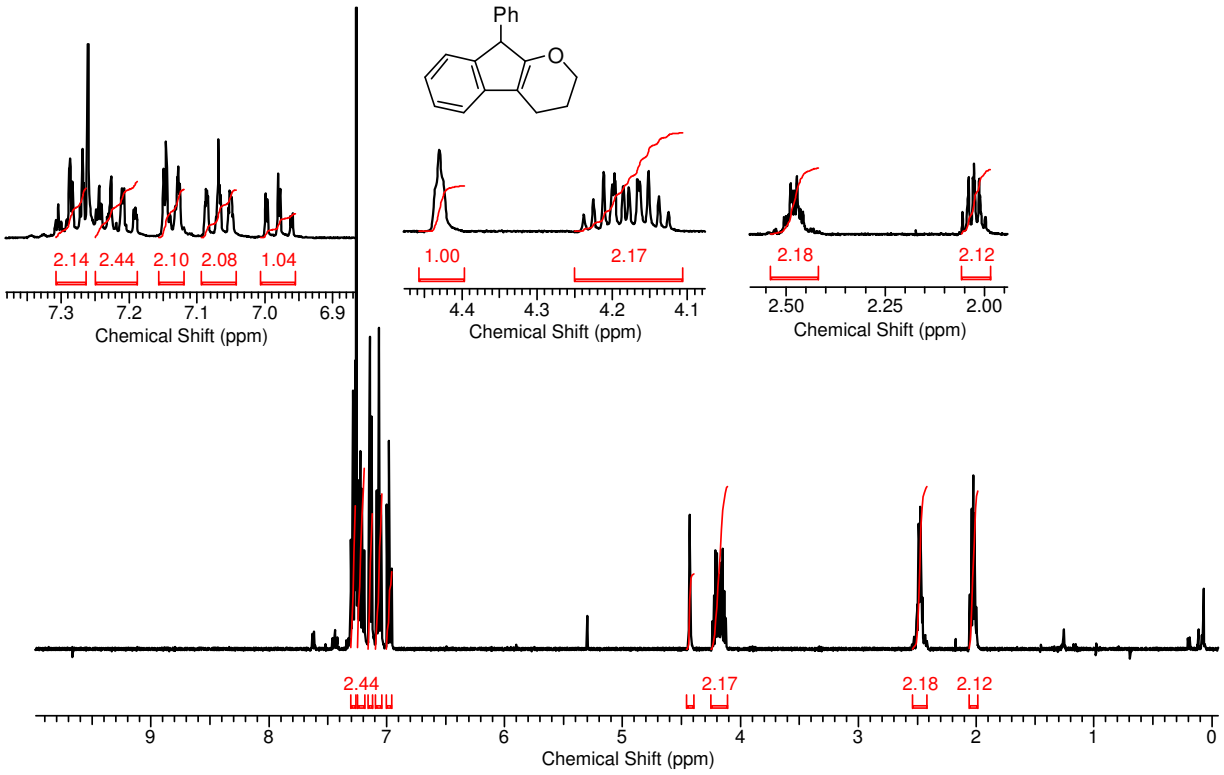

^{13}C NMR

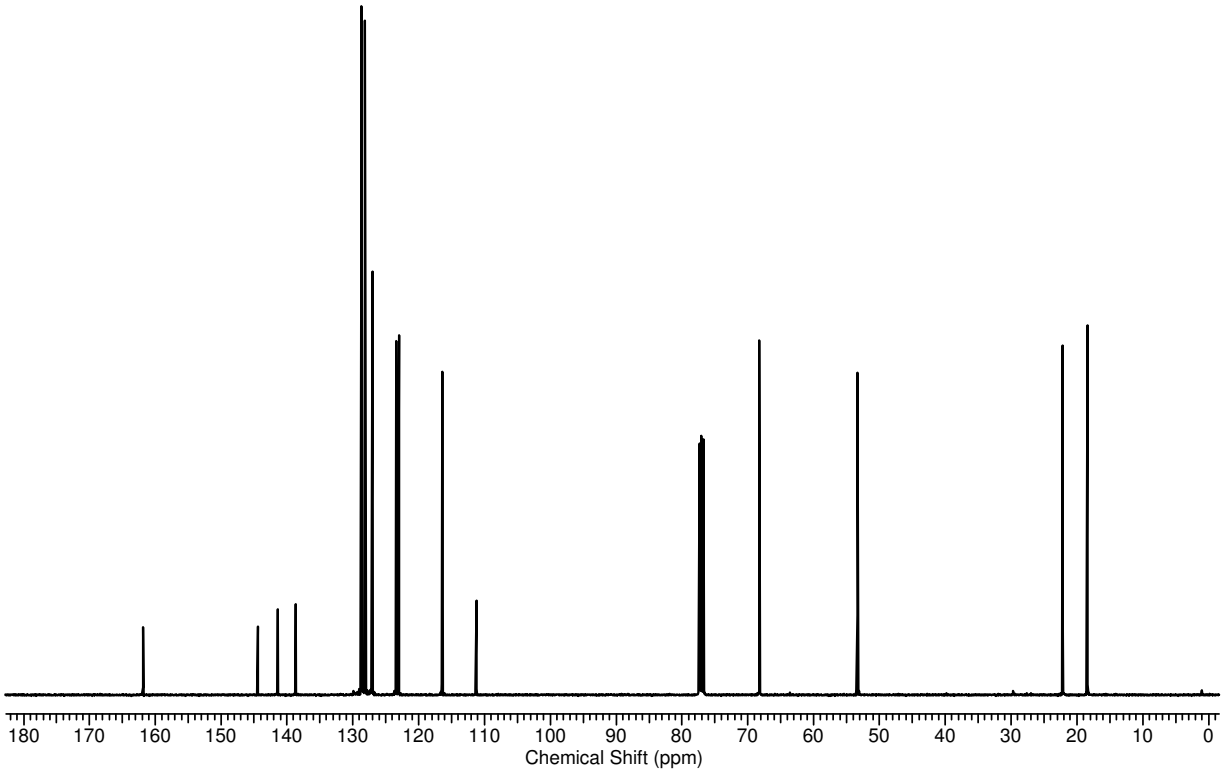

Compound 98

^{1}H NMR

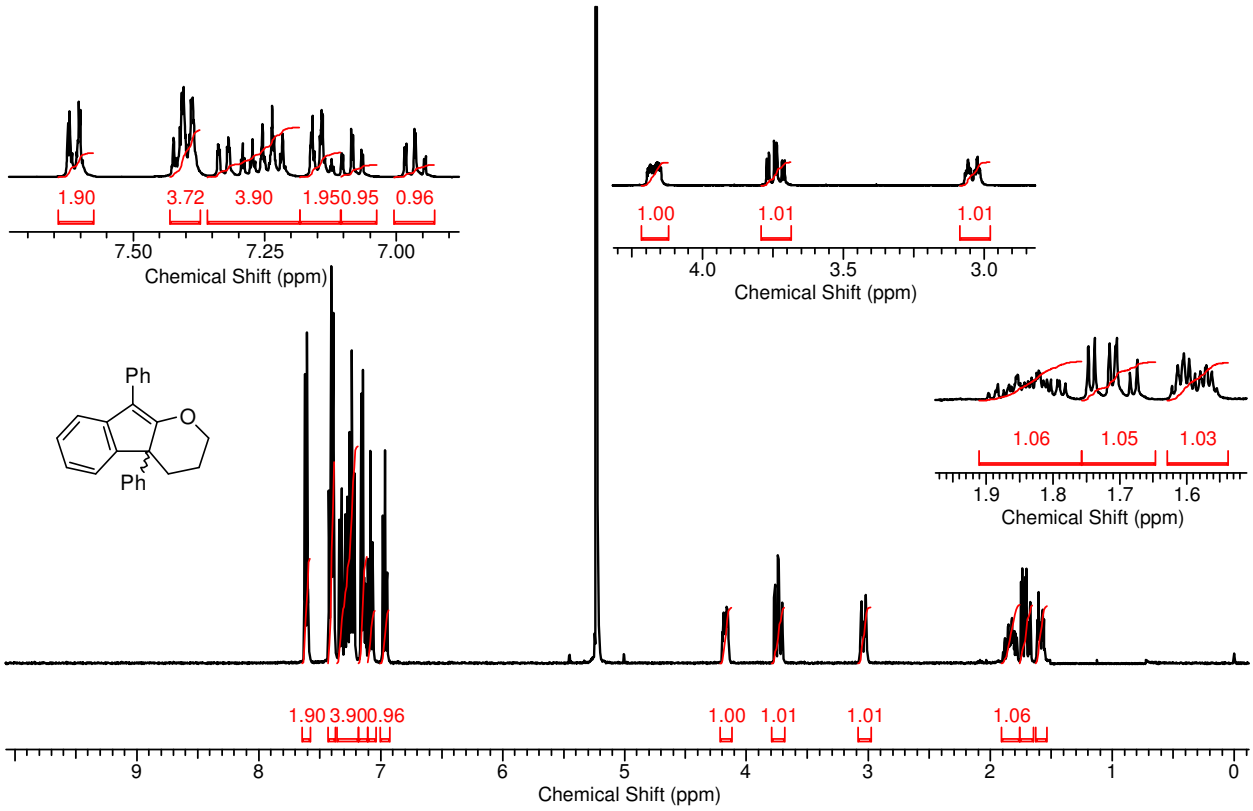

^{13}C NMR

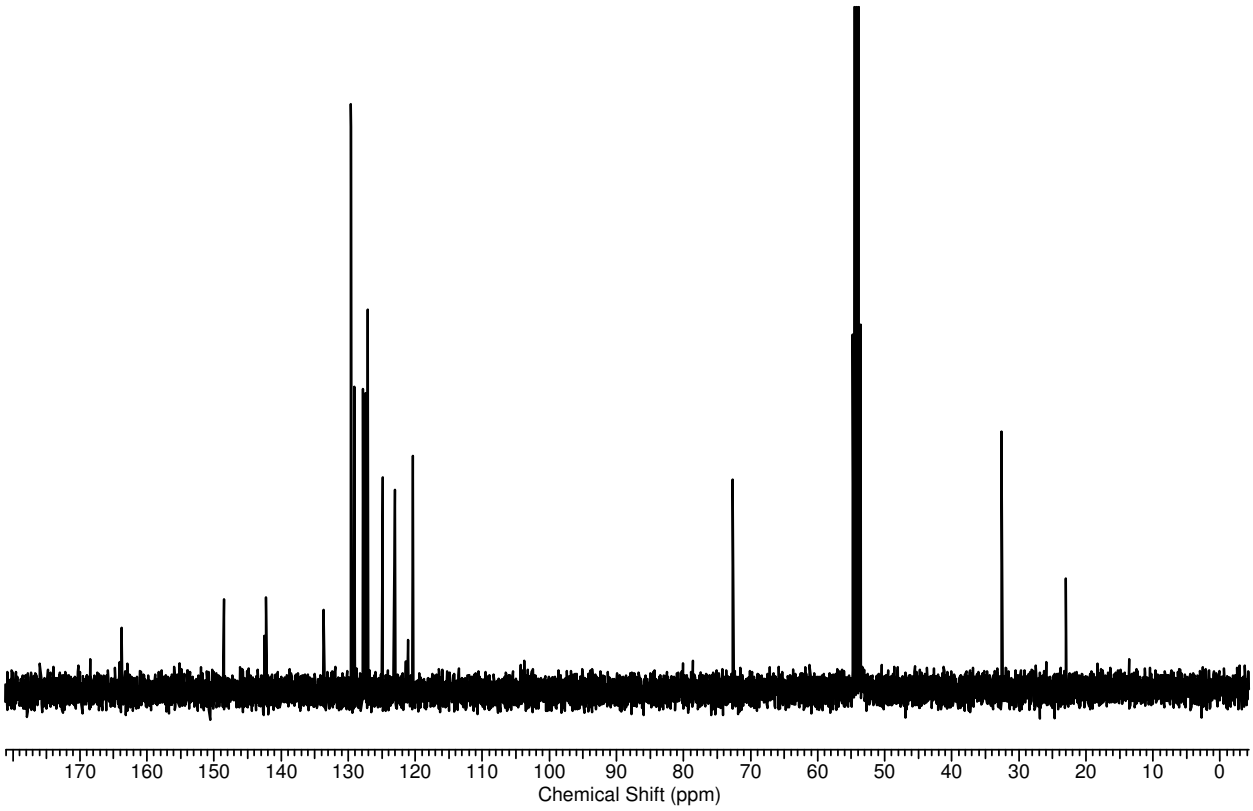

Compound 99

^{1}H NMR

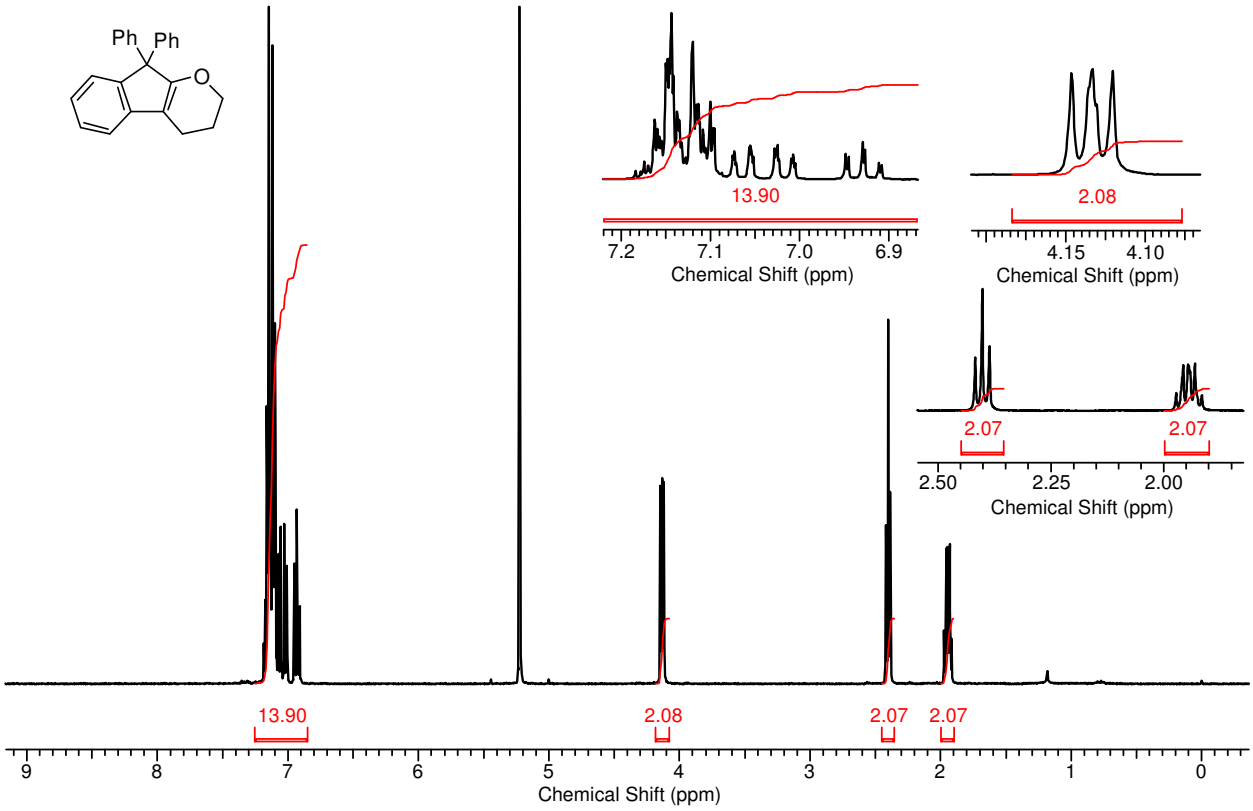

^{13}C NMR

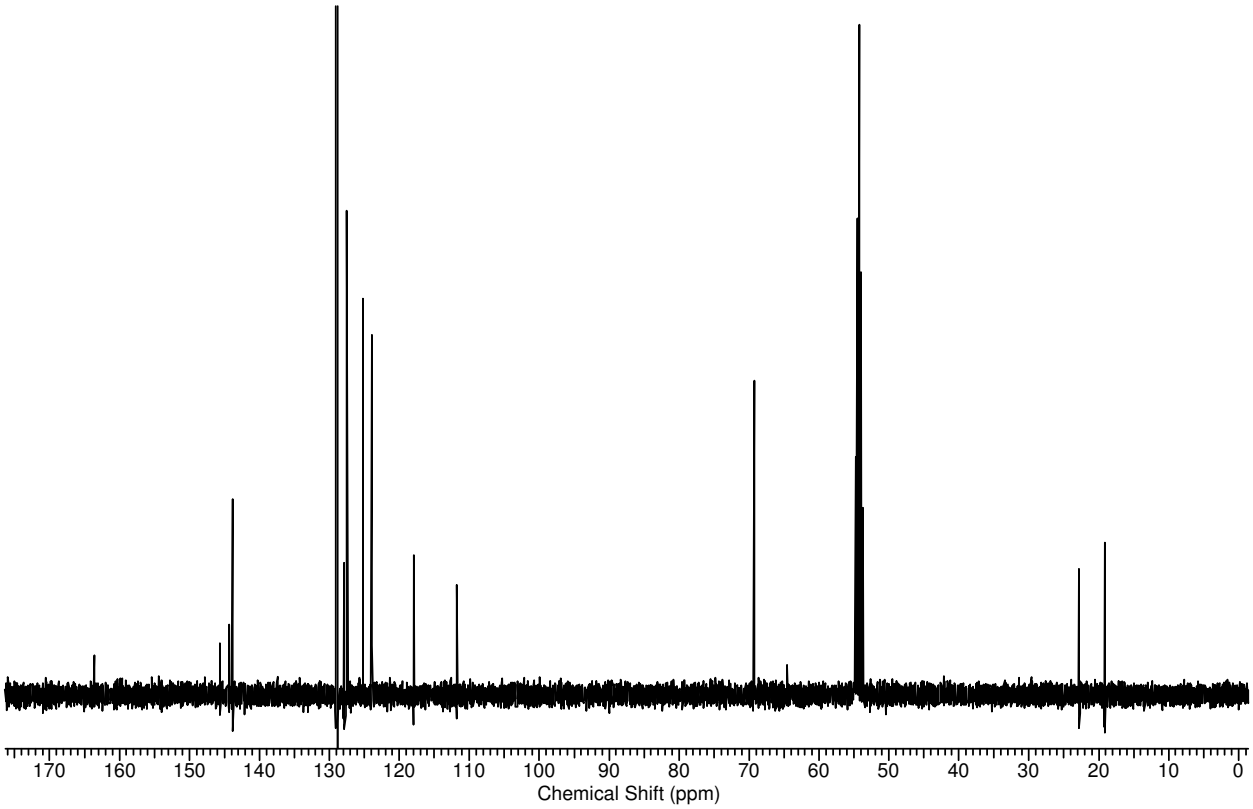

Compound 113a

^{1}H NMR

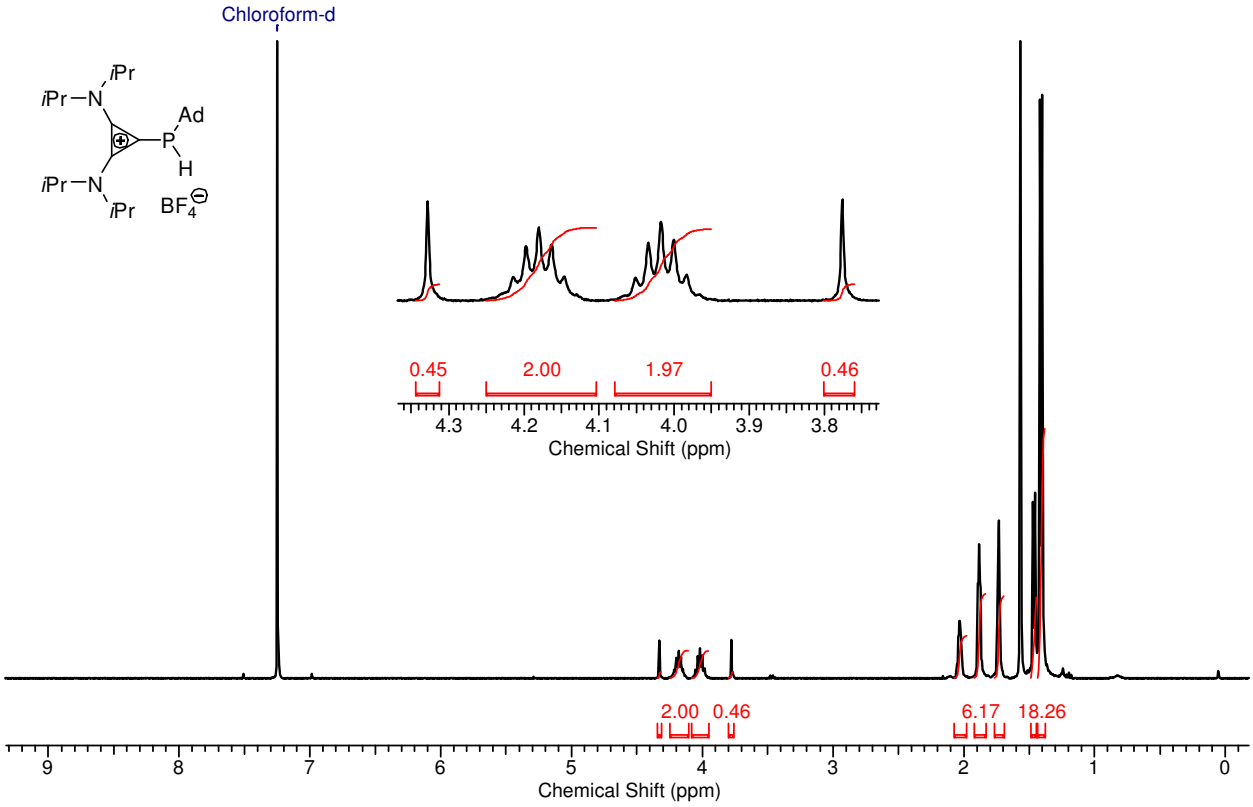

^{31}P NMR

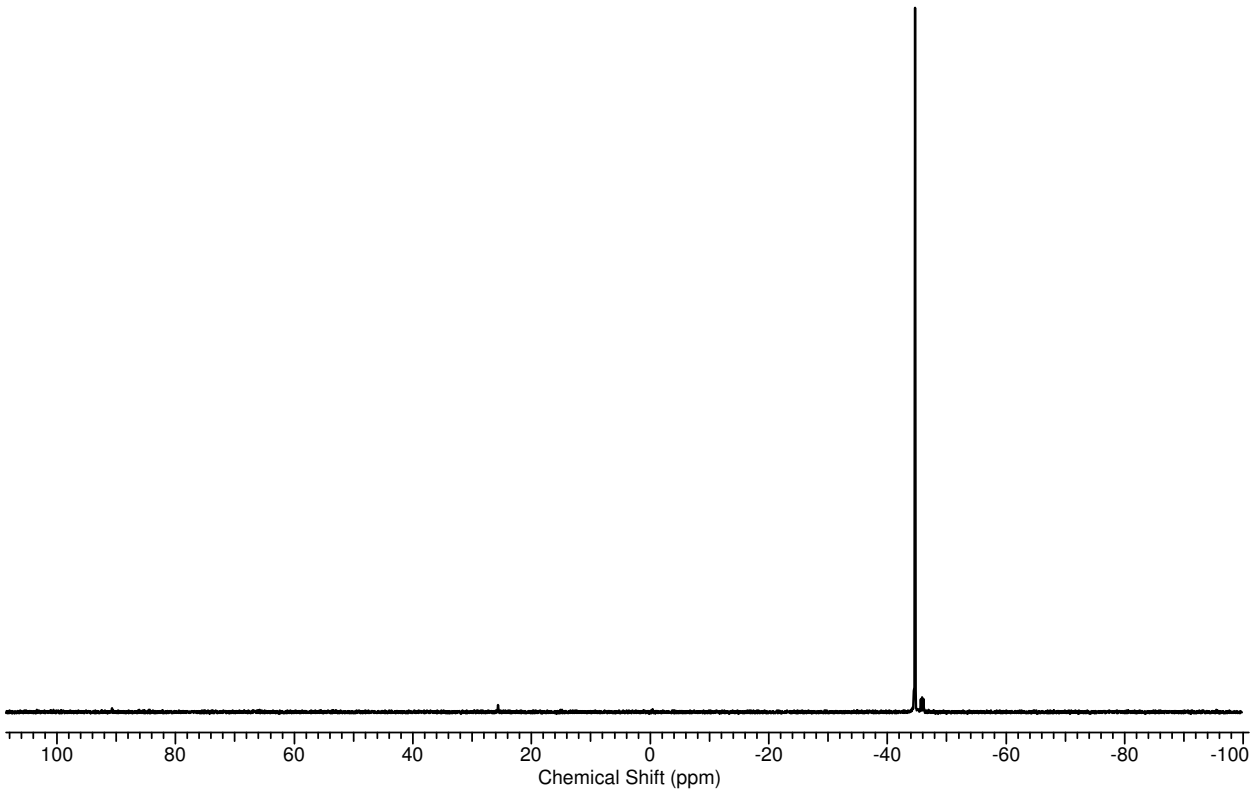

^{13}C NMR

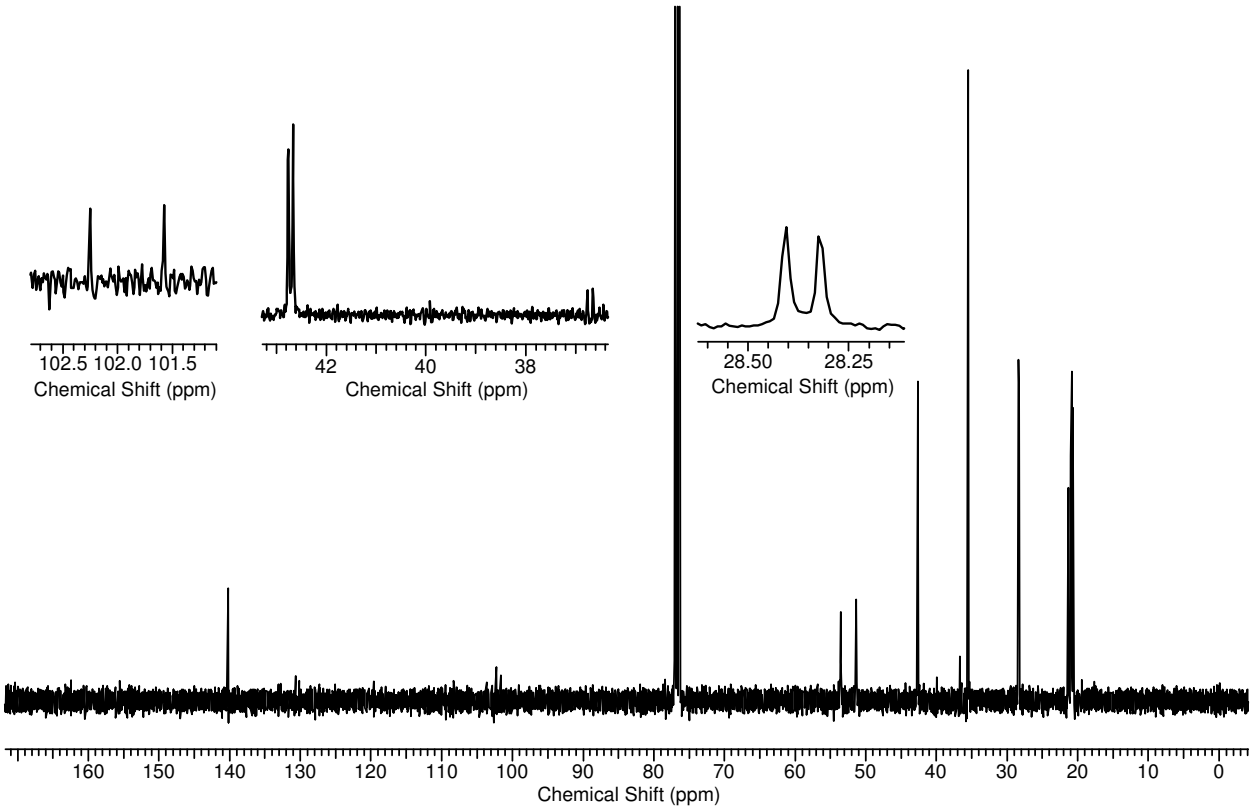

Compound 114a

^{1}H NMR

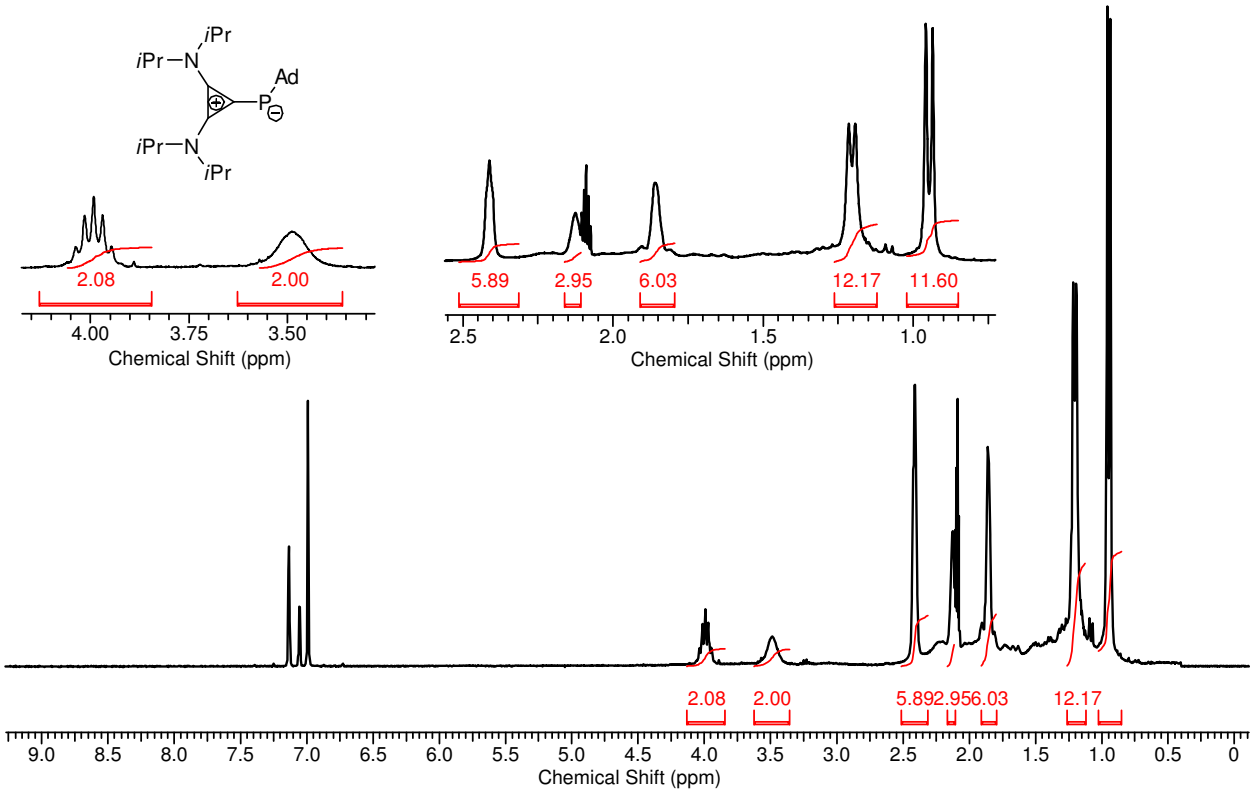

^{31}P NMR

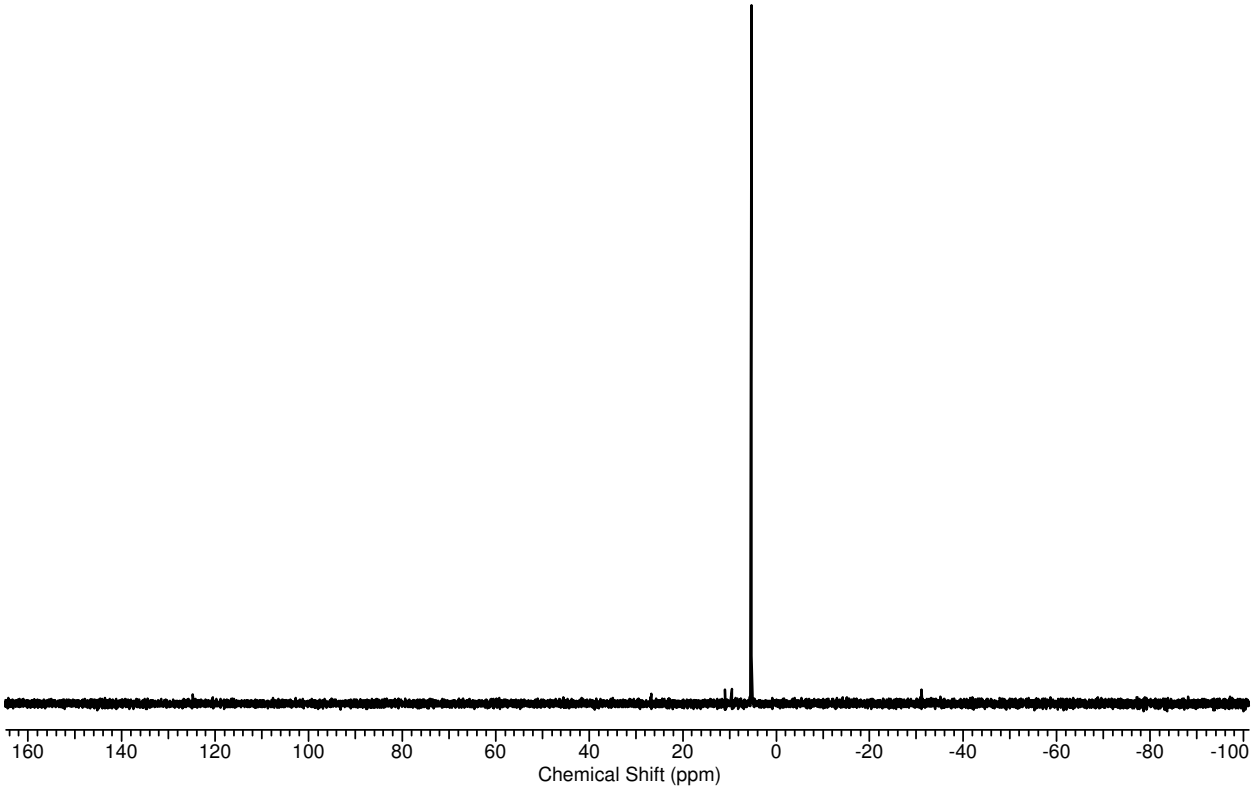

^{13}C NMR

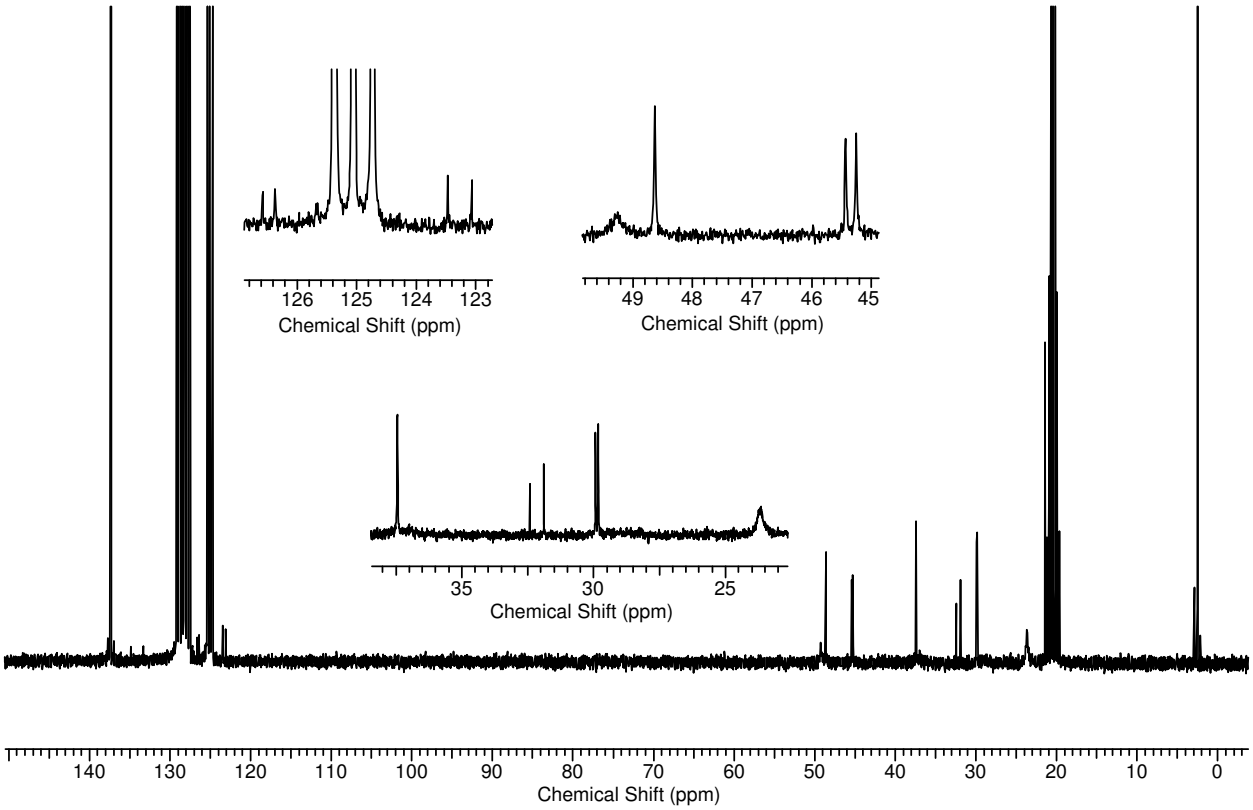

Compound 115

^{1}H NMR

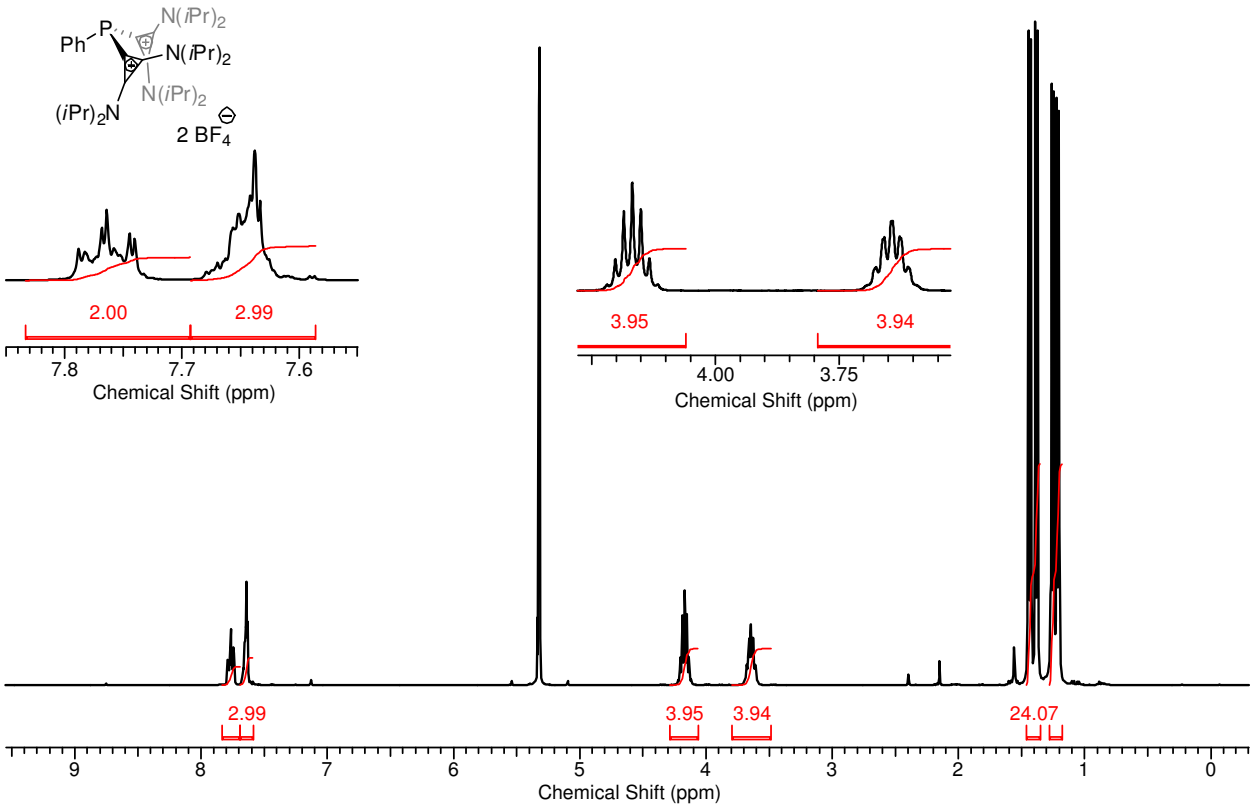

^{31}P NMR

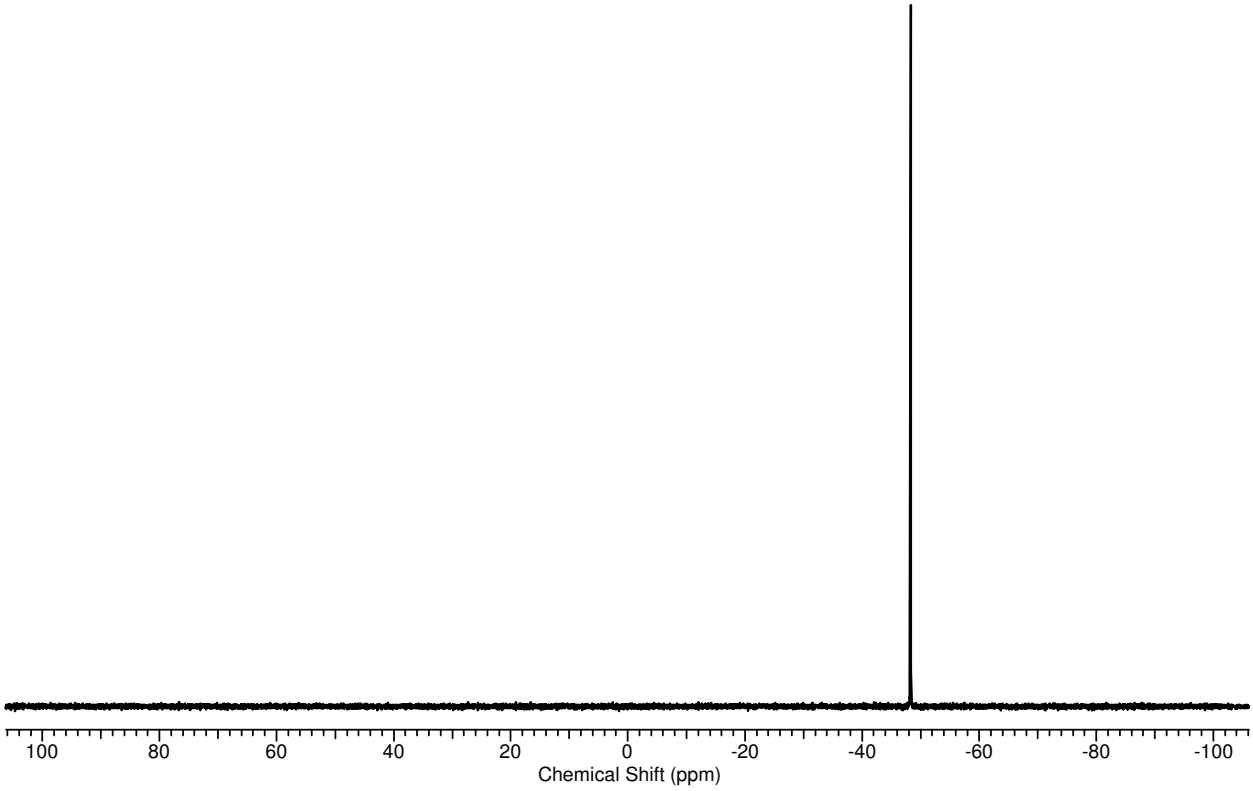

^{13}C NMR

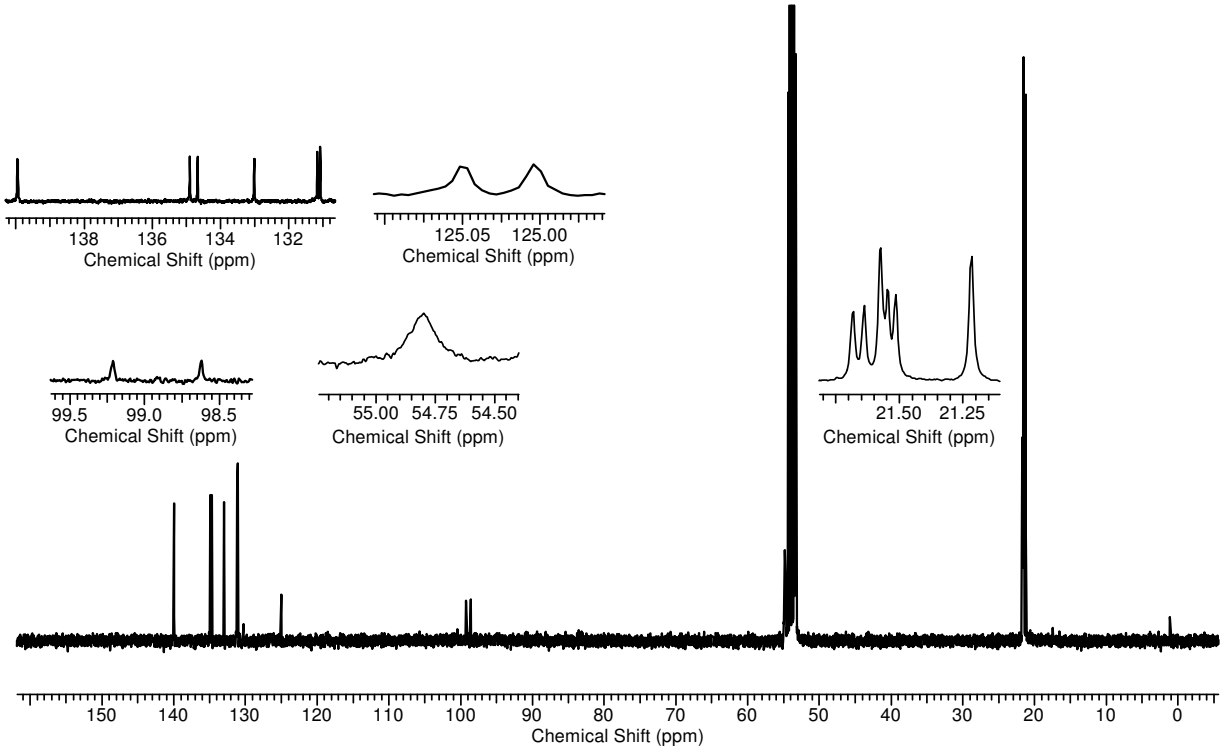

Compound 117

^{1}H NMR

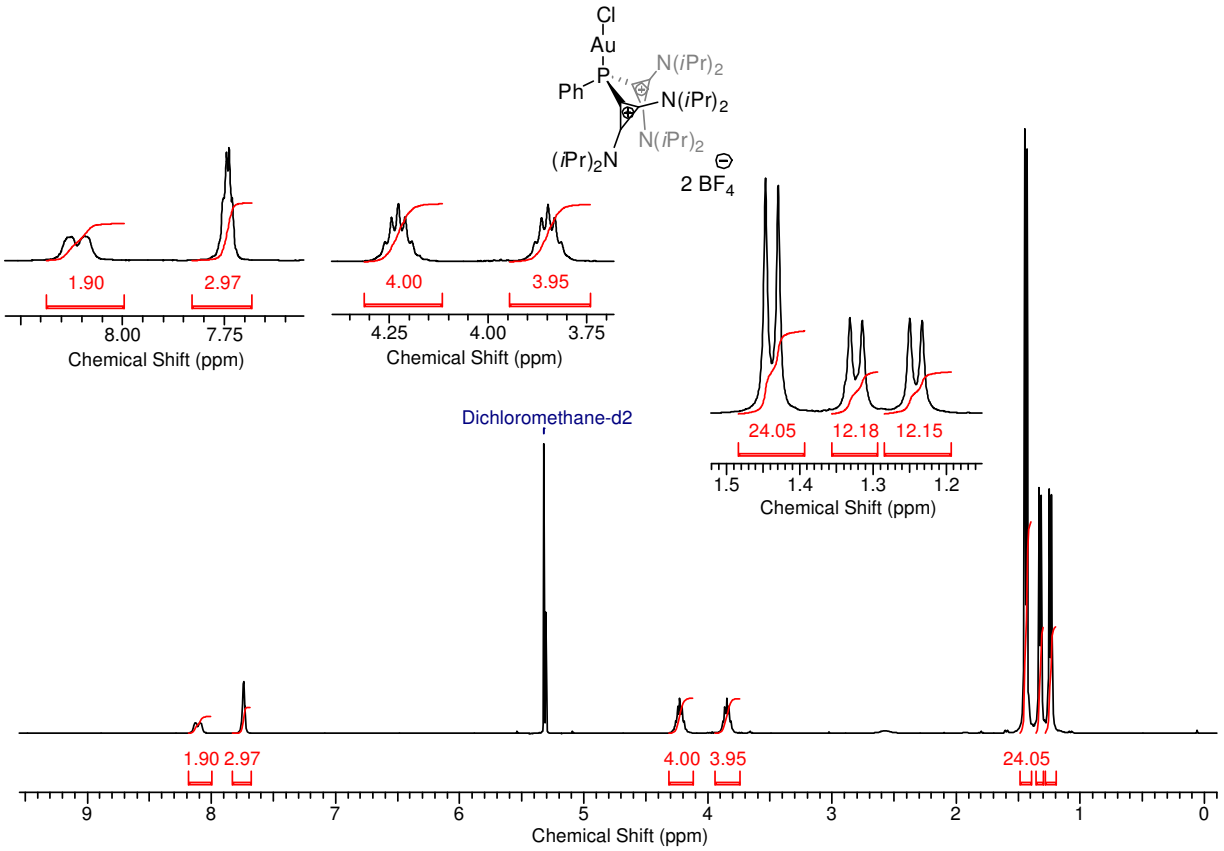

^{31}P NMR

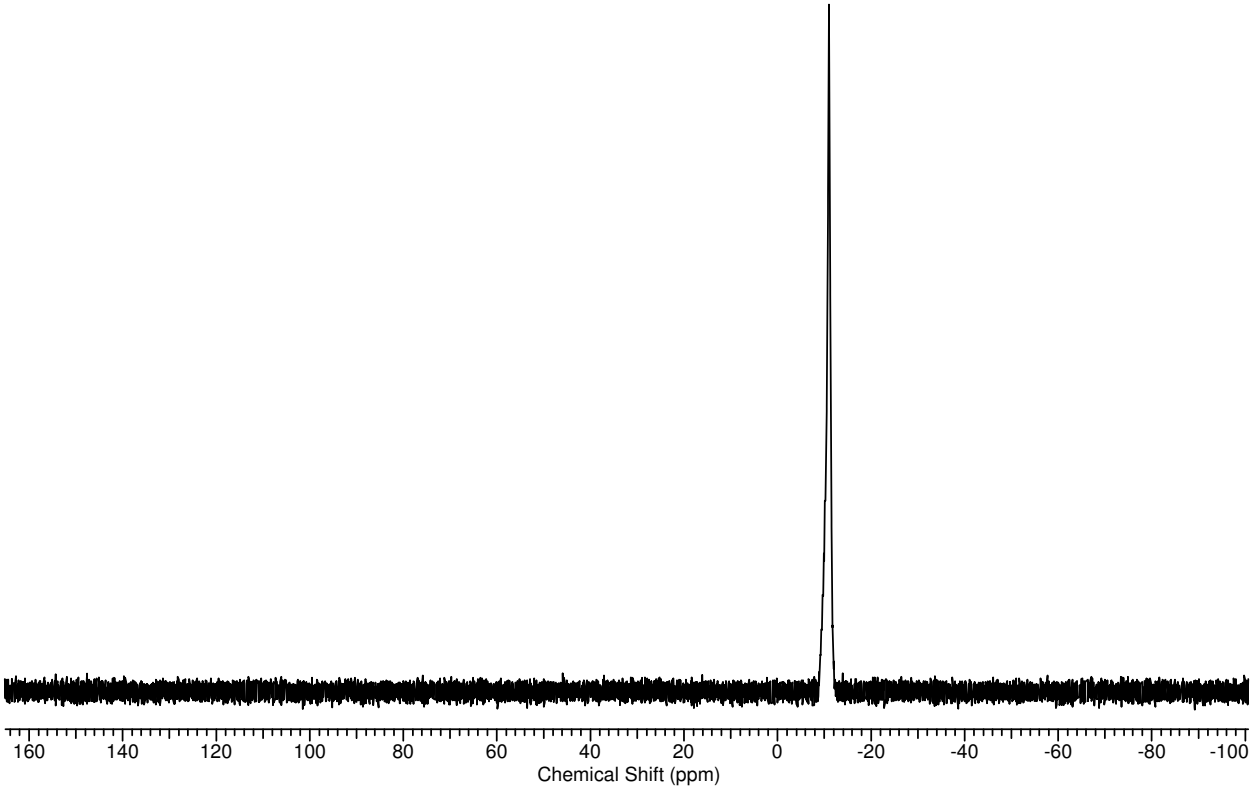

^{13}C NMR

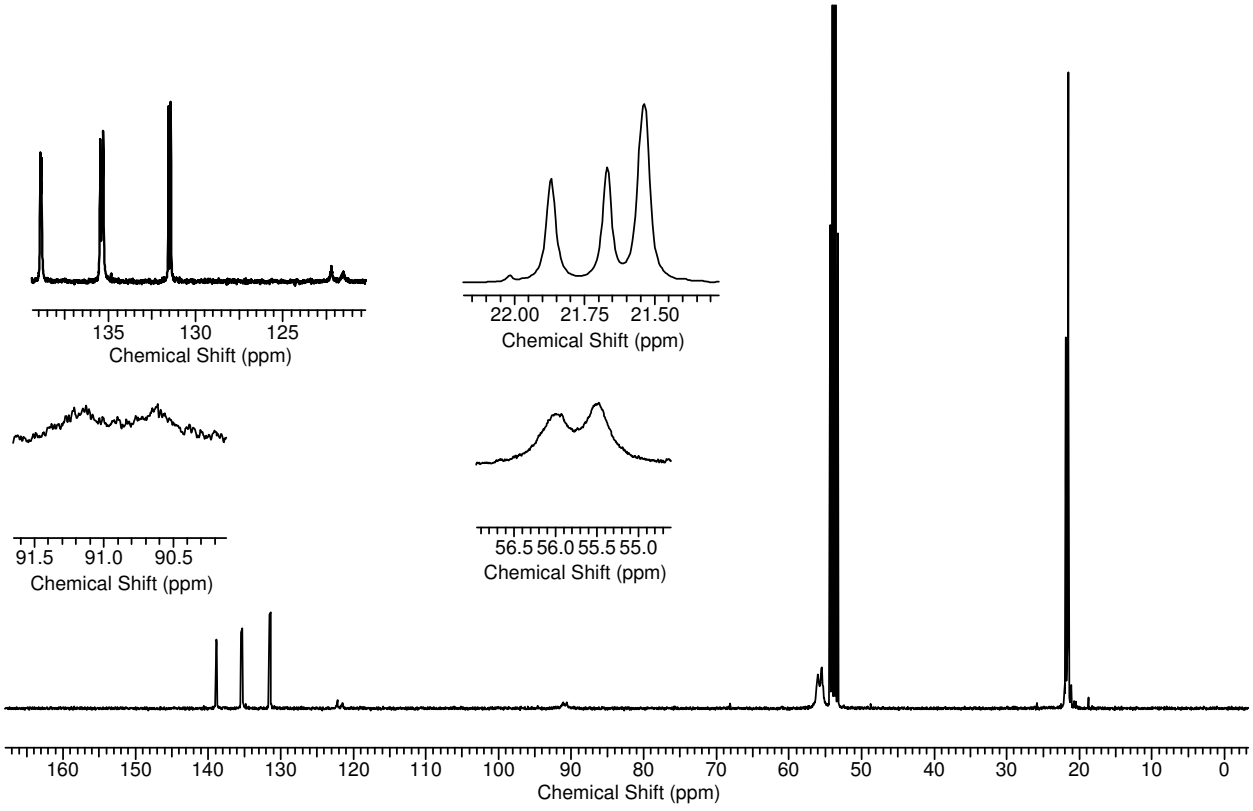

Compound 119

^{1}H NMR

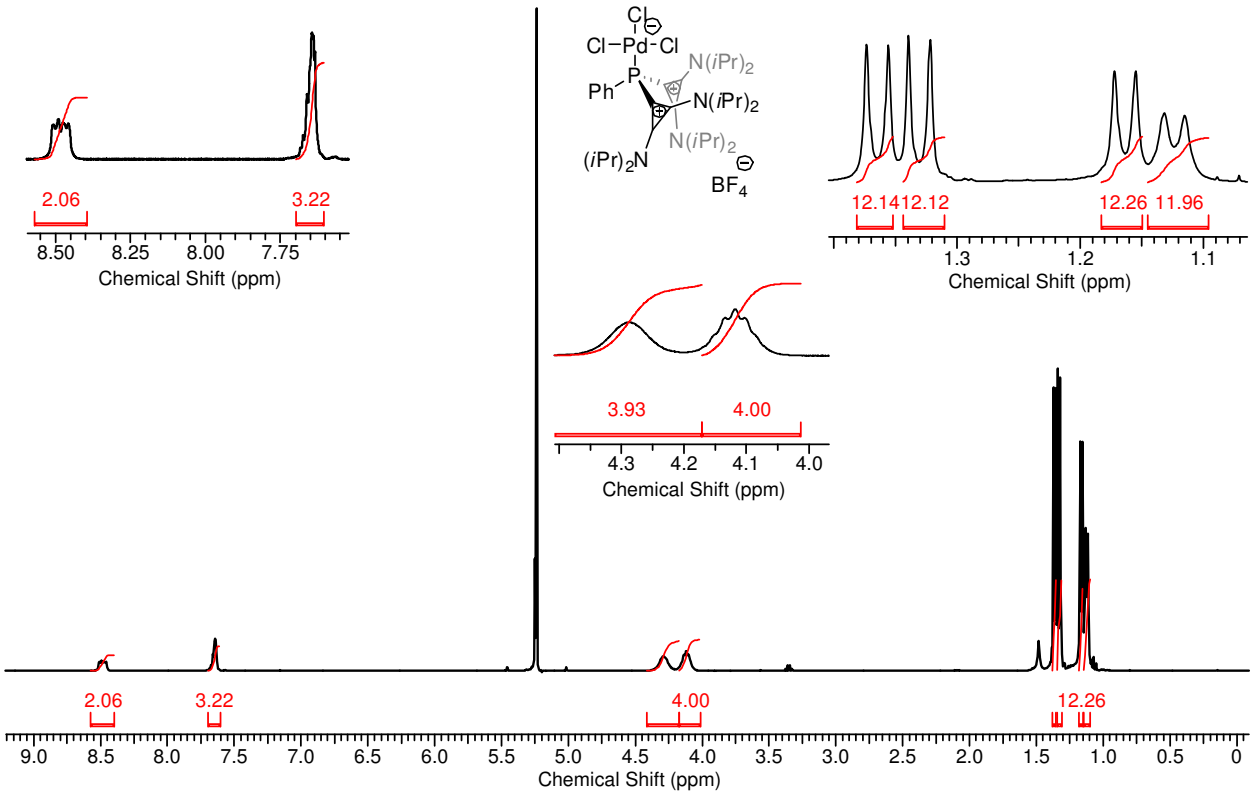

^{31}P NMR

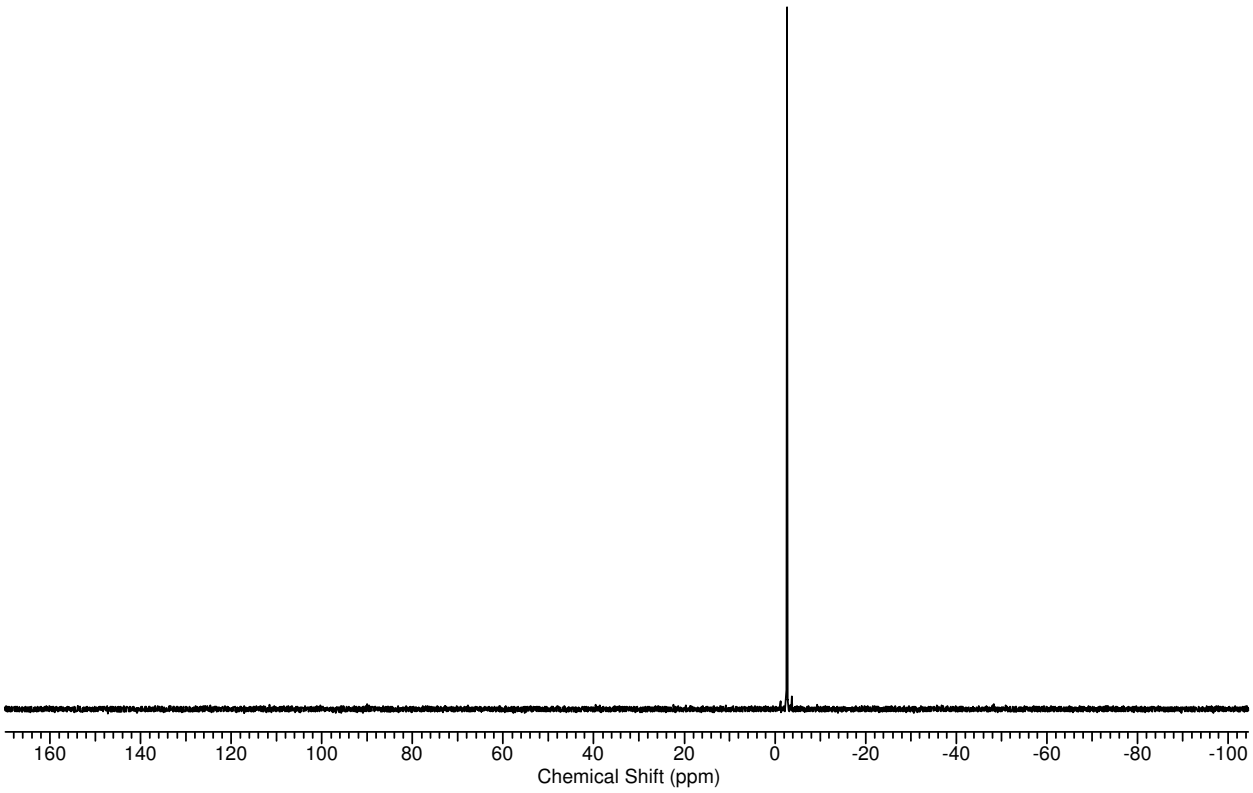

^{13}C NMR

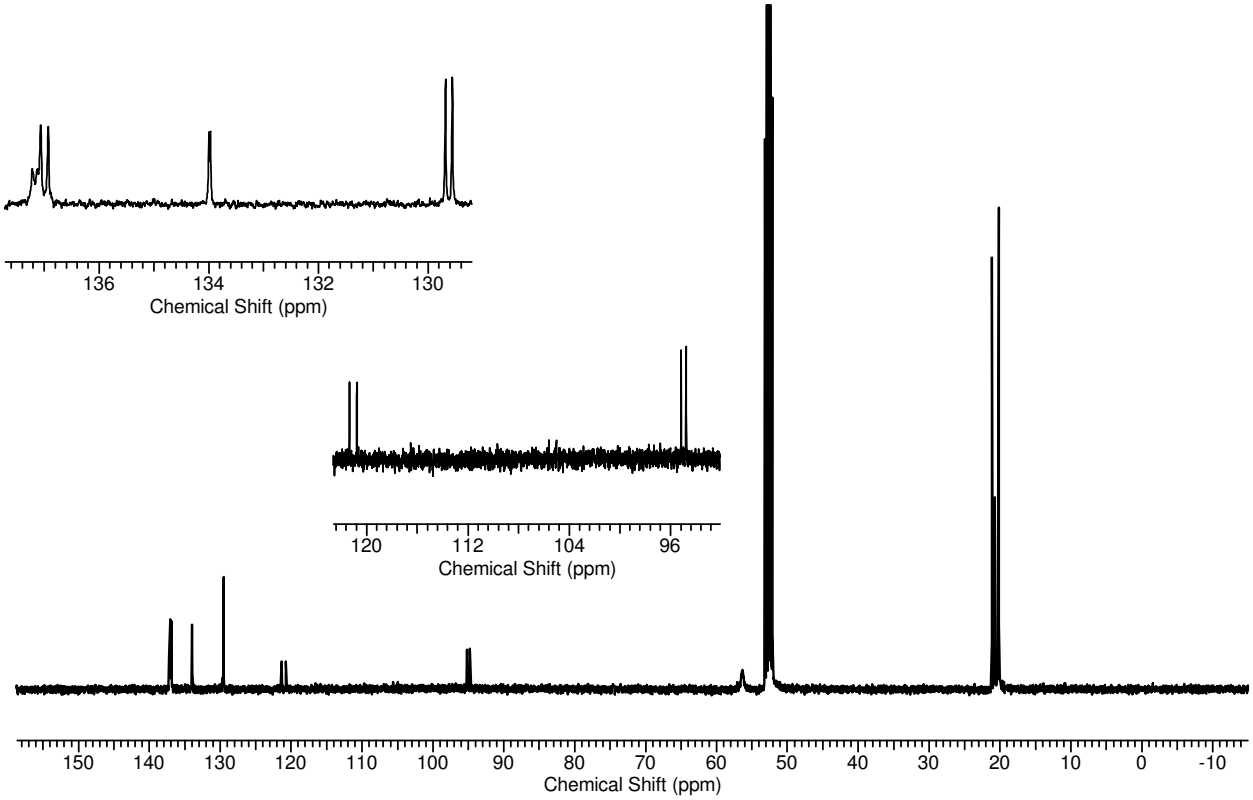

Compound 125

^{1}H NMR

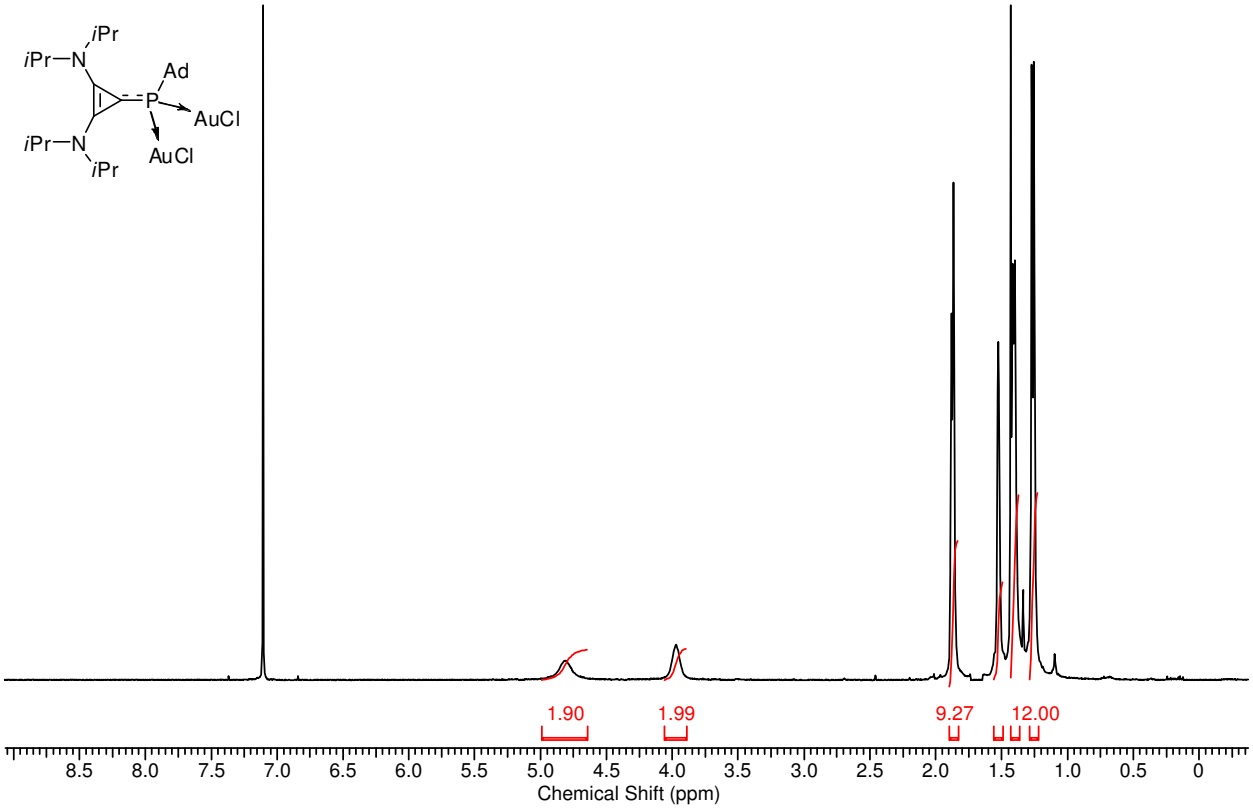

^{31}P NMR

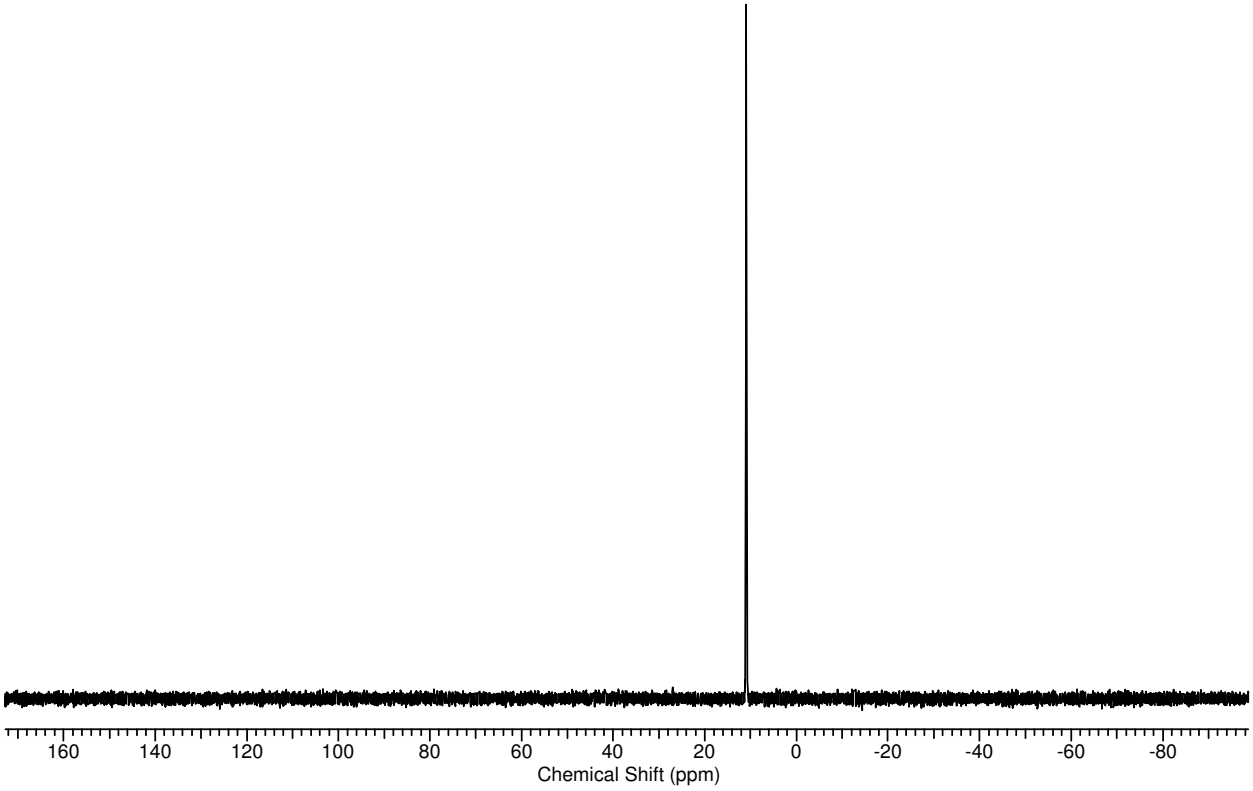

^{13}C NMR

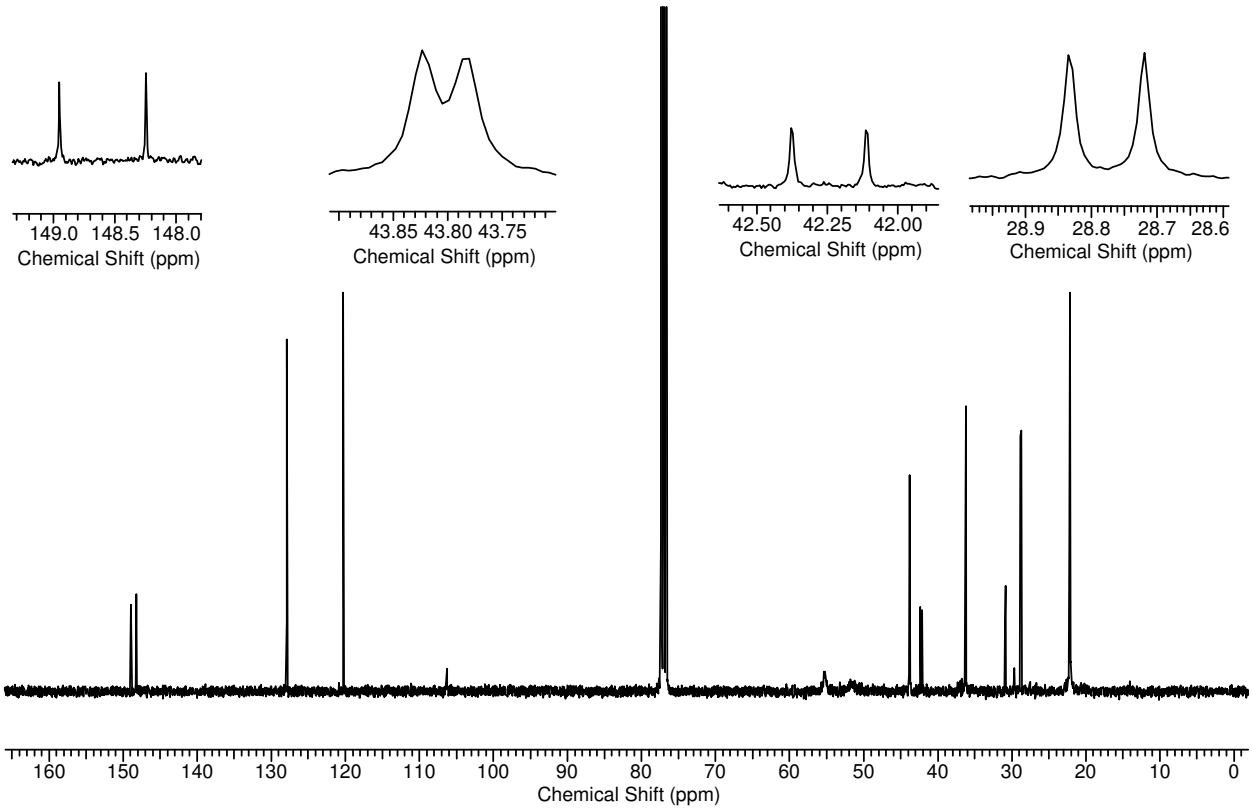

Compound 126

^{1}H NMR

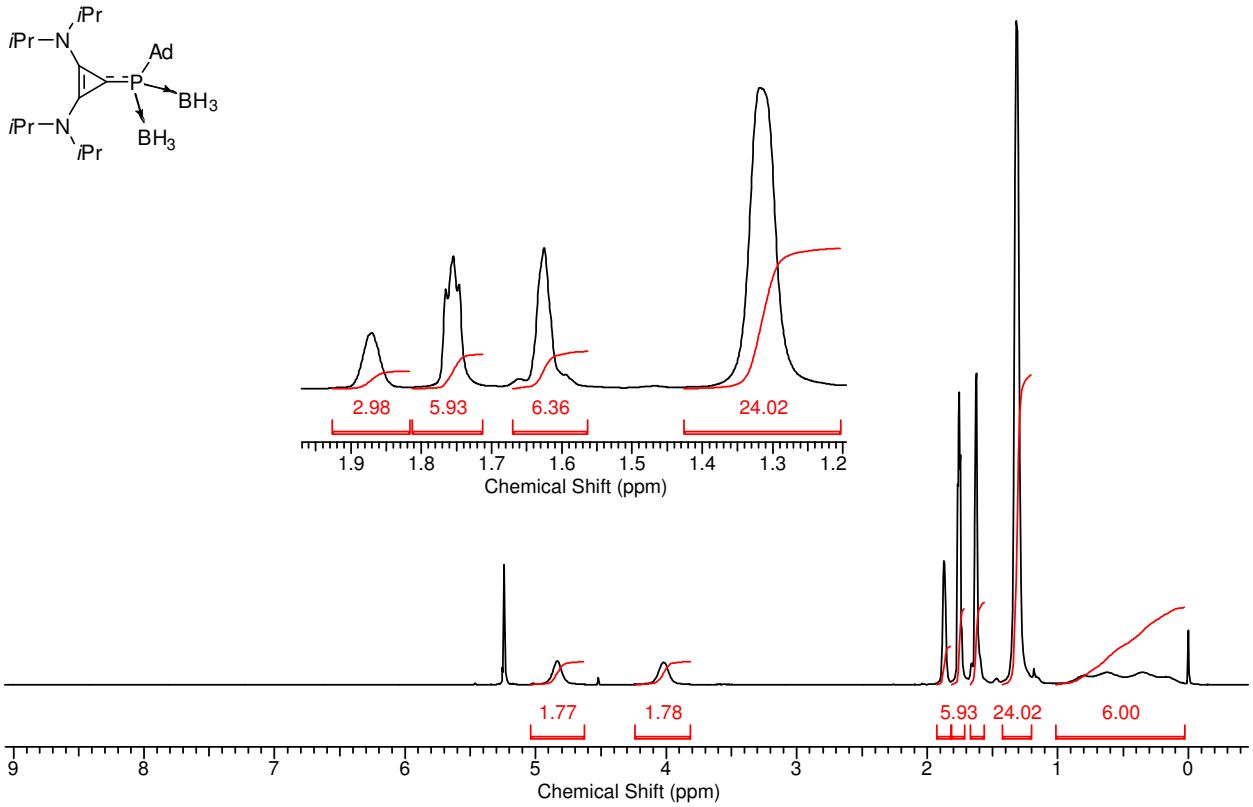

^{31}P NMR

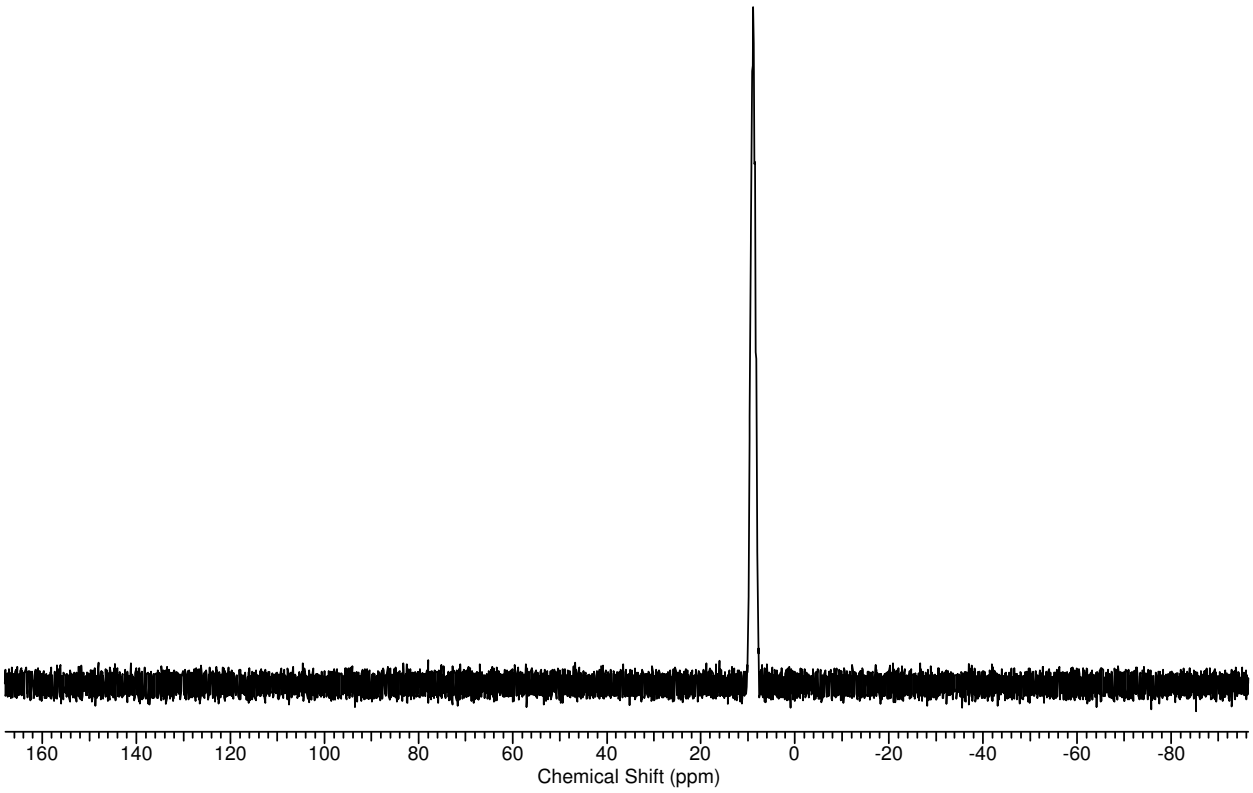

^{11}B NMR

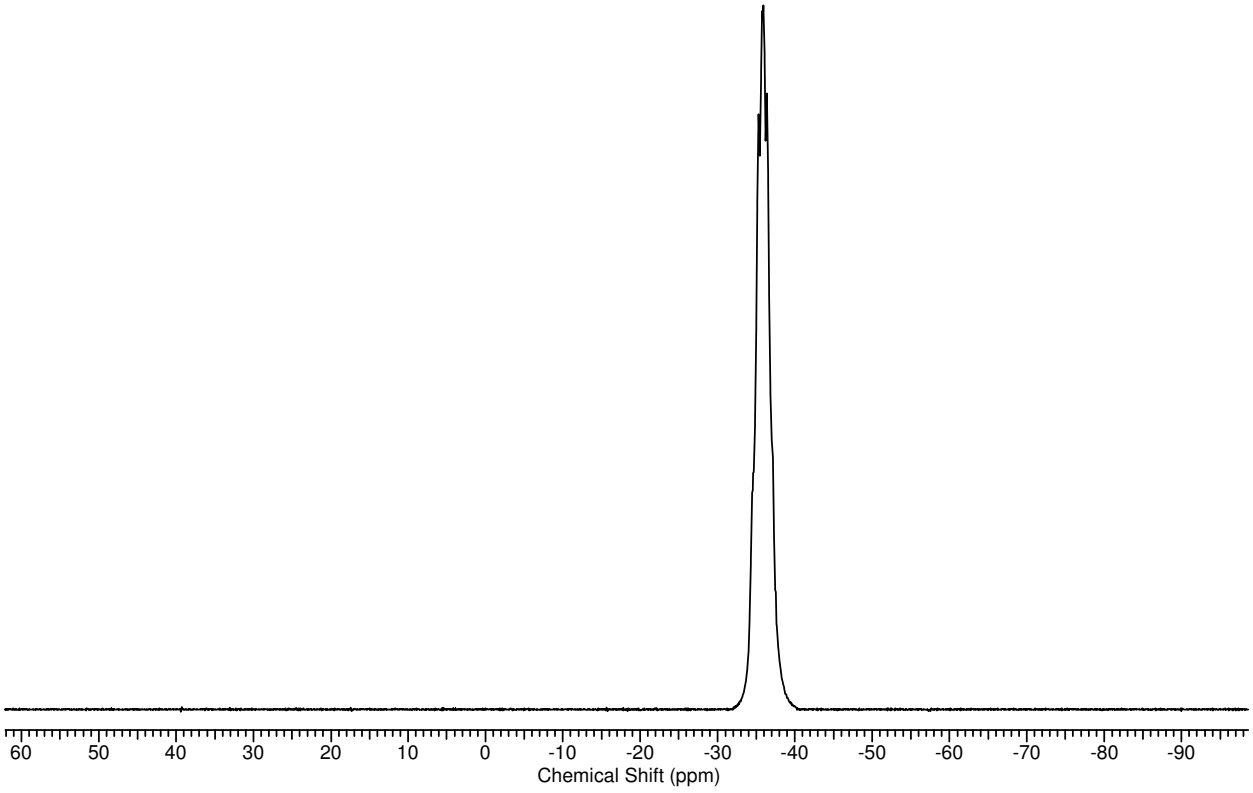

^{13}C NMR

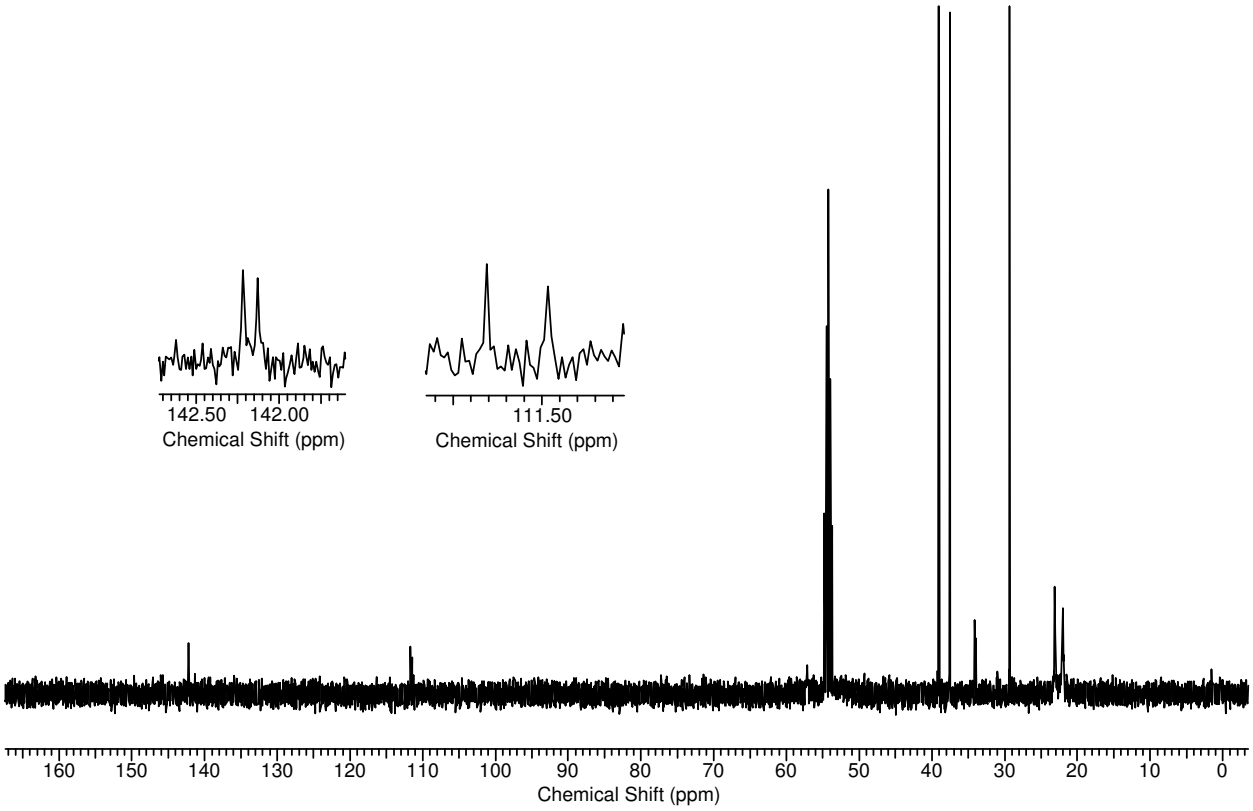

Compound 134

^{1}H NMR

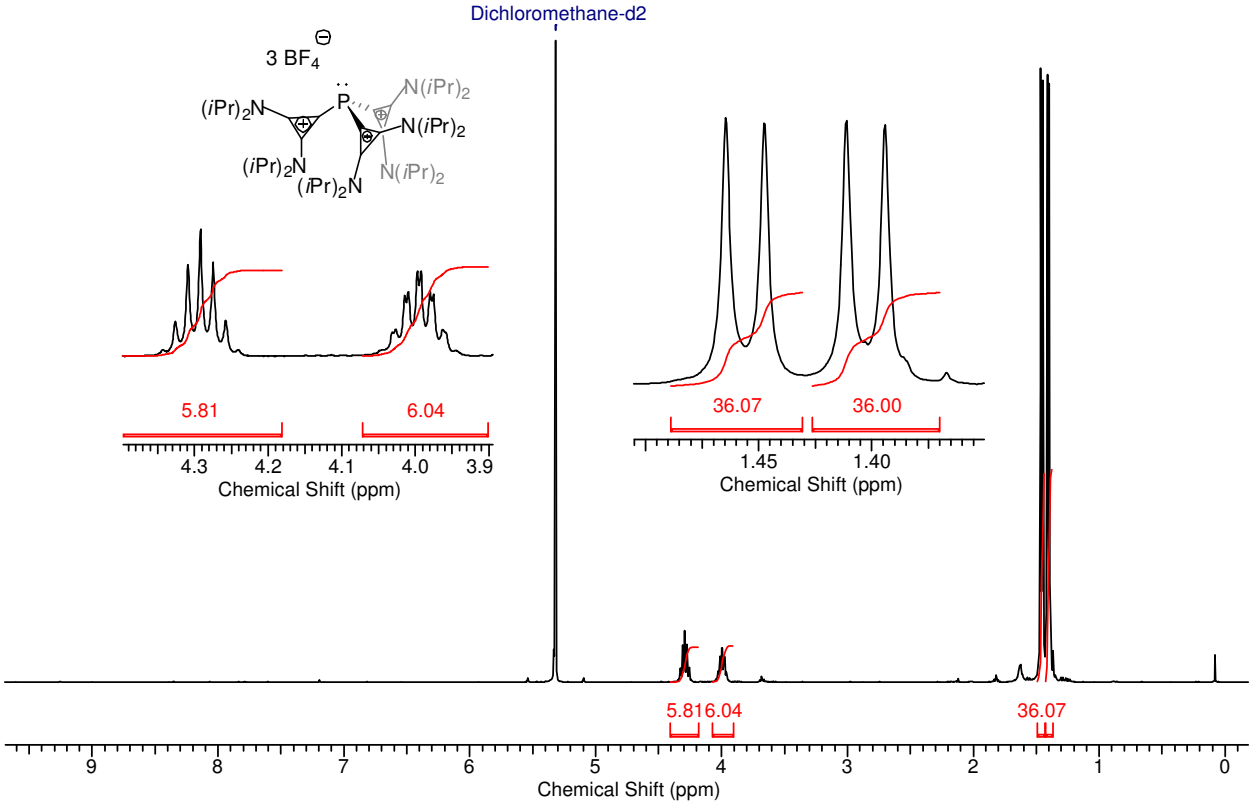

^{31}P NMR

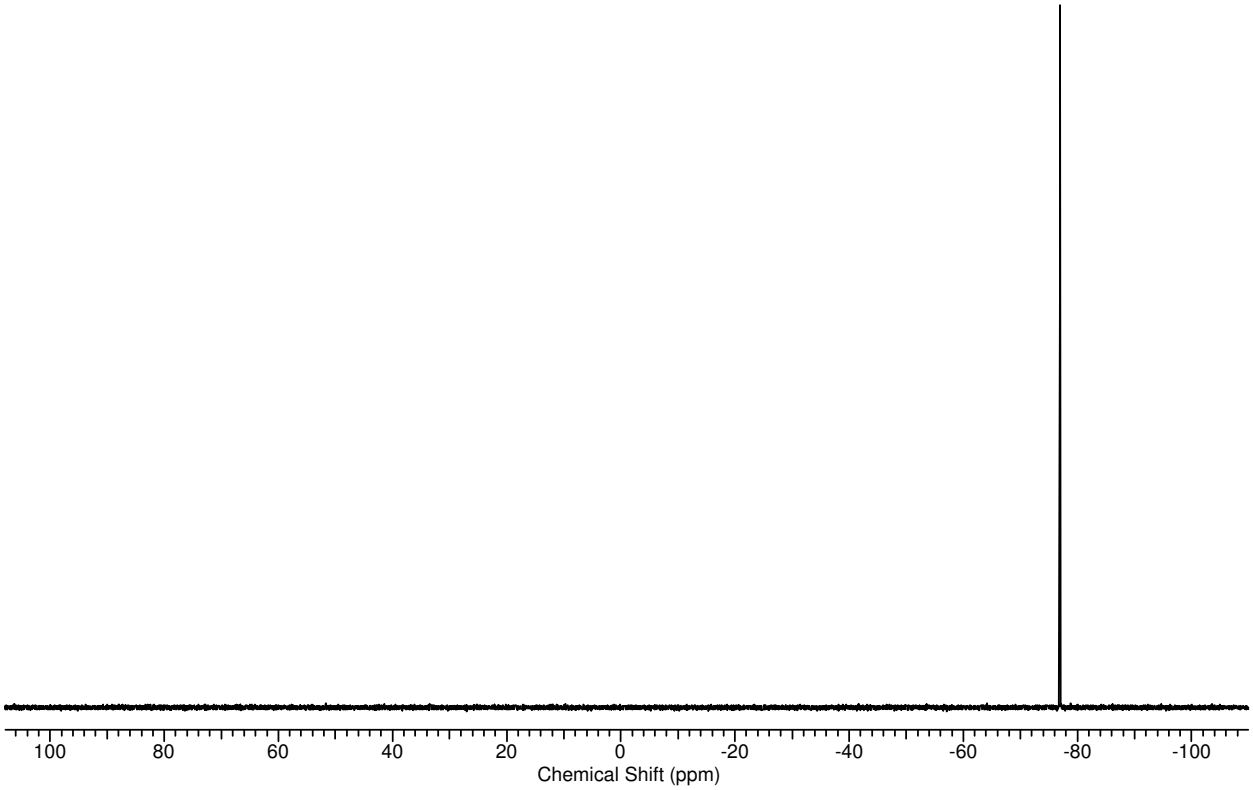

^{13}C NMR

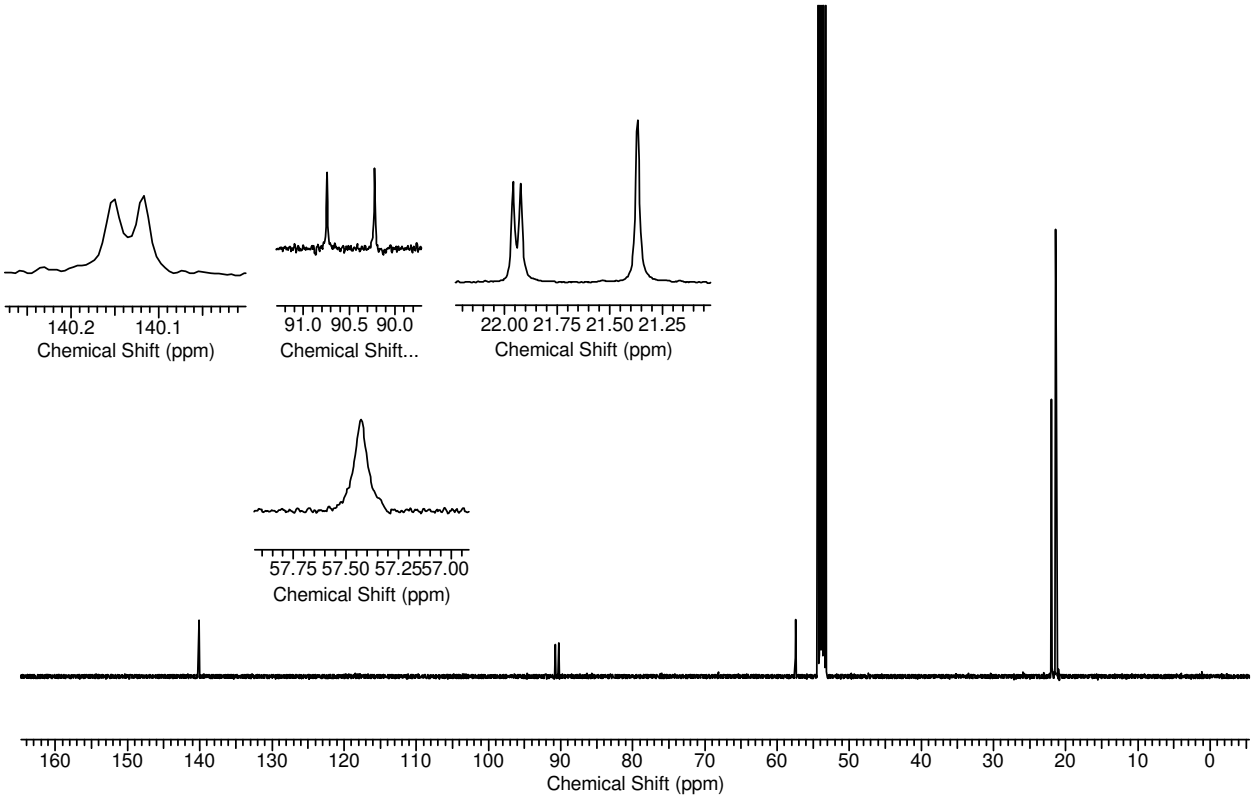

Compound 136

^{1}H NMR

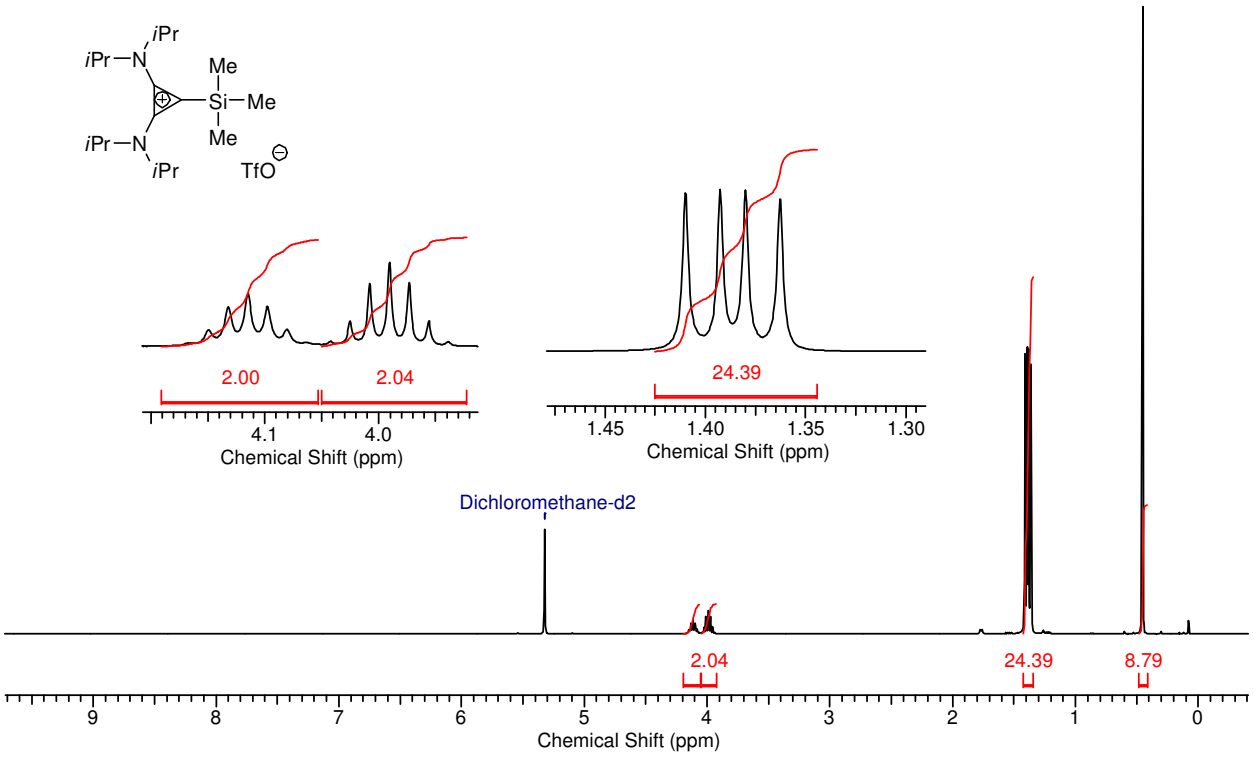

^{13}C NMR

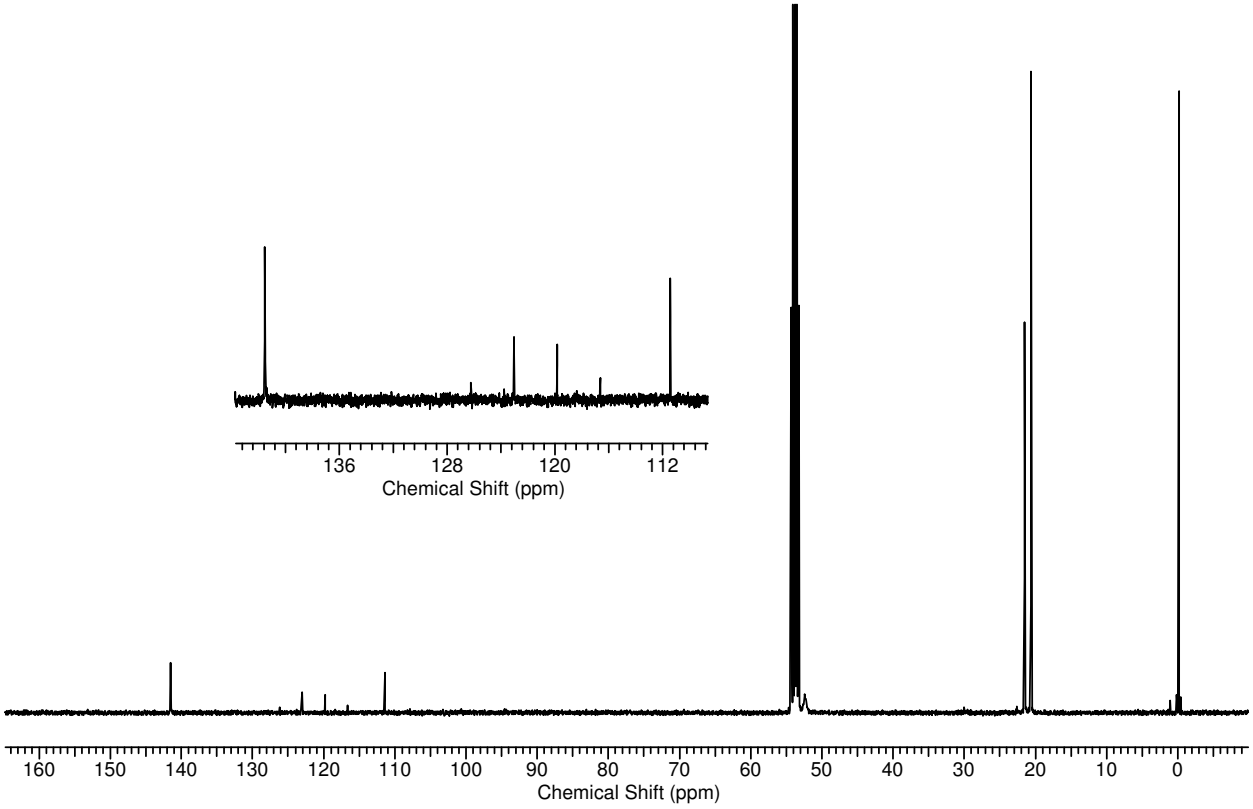

Compound 141

^{1}H NMR

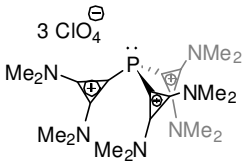

^{31}P NMR

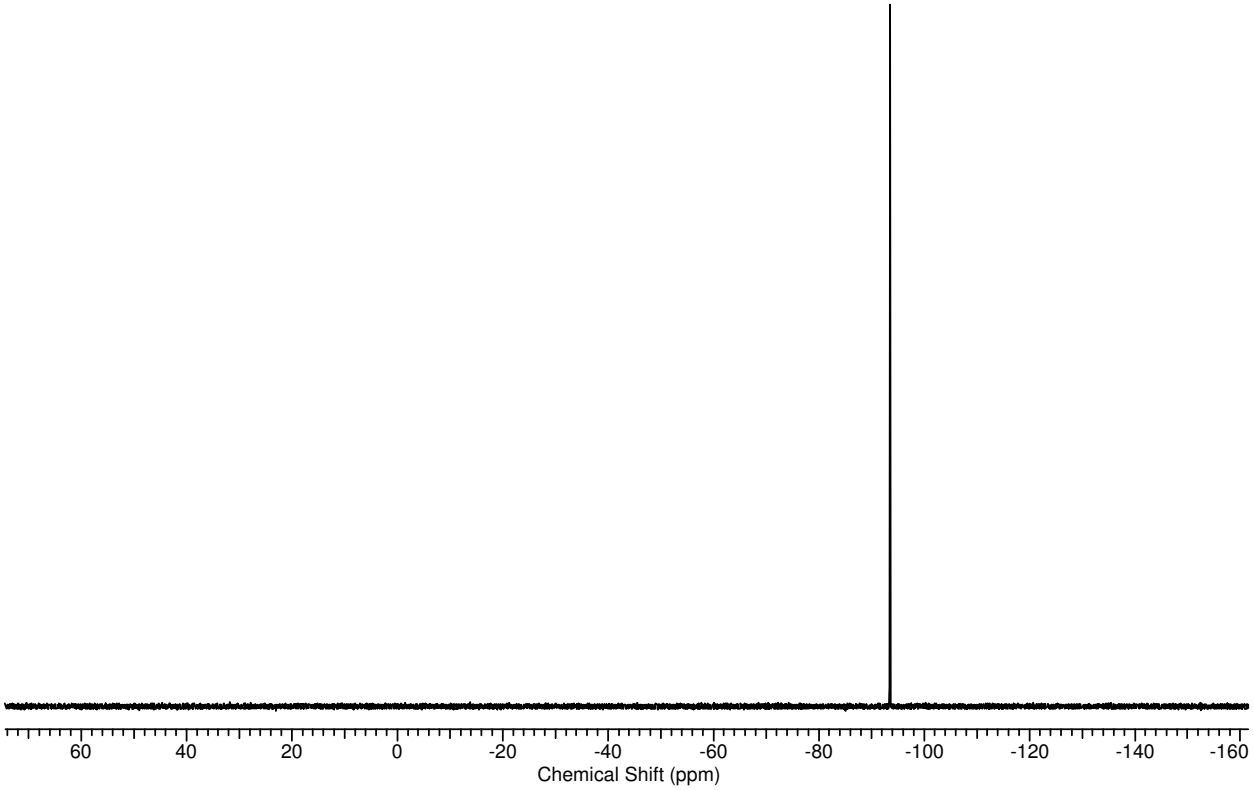

^{13}C NMR

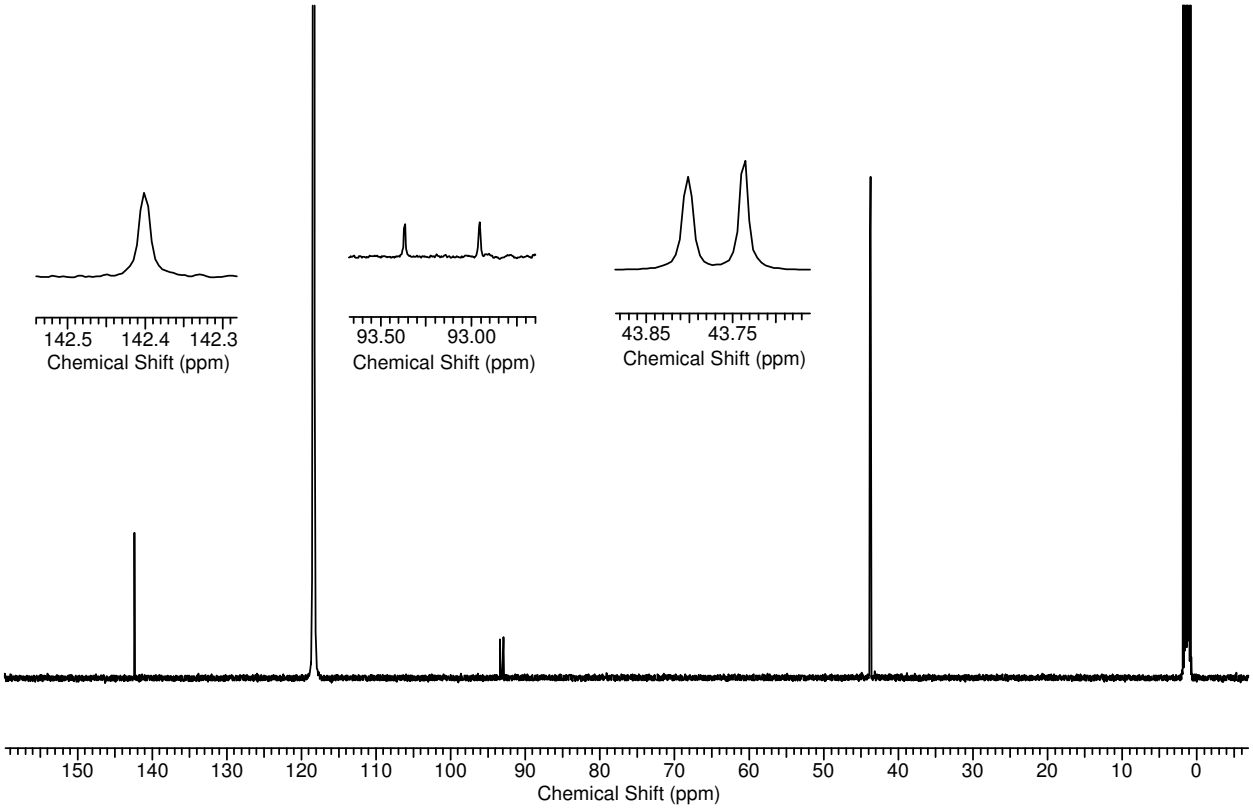

Compound 143

^{1}H NMR

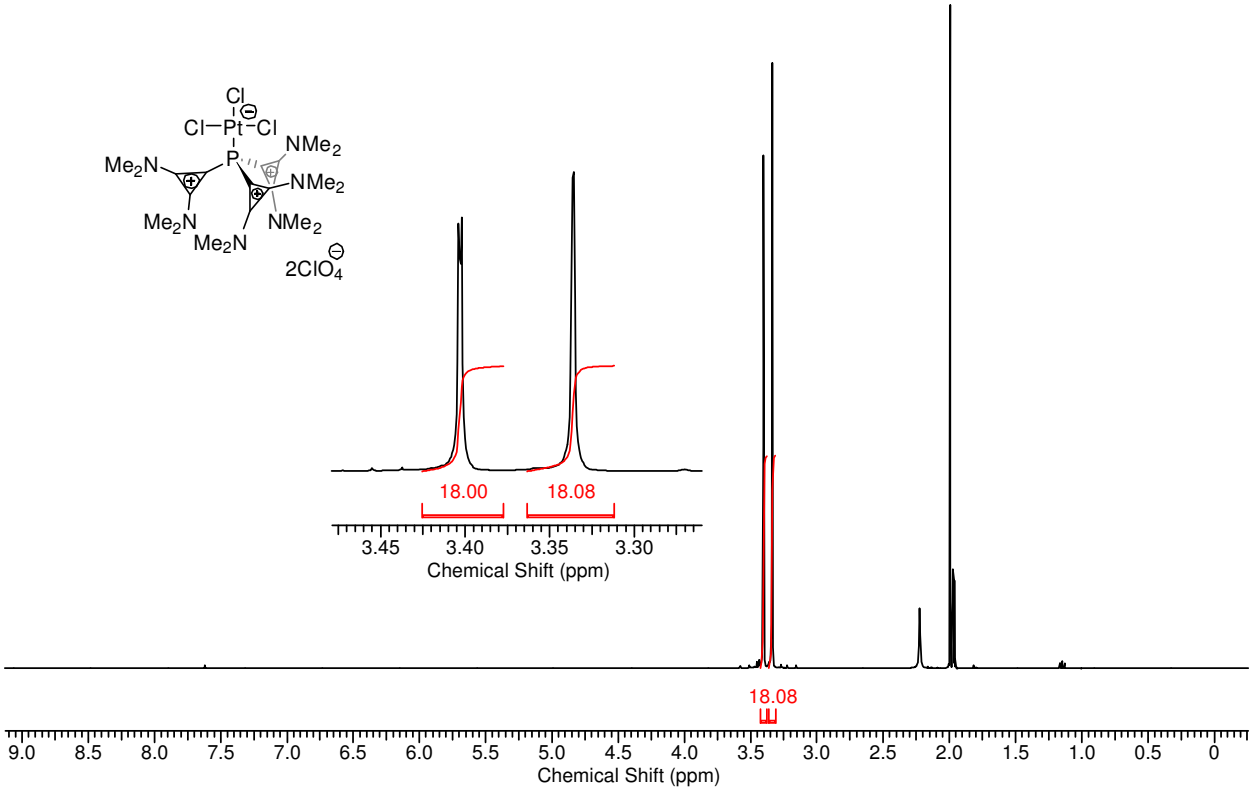

^{31}P NMR

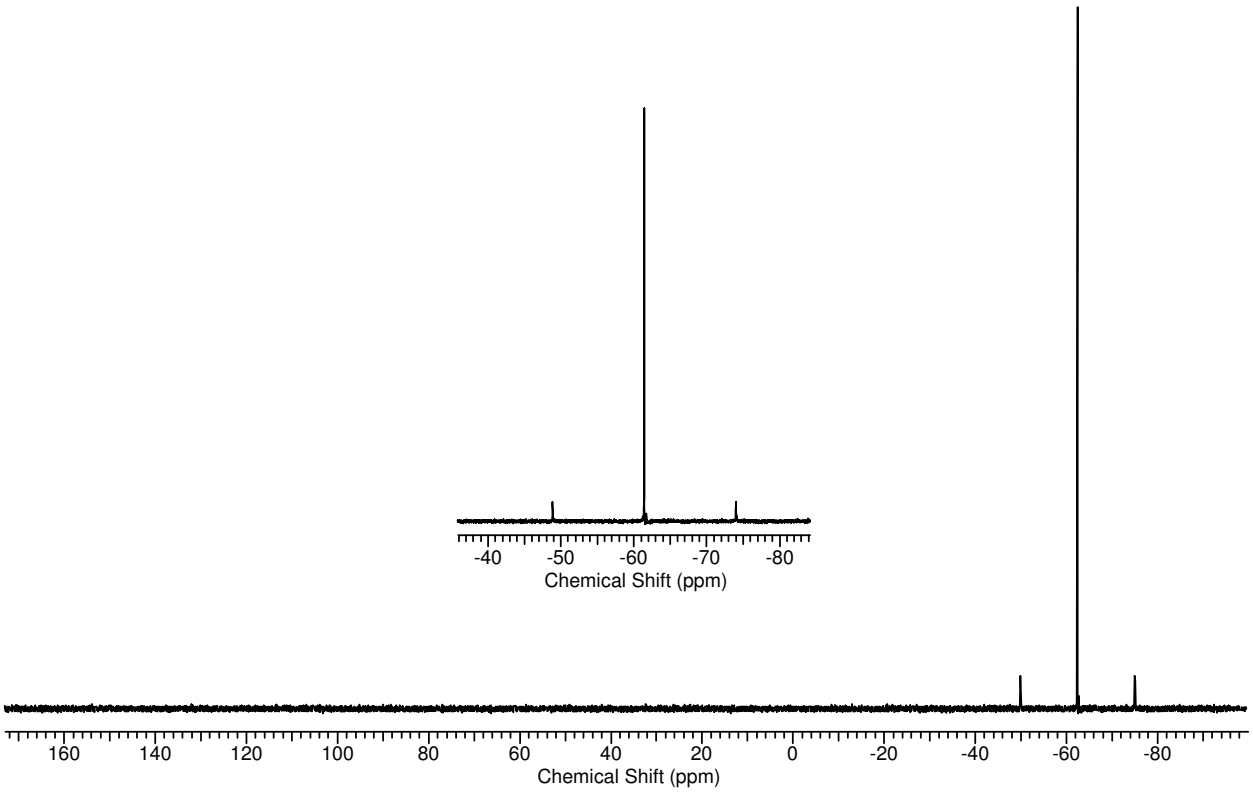

^{13}C NMR

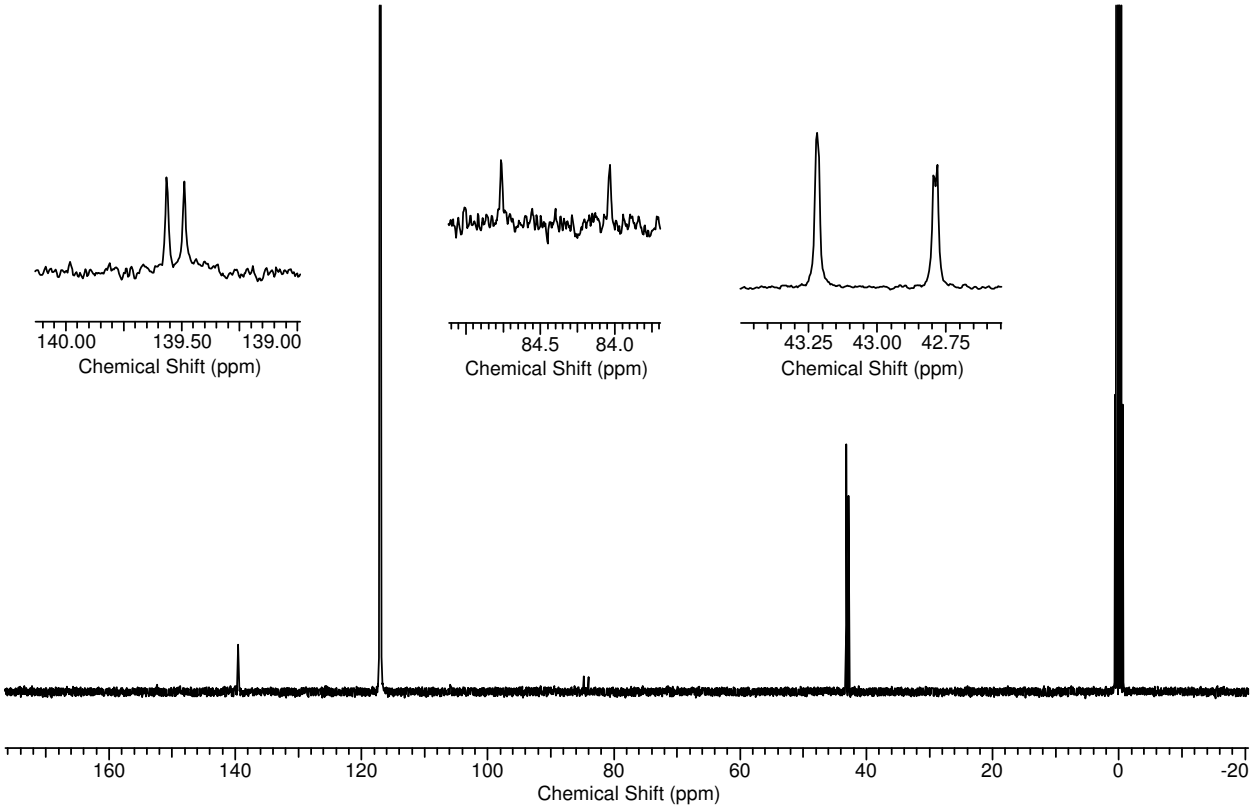

Compound 166b

^{1}H NMR

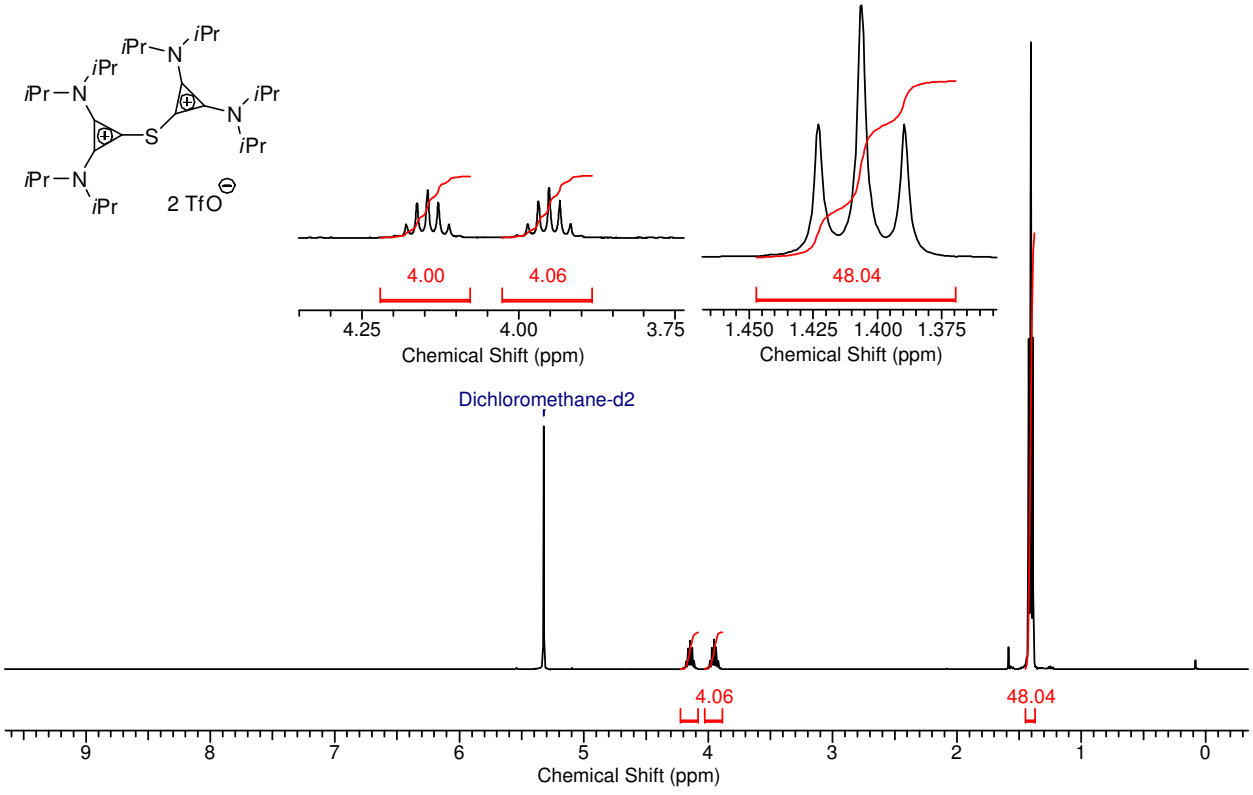

^{13}C NMR

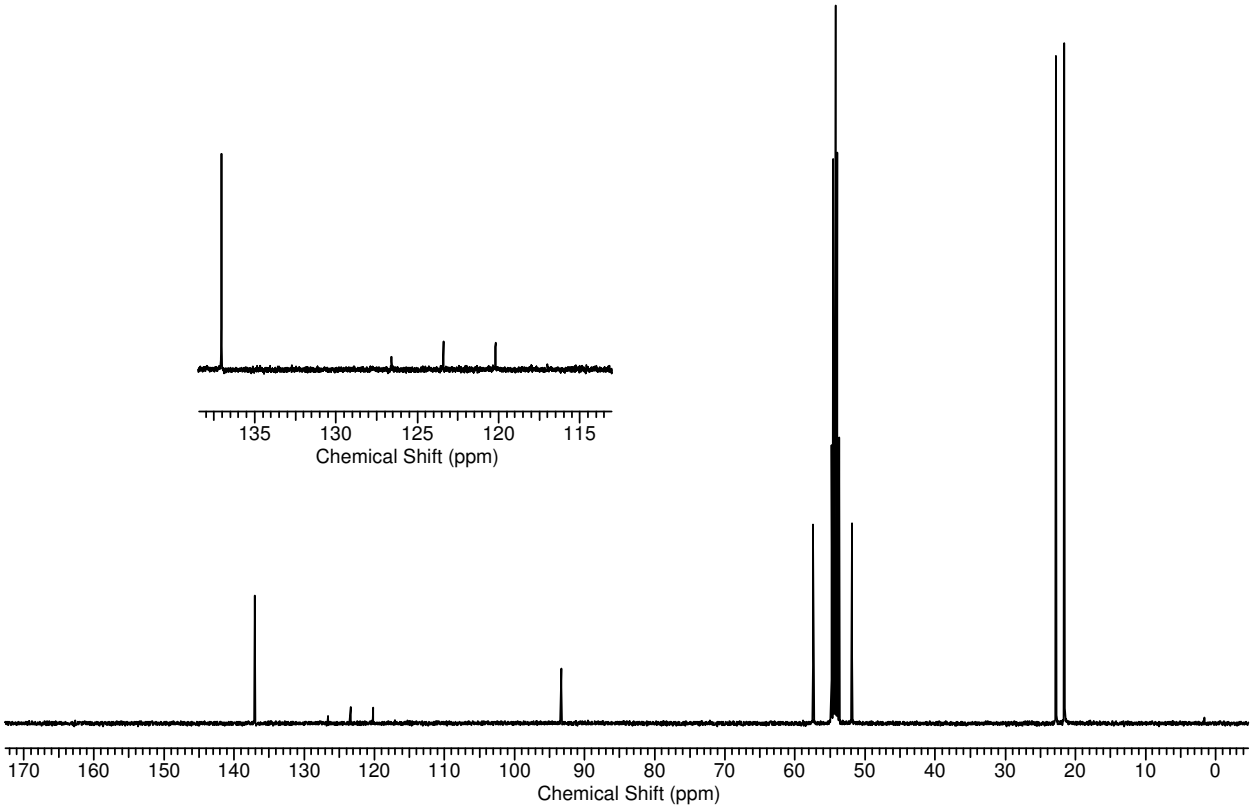

Compound 167a

^{1}H NMR

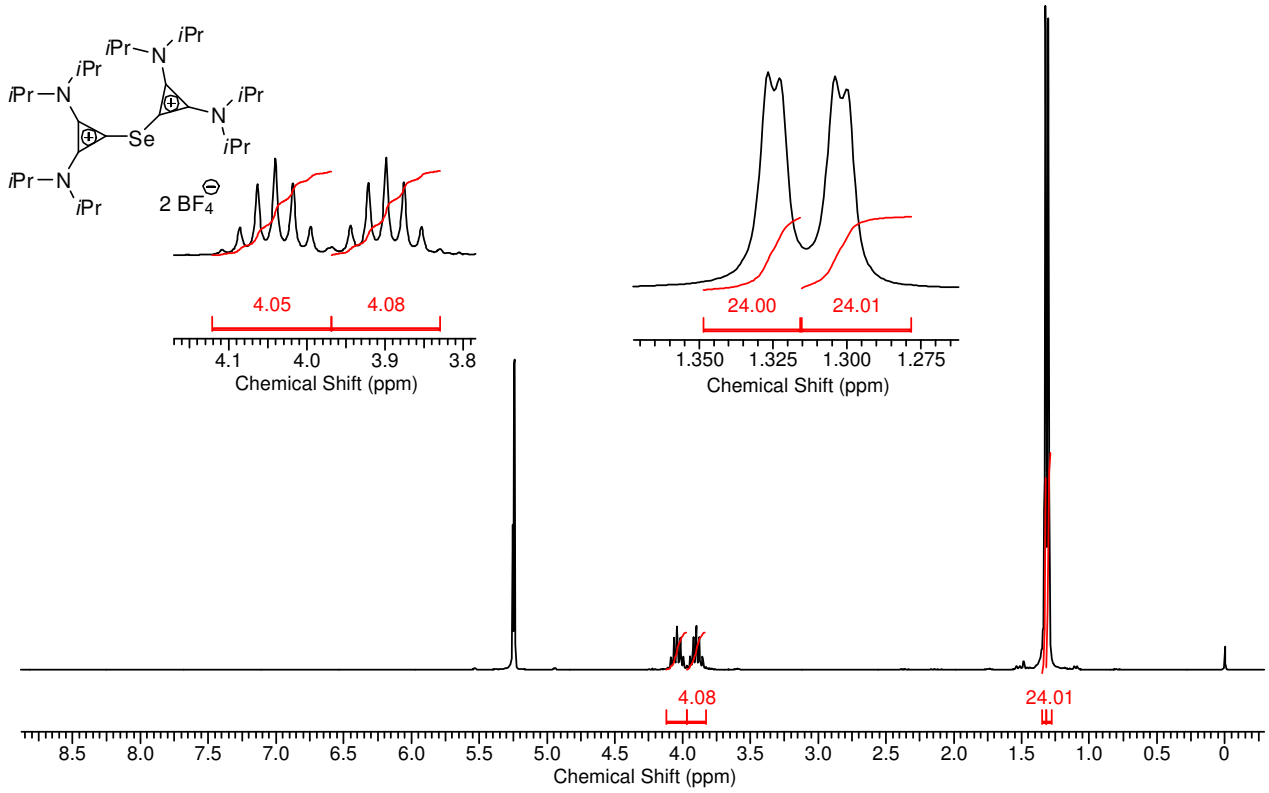

^{13}C NMR

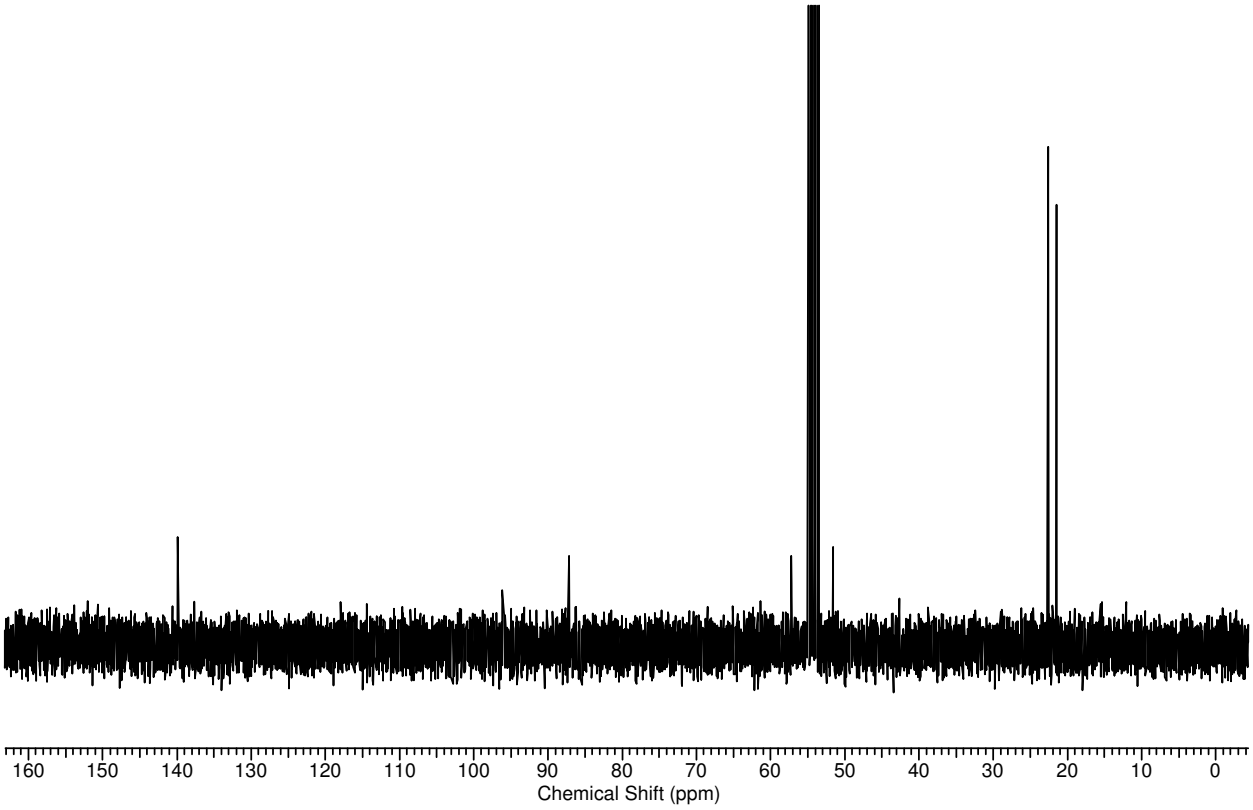

Compound 169b

^{1}H NMR

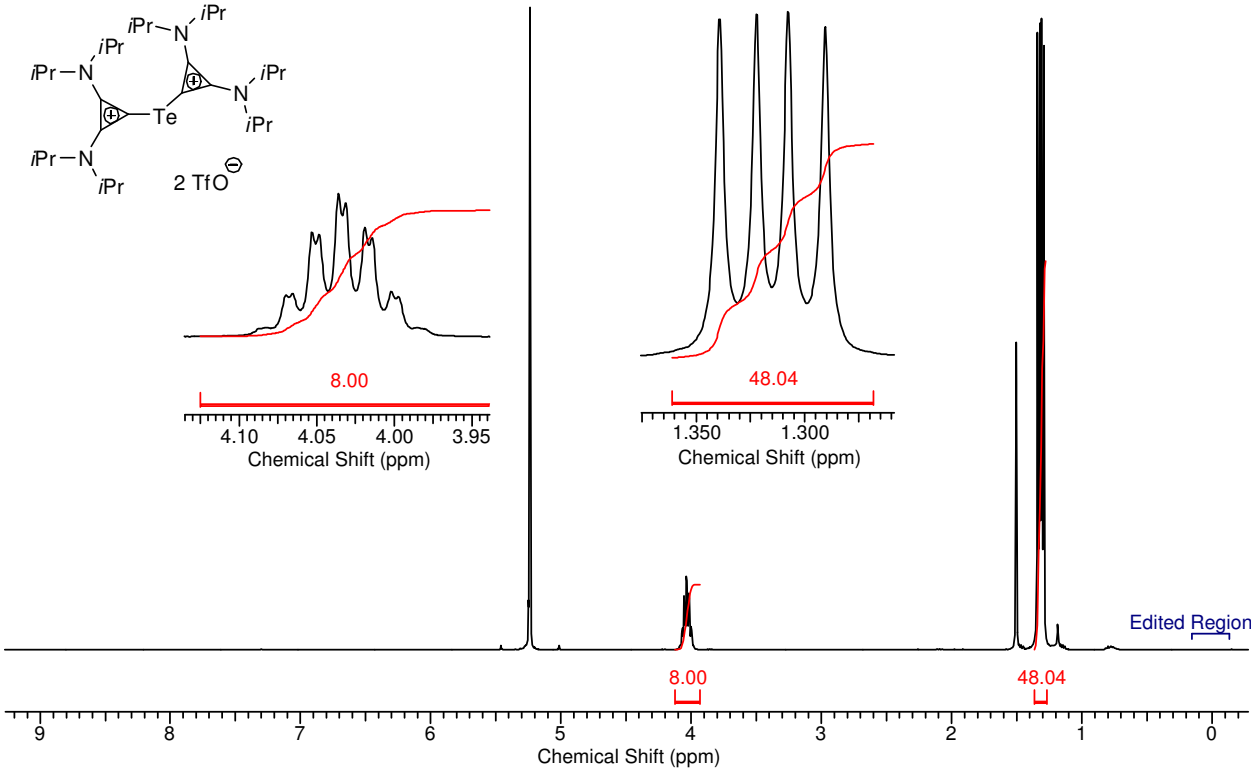

^{13}C NMR

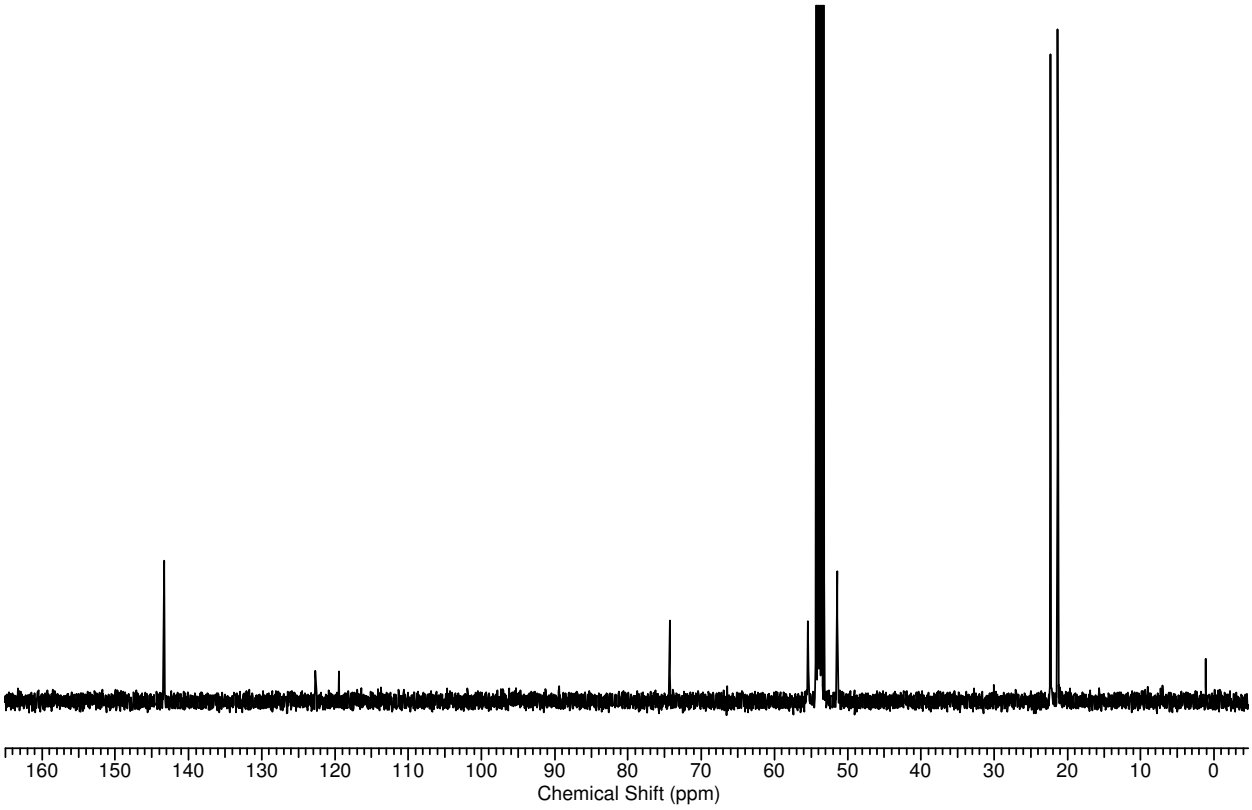

Compound 170

^{1}H NMR

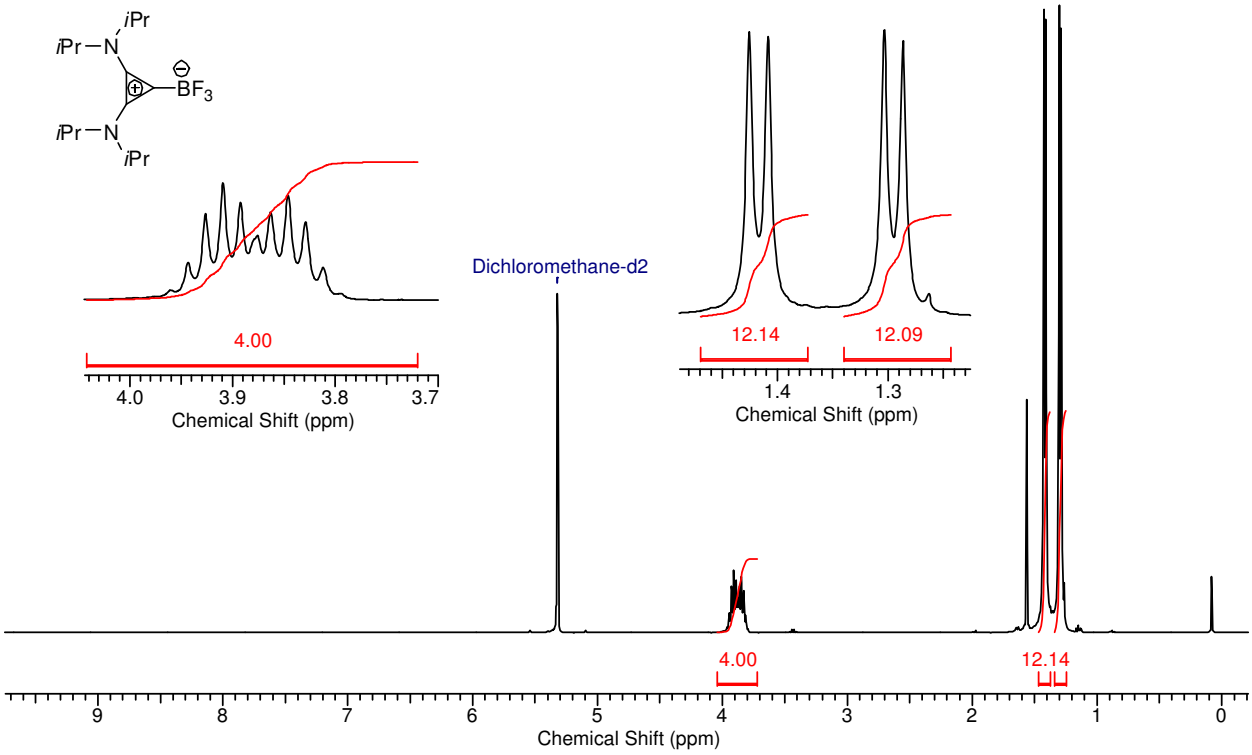

^{11}B NMR

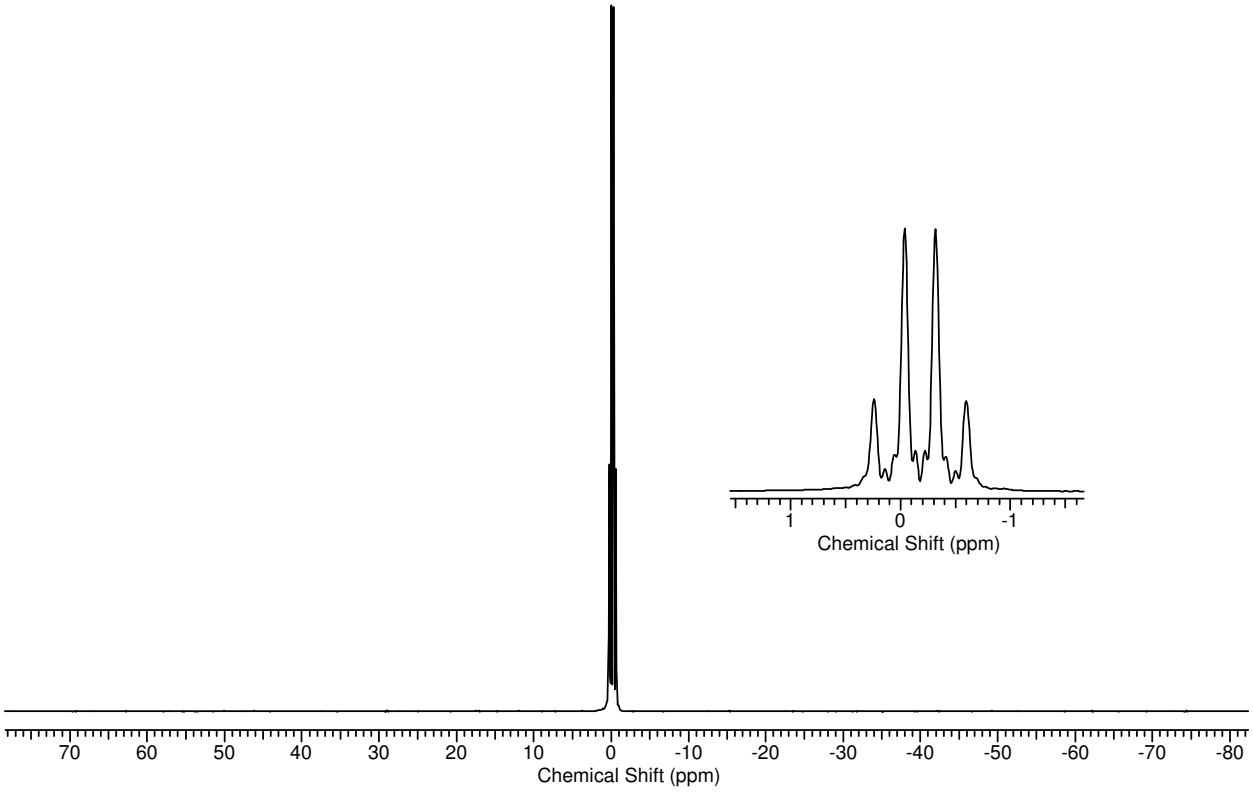

^{19}F NMR

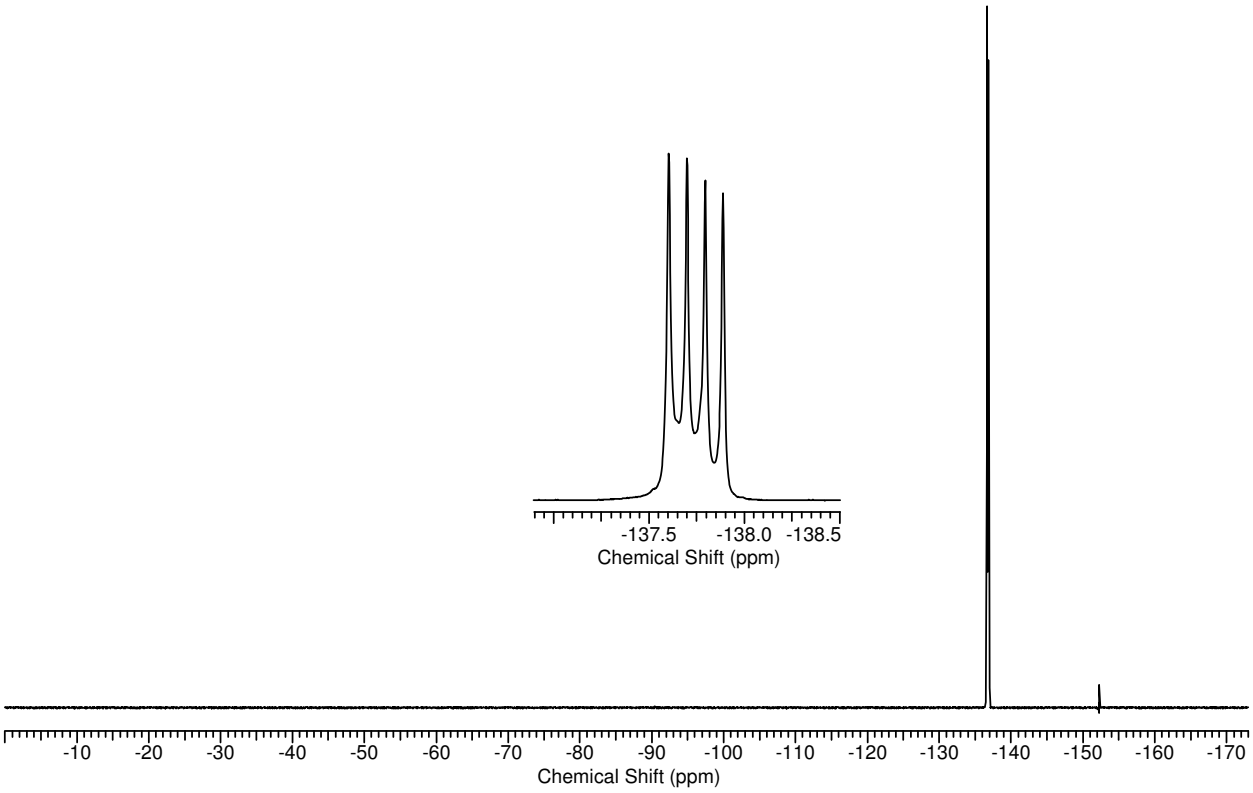

^{13}C NMR

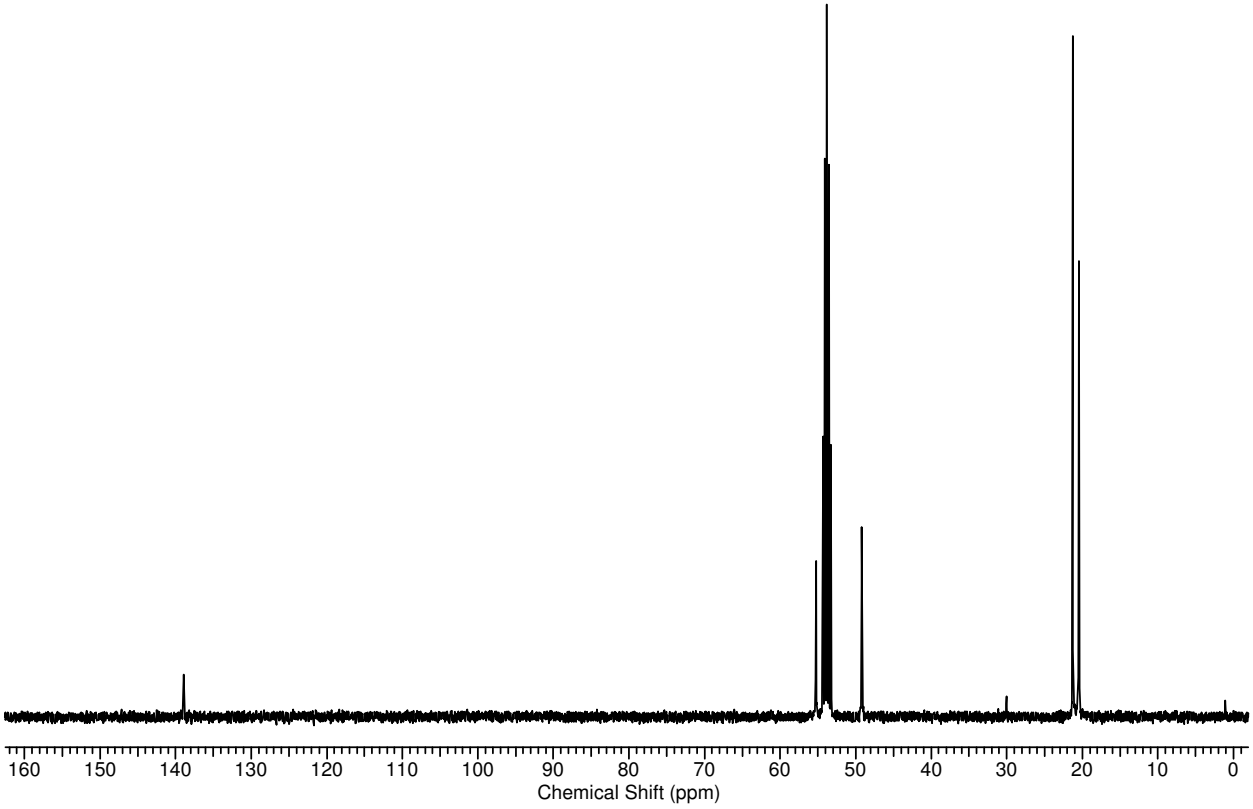
160
150
140
130
120
110
100
90
80
70
60
50
40
30
20
10
0
Chemical Shift (ppm)

7.2 X-ray Structures

7.2.1 Crystal data and structure refinement of compound 43a

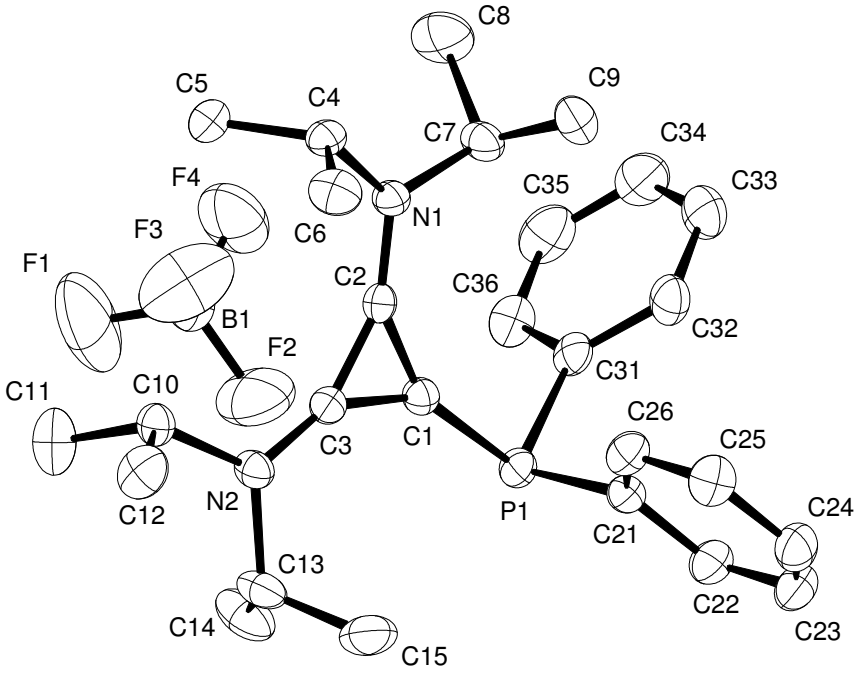

Empirical formula	$C_{27}H_{38}BF_4N_2P$	
Color	colorless	
Formula weight	508.37 $g \cdot mol^{-1}$	
Temperature	100 K	
Wavelength	1.54178 Å	
Crystal system	Monoclinic	
Space group	**$P2_1/n$, (no. 14)**	
Unit cell dimensions	a = 10.0045(4) Å	α= 90°.
	b = 17.9768(7) Å	β= 100.3280(10)°.
	c = 15.8577(6) Å	γ = 90°.
Volume	2805.78(19) $Å^3$	
Z	4	
Density (calculated)	1.203 $Mg \cdot m^{-3}$	
Absorption coefficient	1.242 mm^{-1}	
F(000)	1080 e	

Crystal size	0.6 x 0.6 x 0.4 mm^3	
θ range for data collection	3.75 to 67.35°.	
Index ranges	$-10 \leq h \leq 11$, $-21 \leq k \leq 21$, $-18 \leq l \leq 18$	
Reflections collected	63399	
Independent reflections	4856 [$R_{int} = 0.0305$]	
Reflections with $I>2\sigma(I)$	4785	
Completeness to $\theta = 67.35°$	96.4 %	
Absorption correction	Empirical	
Max. and min. transmission	0.75 and 0.62	
Refinement method	Full-matrix least-squares on F^2	
Data / restraints / parameters	4856 / 0 / 324	
Goodness-of-fit on F^2	1.023	
Final R indices [$I>2\sigma(I)$]	$R_1 = 0.0483$	$wR^2 = 0.1332$
R indices (all data)	$R_1 = 0.0486$	$wR^2 = 0.1334$
Largest diff. peak and hole	0.573 and -0.536 $e \cdot Å^{-3}$	

7.2.2 Crystal data and structure refinement of compound 43d

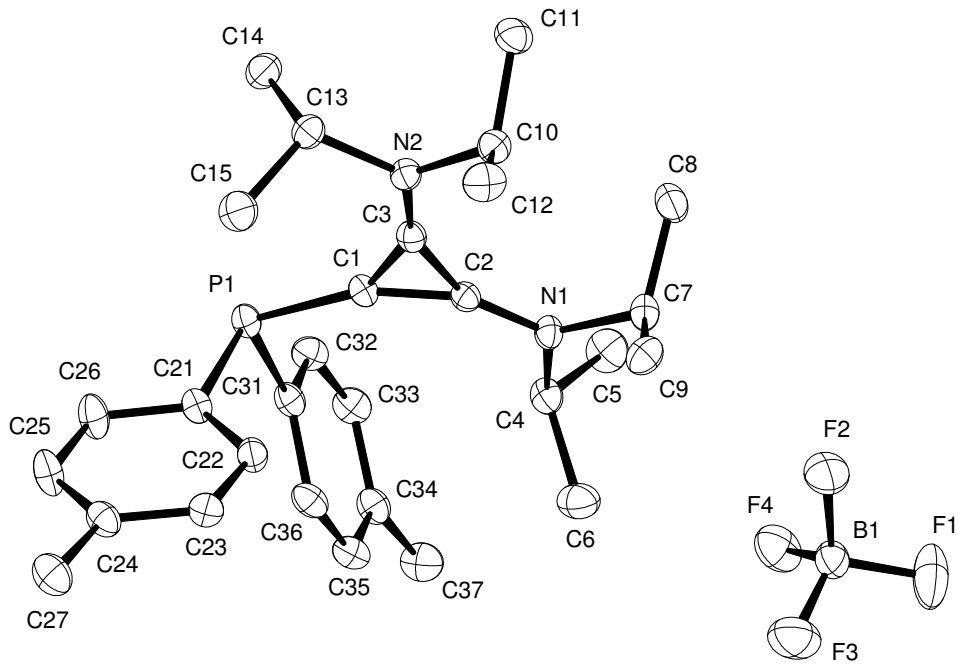

Empirical formula	$C_{29}H_{42}BF_4N_2P$	
Color	colorless	
Formula weight	536.43 $g \cdot mol^{-1}$	
Temperature	100 K	
Wavelength	0.71073 Å	
Crystal system	Monoclinic	
Space group	**C2/c, (no. 15)**	
Unit cell dimensions	a = 22.2571(4) Å	α= 90°.
	b = 19.2743(4) Å	β= 105.3470(10)°.
	c = 14.0616(3) Å	γ = 90°.
Volume	5817.2(2) $Å^3$	
Z	8	
Density (calculated)	1.225 $Mg \cdot m^{-3}$	
Absorption coefficient	0.140 mm^{-1}	
F(000)	2288 e	
Crystal size	0.50 x 0.40 x 0.4 mm^3	
θ range for data collection	2.97 to 33.15°.	
Index ranges	$-24 \le h \le 34$, $-29 \le k \le 29$, $-21 \le l \le 18$	

Reflections collected	33616	
Independent reflections	11096 [R_{int} = 0.0492]	
Reflections with I>2σ(I)	6874	
Completeness to θ = 33.15°	99.9 %	
Absorption correction	Empirical	
Max. and min. transmission	0.97 and 0.75	
Refinement method	Full-matrix least-squares on F^2	
Data / restraints / parameters	11096 / 0 / 344	
Goodness-of-fit on F^2	1.034	
Final R indices [I>2σ(I)]	R_1 = 0.0553	wR^2 = 0.1307
R indices (all data)	R_1 = 0.1067	wR^2 = 0.1567
Largest diff. peak and hole	0.491 and -0.801 e · $Å^{-3}$	

7.2.3 Crystal data and structure refinement of compound 43e

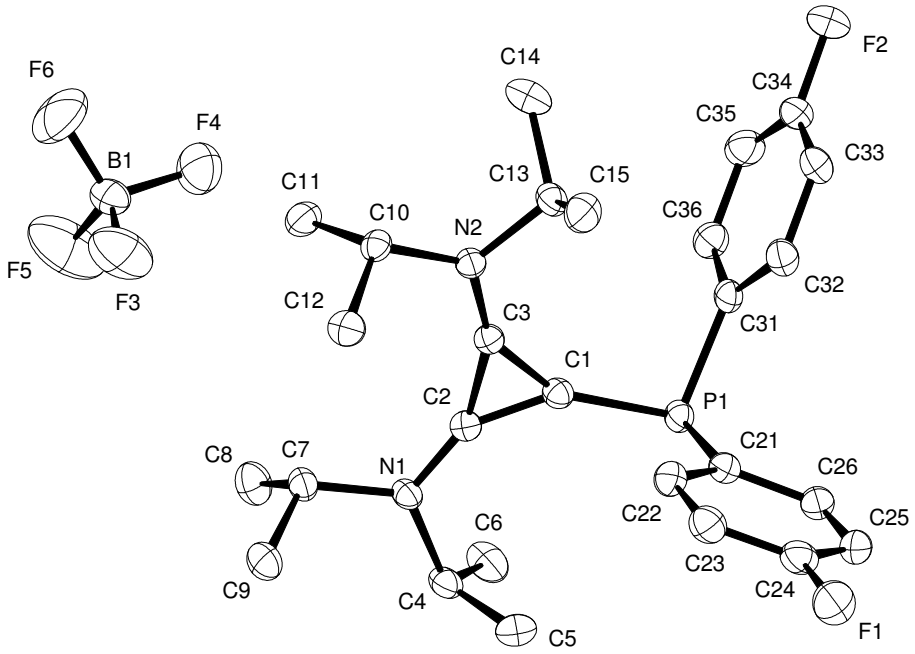

Empirical formula	$C_{27}H_{36}BF_6N_2P$	
Color	colorless	
Formula weight	544.36 $g \cdot mol^{-1}$	
Temperature	100 K	
Wavelength	0.71073 Å	
Crystal system	Monoclinic	
Space group	**$P2_1/n$, (no. 14)**	
Unit cell dimensions	a = 9.9783(2) Å	α= 90°.
	b = 18.3382(6) Å	β= 100.866(2)°.
	c = 15.6515(4) Å	γ = 90°.
Volume	2812.63(13) $Å^3$	
Z	4	
Density (calculated)	1.286 $Mg \cdot m^{-3}$	
Absorption coefficient	0.156 mm^{-1}	
F(000)	1144 e	
Crystal size	0.10 x 0.07 x 0.05 mm^3	
θ range for data collection	3.04 to 31.59°.	

Index ranges	$-14 \leq h \leq 14$, $-26 \leq k \leq 26$, $-23 \leq l \leq 23$	
Reflections collected	45554	
Independent reflections	9392 [$R_{int} = 0.0722$]	
Reflections with $I>2\sigma(I)$	5892	
Completeness to $\theta = 31.59°$	99.6 %	
Absorption correction	Empirical	
Max. and min. transmission	0.99 and 0.74	
Refinement method	Full-matrix least-squares on F^2	
Data / restraints / parameters	9392 / 0 / 342	
Goodness-of-fit on F^2	1.010	
Final R indices [$I>2\sigma(I)$]	$R_1 = 0.0629$	$wR^2 = 0.1299$
R indices (all data)	$R_1 = 0.1161$	$wR^2 = 0.1532$
Largest diff. peak and hole	0.596 and -0.452 e · $Å^{-3}$	

7.2.4 Crystal data and structure refinement of compound 43f

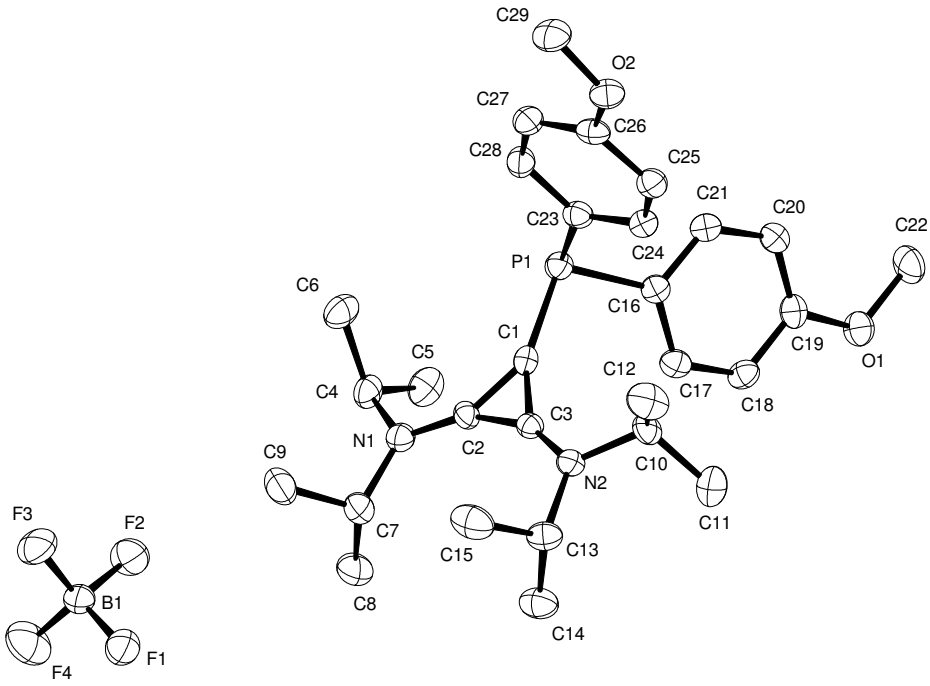

Empirical formula	$C_{29}H_{42}N_2O_2P \cdot BF_4$	
Color	colourless	
Formula weight	568.43 $g \cdot mol^{-1}$	
Temperature	100 K	
Wavelength	1.54178 Å	
Crystal system	Monoclinic	
Space group	**$P2_1$, (no. 4)**	
Unit cell dimensions	a = 10.3056(4) Å	α= 90°.
	b = 14.3756(5) Å	β= 113.206(2)°.
	c = 11.1033(4) Å	γ = 90°.
Volume	1511.86(10) $Å^3$	
Z	2	
Density (calculated)	1.249 $Mg \cdot m^{-3}$	
Absorption coefficient	1.257 mm^{-1}	
F(000)	604 e	
Crystal size	0.48 x 0.06 x 0.06 mm^3	
θ range for data collection	4.33 to 66.69°.	

Index ranges	$-12 \leq h \leq 12$, $-17 \leq k \leq 17$, $-13 \leq l \leq 13$	
Reflections collected	33883	
Independent reflections	5113 [$R_{int} = 0.1041$]	
Reflections with $I>2\sigma(I)$	4410	
Completeness to $\theta = 66.69°$	98.8 %	
Absorption correction	Gaussian	
Max. and min. transmission	0.94 and 0.71	
Refinement method	Full-matrix least-squares on F^2	
Data / restraints / parameters	5113 / 1 / 362	
Goodness-of-fit on F^2	1.086	
Final R indices [$I>2\sigma(I)$]	$R_1 = 0.0605$	$wR^2 = 0.1461$
R indices (all data)	$R_1 = 0.0732$	$wR^2 = 0.1568$
Absolute structure parameter	0.06(3)	
Largest diff. peak and hole	0.750 and -0.479 e · $Å^{-3}$	

7.2.5 Crystal data and structure refinement of compound 44a

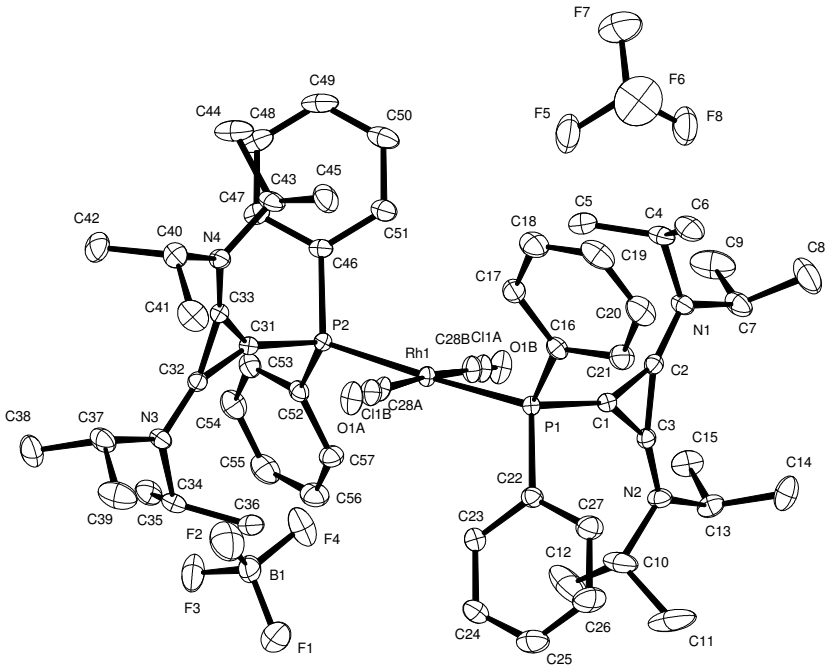

Empirical formula	$C_{55}H_{76}ClN_4OP_2Rh \cdot 2(BF_4^-)$	
Color	black	
Formula weight	1183.12 $g \cdot mol^{-1}$	
Temperature	100 K	
Wavelength	0.71073 Å	
Crystal system	ORTHORHOMBIC	
Space group	**$P2_12_12_1$, (no. 19)**	
Unit cell dimensions	a = 14.1864(16) Å	α= 90°.
	b = 15.8242(18) Å	β= 90°.
	c = 26.542(3) Å	γ = 90°.
Volume	5958.4(12) $Å^3$	
Z	4	
Density (calculated)	1.327 $Mg \cdot m^{-3}$	
Absorption coefficient	0.450 mm^{-1}	
F(000)	2476 e	
Crystal size	0.14 x 0.04 x 0.03 mm^3	
θ range for data collection	1.50 to 30.46°.	
Index ranges	$-20 \le h \le 20$, $-22 \le k \le 22$, $-37 \le l \le 37$	

Reflections collected	170338	
Independent reflections	18132 [R_{int} = 0.0399]	
Reflections with I>2σ(I)	17278	
Completeness to θ = 27.50°	100.0 %	
Absorption correction	Gaussian	
Max. and min. transmission	1.00 and 0.91	
Refinement method	Full-matrix least-squares on F^2	
Data / restraints / parameters	18132 / 0 / 711	
Goodness-of-fit on F^2	1.142	
Final R indices [I>2σ(I)]	R_1 = 0.0282	wR^2 = 0.0720
R indices (all data)	R_1 = 0.0315	wR^2 = 0.0770
Absolute structure parameter	0.00(12)	
Largest diff. peak and hole	1.026 and -0.556 e · $Å^{-3}$	

7.2.6 Crystal data and structure refinement of compound 46a

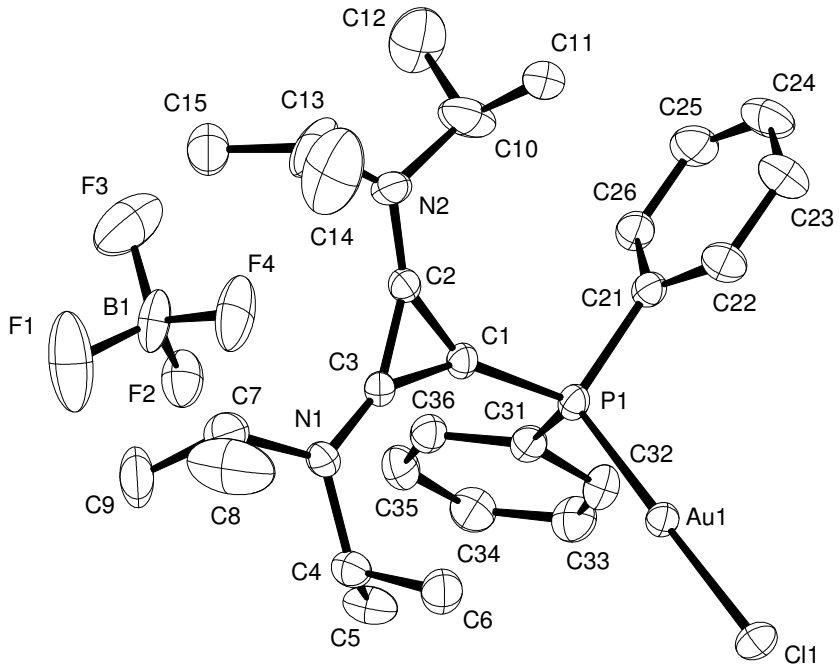

Empirical formula	$C_{27}H_{38}AuBClF_4N_2P$	
Color	colorless	
Formula weight	740.79 $g \cdot mol^{-1}$	
Temperature	100 K	
Wavelength	0.71073 Å	
Crystal system	Monoclinic	
Space group	**$P2_1/c$, (no. 14)**	
Unit cell dimensions	a = 10.6764(2) Å	α= 90°.
	b = 14.4331(2) Å	β= 104.3320(10)°.
	c = 19.9072(4) Å	γ = 90°.
Volume	2972.10(9) $Å^3$	
Z	4	
Density (calculated)	1.656 $Mg \cdot m^{-3}$	
Absorption coefficient	5.138 mm^{-1}	
F(000)	1464 e	
Crystal size	0.27 x 0.07 x 0.07 mm^3	
θ range for data collection	3.01 to 33.19°.	
Index ranges	$-16 \le h \le 16$, $-22 \le k \le 22$, $-30 \le l \le 30$	
Reflections collected	55673	
Independent reflections	11348 [R_{int} = 0.0409]	

Reflections with $I>2\sigma(I)$	9080	
Completeness to $\theta = 33.19°$	99.6 %	
Absorption correction	Empirical	
Max. and min. transmission	0.99 and 0.68	
Refinement method	Full-matrix least-squares on F^2	
Data / restraints / parameters	11348 / 0 / 342	
Goodness-of-fit on F^2	1.026	
Final R indices [$I>2\sigma(I)$]	$R_1 = 0.0377$	$wR^2 = 0.0857$
R indices (all data)	$R_1 = 0.0537$	$wR^2 = 0.0929$
Largest diff. peak and hole	2.285 and -2.185 $e \cdot Å^{-3}$	

7.2.7 Crystal data and structure refinement of compound 46f

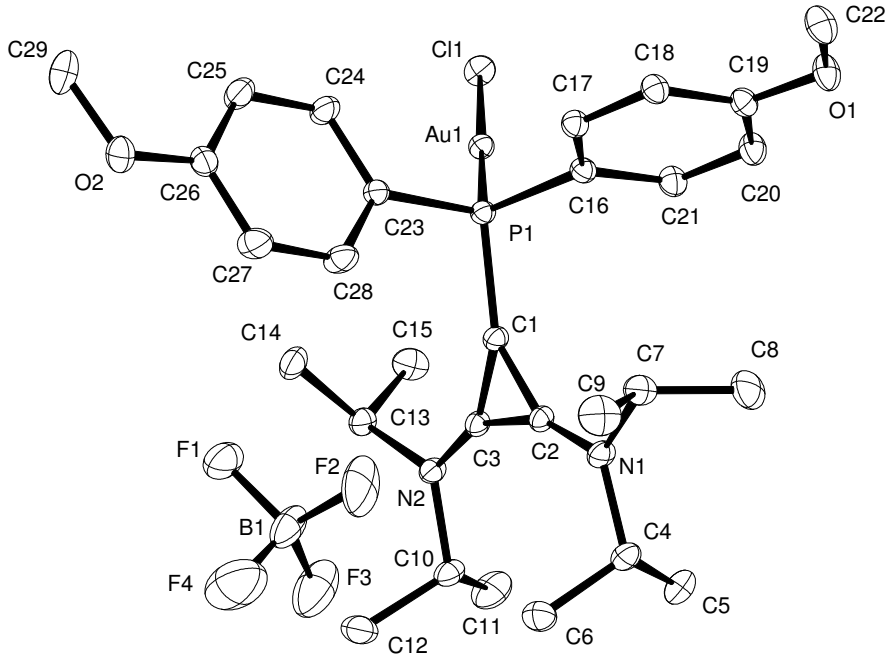

Empirical formula	$C_{29}H_{42}AuBClF_4N_2O_2P$	
Color	colourless	
Formula weight	800.84 g · mol^{-1}	
Temperature	100 K	
Wavelength	0.71073 Å	
Crystal system	Triclinic	
Space group	**P1, (no. 2)**	
Unit cell dimensions	a = 10.5654(8) Å	α= 96.4710(10)°.
	b = 13.3962(10) Å	β= 108.2060(10)°.
	c = 13.5582(10) Å	γ = 111.5600(10)°.
Volume	1638.2(2) Å^3	
Z	2	
Density (calculated)	1.624 Mg · m^{-3}	
Absorption coefficient	4.672 mm^{-1}	
F(000)	796 e	
Crystal size	0.08 x 0.04 x 0.04 mm^3	
θ range for data collection	3.55 to 36.68°.	

Index ranges	$-17 \leq h \leq 17$, $-22 \leq k \leq 22$, $-22 \leq l \leq 22$	
Reflections collected	61814	
Independent reflections	15258 [$R_{int} = 0.0195$]	
Reflections with $I>2\sigma(I)$	14610	
Completeness to $\theta = 36.68°$	93.7 %	
Absorption correction	Gaussian	
Max. and min. transmission	0.88 and 0.78	
Refinement method	Full-matrix least-squares on F^2	
Data / restraints / parameters	15258 / 0 / 380	
Goodness-of-fit on F^2	1.056	
Final R indices [$I>2\sigma(I)$]	$R_1 = 0.0182$	$wR^2 = 0.0503$
R indices (all data)	$R_1 = 0.0195$	$wR^2 = 0.0510$
Largest diff. peak and hole	3.629 and -1.464 e · $Å^{-3}$	

7.2.8 Crystal data and structure refinement of compound 48b

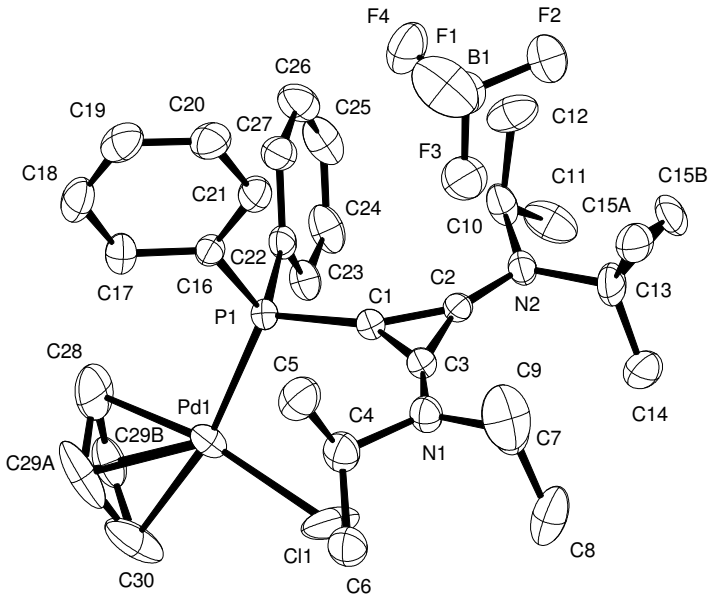

Empirical formula	$C_{30}H_{43}BClF_4N_2PPd$	
Color	yellow	
Formula weight	691.29 $g \cdot mol^{-1}$	
Temperature	100 K	
Wavelength	0.71073 Å	
Crystal system	TRICLINIC	
Space group	**P1, (no. 2)**	
Unit cell dimensions	a = 10.3679(7) Å	α= 80.917(8)°.
	b = 11.1528(12) Å	β= 75.836(7)°.
	c = 14.9063(12) Å	γ = 77.536(7)°.
Volume	1621.8(2) $Å^3$	
Z	2	
Density (calculated)	1.416 $Mg \cdot m^{-3}$	
Absorption coefficient	0.749 mm^{-1}	
F(000)	712 e	
Crystal size	0.12 x 0.12 x 0.08 mm^3	
θ range for data collection	2.75 to 33.23°.	
Index ranges	$-15 \le h \le 15$, $-17 \le k \le 17$, $-22 \le l \le 22$	

Reflections collected	45668	
Independent reflections	12368 [R_{int} = 0.0542]	
Reflections with I>2σ(I)	8816	
Completeness to θ = 33.23°	99.5 %	
Absorption correction	Gaussian	
Max. and min. transmission	0.95 and 0.92	
Refinement method	Full-matrix least-squares on F^2	
Data / restraints / parameters	12368 / 0 / 388	
Goodness-of-fit on F^2	1.034	
Final R indices [I>2σ(I)]	R_1 = 0.0476	wR^2 = 0.0980
R indices (all data)	R_1 = 0.0830	wR^2 = 0.1132
Largest diff. peak and hole	0.821 and -1.408 e · $Å^{-3}$	

7.2.9 Crystal data and structure refinement of compound 48c

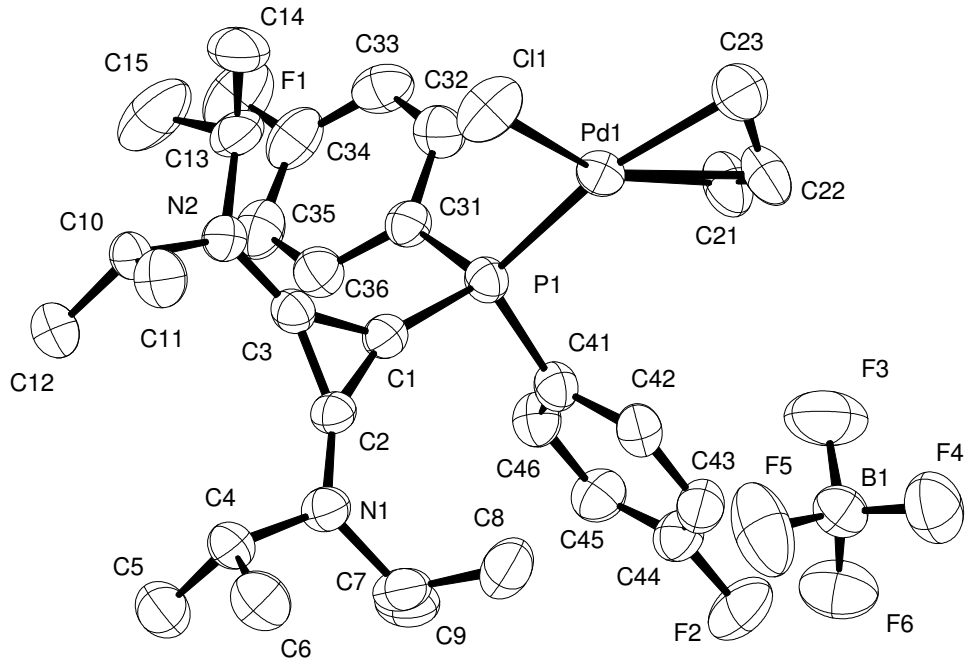

Empirical formula	$C_{30}H_{42}BClF_6N_2PPd$	
Color	yellow	
Formula weight	728.29 $g \cdot mol^{-1}$	
Temperature	100 K	
Wavelength	0.71073 Å	
Crystal system	Orthorhombic	
Space group	**Pbca, (no. 61)**	
Unit cell dimensions	a = 15.8827(7) Å	α= 90°.
	b = 11.0550(5) Å	β= 90°.
	c = 36.5987(16) Å	γ = 90°.
Volume	6426.1(5) $Å^3$	
Z	8	
Density (calculated)	1.506 $Mg \cdot m^{-3}$	
Absorption coefficient	0.769 mm^{-1}	
F(000)	2984 e	
Crystal size	0.30 x 0.17 x 0.12 mm^3	
θ range for data collection	3.16 to 33.19°.	

Index ranges	$-24 \leq h \leq 24$, $-17 \leq k \leq 16$, $-56 \leq l \leq 56$	
Reflections collected	80403	
Independent reflections	12270 [$R_{int} = 0.0797$]	
Reflections with $I>2\sigma(I)$	6885	
Completeness to $\theta = 33.19°$	99.9 %	
Absorption correction	Empirical	
Max. and min. transmission	0.99 and 0.68	
Refinement method	Full-matrix least-squares on F^2	
Data / restraints / parameters	12270 / 0 / 388	
Goodness-of-fit on F^2	1.031	
Final R indices [$I>2\sigma(I)$]	$R_1 = 0.0805$	$wR^2 = 0.2271$
R indices (all data)	$R_1 = 0.1359$	$wR^2 = 0.2741$
Extinction coefficient	0.0024(4)	
Largest diff. peak and hole	2.663 and -2.813 e · $Å^{-3}$	

7.2.10 Crystal data and structure refinement of compound 50

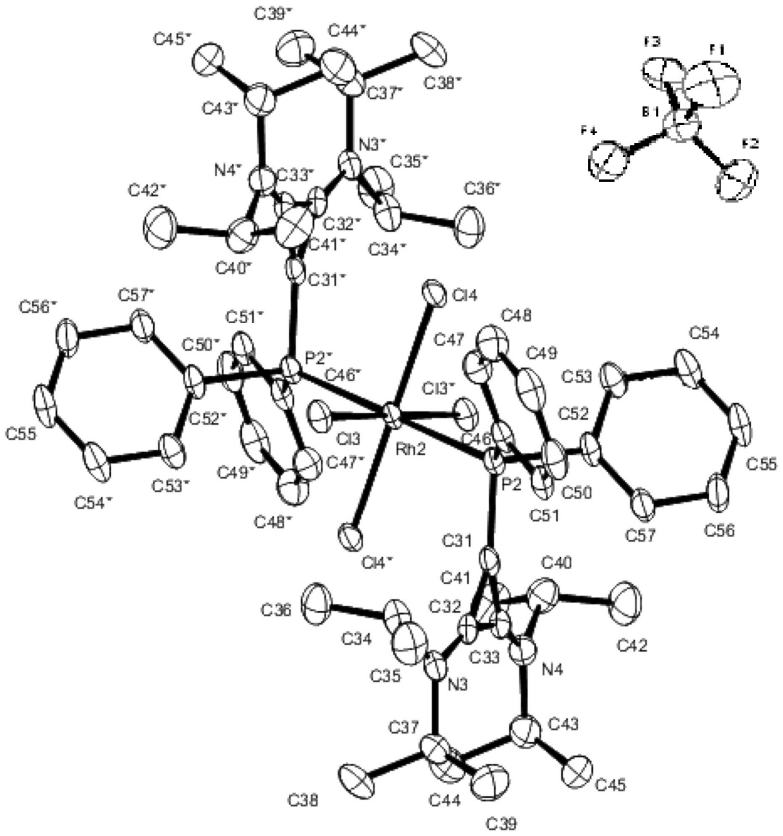

Empirical formula	$C_{54}H_{76}BCl_4F_4N_4P_2Rh$	
Color	colourless	
Formula weight	1174.64 $g \cdot mol^{-1}$	
Temperature	100 K	
Wavelength	0.71073 Å	
Crystal system	Triclinic	
Space group	**P1, (no. 2)**	
Unit cell dimensions	a = 12.4061(18) Å	α= 103.320(3)°
	b = 15.032(2) Å	β= 98.593(3)°
	c = 19.428(3) Å	γ = 104.421(3)°
Volume	3331.3(8) $Å^3$	
Z	2	
Density (calculated)	1.171 $Mg \cdot m^{-3}$	
Absorption coefficient	0.509 mm^{-1}	

F(000)	1224 e	
Crystal size	0.18 x 0.16 x 0.03 mm^3	
θ range for data collection	1.10 to 27.50°.	
Index ranges	$-16 \leq h \leq 16$, $-19 \leq k \leq 19$, $-23 \leq l \leq 25$	
Reflections collected	77788	
Independent reflections	15296 [$R_{int} = 0.0616$]	
Reflections with I>2σ(I)	11430	
Completeness to θ = 27.50°	100.0 %	
Absorption correction	Gaussian	
Max. and min. transmission	1.00 and 0.98	
Refinement method	Full-matrix least-squares on F^2	
Data / restraints / parameters	15296 / 0 / 648	
Goodness-of-fit on F^2	1.106	
Final R indices [I>2σ(I)]	$R_1 = 0.0410$	$wR^2 = 0.1032$
R indices (all data)	$R_1 = 0.0602$	$wR^2 = 0.1094$
Largest diff. peak and hole	1.078 and -0.619 e · $Å^{-3}$	

7.2.11 Crystal data and structure refinement of compound 97

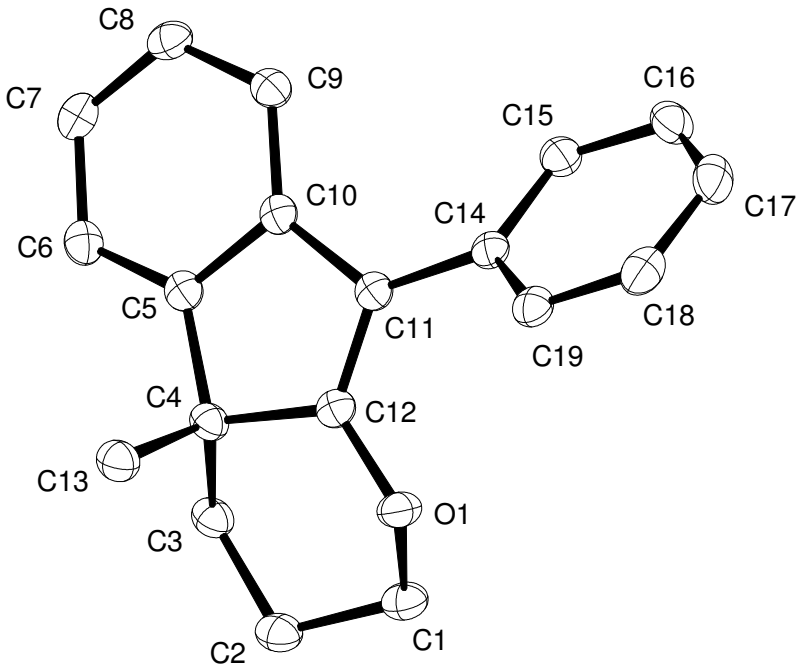

Empirical formula	$C_{19}H_{18}O$	
Color	colourless	
Formula weight	262.33 $g \cdot mol^{-1}$	
Temperature	100 K	
Wavelength	1.54178 Å	
Crystal system	Orthorhombic	
Space group	**Pbca, (no. 61)**	
Unit cell dimensions	a = 14.6635(18) Å	α= 90°.
	b = 7.7159(10) Å	β= 90°.
	c = 24.482(3) Å	γ = 90°.
Volume	2770.0(6) $Å^3$	
Z	8	
Density (calculated)	1.258 $Mg \cdot m^{-3}$	
Absorption coefficient	0.585 mm^{-1}	
F(000)	1120 e	
Crystal size	0.41 x 0.36 x 0.14 mm^3	
θ range for data collection	3.61 to 66.97°.	
Index ranges	$-17 \le h \le 15$, $-9 \le k \le 8$, $-26 \le l \le 28$	

Reflections collected	44701	
Independent reflections	2425 [R_{int} = 0.0433]	
Reflections with I>2σ(I)	2336	
Completeness to θ = 66.97°	98.1 %	
Absorption correction	Gaussian	
Max. and min. transmission	0.92 and 0.79	
Refinement method	Full-matrix least-squares on F^2	
Data / restraints / parameters	2425 / 0 / 182	
Goodness-of-fit on F^2	1.051	
Final R indices [I>2σ(I)]	R_1 = 0.0357	wR^2 = 0.0895
R indices (all data)	R_1 = 0.0367	wR^2 = 0.0902
Largest diff. peak and hole	0.220 and -0.203 e · $Å^{-3}$	

7.2.12 Crystal data and structure refinement of compound 113a

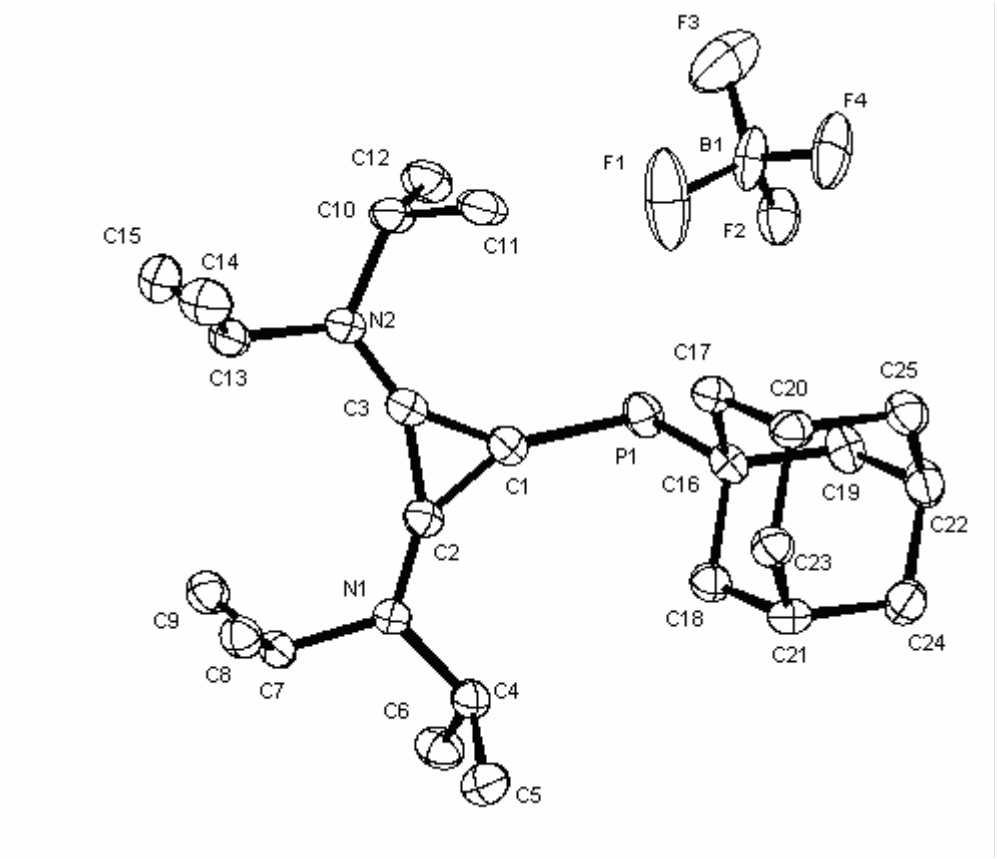

Empirical formula	$C_{25}H_{44}BF_4N_2P$	
Color	colourless	
Formula weight	490.40 $g \cdot mol^{-1}$	
Temperature	100 K	
Wavelength	0.71073 Å	
Crystal system	Monoclinic	
Space group	**$P2_1$, (no. 4)**	
Unit cell dimensions	a = 8.1898(2) Å	α= 90.0°.
	b = 11.3350(3) Å	β= 94.9740(10)°.
	c = 14.5669(3) Å	γ = 90.0°.
Volume	1347.17(6) $Å^3$	
Z	2	
Density (calculated)	1.209 $Mg \cdot m^{-3}$	
Absorption coefficient	0.145 mm^{-1}	
F(000)	528 e	

Crystal size	0.42 x 0.12 x 0.06 mm^3	
θ range for data collection	2.97 to 33.27°.	
Index ranges	$-12 \leq h \leq 12$, $-17 \leq k \leq 17$, $-22 \leq l \leq 22$	
Reflections collected	79951	
Independent reflections	10307 [$R_{int} = 0.0972$]	
Reflections with $I>2\sigma(I)$	6555	
Completeness to $\theta = 33.27°$	99.4 %	
Absorption correction	Gaussian	
Max. and min. transmission	0.99131 and 0.95490	
Refinement method	Full-matrix least-squares on F^2	
Data / restraints / parameters	10307 / 1 / 310	
Goodness-of-fit on F^2	1.021	
Final R indices [$I>2\sigma(I)$]	$R_1 = 0.0560$	$wR^2 = 0.1204$
R indices (all data)	$R_1 = 0.1159$	$wR^2 = 0.1454$
Absolute structure parameter	-0.12(9)	
Largest diff. peak and hole	0.412 and -0.430 e · $Å^{-3}$	

7.2.13 Crystal data and structure refinement of compound 115

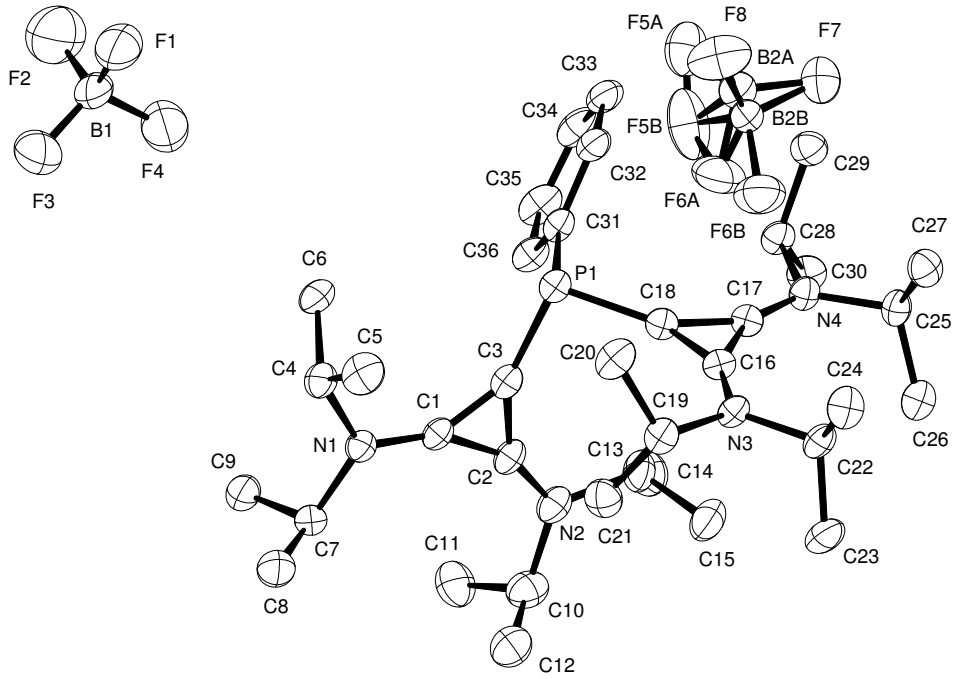

Empirical formula	$C_{36}H_{61}B_2F_8N_4P$	
Color	colourless	
Formula weight	754.48 $g \cdot mol^{-1}$	
Temperature	100 K	
Wavelength	1.54178 Å	
Crystal system	Orthorhombic	
Space group	**Pbcn, (no. 60)**	
Unit cell dimensions	a = 45.8483(14) Å	α= 90°.
	b = 11.6679(3) Å	β= 90°.
	c = 15.3567(5) Å	γ = 90°.
Volume	8215.1(4) $Å^3$	
Z	8	
Density (calculated)	1.220 $Mg \cdot m^{-3}$	
Absorption coefficient	1.160 mm^{-1}	
F(000)	3216 e	
Crystal size	0.59 x 0.51 x 0.04 mm^3	
θ range for data collection	1.93 to 67.48°.	
Index ranges	$-54 \le h \le 54$, $-13 \le k \le 13$, $-18 \le l \le 18$	

Reflections collected	205006	
Independent reflections	7325 [R_{int} = 0.1118]	
Reflections with I>2σ(I)	6324	
Completeness to θ = 67.48°	99.0 %	
Absorption correction	Gaussian	
Max. and min. transmission	0.96 and 0.51	
Refinement method	Full-matrix least-squares on F^2	
Data / restraints / parameters	7325 / 0 / 495	
Goodness-of-fit on F^2	2.065	
Final R indices [I>2σ(I)]	R_1 = 0.0794	wR^2 = 0.1689
R indices (all data)	R_1 = 0.0895	wR^2 = 0.1718
Extinction coefficient	0.00099(8)	
Largest diff. peak and hole	0.608 and -0.429 e · $Å^{-3}$	

7.2.14 Crystal data and structure refinement of compound 117

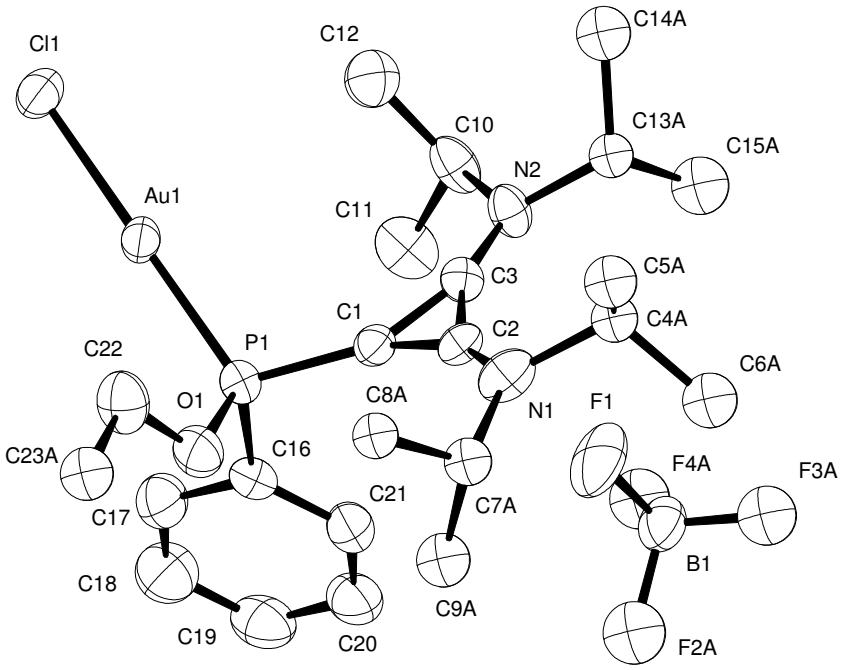

Empirical formula	$C_{23}H_{38}AuClN_2OP^+ \cdot BF_4^-$	
Color	yellow	
Formula weight	708.75 $g \cdot mol^{-1}$	
Temperature	100 K	
Wavelength	0.71073 Å	
Crystal system	MONOCLINIC	
Space group	**$P2_1/n$, (no. 14)**	
Unit cell dimensions	a = 10.6782(11) Å	α= 90°
	b = 13.9102(9) Å	β= 104.871(6)°
	c = 19.8627(18) Å	γ = 90°
Volume	2851.5(4) $Å^3$	
Z	4	
Density (calculated)	1.651 $Mg \cdot m^{-3}$	
Absorption coefficient	5.353 mm^{-1}	
F(000)	1400 e	
Crystal size	0.20 x 0.14 x 0.10 mm^3	
θ range for data collection	2.87 to 27.50°.	
Index ranges	$-13 \le h \le 13$, $-17 \le k \le 18$, $-25 \le l \le 25$	

Reflections collected	43582	
Independent reflections	6536 [R_{int} = 0.0529]	
Reflections with I>2σ(I)	5652	
Completeness to θ = 27.50°	99.9 %	
Absorption correction	Gaussian	
Max. and min. transmission	0.61 and 0.40	
Refinement method	Full-matrix least-squares on F^2	
Data / restraints / parameters	6536 / 0 / 325	
Goodness-of-fit on F^2	1.088	
Final R indices [I>2σ(I)]	R_1 = 0.0407	wR^2 = 0.0930
R indices (all data)	R_1 = 0.0500	wR^2 = 0.0980
Largest diff. peak and hole	3.314 and -1.230 e · $Å^{-3}$	

7.2.15 Crystal data and structure refinement of compound 118

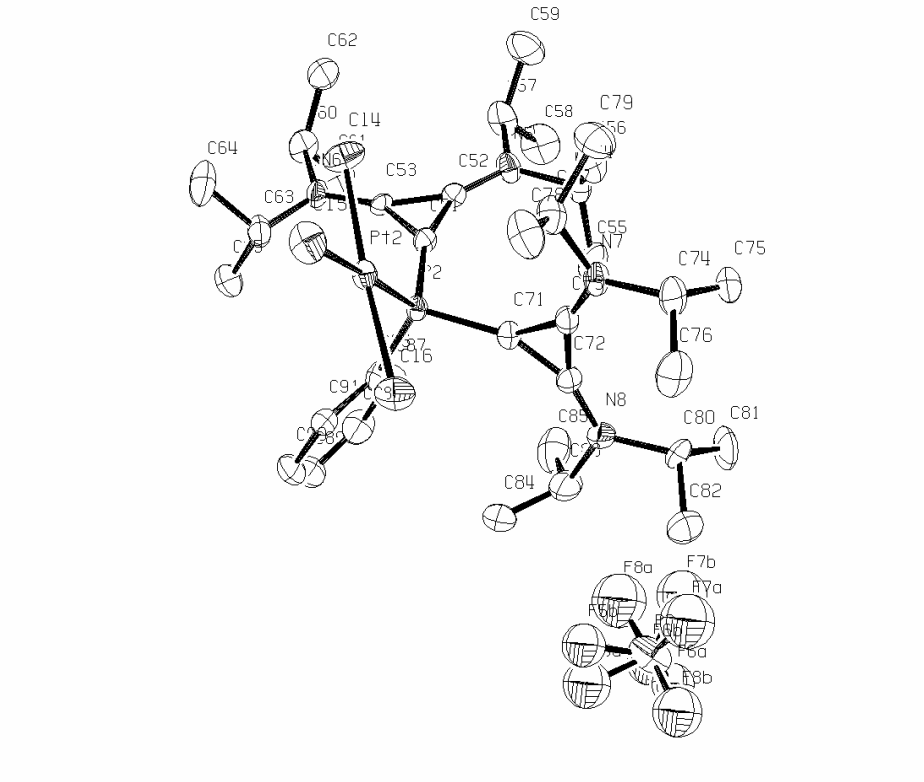

Empirical formula	$C_{37}H_{61.50}BCl_6F_4N_4PPt$	
Color	yellow	
Formula weight	1087.97 $g \cdot mol^{-1}$	
Temperature	200 K	
Wavelength	0.71073 Å	
Crystal system	MONOCLINIC	
Space group	**$P2_1/c$, (no. 14)**	
Unit cell dimensions	a = 25.819(3) Å	α= 90°.
	b = 15.859(2) Å	β= 113.707(6)°.
	c = 25.450(2) Å	γ = 90°.
Volume	9541.1(19) $Å^3$	
Z	8	
Density (calculated)	1.515 $Mg \cdot m^{-3}$	
Absorption coefficient	3.357 mm^{-1}	
F(000)	4380 e	
Crystal size	0.153 x 0.152 x 0.050 mm^3	

θ range for data collection	2.71 to 27.50°.	
Index ranges	$-33 \leq h \leq 33$, $-20 \leq k \leq 20$, $-33 \leq l \leq 32$	
Reflections collected	129550	
Independent reflections	21869 [$R_{int} = 0.0612$]	
Reflections with $I>2\sigma(I)$	18230	
Completeness to $\theta = 27.50°$	99.8 %	
Absorption correction	Gaussian	
Max. and min. transmission	0.85 and 0.35	
Refinement method	Full-matrix least-squares on F^2	
Data / restraints / parameters	21869 / 0 / 998	
Goodness-of-fit on F^2	1.208	
Final R indices [$I>2\sigma(I)$]	$R_1 = 0.0822$	$wR^2 = 0.2045$
R indices (all data)	$R_1 = 0.0969$	$wR^2 = 0.2135$
Largest diff. peak and hole	4.066 and -2.870 e · $Å^{-3}$	

7.2.16 Crystal data and structure refinement of compound 126

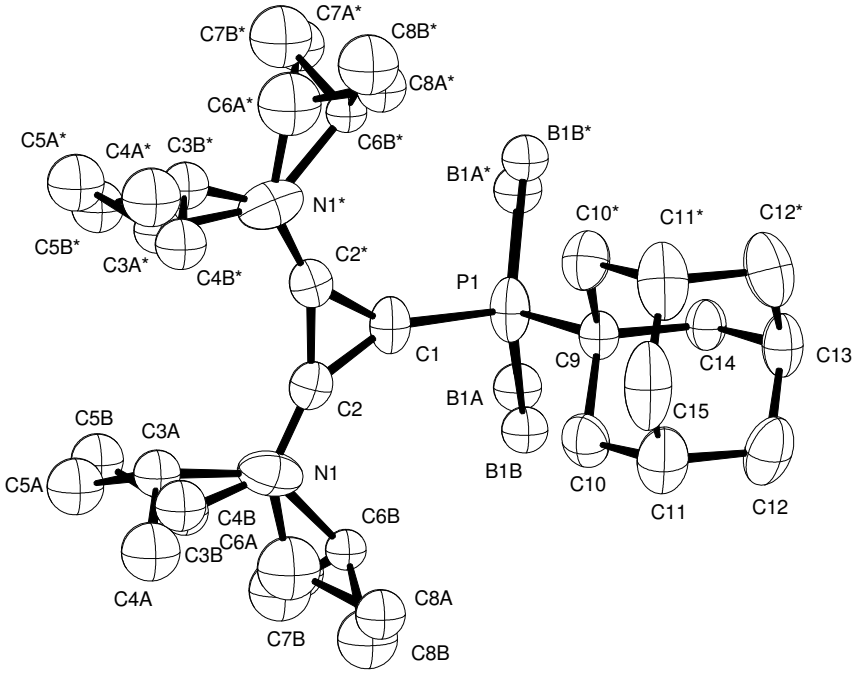

Empirical formula	$C_{25}H_{48}B_2N_2P$	
Color	colorless	
Formula weight	429.24 $g \cdot mol^{-1}$	
Temperature	100 K	
Wavelength	0.71073 Å	
Crystal system	ORTHORHOMBIC	
Space group	**Pnma, (no. 62)**	
Unit cell dimensions	a = 14.3239(2) Å	α= 90°.
	b = 16.1313(2) Å	β= 90°.
	c = 11.9731(2) Å	γ = 90°.
Volume	2766.54(7) $Å^3$	
Z	4	
Density (calculated)	1.031 $Mg \cdot m^{-3}$	
Absorption coefficient	0.113 mm^{-1}	
F(000)	948 e	
Crystal size	0.16 x 0.10 x 0.05 mm^3	
θ range for data collection	3.11 to 27.49°.	

Index ranges	$-18 \leq h \leq 18$, $-20 \leq k \leq 20$, $-15 \leq l \leq 15$	
Reflections collected	41754	
Independent reflections	3291 [$R_{int} = 0.0555$]	
Reflections with $I>2\sigma(I)$	2417	
Completeness to $\theta = 27.49°$	99.8 %	
Absorption correction	Gaussian	
Max. and min. transmission	0.99 and 0.54	
Refinement method	Full-matrix least-squares on F^2	
Data / restraints / parameters	3291 / 1 / 180	
Goodness-of-fit on F^2	1.042	
Final R indices [$I>2\sigma(I)$]	$R_1 = 0.0720$	$wR^2 = 0.1816$
R indices (all data)	$R_1 = 0.0968$	$wR^2 = 0.2067$
Extinction coefficient	0.018(3)	
Largest diff. peak and hole	0.401 and -0.298 e · $Å^{-3}$	

7.2.17 Crystal data and structure refinement of compound 134a

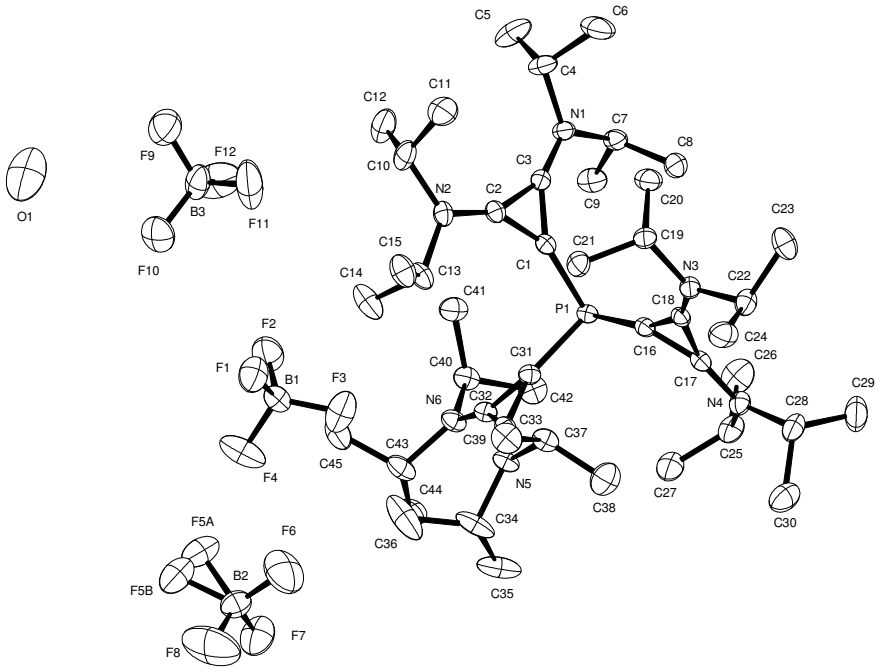

Empirical formula	$C_{45}H_{86}B_3F_{12}N_6OP$	
Color	colourless	
Formula weight	1018.60 g · mol^{-1}	
Temperature	100 K	
Wavelength	1.54178 Å	
Crystal system	MONOCLINIC	
Space group	**$P2_1/c$, (no. 14)**	
Unit cell dimensions	a = 13.2410(6) Å	α= 90°.
	b = 20.3202(9) Å	β= 101.408(2)°.
	c = 21.5275(10) Å	γ = 90°.
Volume	5677.8(4) Å^3	
Z	4	
Density (calculated)	1.192 Mg · m^{-3}	
Absorption coefficient	1.087 mm^{-1}	
F(000)	2176 e	
Crystal size	0.3 x 0.24 x 0.14 mm^3	
θ range for data collection	3.02 to 67.21°.	
Index ranges	-15 ≤ h ≤ 15, -24≤ k ≤ 24, -25 ≤ l ≤ 24	

Reflections collected	246109	
Independent reflections	10120 [R_{int} = 0.0552]	
Reflections with I>2σ(I)	9467	
Completeness to θ = 67.21°	99.7 %	
Absorption correction	Gaussian	
Max. and min. transmission	0.88 and 0.71	
Refinement method	Full-matrix least-squares on F^2	
Data / restraints / parameters	10120 / 0 / 655	
Goodness-of-fit on F^2	1.050	
Final R indices [I>2σ(I)]	R_1 = 0.0500	wR^2 = 0.1255
R indices (all data)	R_1 = 0.0527	wR^2 = 0.1279
Largest diff. peak and hole	0.826 and -0.615 e · $Å^{-3}$	

7.2.18 Crystal data and structure refinement of compound 166a

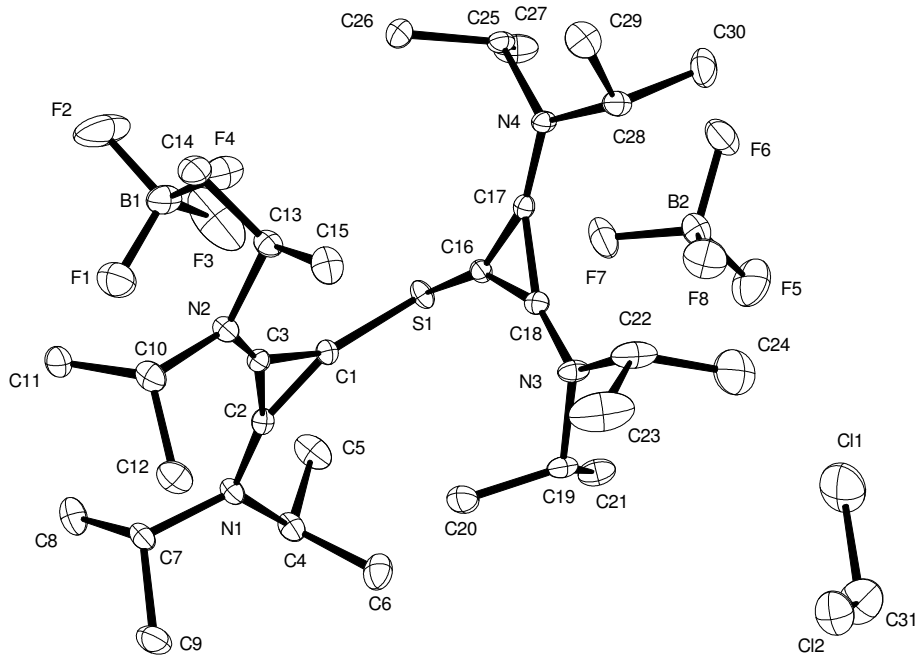

Empirical formula	$C_{31}H_{58}B_2Cl_2F_8N_4S$	
Color	colourless	
Formula weight	763.39 $g \cdot mol^{-1}$	
Temperature	100 K	
Wavelength	0.71073 Å	
Crystal system	ORTHORHOMBIC	
Space group	**Pbca, (no. 61)**	
Unit cell dimensions	a = 15.9281(17) Å	α= 90°.
	b = 16.791(3) Å	β= 90°.
	c = 29.680(2) Å	γ = 90°.
Volume	7937.7(18) $Å^3$	
Z	8	
Density (calculated)	1.278 $Mg \cdot m^{-3}$	
Absorption coefficient	0.281 mm^{-1}	
F(000)	3232 e	
Crystal size	0.32 x 0.16 x 0.16 mm^3	
θ range for data collection	2.71 to 33.10°.	
Index ranges	$-24 \le h \le 24$, $-25 \le k \le 24$, $-44 \le l \le 45$	

Reflections collected	186573	
Independent reflections	15030 [R_{int} = 0.0649]	
Reflections with I>2σ(I)	9521	
Completeness to θ = 30.00°	99.8 %	
Absorption correction	Gaussian	
Max. and min. transmission	0.98 and 0.97	
Refinement method	Full-matrix least-squares on F^2	
Data / restraints / parameters	15030 / 0 / 449	
Goodness-of-fit on F^2	1.039	
Final R indices [I>2σ(I)]	R_1 = 0.0464	wR^2 = 0.1007
R indices (all data)	R_1 = 0.0959	wR^2 = 0.1178
Largest diff. peak and hole	1.036 and -1.045 e · $Å^{-3}$	

7.2.19 Crystal data and structure refinement of compound 167a

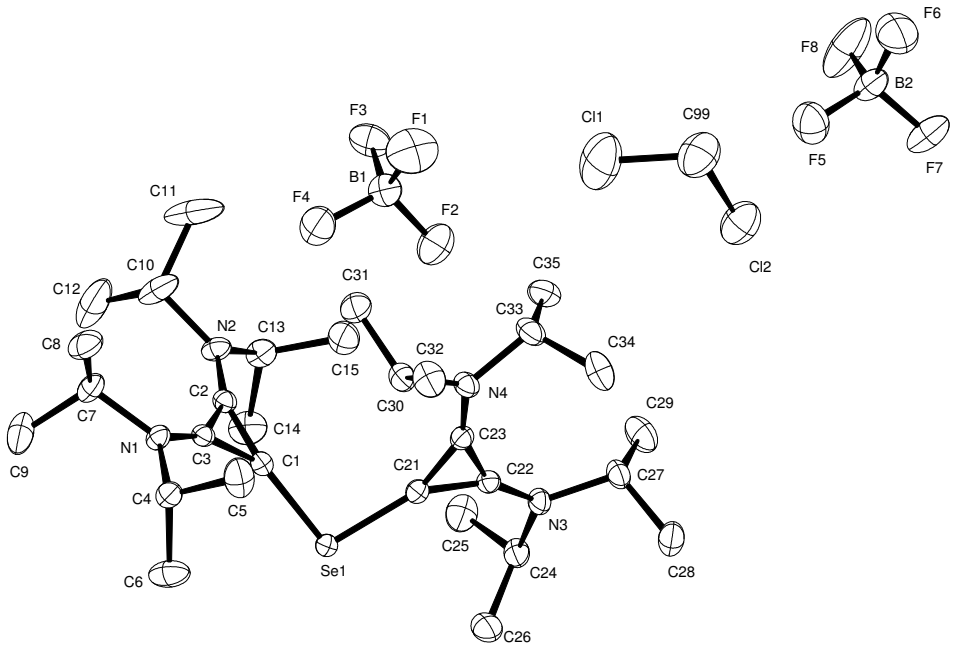

Empirical formula	$C_{31}H_{58}B_2Cl_2F_8N_4Se$	
Color	colorless	
Formula weight	810.29 $g \cdot mol^{-1}$	
Temperature	130 K	
Wavelength	1.54184 Å	
Crystal system	ORTHORHOMBIC	
Space group	**Pbca, (no. 61)**	
Unit cell dimensions	a = 16.0030(6) Å	α= 90°.
	b = 16.9693(7) Å	β= 90°.
	c = 29.6752(12) Å	γ = 90°.
Volume	8058.6(6) $Å^3$	
Z	8	
Density (calculated)	1.336 $Mg \cdot m^{-3}$	
Absorption coefficient	3.034 mm^{-1}	
F(000)	3376 e	
Crystal size	0.24 x 0.23 x 0.21 mm^3	
θ range for data collection	2.98 to 67.28°.	
Index ranges	$-18 \le h \le 18$, $-20 \le k \le 20$, $-35 \le l \le 33$	

Reflections collected	175830	
Independent reflections	7176 [R_{int} = 0.0501]	
Reflections with I>2σ(I)	6719	
Completeness to θ = 67.28°	99.3 %	
Absorption correction	Gaussian	
Max. and min. transmission	0.74 and 0.63	
Refinement method	Full-matrix least-squares on F^2	
Data / restraints / parameters	7176 / 0 / 449	
Goodness-of-fit on F^2	1.025	
Final R indices [I>2σ(I)]	R_1 = 0.0301	wR^2 = 0.0747
R indices (all data)	R_1 = 0.0318	wR^2 = 0.0756
Largest diff. peak and hole	0.711 and -0.765 e · $Å^{-3}$	

7.2.20 Crystal data and structure refinement of compound 169b

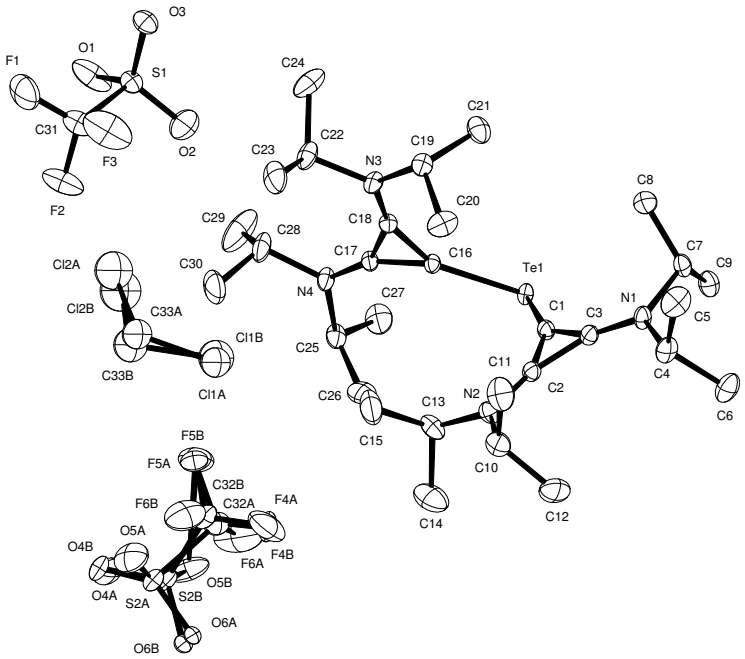

Empirical formula	$C_{33}H_{58}Cl_2F_6N_4O_6S_2Te$	
Color	colorless	
Formula weight	983.45 $g \cdot mol^{-1}$	
Temperature	100 K	
Wavelength	0.71073 Å	
Crystal system	ORTHORHOMBIC	
Space group	**Pbca, (no. 61)**	
Unit cell dimensions	a = 15.536(2) Å	α= 90°.
	b = 18.1269(15) Å	β= 90°.
	c = 32.831(4) Å	γ = 90°.
Volume	9246.1(18) $Å^3$	
Z	8	
Density (calculated)	1.413 $Mg \cdot m^{-3}$	
Absorption coefficient	0.915 mm^{-1}	
F(000)	4032 e	
Crystal size	0.29 x 0.19 x 0.06 mm^3	
θ range for data collection	2.62 to 33.11°.	
Index ranges	$-23 \le h \le 23$, $-27 \le k \le 27$, $-50 \le l \le 50$	

Reflections collected	164134	
Independent reflections	17563 [R_{int} = 0.0530]	
Reflections with I>2σ(I)	13988	
Completeness to θ = 27.50°	99.9 %	
Absorption correction	Gaussian	
Max. and min. transmission	0.95 and 0.88	
Refinement method	Full-matrix least-squares on F^2	
Data / restraints / parameters	17563 / 0 / 572	
Goodness-of-fit on F^2	1.151	
Final R indices [I>2σ(I)]	R_1 = 0.0559	wR^2 = 0.1227
R indices (all data)	R_1 = 0.0741	wR^2 = 0.1299
Largest diff. peak and hole	2.381 and -2.058 e · $Å^{-3}$	

7.2.21 Crystal data and structure refinement of compound 170

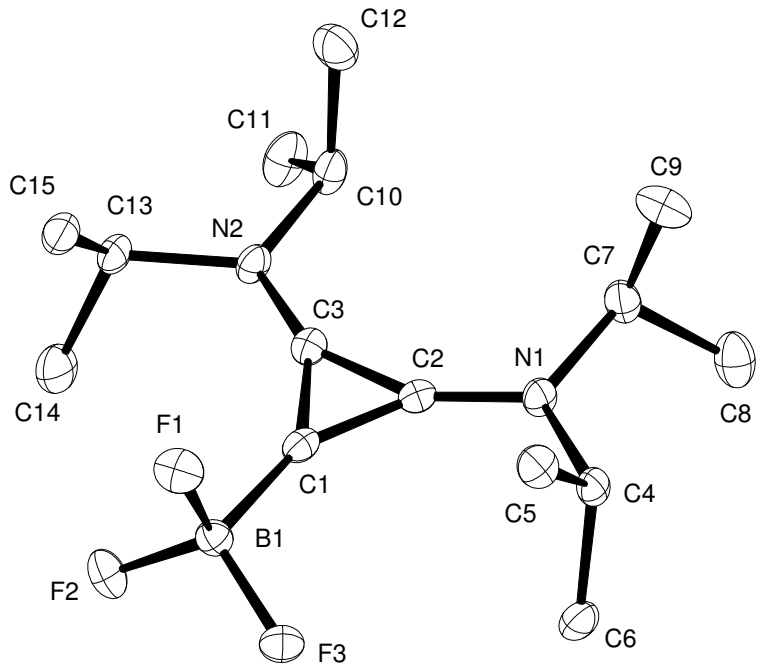

Empirical formula	$C_{15}H_{28}BF_3N_2$	
Color	colourless	
Formula weight	304.20 $g \cdot mol^{-1}$	
Temperature	100 K	
Wavelength	0.71073 Å	
Crystal system	ORTHORHOMBIC	
Space group	**$Pna2_1$, (no. 33)**	
Unit cell dimensions	a = 12.512(3) Å	α= 90°.
	b = 13.905(3) Å	β= 90°.
	c = 9.644(3) Å	γ = 90°.
Volume	1677.9(8) $Å^3$	
Z	4	
Density (calculated)	1.204 $Mg \cdot m^{-3}$	
Absorption coefficient	0.093 mm^{-1}	
F(000)	656 e	
Crystal size	0.20 x 0.19 x 0.05 mm^3	
θ range for data collection	2.93 to 29.89°.	
Index ranges	$-17 \le h \le 17$, $-19 \le k \le 19$, $-13 \le l \le 13$	

Reflections collected	35900	
Independent reflections	4846 [R_{int} = 0.0757]	
Reflections with I>2σ(I)	3995	
Completeness to θ = 27.50°	99.9 %	
Absorption correction	Gaussian	
Max. and min. transmission	0.91 and 0.71	
Refinement method	Full-matrix least-squares on F^2	
Data / restraints / parameters	4846 / 1 / 198	
Goodness-of-fit on F^2	1.084	
Final R indices [I>2σ(I)]	R_1 = 0.0441	wR^2 = 0.0855
R indices (all data)	R_1 = 0.0638	wR^2 = 0.0934
Absolute structure parameter	-0.7(5)	
Largest diff. peak and hole	0.476 and -0.225 e · $Å^{-3}$	

8 Bibliography

[1] D. J. M. Snelders, G. van Koten, R. J. M. Klein Gebbink, *Chem.–Eur. J.* **2011**, *17*, 42 – 57.

[2] I. Kovàcs, M. C. Baird, *J. Organomet. Chem.* **1995**, *502*, 87 – 94.

[3] R. Schibli, K. V. Katti, W. A. Volkert, C. L. Barnes, *Inorg. Chem.* **1998**, *37*, 5306 – 5312.

[4] D. J. M. Snelders, R. Kreiter, J. J. Firet, G. van Koten, R. J. M. Klein Gebbink, *Adv. Synth. Catal.* **2008**, *350*, 262 – 266.

[5] D. J. M. Snelders, G. van Koten, and R. J. M. Klein Gebbink, *J. Am. Chem. Soc.* **2009**, *131*, 11407–11416.

[6] J. Andrieu, M. Azouri, P. Richard, *Inorg. Chem. Commun.* **2008**, *11*, 1401 – 1404.

[7] C. W. Schultz, R. W. Parry, *Inorg. Chem.* **1976**, *15*, 3046 – 3050.

[8] (a) A. H. Cowley, R. A. Kemp, C. A. Stewart, *J. Am. Chem. Soc.* **1982**, *104*, 3239 – 3240; (b) A. H. Cowley, S. K. Mehrotra, *J. Am. Chem. Soc.* **1983**, *105*, 2074 – 2075.

[9] (a) W. B. McCormack, U.S. Patents 2663736, 2663737, **1953**; *Chem. Abstr.* **1955,** *49*, 7601; (b) C. K. SooHoo, *S.* G. Baxter, *J. Am. Chem. Soc.* **1983**, *105*, 7443 – 7444; (c) A. H. Cowley, R. A. Kemp, J. G. Lasch, N. C. Norman, C. A. Stewart, *J. Am. Chem. Soc.* **1983**, *105*, 7444 – 7445.

[10] (a) K. A. Fongers, H. Hogveen, R. F. Kingma, *Tetrahedron Lett.* **1983**, *24*, 643 – 646; (b) R. Breslow, L. A. Duerinn, *Tetrahedron Lett.* **1984**, *25*, 1345 – 1348.

[11] M.-R. Marre, M. Sanchez, R. Wolf, *Phosphorus Sulfur* **1982**, *13*, 27.

[12] A. Schmidpeter, S. Lochschmidt, A. Willham, *Angew. Chem.* **1983**, *95*, 561 – 562.

[13] G. Trinquler, M. R. Marre, *J. Phys. Chem.* **1983**, *87*, 1903 – 1905.

[14] A. Schmidpeter, M. Thiele, *Angew. Chem.* **1991**, *103*, 333 – 335; *Angew. Chem. Int. Ed.* **1991**, *30*, 308 – 310.

[15] A. H. Cowley, R. A. Kemp, *Chem. Rev.* **1985**, *85*, 367 – 382.

[16] D. Gudat, *Coord. Chem. Rev.* **1997**, *163*, 71 – 106.

[17] M. K. Denk, S. Gupta, A. J. Lough, *Eur. J. Inorg. Chem.* **1999**, 41 – 49.

[18] M. K. Denk, S. Gupta, R. Ramachandran, *Tetrahedron Lett.* **1996**, *37*, 9025 – 9028.

[19] (a) R. W. Kopp, A. C. Bond, R. W. Parry, *Inorg. Chem.* **1976**, *15*, 3042 – 3046; (b) C. W. Schultz, R. W. Parry, *Inorg. Chem.* **1976**, *15*, 3046 – 3050.

[20] C. A. Caputo, J. T. Price, M. C. Jennings, R. MacDonald, N. D. Jones, *Dalton Trans.* **2008**, 3461 – 3469.

[21] C. A. Caputo, M. C. Jennings, H. M. Tuononen, N. D. Jones, *Organometallics* **2009,** *28,* 990–1000.

[22] H. M. Tuononen, R. Roesler, J. L. Dutton, P. J. Ragogna, *Inorg. Chem.* **2007**, *46*, 10693 – 10706.

[23] M. B. Abrams, B. L. Scott, R. T. Baker, *Organometallics* **2000**, *19*, 4944 – 4956.

[24] H. A. Spinney, G. P. A. Yap, I. Korobkov, G. DiLabio, D. S. Richeson, *Organometallics* **2006**, *25*, 3541 – 3543.

[25] S. Burck, J. Daniels, T. Gans-Eichler, D. Gudat, K. Nättinen, M. Nieger, *Z. Anorg. Allg. Chem.* **2005**, *631*, 1403 – 1412.

[26] R. Oberdörfer, M. Nieger, E. Niecke, *Chem. Ber.* **1994**, *127*, 2397 – 2401.

[27] S. S. Snow, D. X. Jiang, R. W. Parry, *Inorg. Chem.* **1987**, *26*, 1629 – 1631.

[28] N. J. Hardman, M. B. Abrams, M. A. Pribisko, T. M. Gilbert, R. L. Martin, G. J. Kubas, R. T. Baker, *Angew. Chem.* **2004**, *116*, 1989 – 1992; *Angew. Chem. Int. Ed.* **2004**, *43*, 1955 – 1958.

[29] N. Burford, T. S. Cameron, P. J. Ragogna, *J. Am. Chem. Soc.* **2001**, *123*, 7947-7948.

[30] N. Burford, T. S. Cameron, D. J. LeBlanc, P. Losier, S. Sereda, G. Wu, *Organometallics*, **1997**, *16*, 4712 – 4717.

[31] (a) B. D. Ellis, P. J. Ragogna, C. L. B. MacDonald, *Inorg. Chem.* **2004**, *43*, 7857 – 7867; (b) N. Burford, P. J. Ragogna, *J. Chem. Soc. Dalton Trans.* **2002**, 4307 – 4315; (c) N. Burford, P. J. Ragogna, R. MacDonald, M. J. Ferguson, *J. Am. Chem. Soc.* **2003**, *125*, 14404 – 14410; (d) N. Burford, P. Losier, A. D. Phillips, P. J. Ragogna, T. S. Cameron, *Inorg. Chem.* **2003**, *42*, 1087 – 1091.

[32] S. Saleh, E. Fayad, M. Azouri, J. Hierso, J. Andrieu, M. Picquet, *Adv. Synth. Catal.* **2009**, *351*, 1621 – 1628.

[33] (a) J. Andrieu, M. Azouri, P. Richard, *Inorg. Chem. Commun.* **2008**, *11*, 1401 – 1404; (b) M. Azouri, J. Andrieu, M. Picquet, H. Cattey, *Inorg. Chem.* **2009**, *48*, 1236 – 1242; (c) I. Abdellah, C. Lepetit, Y. Canac, C. Duhayon, R. Chauvin, *Chem. Eur. J.* **2010**, *16*, 13095 – 13108.

[34] N. Kuhn, M. Göhner, *Z. Anorg. Allg. Chem.* **1999**, *625*, 1415-1416.

[35] (a) D. J. Brauer, K. W. Kottsieper, C. Liek, O. Stelzer, H. Waffenschmidt, P. Wasserscheid, *J. Organomet. Chem.* **2001**, *630*, 177 – 184; (b) S.-G. Lee, Y. J. Zhang, J. Y. Piao, C. E. Song, J. H. Choi, J. Hong, *Chem. Commun.* **2003**, 2624 – 2625; (c) R. P. J. Bronger, S. M. Silva, P. C. J. Kamer, P. W. N. M. van Leeuwen, *Dalton Trans.* **2004**, 1590 – 1596; (d) J. Andrieu, M. Azouri, *Inorg. Chim. Acta* **2007**, *360*, 131 – 135.

[36] See ref. 32.

[37] (a) See ref. 15; (b) See ref. 16.

[38] (a) See ref. 17; (b) See ref. 20; (c) See ref. 14; (d) D. Gudat, *Acc. Chem. Res.* **2010**, *43*, 1307 – 1316.

[39] (a) See ref. 31; (b) See ref. 20; (c) N. Kuhn, J. Fahl, D. Bläzer, R. Boese, *Z. Anorg. Allg. Chem.* **1999**, *625*, 729 – 734; (d) N. Burford, P. J. Ragogna, K. Sharp, R. MacDonald, M. J. Ferguson, *Inorg. Chem.* **2005**, *44*, 9453 – 9460; for adducts with pyridine derivatives and other *N*-based ligands, see: (e) See ref. 9a.

[40] (a) H. Nakazawa, *J. Organomet. Chem.* **2000**, *611*, 349 – 363; (b) See ref. 31; (c) See ref. 22; (d) See ref. 28; (e) C. A. Caputo, A. L. Brazeau, Z. Hynes, J. T. Price, H. M. Tounonen, N. D. Jones, *Organometallics* **2009**, *28*, 5261 – 5265.

[41] (a) P. Le Floch, F. Mathey, *Synlett* **1991**, 743 – 744; (b) H. Werner, B. Klingert, *J. Organomet. Chem.* **1981**, *218*, 395 – 407.

[42] (a) See ref. 32; (b) See ref. 33; (c) N. Debono, Y. Canac, C. Duhayon, R. Chauvin, *Eur. J. Inorg. Chem.* **2008**, 2991 – 2999; (d) J. J. Weigand, K. O. Feldmann, F. D. Henne, *J. Am. Chem. Soc.* **2010**, *132*, 16321 – 16323.

[43] (a) *Applied Homogeneous Catalysis with Orgnometallic Compounds Part I+II* (Eds.: B. Cornils, W. A. Herrmann), Wiley-VCH, Weinheim, **1996**; (b) *Aqueous-Phase Organometallic Catalysis* (Eds.: B. Cornils, W. A. Herrmann), Wiley-VCH, Weinheim, **1998**.

[44] (a) O. Back, G. Kuchenbeiser, B. Donnadieu, G. Bertrand, *Angew. Chem.* **2009**, *121*, 5638 – 5641; *Angew. Chem. Int. Ed.* **2009**, *48*, 5530 – 5533; (b) W. Kirmse, *Angew. Chem. Int. Ed.* **2004**, *43*, 1767 – 1769; (c) V. Lavallo, Y. Canac, B. Donnadieu, W. W. Schoeller, G. Bertrand, *Science* **2006**, *312*, 722 – 724; (d) W. W. Schoeller, G. Frey, G. Bertrand, *Chem. Eur. J.* **2008**, *14*, 4711 – 4718; (e) D. M. Chisholm, J. S. McIndoe, *Dalton Trans.* **2008**, 3933 – 3945; (f) for recent work on phosphines attached to imidazolium moieties through a methylene linker, see: A. Dumrath, X. Wu, H. Neumann, A. Spannenberg, R. Jackstell, M. Beller, *Angew. Chem.* **2010**, *122*, 9172 – 9176; *Angew. Chem. Int. Ed.* **2010**, *49*, 8988 – 8992; (g) for the synthesis of a phosphine containing a metalated substituent, see: M. R. Axet, M. Barbazanges, M. Augé, C. Desmarets, J. Moussa, C. Ollivier, C. Aubert, L. Fensterbank, V. Gandon, M. Malacria, L. M. Chamoreau, H. Amouri, *Organometallics* **2010**, *29*, 6636 – 6638.

[45] For the employment of this carbene to stabilize N(I) and P(I) centers, see: H. Bruns, M. Patil, J. Carreras, A. Vàzquez, W. Thiel, R. Goddard, M. Alcarazo, *Angew. Chem.* **2010**, *122*, 3762 – 3766; *Angew. Chem. Int. Ed.* **2010**, *49*, 3680 – 3683;

[46] See ref. 44d.

[47] (a) R. Weiss, K. G. Wagner, C. Priesner, J. Macheleid, *J. Am. Chem. Soc.* **1985**, *107*, 4491 – 4499; (b) a tungsten complex containing a cyclopropenylidene-stabilized phosphenium

cation has been described, although a different synthetic protocol was used, see: N. H. T. Huy, B. Donnadieu, G. Bertrand, F. Mathey, *Chem. Asian J.* **2009**, *4*, 1225 – 1228.

[48] J. C. J. Bart, *J. Chem. Soc. B* **1969**, 350 – 365.

[49] CCDC 805226 (**43a**) and 805225 (**46a**) contain the supplementary crystallographic data for this thesis. These data can be obtained free of charge from The Cambridge Crystallographic Data Centre *via* www.ccdc.cam.ac.uk/data_request/cif.

[50] (a) S. Otto, A. Rodt, *Inorg. Chim. Acta* **2004**, 357, 1–10; (b) D. Gusev, *Organometallics* **2009**, *28*, 763 – 770.

[51] For a similar study on [(NHC)RhCl(cod)] complexes, see: (a) S. Wolf, H. Plenio, *J. Organomet. Chem.* **2009**, *694*, 1487 – 1492; (b) M. Alcarazo, T. Stork, A. Anoop, W. Thiel, A. Fürstner, *Angew. Chem.* **2010**, *122*, 2596 – 2600; *Angew. Chem. Int. Ed.* **2010**, *49*, 2542 – 2546.

[52] N. Mézailles, L. Ricard, F. Gagosz, *Org. Lett.* **2005**, *7*, 4133 – 4136.

[53] For recent reviews on gold-promoted transformations, see: (a) E. Jiménez-Núñez, A. M. Echavarren, *Chem. Rev.* **2008**, *108*, 3326 – 3350; (b) A. Fürstner, P.W. Davies, *Angew. Chem.* **2007**, *119*, 3478 – 3519; *Angew. Chem. Int. Ed.* **2007**, *46*, 3410 – 3449; (c) D. J. Gorin, B. D. Sherry, F. D. Toste, *Chem. Rev.* **2008**, *108*, 3351 – 3378.

[54] M. R. Luzung, P. Mauleón, F. D. Toste, *J. Am. Chem. Soc.* **2007**, *129*, 12402 – 12403.

[55] F. Chávez, R. Godinez, *Synth. Commun.* **1992**, *22*, 159 – 164.

[56] M. Murakami, S. Kadowaki, T. Matsuda, *Org. Lett.* **2005**, *7*, 3953 – 3956.

[57] A. Doutheau, A. Saba, J. Goré, *Synth. Commun.* **1982**, *12*, 557-563.

[58] T. Makino, K. Itoh, *J. Org. Chem.* **2004**, *69*, 395-405.

[59] (a) See ref. 54; (b) See ref. 51b.

[60] (a) I. Alonso, B. Trillo, F. López, S. Montserrat, G. Ujaque, L. Castedo, A. Lledós, J. L. Mascareñas, *J. Am. Chem. Soc.* **2009**, *131*, 13020 – 13030; (b) P. Mauleón, R. M. Zeldin, A. Z. González, F. D. Toste, *J. Am. Chem. Soc.* **2009**, *131*, 6348 – 6349; (c) D. Benítez, E. Tkatchouk, A. Z. González, W. A. Goddard III, F. D. Toste, *Org. Lett.* **2009**, *11*, 4798 – 4801.

[61] A. Z. González, F. D. Toste *Org. Lett.* **2010**, *12*, 200 – 203.

[62] M. N. Paddon-Row, A. I. Longshaw, A. C. Willis, M. S. Sherburn, *Chem.-Asian J.* **2009**, *4*, 126 – 134.

[63] V. Mamane, P. Hannen, A. Fürstner, *Chem. Eur. J.* **2004**, *10*, 4556 – 4575.

[64] Synthesized by V. Mamane at the Max Planck Institute for Coal Research in Mülheim an der Ruhr.

[65] For a related transformation, see: P. Cordier, C. Aubert, M. Malacria, E. Lacôte, V. Gandon, *Angew. Chem.* **2009**, *121*, 8913 – 8916; *Angew. Chem. Int. Ed.* **2009**, *48*, 8757 – 8760.

[66] (a) K. Mikami, K. Takahashi, T. Nakai, *Synlett* **1989**, 45 – 47; (b) B. W. Boal, A. W. Schammel, N. K. Garg, *Org. Lett.* **2009**, *11*, 3458 – 3461.

[67] G. F. Weber, S. S. Hall, *J. Org. Chem.* **1979**, *44*, 364 – 368.

[68] J. D. Rosen, T. D. Nelson, M. A. Huffman, J. M. McNamara, *Tetrahedron Lett.* **2003**, *44*, 365 – 368.

[69] Synthesized by T. Gress at the Max Planck Institute for Coal Research in Mülheim an der Ruhr.

[70] C. M. Martin, P. J. Ragogna, *Inorg. Chem.* **2010**, *49*, 8164 – 8172.

[71] See ref. 33c.

[72] See ref. 33b.

[73] Y. Wang, Y. Xie, M. Y. Abraham, R. J. Gilliard, P. Wei, H. F. Schaefer, P.v.R. Schleyer, G. H. Robinson, *Organometallics* **2010**, *29*, 4778 – 4780.

[74] (a) B. D. Ellis, C. A. Dyer, A. Decken, C. L. B. Macdonald, *Chem. Commun.* **2005**, 1965 – 1967; (b) B. D. Ellis, C. L. B. Macdonald, *Coord. Chem. Rev.* **2007**, *251*, 936 – 973; (c) See ref. 10b.

[75] See ref. 42d.

[76] The synthesis was realized by S. Holle at the Max Planck Institute for Coal Research in Mülheim an der Ruhr.

[77] See ref. 33b.

[78] The C–P bond distance in the unstabilized ylide $Ph_3P{=}CH_2$ is 1.662(8) Å. J. C. J. Bart, *J. Chem. Soc. B* **1969**, 350 – 365.

[79] Z. B. Maksić, B. Kovaĉević, *J. Chem. Soc. Perkin Trans. 2* **1999**, 2623 – 2629.

[80] A. Fürstner, F. Stelzer, H. Szillat, *J. Am. Chem. Soc.* **2001**, *123*, 11863 – 11869.

[81] A. Fürstner, P. W. Davies, T. Gress, *J. Am. Chem. Soc.* **2005**, *127*, 8244 – 8245.

[82] See ref. 69.

[83] See ref. 69.

[84] (a) R. Weiss, R. Roth, *Synthesis* **1987**, 870 – 872; (b) E. Anders, A. Stankowiak, A. Meske, J. Tropsch, G. Maas, *Chem. Ber.* **1987**, *120*, 735 – 745.

[85] R. Weiss, S. Engel, *Synthesis* **1991**, 1077 – 1079.

[86] G. Bouhadir, R. W. Reed, R. Réau, G. Bertrand, *Heteroat. Chem.* **1995**, *6*, 371 – 375.

[87] (a) A. P. Rupar, V. N. Staroverov, P. J. Ragogna, K. M. Baines, *J. Am. Chem. Soc.* **2007**, *129*, 15138 – 15139; (b) D. J. Williams, P. H. Poor, G. Ramírez, *Inorg. Chim. Acta* **1989**, *165*, 167 – 172; (c) J. L. Dutton, T. L. Battista, M. J. Sgro, P. J. Ragogna, *Chem. Commun.* **2010**, *46*, 1041 – 1043.

[88] (a) See ref. 45; (b) J. Petuškova, H. Bruns, M. Alcarazo, *Angew. Chem. Int. Ed.* **2011**, *50*, 3799 – 3802.

[89] (a) H. Clavier, S. P. Nolan, *Chem. Commun.* **2010**, *46*, 841 – 861; (b) D. G. Gusev, *Organometallics* **2009**, *28*, 6458 – 6461; (c) T. Dröge, F. Glorius, *Angew. Chem. Int. Ed.* **2010**, *49*, 6940 –6952; (d) G. Kuchenbeiser, B. Donnadieu, G. Bertrand, *J. Organomet. Chem.* **2008**, *693*, 899 – 904.

[90] (a) See ref. 44c; (b) W. W. Schoeller, G. Frey, G. Bertrand, *Chem.–Eur. J.* **2008**, *14*, 4711 – 4718; (c) See ref. 47b.

[91] For the synthesis of analogous O- and S-centered dications, see: (a) Z. Yoshida, H. Konishi, H. Ogoshi, *Isr. J. Chem.* **1981**, *21*, 139 – 165; (b) G. Mass, P. J. Stang, *J. Org. Chem.* **1983**, *48*, 3038 – 3043.

[92] V. Lavallo, Y. Ishida, B. Donnadieu, G. Bertrand, *Angew. Chem. Int. Ed.* **2006**, *45*, 6652 – 6655.

[93] See ref. 76.

[94] (a) Z. Yoshida, Y. Tawara, *J. Am. Chem. Soc.* **1971**, *93*, 2573 – 2574; (b) C. Wilcox, R. Breslow, *Tetrahedron Lett.* **1980**, *21*, 3241 – 3242; (c) A. Landau, G. Seitz, *Chem. Ber.* **1991**, *124*, 665 – 669.

[95] See ref. 33b.

[96] (a) See ref. 10b; (b) Y. Tulchinky, M. A. Iron, M. Botoshansky, M. Gandelman, *Nat. Chem.* **2011**, *3*, 525 – 531; (c) M. P. Cloes, P. B. Hitchcock, *Chem. Commun.* **2007**, 5229 – 5231.

[97] Q. Tho DO, D. Elothmani, G. Le Guillanton, *Tetrahedron Lett.* **1998**, *39*, 4657 – 4658.

[98] (a) See ref. 70; (b) See ref. 87c; (c) J. I. Dutton, P. J. Ragogna, *Coord. Chem. Rev.* **2011**, *255*, 1414 – 1425; (d) C. D. Martin, P. J. Ragogna, *Annu. Rep. Prog.Chem., Sec. A* **2011**, *107*, 110 – 124.

[99] See. ref. 98c.

[100] H. Fujihara, H. Mima, N. Furukawa, *J. Am. Chem. Soc.* **1995**, *117*, 10153 – 10154.

[101] See ref. 87c.

[102] K. T. Higa, D. C. Harris, *Organometallics*, **1989**, *8*, 1674 – 1678.

[103] B. Trillo, F. Lopéz, S. Monserrat, G. Ujaque, L. Castedo, A. Lledós, J. L. Mascareñas, *Chem. Eur. J.* **2009**, *15*, 3336 – 3339.

[104] See ref. 60b.

[105] See. ref. 94a.

[106] See. ref. 94b.

[107] See. ref. 94c.

[108] See. ref. 94c.